

236940

Westinghouse Non-Proprietary Class 3

WCAP-15958
Revision 0

January 2003

Analysis of Capsule V from Pacific Gas and Electric Company Diablo Canyon Unit 1 Reactor Vessel Radiation Surveillance Program



236940



Westinghouse Electric Company
Nuclear Services
P.O. Box 355
Pittsburgh, Pennsylvania 15230-0355
USA

Mr. Bill Bojduj
Pacific Gas and Electric Company
Diablo Canyon Power Plant
P.O. Box 56
Avila Beach, CA 93424

Direct tel: 412-374-6345
Direct fax: 412-374-3451
e-mail: rice1wr@westinghouse.com
Westinghouse S.O.: 13660
Customer P.O. 4500635504
Our ref: PGE-03-8

February 6, 2003

PACIFIC GAS & ELECTRIC COMPANY
NUCLEAR PLANT, DIABLO CANYON UNIT 1
Surveillance Capsule Analysis

Dear Mr. Bojduj:

Please find attached ten (10) copies of WCAP-15958, "Analysis of Capsule V from Pacific Gas and Electric Company Diablo Canyon Unit 1 Reactor Vessel Radiation Surveillance Program," January 2003.

If you have any questions regarding this WCAP, please contact Mr. Tom Laubham at 412-374-6788, or me.

Very truly yours,

A handwritten signature in black ink, appearing to read 'William R. Rice'.

W. R. Rice
Customer Project Manager

Attachment

cc: DCPD Chrono	PGE - 1L
Dave Miklush	PGE - 1L
Steve Chesnut	PGE - 1L
Larry Cossette	PGE - 1L

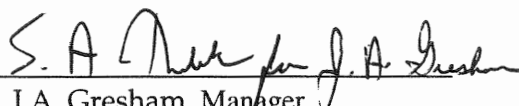
1

WCAP-15958, Revision 0

Analysis of Capsule V from Pacific Gas and Electric Company Diablo Canyon Unit 1 Reactor Vessel Radiation Surveillance Program

**A. R. Rawluszki
J. Conermann
R. J. Hagler**

January 2003

Approved: 
J.A. Gresham, Manager
Engineering & Materials Technology

Westinghouse Electric Company LLC
Energy Systems
P.O. Box 355
Pittsburgh, PA 15230-0355

©2003 Westinghouse Electric Company LLC
All Rights Reserved

TABLE OF CONTENTS

236940

LIST OF TABLES	iv
LIST OF FIGURES	vi
PREFACE	viii
EXECUTIVE SUMMARY	ix
1 SUMMARY OF RESULTS.....	1-1
2 INTRODUCTION	2-1
3 BACKGROUND	3-1
4 DESCRIPTION OF PROGRAM	4-1
5 TESTING OF SPECIMENS FROM CAPSULE V.....	5-1
5.1 OVERVIEW.....	5-1
5.2 CHARPY V-NOTCH IMPACT TEST RESULTS	5-3
5.3 TENSILE TEST RESULTS	5-5
5.4 WEDGE OPENING LOADING TESTS	5-5
6 RADIATION ANALYSIS AND NEUTRON DOSIMETRY	6-1
6.1 INTRODUCTION	6-1
6.2 DISCRETE ORDINATES ANALYSIS.....	6-2
6.3 NEUTRON DOSIMETRY	6-5
6.4 CALCULATIONAL UNCERTAINTIES	6-6
7 SURVEILLANCE CAPSULE REMOVAL SCHEDULE.....	7-1
8 REFERENCES	8-1
APPENDIX A LOAD-TIME RECORDS FOR CHARPY SPECIMEN TESTS	A-0
APPENDIX B CHARPY V-NOTCH SHIFT RESULTS FOR EACH CAPSULE PREVIOUS FIT VS. SYMMETRIC HYPERBOLIC TANGENT CURVE-FITTING METHOD (CVGRAPH, VERSION 4.1).....	B-0
APPENDIX C CHARPY V-NOTCH PLOTS FOR EACH CAPSULE USING SYMMETRIC HYPERBOLIC TANGENT CURVE-FITTING METHOD	C-0
APPENDIX D DIABLO CANYON UNIT 1 SURVEILLANCE PROGRAM CREDIBILITY ANALYSIS	D-0
APPENDIX E VALIDATION OF THE RADIATION TRANSPORT MODELS BASED ON NEUTRON DOSIMETRY MEASUREMENTS.....	E-0

LIST OF TABLES

Table 4-1	Heat Treatment History of the Diablo Canyon Unit 1 Reactor Vessel Surveillance Materials.....	4-3
Table 4-2	Heat Treatment History of the HSST 02 Correlation Monitor Plate Material.....	4-3
Table 4-3	Chemical Composition (wt %) of the Diablo Canyon Unit 1 Reactor Vessel Surveillance Materials (Unirradiated).....	4-4
Table 5-1	Charpy V-Notch Data for the Diablo Canyon Unit 1 Intermediate Shell Plate B4106-3 Irradiated to a Fluence of 1.37×10^{19} n/cm ² (E > 1.0 MeV) (Longitudinal Orientation)	5-6
Table 5-2	Charpy V-notch Data for the Diablo Canyon Unit 1 Surveillance Weld Material Irradiated to a Fluence of 1.37×10^{19} n/cm ² (E> 1.0 MeV)	5-7
Table 5-3	Charpy V-notch Data for the Diablo Canyon Unit 1 Heat-Affected-Zone (HAZ) Material Irradiated to a Fluence of 1.37×10^{19} n/cm ² (E> 1.0 MeV)	5-8
Table 5-4	Charpy V-notch Data for the Diablo Canyon Unit 1 Correlation Monitor Material Irradiated to a Fluence of 1.37×10^{19} n/cm ² (E> 1.0 MeV)	5-9
Table 5-5	Instrumented Charpy Impact Test Results for the Diablo Canyon Unit 1 Intermediate Shell Plate B4106-3 Irradiated to a Fluence of 1.37×10^{19} n/cm ² (E> 1.0 MeV) (Longitudinal Orientation)	5-10
Table 5-6	Instrumented Charpy Impact Test Results for the Diablo Canyon Unit 1 Surveillance Weld Metal Irradiated to a Fluence of 1.37×10^{19} n/cm ² (E> 1.0 MeV)	5-11
Table 5-7	Instrumented Charpy Impact Test Results for the Diablo Canyon Unit 1 Heat-Affected-Zone (HAZ) Irradiated to a Fluence of 1.37×10^{19} n/cm ² (E> 1.0MeV)	5-12
Table 5-8	Instrumented Charpy Impact Test Results for the Diablo Canyon Unit 1 Correlation Monitor Metal Irradiated to a Fluence of 1.37×10^{19} n/cm ² (E> 1.0MeV)	5-13
Table 5-9	Effect of Irradiation to 1.37×10^{19} n/cm ² (E> 1.0 MeV) on the Capsule V Notch Toughness Properties of the Diablo Canyon Unit 1 Reactor Vessel Surveillance Materials.....	5-14
Table 5-10	Comparison of the Diablo Canyon Unit 1 Surveillance Material 30 ft-lb Transition Temperature Shifts and Upper Shelf Energy Decreases with Regulatory Guide 1.99, Revision 2, Predictions.....	5-15
Table 5-11	Tensile Properties of the Diablo Canyon Unit 1 Capsule V Reactor Vessel Surveillance Materials Irradiated to 1.37×10^{19} n/cm ² (E> 1.0MeV).....	5-16

LIST OF TABLES (Cont.)

Table 6-1	Calculated Neutron Exposure Rates and Integrated Exposures At The Surveillance Capsule Center.....	6-10
Table 6-2	Calculated Azimuthal Variation of Maximum Exposure Rates And Integrated Exposures at the Reactor Vessel Clad/Base Metal Interface	6-14
Table 6-3	Relative Radial Distribution Of Neutron Fluence ($E > 1.0$ MeV) Within The Reactor Vessel Wall	6-18
Table 6-4	Relative Radial Distribution of Iron Atom Displacements (dpa) Within The Reactor Vessel Wall	6-18
Table 6-5	Calculated Fast Neutron Exposure of Surveillance Capsules Withdrawn from Diablo Canyon Unit 1	6-19
Table 6-6	Calculated Surveillance Capsule Lead Factors.....	6-19
Table 7-1	Diablo Canyon Unit 1 Reactor Vessel Surveillance Capsule Withdrawal Schedule	7-1

LIST OF FIGURES

Figure 4-1	Arrangement of Surveillance Capsules in the Diablo Canyon Unit 1 Reactor Vessel....	4-6
Figure 4-2	Capsule V Diagram Showing the Location of Specimens, Thermal Monitors, and Dosimeters	4-7
Figure 5-1	Charpy V-Notch Impact Energy vs. Temperature for Diablo Canyon Unit 1 Reactor Vessel Intermediate Shell Plate B4106-3 (Longitudinal Orientation)	5-17
Figure 5-2	Charpy V-Notch Lateral Expansion vs. Temperature for Diablo Canyon Unit 1 Reactor Vessel Intermediate Shell Plate B4106-3 (Longitudinal Orientation)	5-18
Figure 5-3	Charpy V-Notch Percent Shear vs. Temperature for Diablo Canyon Unit 1 Reactor Vessel Intermediate Shell Plate B4106-3 (Longitudinal Orientation)	5-19
Figure 5-4	Charpy V-Notch Impact Energy vs. Temperature for Diablo Canyon Unit 1 Reactor Vessel Weld Metal.....	5-20
Figure 5-5	Charpy V-Notch Lateral Expansion vs. Temperature for Diablo Canyon Unit 1 Reactor Weld Metal.....	5-21
Figure 5-6	Charpy V-Notch Percent Shear vs. Temperature for Diablo Canyon Unit 1 Reactor Vessel Weld Metal.....	5-22
Figure 5-7	Charpy V-Notch Impact Energy vs. Temperature for Diablo Canyon Unit 1 Reactor Vessel Heat-Affected-Zone Material.....	5-23
Figure 5-8	Charpy V-Notch Lateral Expansion vs. Temperature for Diablo Canyon Unit 1 Reactor Vessel Heat-Affected-Zone Material	5-24
Figure 5-9	Charpy V-Notch Percent Shear vs. Temperature for Diablo Canyon Unit 1 Reactor Vessel Heat-Affected-Zone Material.....	5-25
Figure 5-10	Charpy V-Notch Impact Energy vs. Temperature for Diablo Canyon Unit 1 Reactor Vessel Correlation Monitor Material	5-26
Figure 5-11	Charpy V-Notch Lateral Expansion vs. Temperature for Diablo Canyon Unit 1 Reactor Vessel Correlation Monitor Material	5-27
Figure 5-12	Charpy V-Notch Percent Shear vs. Temperature for Diablo Canyon Unit 1 Reactor Vessel Correlation Monitor Material	5-28
Figure 5-13	Charpy Impact Specimen Fracture Surfaces for Diablo Canyon Unit 1 Reactor Vessel Intermediate Shell Plate B4106-3 (Longitudinal Orientation)	5-29

236940

LIST OF FIGURES (Cont.)

Figure 5-14	Charpy Impact Specimen Fracture Surfaces for Diablo Canyon Unit 1 Reactor Vessel Weld Metal.....	5-30
Figure 5-15	Charpy Impact Specimen Fracture Surfaces for Diablo Canyon Unit 1 Reactor Vessel Heat-Affected-Zone Metal.....	5-31
Figure 5-16	Charpy Impact Specimen Fracture Surfaces for Diablo Canyon Unit 1 Reactor Vessel Correlation Monitor Material	5-32
Figure 5-17	Tensile Properties for Diablo Canyon Unit 1 Reactor Vessel Intermediate Shell Plate B4106-3 (Longitudinal Orientation)	5-33
Figure 5-18	Tensile Properties for Diablo Canyon Unit 1 Reactor Vessel Weld Metal	5-34
Figure 5-19	Fractured Tensile Specimens from Diablo Canyon Unit 1 Reactor Vessel Intermediate Shell Plate B4106-3 (Longitudinal Orientation).....	5-35
Figure 5-20	Fractured Tensile Specimens from Diablo Canyon Unit 1 Reactor Vessel Weld Metal.....	5-36
Figure 5-21	Engineering Stress-Strain Curves for Intermediate Shell Plate B4106-3 Tensile Specimens E8 and E9 (Longitudinal Orientation).....	5-37
Figure 5-22	Engineering Stress-Strain Curves for Weld Metal Tensile Specimens W3 and W4	5-38
Figure 6-1	Diablo Canyon Unit 1 r, θ Reactor Geometry at the Core Midplane.....	6-8
Figure 6-2	Diablo Canyon Unit 1 r,z Reactor Geometry	6-9

PREFACE

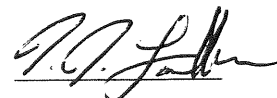
236940

This report has been technically reviewed and verified by:

Reviewer:

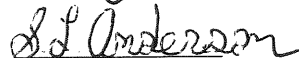
Sections 1 through 5, 7, 8, Appendices A, B, C and D

T. J. Laubham



Section 6 and Appendix E

S. L. Anderson



EXECUTIVE SUMMARY

The purpose of this report is to document the results of the testing of surveillance Capsule V from Diablo Canyon Unit 1. Capsule V was removed at 14.27 EFPY and post irradiation mechanical tests of the Charpy V-notch and tensile specimens were performed. A fluence evaluation utilizing the recently released neutron transport and dosimetry cross-section libraries was derived from the ENDF/B-VI database. Capsule V received a fluence of 1.37×10^{19} n/cm² after irradiation to 14.27 EFPY. This is equivalent to a vessel fluence at the end of the current license (32 EFPY). The peak clad/base metal interface vessel fluence after 14.27 EFPY of plant operation was 6.07×10^{18} n/cm². This evaluation lead to the following conclusions: Specimen results are behaving in accordance with predictions. The surveillance program, however, does not meet the regulatory criteria for credibility. Regulatory Guide 1.99 requires that all five criteria for credibility be met. For the Diablo Canyon Unit 1 surveillance program, four out of five of the criteria for credibility were met. A brief summary of the Charpy V-notch testing can be found in Section 1. All Charpy V-notch data was plotted using a symmetric hyperbolic tangent curve fitting program.

1 SUMMARY OF RESULTS

The analysis of the reactor vessel materials contained in surveillance Capsule V, the fifth capsule removed (third capsule tested) from the Diablo Canyon Unit 1 reactor pressure vessel, led to the following conclusions:

- The Charpy V-notch data presented in WCAP-8465^[3], WCAP-11567^[4] and WCAP-13750^[5] were based on Charpy curves using a hyperbolic tangent curve-fitting routine. The results presented in this report are based on a re-plot of all capsule data using CVGRAPH, Version 4.1, which is a symmetric hyperbolic tangent curve-fitting program. Appendix B presents a comparison of the Charpy V-Notch test results for each capsule based on previous fit vs. symmetric hyperbolic tangent fit. Appendix C presents the CVGRAPH, Version 4.1, Charpy V-notch plots and the program input data.
- Capsule V received an average fast neutron fluence ($E > 1.0$ MeV) of 1.37×10^{19} n/cm² after 14.27 effective full power years (EFPY) of plant operation.
- Irradiation of the reactor vessel intermediate shell plate B4106-3 (heat number C2793-1) Charpy specimens, oriented with the longitudinal axis of the specimen parallel to the major working direction (longitudinal orientation), resulted in an irradiated 30 ft-lb transition temperature of 39.46°F and an irradiated 50 ft-lb transition temperature of 77.51°F. This results in a 30 ft-lb transition temperature increase of 34.32°F and a 50 ft-lb transition temperature increase of 38.19°F for the longitudinal oriented specimens. See Table 5-9.
- Irradiation of the weld metal (heat number 27204) Charpy specimens resulted in an irradiated 30 ft-lb transition temperature of 135.45°F and an irradiated 50 ft-lb transition temperature of 219.26°F. This results in a 30 ft-lb transition temperature increase of 201.07°F and a 50 ft-lb transition temperature increase of 243.43°F. See Table 5-9.
- Irradiation of the weld Heat-Affected-Zone (HAZ) metal Charpy specimens resulted in an irradiated 30 ft-lb transition temperature of -52.65°F and an irradiated 50 ft-lb transition temperature of -1.98°F. This results in a 30 ft-lb transition temperature increase of 110.9°F and a 50 ft-lb transition temperature increase of 109.77°F. See Table 5-9.
- Irradiation of the Correlation Monitor Material Plate HSST02 Charpy specimens resulted in an irradiated 30 ft-lb transition temperature of 163.05°F and an irradiated 50 ft-lb transition temperature of 197.42°F. This results in a 30 ft-lb transition temperature increase of 116.61°F and a 50 ft-lb transition temperature increase of 119.12°F. See Table 5-9.
- The average upper shelf energy of the intermediate shell plate B4106-3 (longitudinal orientation) resulted in no energy decrease after irradiation. This results in an irradiated average upper shelf energy of 118 ft-lb for the longitudinal oriented specimens. See Table 5-9.

- The average upper shelf energy of the weld metal Charpy specimens resulted in an average energy decrease of 25 ft-lb after irradiation. This results in an irradiated average upper shelf energy of 66 ft-lb for the weld metal specimens. See Table 5-9.
- The average upper shelf energy of the weld HAZ metal Charpy specimens resulted in an average energy decrease of 20 ft-lb after irradiation. This results in an irradiated average upper shelf energy of 116 ft-lb for the weld HAZ metal. See Table 5-9.
- The average upper shelf energy of the Correlation Monitor Material Plate HSST02 Charpy specimens resulted in an average energy decrease of 6 ft-lb after irradiation. This results in an irradiated average upper shelf energy of 117 ft-lb for the weld correlation monitor metal. See Table 5-9.
- A comparison, as presented in Table 5-10, of the Diablo Canyon Unit 1 reactor vessel surveillance material test results with the Regulatory Guide 1.99, Revision 2^[1] predictions led to the following conclusions:
 - The measured 30 ft-lb shift in transition temperature for all the surveillance materials of Capsule V contained in the Diablo Canyon Unit 1 surveillance program are in good agreement or less than the Regulatory Guide 1.99, Revision 2, predictions.
 - The measured percent decrease in upper shelf energy for all the surveillance materials of Capsules V contained in the Diablo Canyon Unit 1 surveillance program are less than the Regulatory Guide 1.99, Revision 2 predictions.
- The credibility evaluation of the Diablo Canyon Unit 1 surveillance program presented in Appendix D of this report indicates that the surveillance results are not credible. This is based on not satisfying the third criterion for credibility.
- All beltline materials exhibit a more than adequate upper shelf energy level for continued safe plant operation and are predicted to maintain an upper shelf energy greater than 50 ft-lb throughout the life of the vessel (32 EFY) as required by 10CFR50, Appendix G^[2].
- The calculated and best estimate end-of-license (32 EFY) neutron fluence ($E > 1.0$ MeV) at the core midplane for the Diablo Canyon Unit 1 reactor vessel using the Regulatory Guide 1.99, Revision 2 attenuation formula (i.e., Equation #3 in the guide) are as follows:

Calculated: Vessel inner radius* = 1.26×10^{19} n/cm²
 Vessel 1/4 thickness = 7.51×10^{18} n/cm²
 Vessel 3/4 thickness = 2.67×10^{18} n/cm²

Best Estimate: Vessel inner radius* = $1.14 \times 10^{19} \text{ n/cm}^2$

Vessel 1/4 thickness = $6.79 \times 10^{18} \text{ n/cm}^2$

Vessel 3/4 thickness = $2.41 \times 10^{18} \text{ n/cm}^2$

*Clad/base metal interface

2 INTRODUCTION

This report presents the results of the examination of Capsule V, the third capsule removed and tested from the reactor in the continuing surveillance program which monitors the effects of neutron irradiation on the Pacific Gas and Electric Company Diablo Canyon Unit 1 reactor pressure vessel materials under actual operating conditions.

The surveillance program for the Pacific Gas and Electric Company Diablo Canyon Unit 1 reactor pressure vessel materials was designed and recommended by the Westinghouse Electric Corporation. A description of the surveillance program and the pre-irradiation mechanical properties of the reactor vessel materials are presented in WCAP-8465, "Pacific Gas and Electric Company Diablo Canyon Unit No. 1 Reactor Vessel Radiation Surveillance Program"^[3]. The original surveillance program was planned to cover the 40-year design life of the reactor pressure vessel and was based on ASTM E185-70, "Recommended Practice for Surveillance Tests for Nuclear Reactor Vessels." In 1992, Diablo Canyon implemented a Supplemental Surveillance Program^[25,26] to cover a 20 year extension on the current design life of the reactor vessel. The Supplemental Program was based on guidance from ASTM-E185-82, draft edition of ASTM-E185-92 and EPRI report, "Supplemental Reactor Vessel Surveillance Program Guidelines," dated December 1991. Capsule V was removed from the reactor after 14.27 EFPY of exposure and shipped to the Westinghouse Science and Technology Center Hot Cell Facility, where the post-irradiation mechanical testing of the Charpy V-notch impact and tensile surveillance specimens was performed.

The Charpy V-notch data presented in WCAP-8465^[3], WCAP-11567^[4] and WCAP-13750^[5] were based on a combination of hand-fit Charpy curves using engineering judgment and hyperbolic tangent curve-fitting. The only "hand fit" curves in the Diablo Canyon Unit 1 surveillance program were the unirradiated data curve fits done by W in WCAP-8465. The results presented in this report are based on a re-plot of all capsule data using CVGRAPH, Version 4.1, which is a symmetric hyperbolic tangent curve-fitting program. Appendix B presents a comparison of the Charpy V-Notch test results of previous curve fits vs. the symmetric hyperbolic tangent fit. Appendix C presents the CVGRAPH, Version 4.1, Charpy V-notch plots and the program input data.

3 BACKGROUND

The ability of the large steel pressure vessel containing the reactor core and its primary coolant to resist fracture constitutes an important factor in ensuring safety in the nuclear industry. The beltline region of the reactor pressure vessel is the most critical region of the vessel because it is subjected to significant fast neutron bombardment. The overall effects of fast neutron irradiation on the mechanical properties of low alloy, ferritic pressure vessel steels such as SA533 Grade B Class 1 (base material of the Diablo Canyon Unit 1 reactor pressure vessel beltline) are well documented in the literature. Generally, low alloy ferritic materials show an increase in hardness and tensile properties and a decrease in ductility and toughness during high-energy irradiation.

A method for ensuring the integrity of reactor pressure vessels has been presented in "Fracture Toughness Criteria for Protection Against Failure," Appendix G to Section XI of the ASME Boiler and Pressure Vessel Code^[16]. The method uses fracture mechanics concepts and is based on the reference nil-ductility transition temperature (RT_{NDT}).

RT_{NDT} is defined as the greater of either the drop weight nil-ductility transition temperature (NDTT per ASTM E-208^[15]) or the temperature 60°F less than the 50 ft-lb (and 35-mil lateral expansion) temperature as determined from Charpy specimens oriented perpendicular (transverse) to the major working direction of the plate. The RT_{NDT} of a given material is used to index that material to a reference stress intensity factor curve (K_{Ic} curve) which appears in Appendix G to the ASME Code^[16]. The K_{Ic} curve is a lower bound of static fracture toughness results obtained from several heats of pressure vessel steel. When a given material is indexed to the K_{Ic} curve, allowable stress intensity factors can be obtained for this material as a function of temperature. Allowable operating limits can then be determined using these allowable stress intensity factors.

RT_{NDT} and, in turn, the operating limits of nuclear power plants can be adjusted to account for the effects of radiation on the reactor vessel material properties. The changes in mechanical properties of a given reactor pressure vessel steel, due to irradiation, can be monitored by a reactor vessel surveillance program, such as the Diablo Canyon Unit 1 reactor vessel radiation surveillance program^[3], in which a surveillance capsule is periodically removed from the operating nuclear reactor and the encapsulated specimens tested. The increase in the average Charpy V-notch 30 ft-lb temperature (ΔRT_{NDT}) due to irradiation is added to the initial RT_{NDT} , along with a margin (M) to cover uncertainties, to adjust the RT_{NDT} (ART) for radiation embrittlement. This ART (RT_{NDT} initial + M + ΔRT_{NDT}) is used to index the material to the K_{Ic} curve and, in turn, to set operating limits for the nuclear power plant that take into account the effects of irradiation on the reactor vessel materials.

4 DESCRIPTION OF PROGRAM

Eight surveillance capsules for monitoring the effects of neutron exposure on the Diablo Canyon Unit 1 reactor pressure vessel core region (beltline) materials were inserted in the reactor vessel prior to initial plant start-up. The eight capsules were positioned in the reactor vessel between the thermal shield and the vessel wall as shown in Figure 4-1. The vertical center of the capsules is opposite the vertical center of the core. Three of the capsules contain specimens made from intermediate shell plate B4106-3, weld metal made with the same heat of weld wire (Heat No. 27204) as the limiting reactor vessel weld seam 3-442C and Correlation Monitor Plate HSST 02. The other five capsules contain specimens made from intermediate shell plates B4106-1, B4106-2, B4106-3 and Correlation Monitor Plate HSST 02.

Capsule V was removed after 14.27 effective full power years (EFPY) of plant operation. This capsule contained Charpy V-notch, tensile, and Wedge Opening Loading (WOL) specimens made from intermediate shell plate B4106-3 (heat number C2793-1) and submerged arc weld metal fabricated with the same weld wire heat 27204 and Linde 1092 flux type as used in the reactor vessel intermediate and lower shell longitudinal weld seams. In addition, this capsule contained Charpy V-notch specimens from the weld Heat-Affected-Zone (HAZ) metal of plate B4106-3 and SA533 Grade B Class 1 plate correlation monitor material.

Test material obtained from the Intermediate Shell Plate (after the thermal heat treatment and forming of the plate) was taken at least one plate thickness (9 5/8 inches) from the quenched edges of the plate. All test specimens were machined from the 1/4 thickness location of the plate after performing a simulated post-weld stress-relieving treatment. Specimens were machined from weld metal and heat-affected-zone metal from a stress-relieved weldment joining plates B4106-3 and B4106-1. All heat-affected-zone specimens were obtained from the weld heat-affected-zone of plate B4106-3.

Charpy V-notch impact specimens from intermediate shell plate B4106-3 were machined in the longitudinal orientation (longitudinal axis of the specimen parallel to the major rolling direction). The core region weld Charpy impact specimens were machined from the weldment such that the long dimension of each Charpy specimen was perpendicular to the weld direction. The notch of the weld metal Charpy specimens was machined such that the direction of crack propagation in the specimen was in the welding direction.

Tensile specimens from intermediate shell plate B4106-3 were machined in the longitudinal orientation. Tensile specimens from the weld metal were oriented with the long dimension of the specimen perpendicular to the weld direction.

WOL specimens from intermediate shell plate B4106-3 and weld metal were machined such that the simulated crack in the specimen would propagate normal and parallel to the major working direction for the plate specimen and parallel to the weld direction.

The heat treatment of the surveillance materials is presented in Tables 4-1 and 4-2. The chemical composition of the unirradiated surveillance material^[3] is presented in Table 4-3. No chemical analyses were performed for the surveillance materials in capsule V.

Capsule V contained dosimeter wires of pure copper, nickel, and aluminum 0.15 weight percent cobalt (cadmium-shielded and unshielded). In addition, cadmium shielded fission monitors of neptunium (Np^{237}) and uranium (U^{238}) were placed in the capsule to measure the integrated flux at specific neutron energy levels.

The capsule contained thermal monitors made from two low-melting-point eutectic alloys and sealed in Pyrex tubes. These thermal monitors were used to define the maximum temperature attained by the test specimens during irradiation. The composition of the two eutectic alloys and their melting points are as follows:

2.5% Ag, 97.5% Pb	Melting Point: 579°F (304°C)
1.75% Ag, 0.75% Sn, 97.5% Pb	Melting Point: 590°F (310°C)

The arrangement of the various mechanical specimens, dosimeters and thermal monitors contained in Capsule V is shown in Figure 4-2.

Table 4-1 Heat Treatment History of the Diablo Canyon Unit 1 Reactor Vessel Surveillance Materials^(a)			
Material	Temperature (°F)	Time (hrs.)	Coolant
Intermediate Shell Plate B4106-3	1600 ± 50	4	Water Quench
	1225 ± 25	4	Air Cool
	1150 ± 25	40	Furnace Cool to 600°F
Weld Metal (heat # 27204)	1150 ± 25	40	Furnace Cool to 600°F

Notes:

(a) This table was taken from WCAP-13750^[5].

Table 4-2 Heat Treatment History of the HSST 02 Correlation Monitor Plate Material^(a)		
Temperature (°F)	Time (hrs.)	Coolant
1675 ± 25	4	Air Cool
1600 ± 25	4	Water Quench
1225 ± 25	4	Furnace Cool
1150 ± 25	40	Furnace Cool to 600°F

Notes:

(a) This table was taken from WCAP-13750^[5].

236340

**Table 4-3 Chemical Composition (wt%) of the Diablo Canyon Unit 1
Reactor Vessel Surveillance Materials (Unirradiated)^(c)**

Element	Intermediate Shell Plate B4106-3	Weld Metal ^(b)	HSST 02	
			Ladle	Check
N	0.010	0.009	-	-
C	0.200	0.140	0.22	0.22
Si	0.250	0.450	0.22	0.25
Mo	0.460	0.480	0.53	0.52
Cu	0.077	0.210	-	0.14
Ni	0.460	0.980	0.62	0.68
Mn	1.330	1.360	1.45	1.48
Cr	0.035	0.060	-	-
V	0.001	0.001	-	-
Co	0.001 ^(a)	0.001 ^(a)	-	-
Sn	0.007	0.010	-	-
Zn	0.001 ^(a)	0.056	-	-
Ti	0.001 ^(a)	0.010	-	-
Zr	0.001 ^(a)	0.030	-	-
As	0.009	0.016	-	-
Sb	0.001	0.003	-	-
S	0.012	0.025	0.019	0.018
P	0.011	0.016	0.011	0.012
Al	0.036	0.018	-	-
B	0.003 ^(a)	0.03 ^(a)	-	-

Notes:

(a) Not detected, the number represents the minimum of detection.

(b) Surveillance weld was made of the same weld wire Heat 27204 and Linde 1092 Flux as the beltline region reactor vessel intermediate and lower shell longitudinal weld seams. Linde 1092 flux lot 3714 was used to fabricate the surveillance weld whereas flux lot 3724 and 3774 was used to fabricate the intermediate and lower shell longitudinal weld seams respectively.

(c) This table was taken from WCAP-13750^[5].

The best estimate copper and nickel weight percent remains as presented in the Diablo Canyon Unit 1 FSAR. The values used for the intermediate shell plate B4106-3 (Heat Number C2793-1) in all calculations documented in this report are as follows:

Cu wt. % = 0.086, and

Ni wt. % = 0.476

The values used for the surveillance weld (Heat Number 27204)* in all calculations documented in this report are as follows:

Cu wt. % = 0.198, and

Ni wt. % = 0.999

* The overall best estimate Cu and Ni for heat 27204 is 0.203 Cu and 1.018 Ni. These values are documented in the Diablo Canyon Unit 1 FSAR.

236940

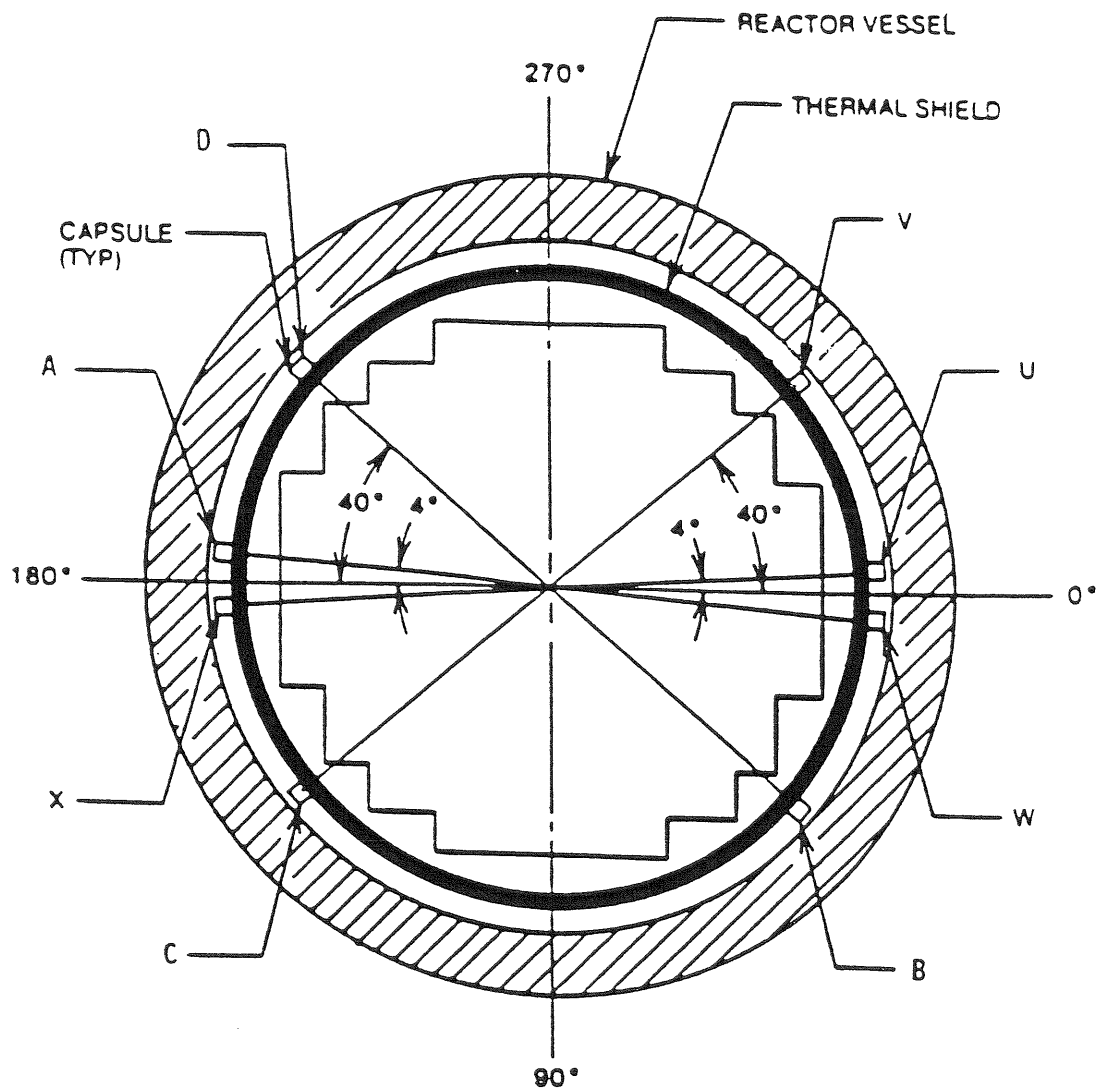


Figure 4-1 Arrangement of Surveillance Capsules in the Diablo Canyon Unit 1 Reactor Vessel

236940

SPECIMEN NUMBERING CODE

E – PLATE B4106-3
 W – WELD METAL
 H – HEAT-AFFECTED ZONE
 R – CORRELATION MONITOR MATERIAL

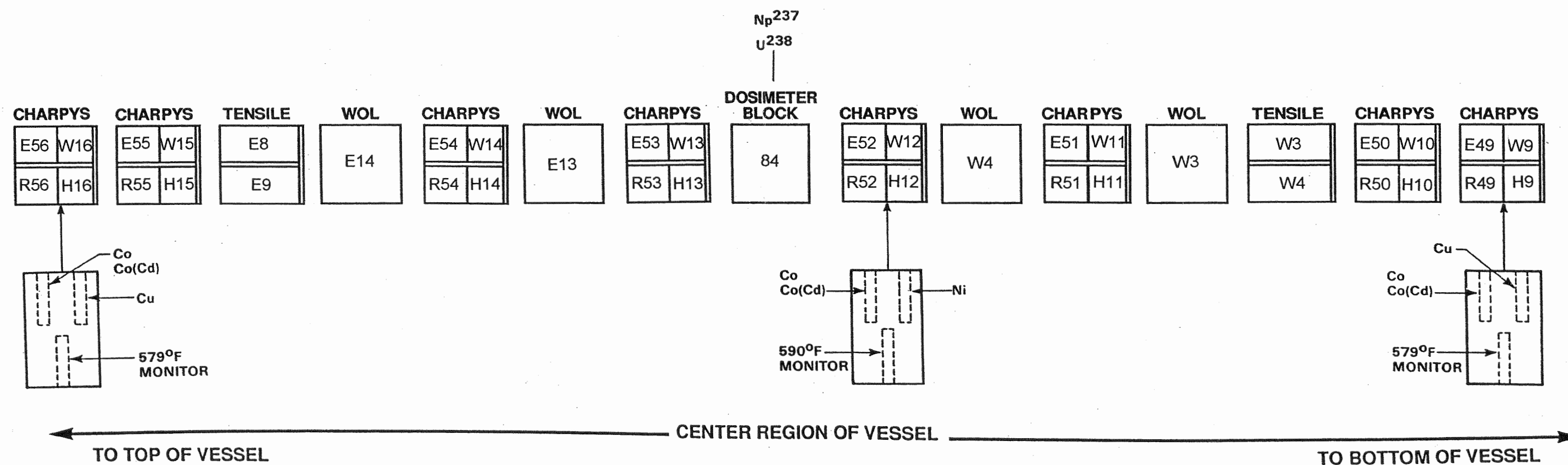
SURVEILLANCE CAPSULE V

Figure 4-2 Capsule V Diagram Showing the Location of Specimens, Thermal Monitors, and Dosimeters

5 TESTING OF SPECIMENS FROM CAPSULE V

5.1 OVERVIEW

The post-irradiation mechanical testing of the Charpy V-notch impact specimens and tensile specimens was performed in the Remote Metallographic Facility (RMF) at the Westinghouse Science and Technology Center. Testing was performed in accordance with 10CFR50, Appendices G and H^[2], ASTM Specification E185-82^[6], and Westinghouse Procedure RMF 8402^[11], Revision 2 as modified by Westinghouse RMF Procedures 8102^[12], Revision 1, and 8103^[13], Revision 1.

Upon receipt of the capsule at the hot cell laboratory, the specimens and spacer blocks were carefully removed, inspected for identification number, and checked against the master list in WCAP-8465^[3]. No discrepancies were found.

Examination of the two low-melting point 579°F (304°C) and 590°F (310°C) eutectic alloys indicated no melting of either type of thermal monitor. Based on this examination, the maximum temperature to which the test specimens were exposed was less than 579°F (304°C).

The Charpy impact tests were performed per ASTM Specification E23-98^[7] and RMF Procedure 8103 on a Tinius-Olsen Model 74, 358J machine. The tup (striker) of the Charpy impact test machine is instrumented with an Instron Dynatup Impulse instrumentation system, feeding information into an IBM compatible computer. With this system, load-time and energy-time signals can be recorded in addition to the standard measurement of Charpy energy (E_D). From the load-time curve (Appendix A), the load of general yielding (P_{GY}), the time to general yielding (t_{GY}), the maximum load (P_M), and the time to maximum load (t_M) can be determined. Under some test conditions, a sharp drop in load indicative of fast fracture was observed. The load at which fast fracture was initiated is identified as the fast fracture load (P_F), and the load at which fast fracture terminated is identified as the arrest load (P_A).

The energy at maximum load (E_M) was determined by comparing the energy-time record and the load-time record. The energy at maximum load is approximately equivalent to the energy required to initiate a crack in the specimen. Therefore, the propagation energy for the crack (E_p) is the difference between the total energy to fracture (E_D) and the energy at maximum load (E_M).

The yield stress (σ_Y) was calculated from the three-point bend formula having the following expression:

$$\sigma_Y = (P_{GY} * L) / [B * (W - a)^2 * C] \quad (1)$$

where: L = distance between the specimen supports in the impact machine
B = the width of the specimen measured parallel to the notch
W = height of the specimen, measured perpendicularly to the notch
a = notch depth

The constant C is dependent on the notch flank angle (ϕ), notch root radius (ρ) and the type of loading (i.e., pure bending or three-point bending). In three-point bending, for a Charpy specimen in which $\phi = 45^\circ$ and $\rho = 0.010$ inch, Equation 1 is valid with $C = 1.21$. Therefore, (for $L = 4W$),

$$\sigma_y = (P_{GY} * L) / [B * (W - a)^2 * 1.21] = (3.33 * P_{GY} * W) / [B * (W - a)^2] \quad (2)$$

For the Charpy specimen, $B = 0.394$ inch, $W = 0.394$ inch and $a = 0.079$ inch. Equation 2 then reduces to:

$$\sigma_y = 33.3 * P_{GY} \quad (3)$$

where σ_y is in units of psi and P_{GY} is in units of lbs. The flow stress was calculated from the average of the yield and maximum loads, also using the three-point bend formula.

The symbol A in columns 4, 5, and 6 of Tables 5-5 through 5-8 is the cross-section area under the notch of the Charpy specimens:

$$A = B * (W - a) = 0.1241 \text{ sq.in.} \quad (4)$$

Percent shear was determined from post-fracture photographs using the ratio-of-areas methods in compliance with ASTM Specification E23-98 and A370-97a^[8]. The lateral expansion was measured using a dial gage rig similar to that shown in the same specification.

Tensile tests were performed on a 20,000-pound Instron, split-console test machine (Model 1115) per ASTM Specification E8-99^[9] and E21-92 (1998)^[10], and Procedure RMF 8102. All pull rods, grips, and pins were made of Inconel 718. The upper pull rod was connected through a universal joint to improve axially of loading. The tests were conducted at a constant crosshead speed of 0.05 inches per minute throughout the test.

Extension measurements were made with a linear variable displacement transducer extensometer. The extensometer knife edges were spring-loaded to the specimen and operated through specimen failure. The extensometer gage length was 1.00 inch. The extensometer is rated as Class B-2 per ASTM E83-93^[18].

Elevated test temperatures were obtained with a three-zone electric resistance split-tube furnace with a 9-inch hot zone. All tests were conducted in air. Because of the difficulty in remotely attaching a thermocouple directly to the specimen, the following procedure was used to monitor specimen temperatures. Chromel-Alumel thermocouples were positioned at the center and at each end of the gage section of a dummy specimen and in each tensile machine gripper. In the test configuration, with a slight load on the specimen, a plot of specimen temperature versus upper and lower tensile machine gripper and controller temperatures was developed over the range from room temperature to 550°F. During the actual testing, the grip temperatures were used to obtain desired specimen temperatures. Experiments have indicated that this method is accurate to $\pm 2^\circ\text{F}$.

The yield load, ultimate load, fracture load, total elongation, and uniform elongation were determined directly from the load-extension curve. The yield strength, ultimate strength, and fracture strength were

calculated using the original cross-sectional area. The final diameter and final gage length were determined from post-fracture photographs. The fracture area used to calculate the fracture stress (true stress at fracture) and percent reduction in area was computed using the final diameter measurement.

5.2 CHARPY V-NOTCH IMPACT TEST RESULTS

The results of the Charpy V-notch impact tests performed on the various materials contained in Capsule V, which received a fluence of 1.37×10^{19} n/cm² ($E > 1.0$ MeV) in 14.27 EFPY of operation, are presented in Tables 5-1 through 5-8 and are compared with unirradiated results^[3] as shown in Figures 5-1 through 5-12.

The transition temperature increases and upper shelf energy decreases for the Capsule V materials are summarized in Table 5-9 and led to the following results:

Irradiation of the reactor vessel Intermediate Shell Plate B4106-3 (heat number C2793-1) Charpy specimens, oriented with the longitudinal axis of the specimen parallel to the major working direction (longitudinal orientation) resulted in an irradiated 30 ft-lb transition temperature of 39.46°F and an irradiated 50 ft-lb transition temperature of 77.51°F. This results in a 30 ft-lb transition temperature increase of 34.32°F and a 50 ft-lb transition temperature increase of 38.19°F for the longitudinal oriented specimens. See Table 5-9.

Irradiation of the weld metal (heat number 27204) Charpy specimens resulted in an irradiated 30 ft-lb transition temperature of 135.45°F and an irradiated 50 ft-lb transition temperature of 219.26°F. This results in a 30 ft-lb transition temperature increase of 201.07°F and a 50 ft-lb transition temperature increase of 243.43°F. See Table 5-9.

Irradiation of the weld Heat-Affected-Zone (HAZ) metal Charpy specimens resulted in an irradiated 30 ft-lb transition temperature of -52.65°F and an irradiated 50 ft-lb transition temperature of -1.98°F. This results in a 30 ft-lb transition temperature increase of 110.9°F and a 50 ft-lb transition temperature increase of 109.77°F. See Table 5-9.

Irradiation of the Correlation Monitor Material Plate HSST02 Charpy specimens resulted in an irradiated 30 ft-lb transition temperature of 163.05°F and an irradiated 50 ft-lb transition temperature of 197.42°F. This results in a 30 ft-lb transition temperature increase of 116.61°F and a 50 ft-lb transition temperature increase of 119.12°F. See Table 5-9.

The average upper shelf energy of the Intermediate Shell Plate B4106-3 (longitudinal orientation) resulted in no energy decrease after irradiation. This results in an irradiated average upper shelf energy of 118 ft-lb for the longitudinal oriented specimens. See Table 5-9.

The average upper shelf energy of the weld metal Charpy specimens resulted in an average energy decrease of 25 ft-lb after irradiation. This results in an irradiated average upper shelf energy of 66 ft-lb for the weld metal specimens. See Table 5-9.

The average upper shelf energy of the weld HAZ metal Charpy specimens resulted in an average energy decrease of 20 ft-lb after irradiation. This results in an irradiated average upper shelf energy of 116 ft-lb for the weld HAZ metal. See Table 5-9.

The average upper shelf energy of the weld correlation monitor metal Charpy specimens resulted in an average energy decrease of 6 ft-lb after irradiation. This results in an irradiated average upper shelf energy of 117 ft-lb for the weld correlation monitor metal. See Table 5-9.

A comparison, as presented in Table 5-10, of the Diablo Canyon Unit 1 reactor vessel beltline material test results with the Regulatory Guide 1.99, Revision 2^[1] predictions led to the following conclusions:

- The measured 30 ft-lb shift in transition temperature for all the surveillance materials of Capsule V contained in the Diablo Canyon Unit 1 surveillance program are in good agreement or less than the Regulatory Guide 1.99, Revision 2, predictions.
- The measured percent decrease in upper shelf energy for all the surveillance materials of Capsules V contained in the Diablo Canyon Unit 1 surveillance program are less than the Regulatory Guide 1.99, Revision 2 predictions.

The fracture appearance of each irradiated Charpy specimen from the various surveillance Capsule V materials is shown in Figures 5-13 through 5-16 and shows an increasingly ductile or tougher appearance with increasing test temperature.

All beltline materials exhibit a more than adequate upper shelf energy level for continued safe plant operation and are predicted to maintain an upper shelf energy greater than 50 ft-lb throughout the life of the vessel (32 EFY) as required by 10CFR50, Appendix G^[2].

The load-time records for individual instrumented Charpy specimen tests are shown in Appendix A.

The Charpy V-notch data presented in WCAP-8465^[3], WCAP-11567^[4] and WCAP-13750^[5] were based on hyperbolic tangent curve fitting. The results presented in this report are based on a re-plot of all capsule data using CVGRAPH, Version 4.1^[14], which is a symmetric hyperbolic tangent curve-fitting program. Appendix B presents a comparison of the Charpy V-Notch test results for each capsule based on previous fit vs. symmetric hyperbolic tangent fit. Appendix C presents the CVGRAPH, Version 4.1, Charpy V-notch plots and the program input data.

5.3 TENSILE TEST RESULTS

The results of the tensile tests performed on the various materials contained in Capsule V irradiated to $1.37 \times 10^{19} \text{ n/cm}^2$ ($E > 1.0 \text{ MeV}$) are presented in Table 5-11 and are compared with unirradiated results^[3] as shown in Figures 5-17 and 5-18.

The results of the tensile tests performed on the Intermediate Shell Plate B4106-3 (longitudinal orientation) indicated that irradiation to $1.37 \times 10^{19} \text{ n/cm}^2$ ($E > 1.0 \text{ MeV}$) caused approximately a 7 to 12 ksi increase in the 0.2 percent offset yield strength and approximately a 5-11 ksi increase in the ultimate tensile strength when compared to unirradiated data^[3]. See Figure 5-17.

The results of the tensile tests performed on the surveillance weld metal indicated that irradiation to $1.37 \times 10^{19} \text{ n/cm}^2$ ($E > 1.0 \text{ MeV}$) caused approximately a 21 to 29 ksi increase in the 0.2 percent offset yield strength and approximately a 15 to 26 ksi increase in the ultimate tensile strength when compared to unirradiated data^[3]. See Figure 5-18.

The fractured tensile specimens for the Intermediate Shell Plate B4106-3 material are shown in Figure 5-19, while the fractured tensile specimens for the surveillance weld metal are shown in Figure 5-20. The engineering stress-strain curves for the tensile tests are shown in Figures 5-21 and 5-22.

5.4 WEDGE OPENING LOADING TESTS

Per the surveillance capsule testing contract, the Wedge Opening Loading (WOL) Specimens were not tested and are being stored at the Westinghouse Science and Technology Center Hot Cell facility.

Table 5-1 Charpy V-notch Data for the Diablo Canyon Unit 1 Intermediate Shell Plate B4106-3 Irradiated to a Fluence of 1.37×10^{19} n/cm² (E > 1.0 MeV) (Longitudinal Orientation)

Sample Number	Temperature		Impact Energy		Lateral Expansion		Shear
	°F	°C	ft-lbs	Joules	mils	mm	%
E52	-25	-32	15	20	5	0.13	5
E49	25	-4	32	43	19	0.48	10
E55	75	24	33	45	21	0.53	15
E51	110	43	70	95	46	1.17	45
E53	125	52	92	125	57	1.45	65
E50	175	79	94	127	56	1.42	75
E54	250	121	122	165	78	1.98	100
E56	275	135	119	161	80	2.03	100

**Table 5-2 Charpy V-notch Data for the Diablo Canyon Unit 1 Surveillance Weld Metal
Irradiated to a Fluence of 1.37×10^{19} n/cm² (E> 1.0 MeV)**

Sample Number	Temperature		Impact Energy		Lateral Expansion		Shear
	°F	°C	ft-lbs	Joules	mils	mm	%
W11	25	-4	11	15	1	0.03	5
W13	100	38	23	31	13	0.33	15
W12	150	66	36	49	25	0.64	25
W9	200	93	37	50	24	0.61	30
W10	225	107	52	71	37	0.94	80
W15	300	149	71	96	51	1.30	100
W14	325	163	60	81	50	1.27	100
W16	350	177	66	89	48	1.22	100

Table 5-3 Charpy V-notch Data for the Diablo Canyon Unit 1 Heat-Affected-Zone (HAZ)
Material Irradiated to a Fluence of 1.37×10^{19} n/cm² (E > 1.0 MeV)

Sample Number	Temperature		Impact Energy		Lateral Expansion		Shear %
	°F	°C	Ft-lbs	Joules	mils	mm	
H14	-125	-87	19	26	4	0.10	10
H12	-50	-46	36	49	22	0.56	45
H11	0	-18	47	64	31	0.79	50
H10	72	22	66	89	45	1.14	75
H9	100	38	88	119	56	1.42	90
H15	125	52	128	174	71	1.80	100
H16	175	79	95	129	65	1.65	100
H13	225	107	124	168	79	2.01	100

Table 5-4 Charpy V-notch Data for the Diablo Canyon Unit 1 Correlation Monitor Material Irradiated to a Fluence of 1.37×10^{19} n/cm² (E > 1.0 MeV)

Sample Number	Temperature		Impact Energy		Lateral Expansion		Shear
	°F	°C	Ft-lbs	Joules	mils	mm	%
R49	25	-4	4	5	0	0.00	5
R51	50	10	8	11	3	0.08	10
R56	100	38	10	14	4	0.10	15
R55	150	66	33	45	20	0.51	30
R53	200	93	47	64	31	0.79	40
R54	250	121	74	100	48	1.22	65
R50	300	149	114	155	72	1.83	100
R52	325	163	120	163	80	2.03	100

**Table 5-5 Instrumented Charpy Impact Test Results for the Diablo Canyon Unit 1 Intermediate Shell Plate B4106-3
Irradiated to a Fluence of $1.37 \times 10^{19} \text{ n/cm}^2$ ($E > 1.0 \text{ MeV}$) (Longitudinal Orientation)**

Sample No.	Test Temp. (°F)	Charpy Energy E_D (ft-lb)	Normalized Energies (ft-lb/in ²)			Yield Load P_{GY} (lb)	Time to Yield t_{GY} (msec)	Max. Load P_M (lb)	Time to Max. t_M (msec)	Fast Fract. Load P_F (lb)	Arrest Load P_A (lb)	Yield Stress S_Y (ksi)	Flow Stress (ksi)
			Charpy E_D/A	Max. E_M/A	Prop. E_P/A								
E52	-25	15	121	72	49	3939	0.19	4304	0.24	4289	0	131	137
E49	25	32	258	196	62	3323	0.14	4438	0.46	4409	0	111	129
E55	75	33	266	173	93	3222	0.15	4259	0.42	4251	702	107	125
E51	110	70	564	316	248	3241	0.15	4466	0.68	4237	751	108	128
E53	125	92	741	321	421	3306	0.16	4462	0.69	3569	1022	110	129
E50	175	94	757	296	461	2954	0.14	4288	0.67	3749	2058	98	121
E54	250	122	983	302	681	2957	0.15	4228	0.69	n/a	n/a	98	120
E56	275	119	959	290	669	3000	0.15	4182	0.67	n/a	n/a	100	120

Table 5-6 Instrumented Charpy Impact Test Results for the Diablo Canyon Unit 1 Surveillance Weld Metal Irradiated to a Fluence of $1.37 \times 10^{19} \text{ n/cm}^2$ ($E > 1.0 \text{ MeV}$)

Sample No.	Test Temp. (°F)	Charpy Energy E_D (ft-lb)	Normalized Energies (ft-lb/in ²)			Yield Load P_{CY} (lb)	Time to Yield t_{CY} (msec)	Max. Load P_M (lb)	Time to Max. t_M (msec)	Fast Fract. Load P_F (lb)	Arrest Load P_A (lb)	Yield Stress S_y (ksi)	Flow Stress (ksi)
			Charpy E_D/A	Max. E_M/A	Prop. E_P/A								
W11	25	11	89	47	42	3939	0.15	4227	0.18	4217	0	131	136
W13	100	23	185	74	112	3426	0.14	4473	0.23	4405	267	114	132
W12	150	36	290	202	89	3440	0.15	4431	0.46	4422	573	115	131
W9	200	37	298	198	100	3281	0.15	4395	0.46	4315	206	109	128
W10	225	52	419	202	217	3354	0.15	4443	0.46	4272	1309	112	130
W15	300	71	572	211	361	3276	0.15	4290	0.49	n/a	n/a	109	126
W14	325	60	483	191	293	3141	0.14	4051	0.47	n/a	n/a	105	120
W16	350	66	532	203	329	3138	0.15	4182	0.48	n/a	n/a	104	122

236840

236940

Table 5-7 Instrumented Charpy Impact Test Results for the Diablo Canyon Unit 1 Heat-Affected-Zone (HAZ) Metal Irradiated to a Fluence of $1.37 \times 10^{19} \text{ n/cm}^2$ ($E > 1.0 \text{ MeV}$)

Sample No.	Test Temp. (°F)	Charpy Energy E_D (ft-lb)	Normalized Energies (ft-lb/in ²)			Yield Load P_{CY} (lb)	Time to Yield t_{CY} (msec)	Max. Load P_M (lb)	Time to Max. t_M (msec)	Fast Fract. Load P_F (lb)	Arrest Load P_A (lb)	Yield Stress S_Y (ksi)	Flow Stress (ksi)
			Charpy E_D/A	Max. E_M/A	Prop. E_P/A								
H14	-125	19	153	89	64	4907	0.19	5398	0.24	5388	0	163	172
H12	-50	36	290	79	212	3903	0.15	4927	0.23	4840	777.75	130	147
H11	0	47	379	80	299	4152	0.17	4822	0.24	4703	1027	138	149
H10	72	66	532	222	310	3733	0.15	4778	0.47	4099	2065	124	142
H9	100	88	709	248	461	3516	0.15	4700	0.53	3662	2376	117	137
H15	125	128	1031	247	785	3490	0.15	4676	0.53	n/a	n/a	116	136
H16	175	95	765	237	528	3406	0.15	4601	0.52	n/a	n/a	113	133
H13	225	124	999	236	763	3312	0.15	4505	0.53	n/a	n/a	110	130

Table 5-8 Instrumented Charpy Impact Test Results for the Diablo Canyon Unit 1 Correlation Monitor Metal Irradiated to a Fluence of $1.37 \times 10^{19} \text{ n/cm}^2$ ($E > 1.0 \text{ MeV}$)

Sample No.	Test Temp. ($^{\circ}\text{F}$)	Charpy Energy E_D (ft-lb)	Normalized Energies (ft-lb/in ²)			Yield Load P_{CY} (lb)	Time to Yield t_{CY} (msec)	Max. Load P_M (lb)	Time to Max. t_M (msec)	Fast Fract. Load P_F (lb)	Arrest Load P_A (lb)	Yield Stress S_Y (ksi)	Flow Stress (ksi)
			Charpy E_D/A	Max. E_M/A	Prop. E_P/A								
R49	25	4	32	14	18	1781	0.11	1839	0.12	1822	0	59	60
R51	50	8	64	36	29	3483	0.15	3593	0.16	3588	0	116	118
R56	100	10	81	36	44	3355	0.15	3465	0.17	3450	0	112	114
R55	150	33	266	185	81	3247	0.15	4399	0.44	4394	472	108	127
R53	200	47	379	229	150	3129	0.15	4449	0.53	4301	998	104	126
R54	250	74	596	301	295	3157	0.15	4377	0.67	4185	2576	105	125
R50	300	114	919	304	615	2971	0.15	4298	0.68	n/a	n/a	99	121
R52	325	120	967	313	654	3101	0.19	4228	0.73	n/a	n/a	103	122

236940

Table 5-9 Effect of Irradiation to 1.37×10^{19} n/cm² (E>1.0 MeV) on the Capsule V Notch Toughness Properties of the Diablo Canyon Unit 1 Reactor Vessel Surveillance Materials^(c)

Material	Average 30 (ft-lb) ^(a) Transition Temperature (°F)			Average 35 mil Lateral ^(b) Expansion Temperature (°F)			Average 50 ft-lb ^(a) Transition Temperature (°F)			Average Energy Absorption ^(a) at Full Shear (ft-lb)		
	Unirradiated	Irradiated	ΔT	Unirradiated	Irradiated	ΔT	Unirradiated	Irradiated	ΔT	Unirradiated	Irradiated	ΔE
Intermediate Shell Plate B4106-3 (Longitudinal)	5.14	39.46	34.32	28.65	89.72	61.07	39.31	77.51	38.19	118	121	3
Weld Metal (heat # 27204)	-65.62	135.45	201.07	-46.52	220.66	267.19	-24.16	219.26	243.43	91	66	-25
HAZ Metal	-163.55	-52.65	110.9	-107.5	18.76	126.27	-111.75	-1.98	109.77	136	116	-20
Correlation Monitor Material	46.44	163.05	116.61	58.96	213.46	154.49	78.3	197.42	119.12	123	117	-6

a. "Average" is defined as the value read from the curve fit through the data points of the Charpy tests (see Figures 5-1, 5-4, 5-7 and 5-10).

b. "Average" is defined as the value read from the curve fit through the data points of the Charpy tests (see Figures 5-2, 5-5, 5-8 and 5-11).

c. Any difference in unirradiated properties reported in this Table in comparison to WCAP-8465, WCAP-11567 and WCAP-13750, are due to now using a symmetric hyperbolic tangent curve fitting of the Charpy data versus the method used in the previous analyses. See Appendix B.

Table 5-10 Comparison of the Diablo Canyon Unit 1 Surveillance Material 30 ft-lb Transition Temperature Shifts and Upper Shelf Energy Decreases with Regulatory Guide 1.99, Revision 2, Predictions

Material	Capsule	Fluence ^(d) ($\times 10^{19}$ n/cm ² , E > 1.0 MeV)	30 ft-lb Transition Temperature Shift		Upper Shelf Energy Decrease	
			Predicted (°F) ^(a)	Measured (°F) ^(b)	Predicted (%) ^(a)	Measured (%) ^(c)
Inter. Shell Plate B4106-3 (Longitudinal)	S	0.284	36.2	-1.78	14	0
	Y	1.05	56.0	48.66	19	6.8
	V	1.37	60.0	34.32	20	0
Weld Metal (heat # 27204)	S	0.284	145.8	110.79	25.5	11.0
	Y	1.05	225.4	232.59	34.5	34.1
	V	1.37	241.6	201.07	36.5	27.5
HAZ Metal	S	0.284	--	72.31	--	8.1
	Y	1.05	--	79.77	--	19.9
	V	1.37	--	110.9	--	14.7
Correlation Monitor Material	S	0.284	73.01	65.62	--	2.4
	Y	1.05	112.9	115.79	--	8.9
	V	1.37	121.0	116.61	--	4.9

Notes:

- (a) Based on Regulatory Guide 1.99, Revision 2, methodology using the mean weight percent values of copper and nickel of the surveillance material.
- (b) Calculated using measured Charpy data plotted using CVGRAPH, Version 4.1 (See Appendix C)
- (c) Values are based on the definition of upper shelf energy given in ASTM E185-82.
- (d) The fluence values presented here are the calculated fluence values, not the best estimate. For best estimate values see Section 6 of this report.

Table 5-11 Tensile Properties of the Diablo Canyon Unit 1 Capsule V Reactor Vessel Surveillance Materials Irradiated to 1.37×10^{19} n/cm² (E > 1.0 MeV)

Material	Sample Number	Test Temp. (°F)	0.2% Yield Strength (ksi)	Ultimate Strength (ksi)	Fracture Load (kip)	Fracture Stress (ksi)	Fracture Strength (ksi)	Uniform Elongation (%)	Total Elongation (%)	Reduction in Area (%)
Intermediate Shell Plate B4106-3 (Longitudinal)	E8	200	71.3	91.3	3.07	188.6	62.6	8.6	20.5	67
	E9	550	66.6	91.9	3.28	165.4	66.7	10.2	21.2	60
Weld Metal (heat # 27204)	W3	200	94.8	108.0	3.87	176.7	78.8	9.0	20.3	55
	W4	550	86.1	102.7	4.30	150.1	87.6	8.5	15.5	42

235340

INTERMEDIATE SHELL PLATE B4106-3 (LONG)

CVGRAPH 4.1 Hyperbolic Tangent Curve Printed at 11:21:33 on 08-19-2002

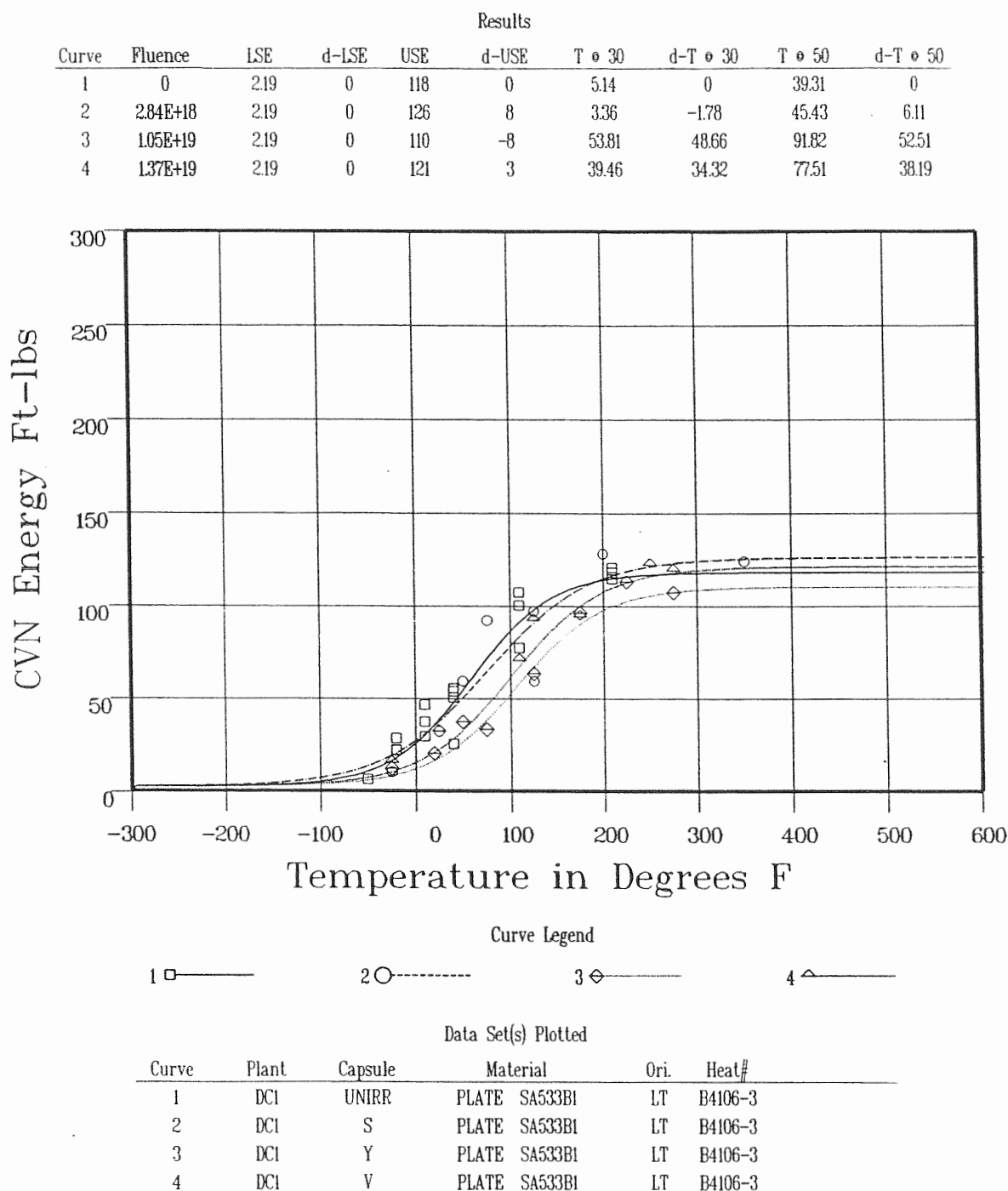


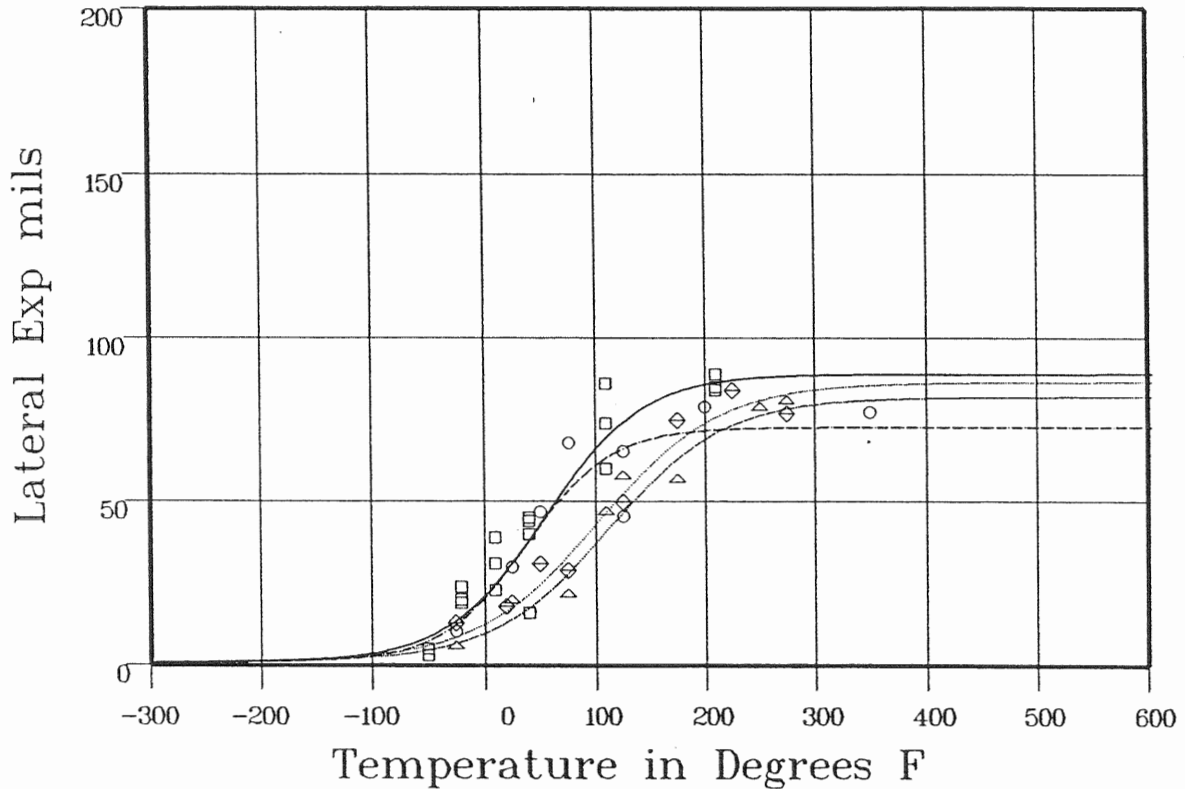
Figure 5-1 Charpy V-Notch Impact Energy vs. Temperature for Diablo Canyon Unit 1 Reactor Vessel Intermediate Shell Plate B4106-3 (Longitudinal Orientation)

INTERMEDIATE SHELL PLATE B4106-3 (LONG)

CVGRAPH 4.1 Hyperbolic Tangent Curve Printed at 11:38:29 on 08-19-2002

Results

Curve	Fluence	USE	d-USE	T σ LE35	d-T σ LE35
1	0	89.02	0	28.65	0
2	2.84E+18	72.72	-16.3	28.92	27
3	1.05E+19	86.52	-2.5	74.89	46.24
4	1.37E+19	81.97	-7.05	89.72	61.07



Curve Legend

1 \square ——— 2 \circ - - - - - 3 \diamond ——— 4 \triangle ———

Data Set(s) Plotted

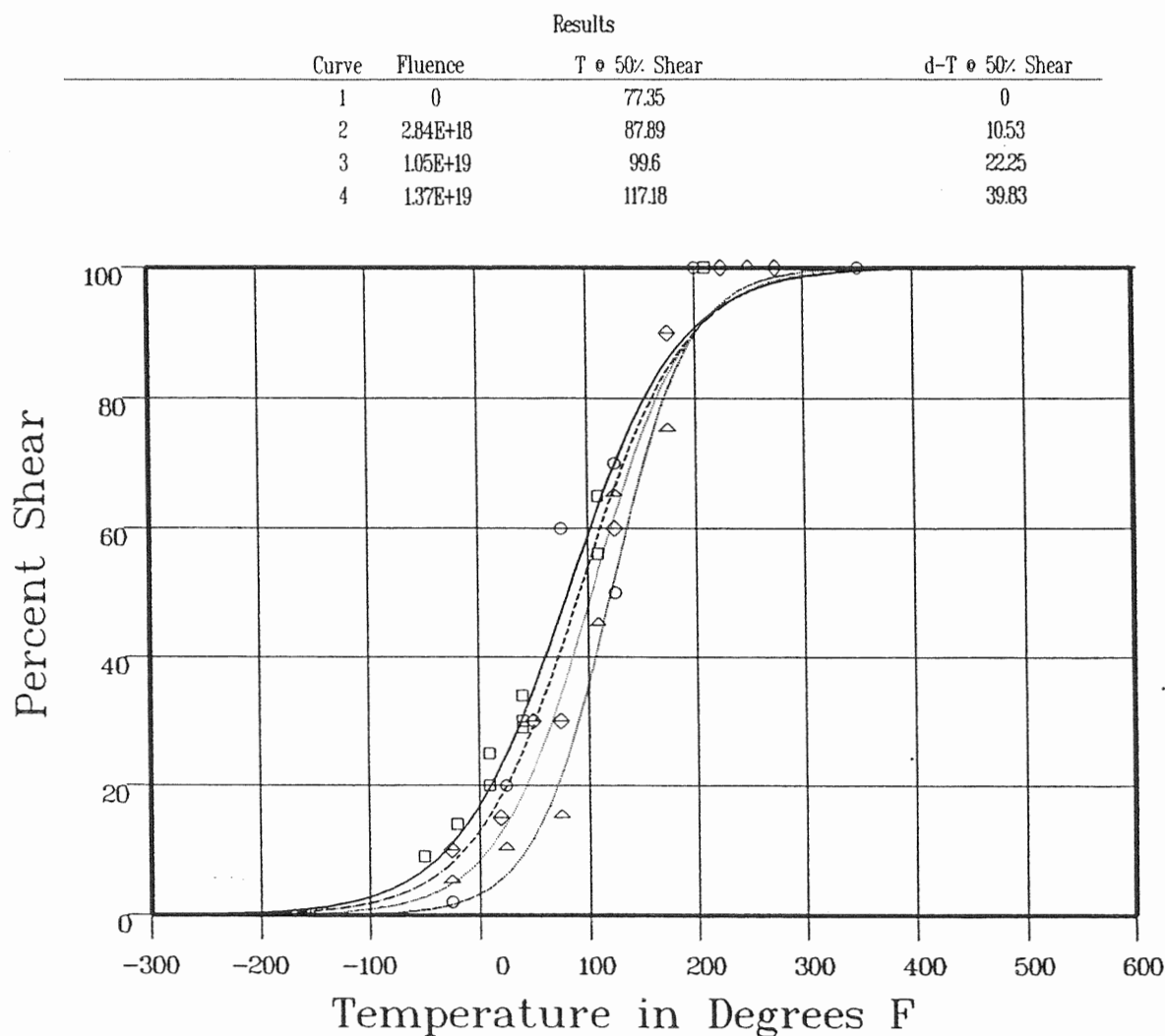
Curve	Plant	Capsule	Material	Ori.	Heat#
1	DC1	UNIRR	PLATE SA533B1	LT	B4106-3
2	DC1	S	PLATE SA533B1	LT	B4106-3
3	DC1	Y	PLATE SA533B1	LT	B4106-3
4	DC1	V	PLATE SA533B1	LT	B4106-3

Figure 5-2 Charpy V-Notch Lateral Expansion vs. Temperature for Diablo Canyon Unit 1 Reactor Vessel Intermediate Shell Plate B4106-3 (Longitudinal Orientation)

INTERMEDIATE SHELL PLATE B4106-3

CVGRAPH 41 Hyperbolic Tangent Curve Printed at 11:49:00 on 08-19-2002

236340



Curve Legend

1 \square ——— 2 \circ - - - - - 3 \diamond ——— 4 \triangle ———

Data Set(s) Plotted

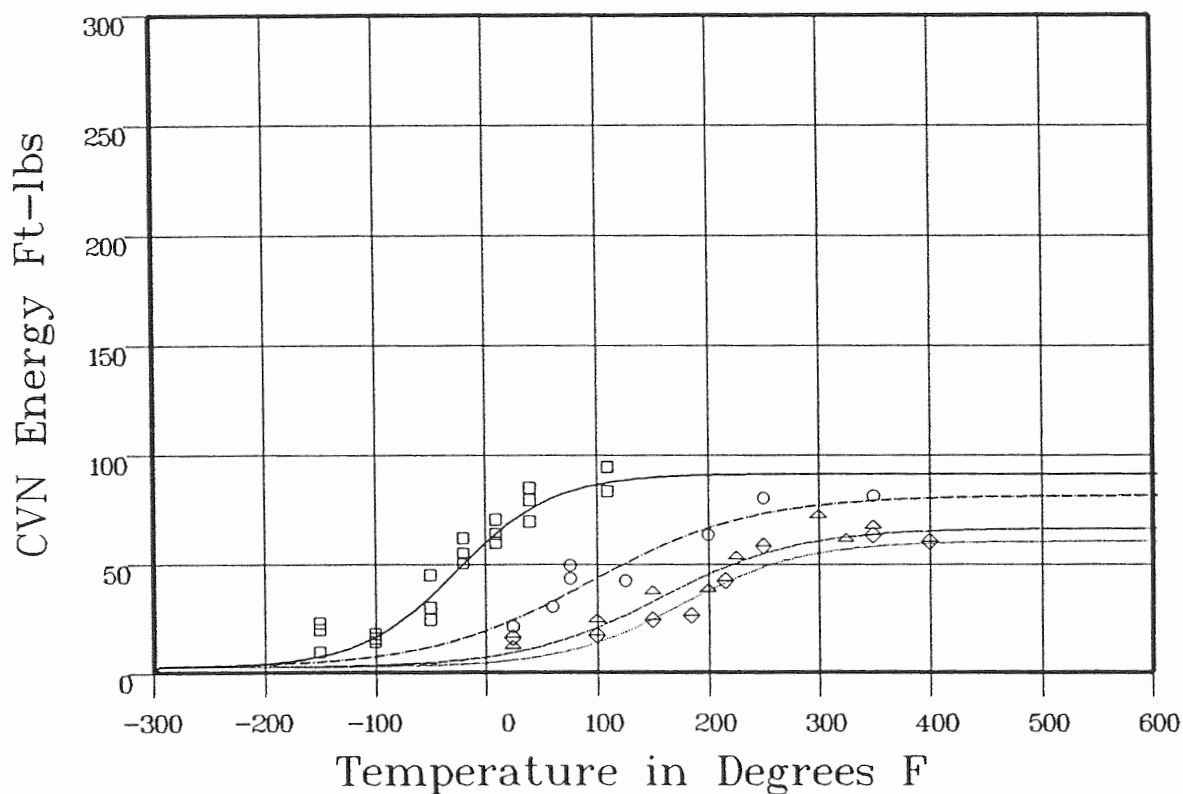
Curve	Plant	Capsule	Material	Ori.	Heat#
1	DCI	UNIRR	PLATE SA533B1	LT	B4106-3
2	DCI	S	PLATE SA533B1	LT	B4106-3
3	DCI	Y	PLATE SA533B1	LT	B4106-3
4	DCI	V	PLATE SA533B1	LT	B4106-3

Figure 5-3 Charpy V-Notch Percent Shear vs. Temperature for Diablo Canyon Unit 1 Reactor Vessel Intermediate Shell Plate B4106-3 (Longitudinal Orientation)

SURVEILLANCE WELD METAL

CVGRAPH 4.1 Hyperbolic Tangent Curve Printed at 12:20:17 on 08-19-2002

Curve	Fluence	Results							
		LSE	d-LSE	USE	d-USE	T σ 30	d-T σ 30	T σ 50	d-T σ 50
1	0	2.19	0	91	0	-65.62	0	-24.16	0
2	2.84E+18	2.19	0	81	-10	45.17	110.79	120.38	144.54
3	1.05E+19	2.2	0	60	-31	166.97	232.59	255.73	279.9
4	1.37E+19	2.19	0	66	-25	135.45	201.07	219.26	243.43



Curve Legend

1 \square ——— 2 \circ - - - - - 3 \diamond ——— 4 \triangle ———

Data Set(s) Plotted

Curve	Plant	Capsule	Material	Ori.	Heat#
1	DC1	UNIRR	WELD LINDE 1092	27204	FLUX LOT 3714
2	DC1	S	WELD LINDE 1092	27204	FLUX LOT 3714
3	DC1	Y	WELD LINDE 1092	27204	FLUX LOT 3714
4	DC1	V	WELD LINDE 1092	27204	FLUX LOT 3714

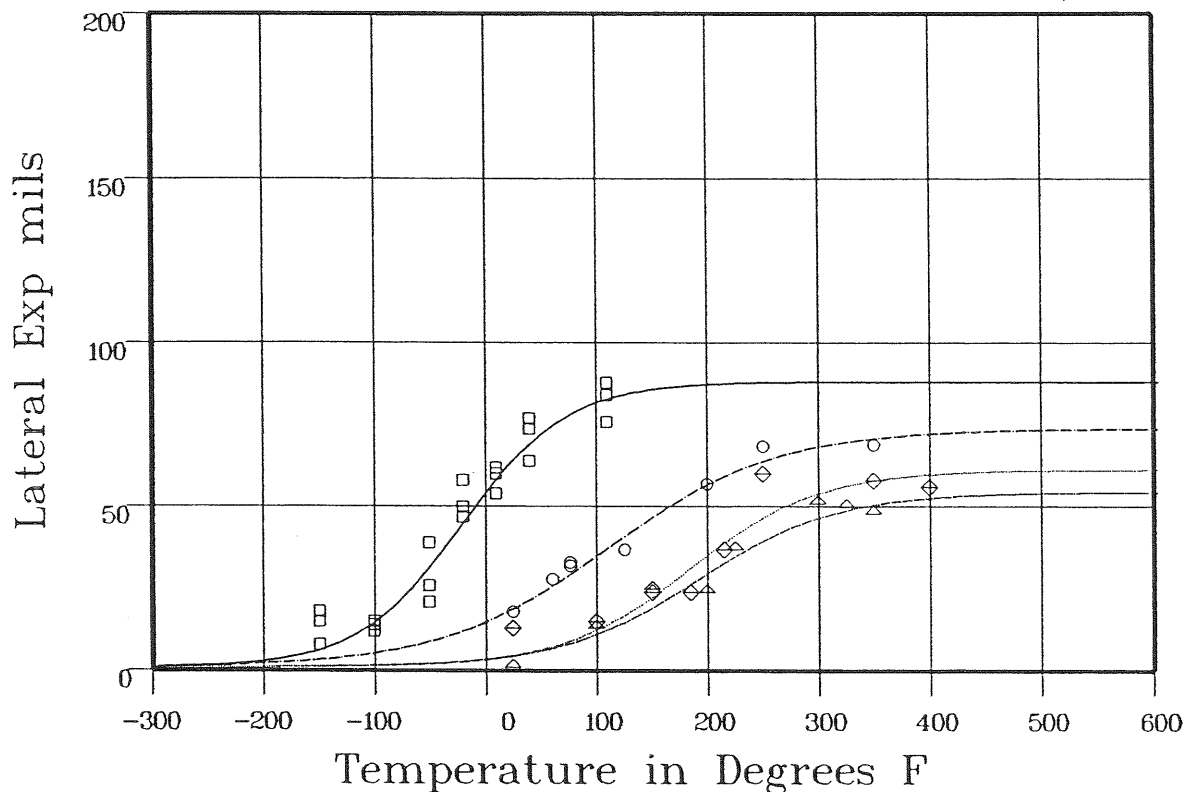
Figure 5-4 Charpy V-Notch Impact Energy vs. Temperature for Diablo Canyon Unit 1 Reactor Vessel Weld Metal

SURVEILLANCE PROGRAM WELD METAL

CVGRAPH 41 Hyperbolic Tangent Curve Printed at 123039 on 08-19-2002

Results

Curve	Fluence	USE	d-USE	T σ LE35	d-T σ LE35
1	0	88.17	0	-46.52	0
2	2.84E+18	73.91	-14.25	95.28	141.81
3	1.05E+19	61.24	-26.93	194.25	240.77
4	1.37E+19	54.47	-33.7	220.66	267.19



Curve Legend

1 \square ——— 2 \circ - - - - - 3 \diamond ——— 4 \triangle ———

Data Set(s) Plotted

Curve	Plant	Capsule	Material	Ori.	Heat#
1	DCI	UNIRR	WELD LINDE 1092	27204 FLUX LOT 3714	
2	DCI	S	WELD LINDE 1092	27204 FLUX LOT 3714	
3	DCI	Y	WELD LINDE 1092	27204 FLUX LOT 3714	
4	DCI	V	WELD LINDE 1092	27204 FLUX LOT 3714	

Figure 5-5 Charpy V-Notch Lateral Expansion vs. Temperature for Diablo Canyon Unit 1 Reactor Vessel Weld Metal

SURVEILLANCE PROGRAM WELD METAL

CVGRAPH 4.1 Hyperbolic Tangent Curve Printed at 12:44:50 on 08-19-2002

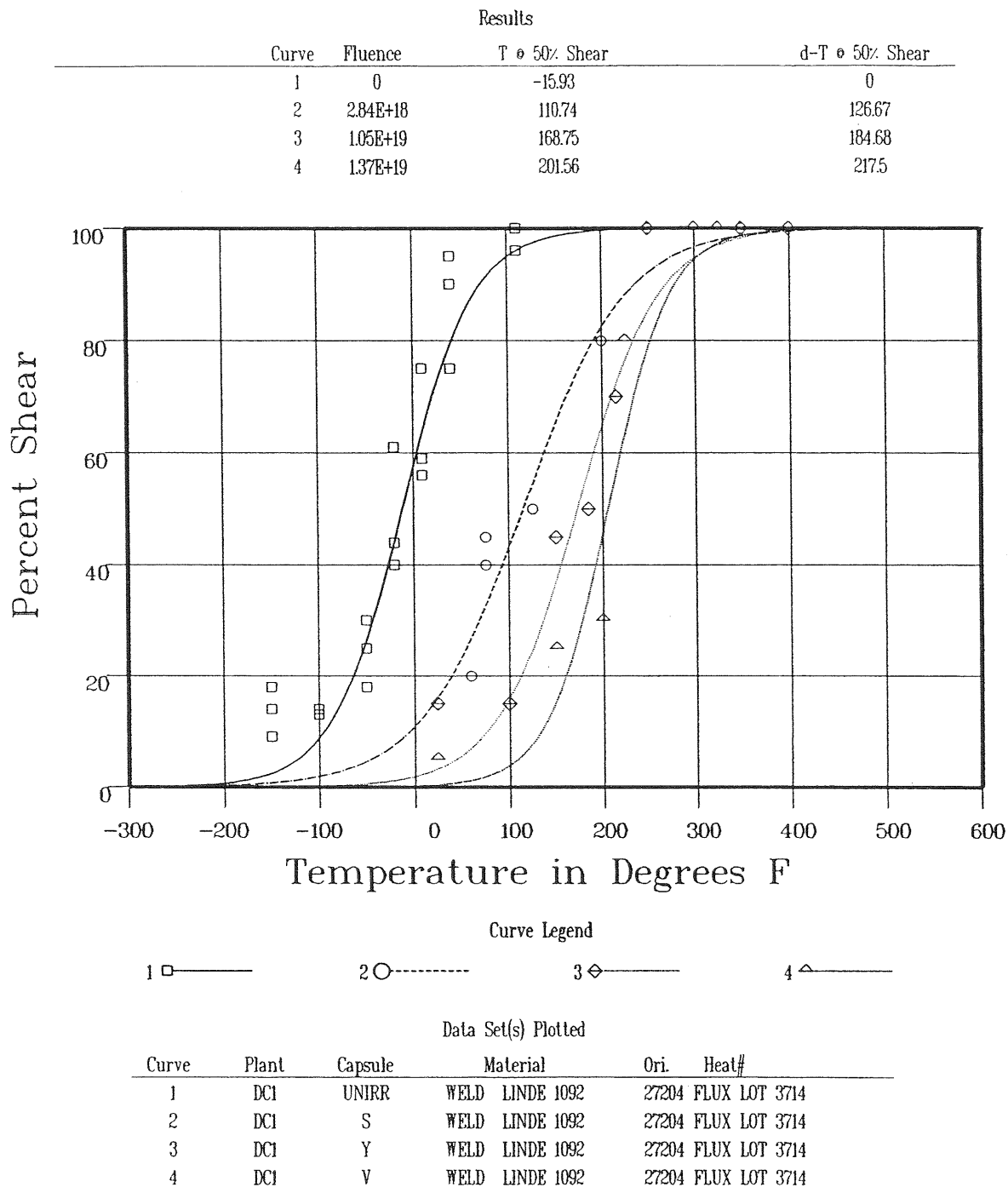


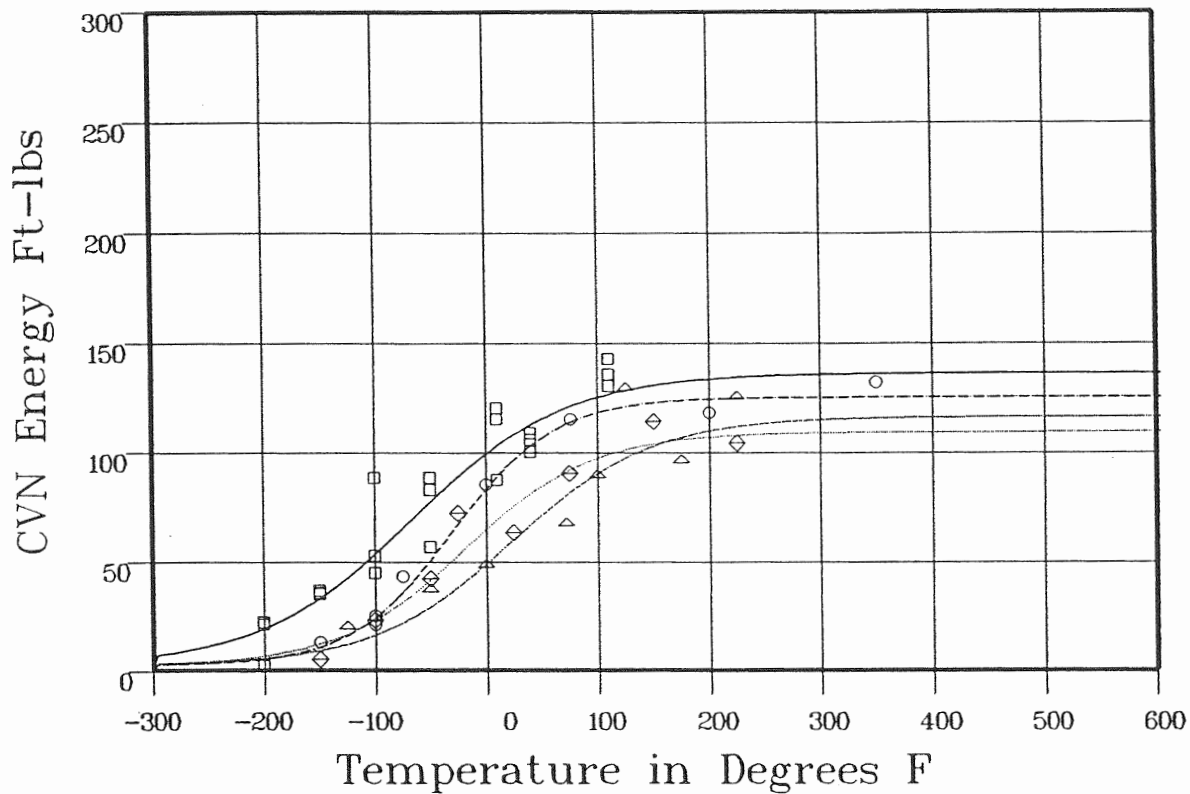
Figure 5-6 Charpy V-Notch Percent Shear vs Temperature for Diablo Canyon Unit 1 Reactor Vessel Weld Metal

HEAT AFFECTED ZONE

CVGRAPH 4J Hyperbolic Tangent Curve Printed at 13:33:29 on 08-19-2002

Results

Curve	Fluence	LSE	d-LSE	USE	d-USE	T @ 30	d-T @ 30	T @ 50	d-T @ 50
1	0	2.19	0	136	0	-163.55	0	-111.75	0
2	2.84E+18	2.19	0	125	-11	-91.24	72.31	-55.29	56.46
3	1.05E+19	2.19	0	109	-27	-83.77	79.77	-35.96	75.78
4	1.37E+19	2.19	0	116	-20	-52.65	110.9	-1.98	109.77



Curve Legend

1 \square ——— 2 \circ - - - - - 3 \diamond ——— 4 \triangle ———

Data Set(s) Plotted

Curve	Plant	Capsule	Material	Ori.	Heat#
1	DCI	UNIRR	HEAT AFFD ZONE		
2	DCI	S	HEAT AFFD ZONE		
3	DCI	Y	HEAT AFFD ZONE		
4	DCI	V	HEAT AFFD ZONE		

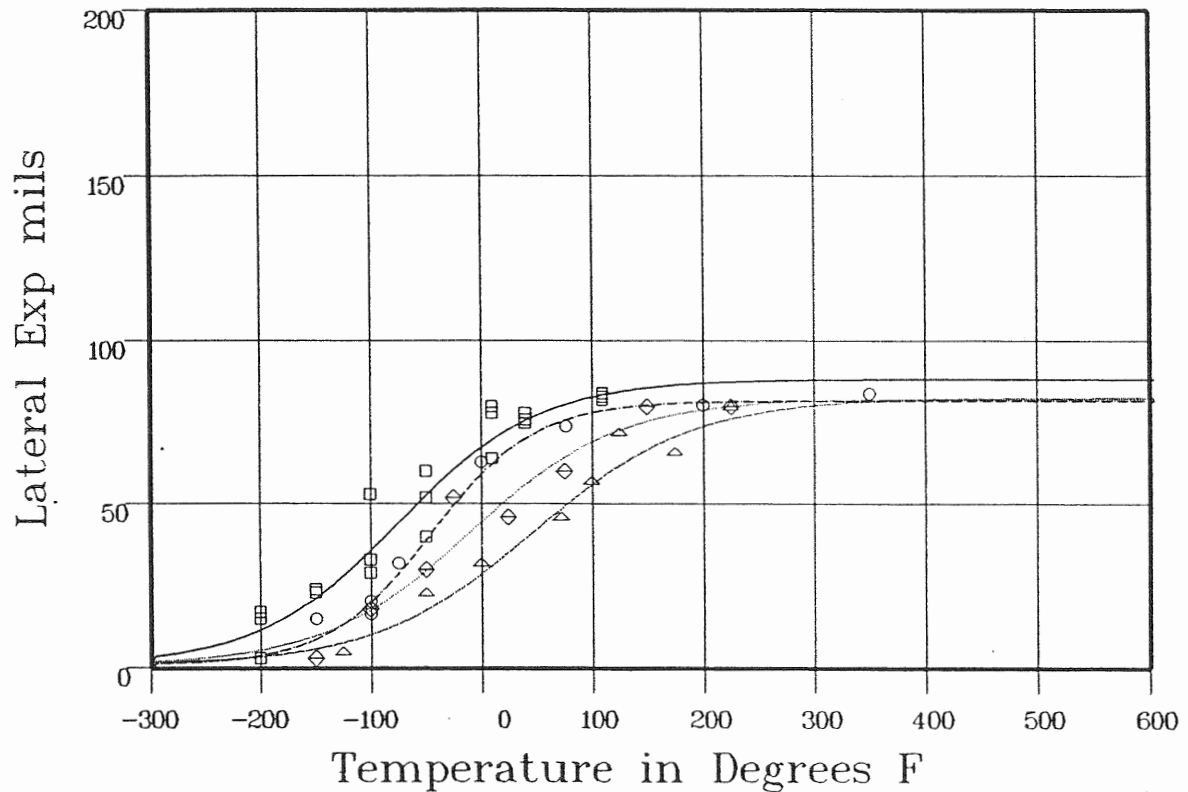
Figure 5-7 Charpy V-Notch Impact Energy vs. Temperature for Diablo Canyon Unit 1 Reactor Vessel Heat-Affected-Zone Material

HEAT AFFECTED ZONE

CVGRAPH 4.1 Hyperbolic Tangent Curve Printed at 14:27:03 on 08-19-2002

Results

Curve	Fluence	USE	d-USE	T ϕ LE35	d-T ϕ LE35
1	0	88.3	0	-107.5	0
2	2.84E+18	81.74	-6.56	-64.26	43.24
3	1.05E+19	82.45	-5.85	-36.47	71.03
4	1.37E+19	82.69	-5.61	18.76	126.27



Curve Legend

1 \square ——— 2 \circ - - - - - 3 \diamond ——— 4 \triangle ———

Data Set(s) Plotted

Curve	Plant	Capsule	Material	Ori.	Heat#
1	DC1	UNIRR	HEAT AFFD ZONE		
2	DC1	S	HEAT AFFD ZONE		
3	DC1	Y	HEAT AFFD ZONE		
4	DC1	V	HEAT AFFD ZONE		

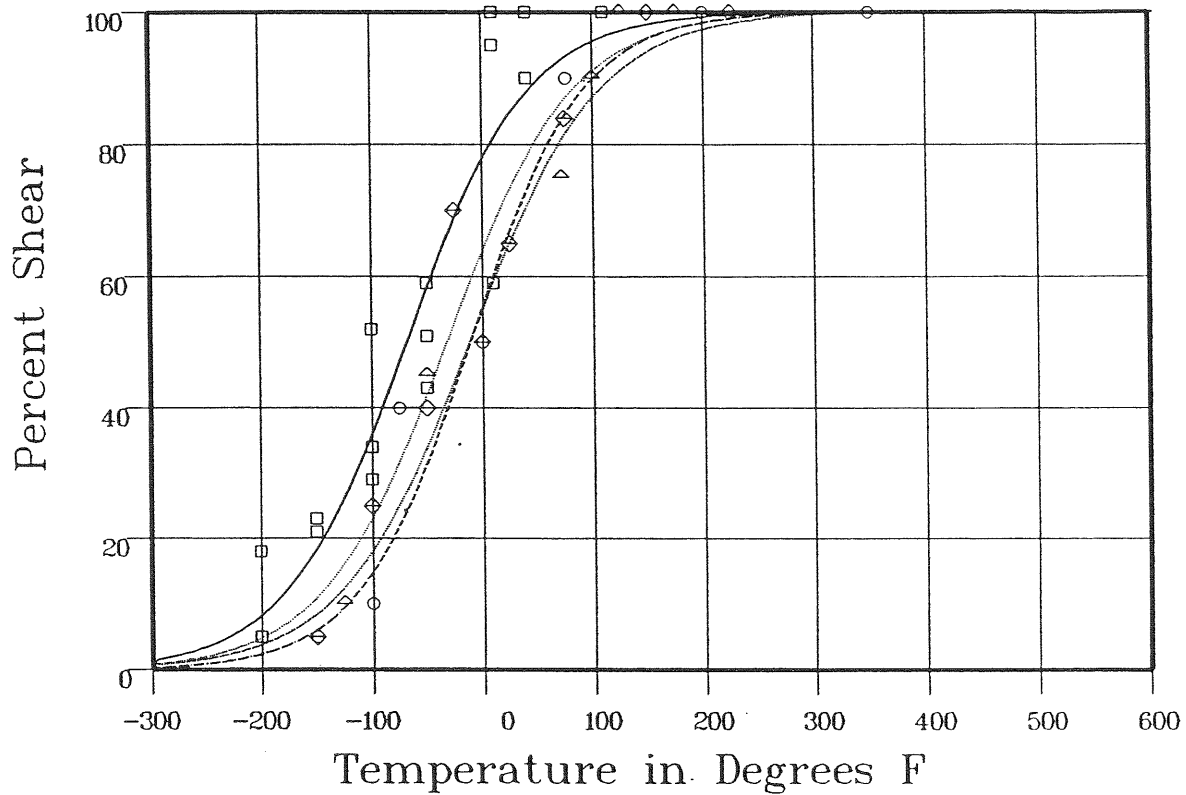
Figure 5-8 Charpy V-Notch Lateral Expansion vs. Temperature for Diablo Canyon Unit 1 Reactor Vessel Heat-Affected-Zone Material

HEAT AFFECTED ZONE

CVGRAPH 4.1 Hyperbolic Tangent Curve Printed at 14:01:24 on 09-03-2002

Results

Curve	Fluence	T @ 50% Shear	d-T @ 50% Shear
1	0	-72.94	0
2	2.84E+18	-15.46	57.47
3	1.05E+19	-36.27	36.66
4	1.37E+19	-15.93	57



Curve Legend

1 \square ——— 2 \circ - - - - - 3 \diamond ——— 4 \triangle ———

Data Set(s) Plotted

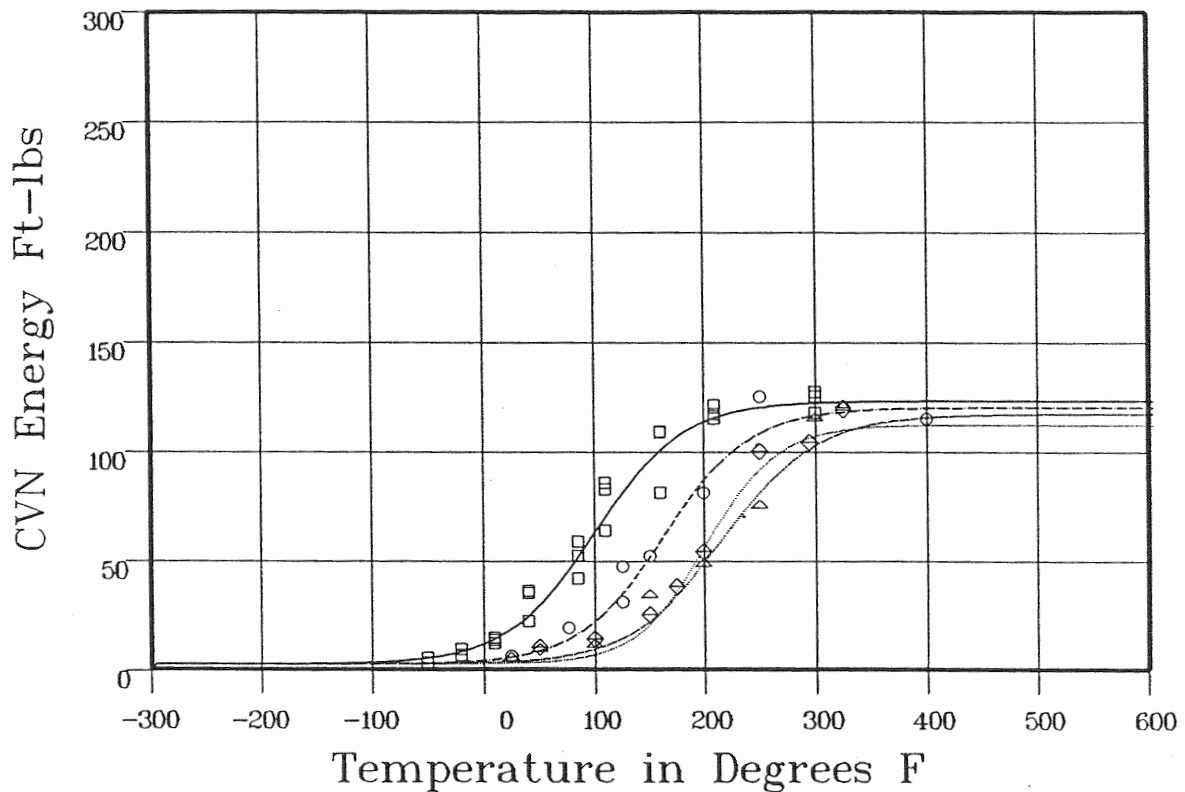
Curve	Plant	Capsule	Material	Ori.	Heat#
1	DCI	UNIRR	HEAT AFF'D ZONE		
2	DCI	S	HEAT AFF'D ZONE		
3	DCI	Y	HEAT AFF'D ZONE		
4	DCI	V	HEAT AFF'D ZONE		

Figure 5-9 Charpy V-Notch Percent Shear vs. Temperature for Diablo Canyon Unit 1 Reactor Vessel Heat-Affected-Zone Material

STANDARD REFERENCE MATERIAL

CVGRAPH 4J Hyperbolic Tangent Curve Printed at 11:05:06 on 09-06-2002

Curve	Fluence	LSE	d-LSE	USE	Results				
					d-USE	T @ 30	d-T @ 30	T @ 50	d-T @ 50
1	0	2.19	0	123	0	46.44	0	78.3	0
2	2.84E+18	2.19	0	120	-3	112.06	65.62	143.42	65.11
3	1.05E+19	2.19	0	112	-11	162.23	115.79	188.9	110.59
4	1.37E+19	2.19	0	117	-6	163.05	116.61	197.42	119.12



Curve Legend

1 \square ——— 2 \circ - - - - - 3 \diamond ——— 4 \triangle ———

Data Set(s) Plotted					
Curve	Plant	Capsule	Material	Ori.	Heat#
1	DC1	UNIRR	SRM SA533B1	LT	
2	DC1	S	SRM SA533B1	LT	
3	DC1	Y	SRM SA533B1	LT	
4	DC1	V	SRM SA533B1	LT	

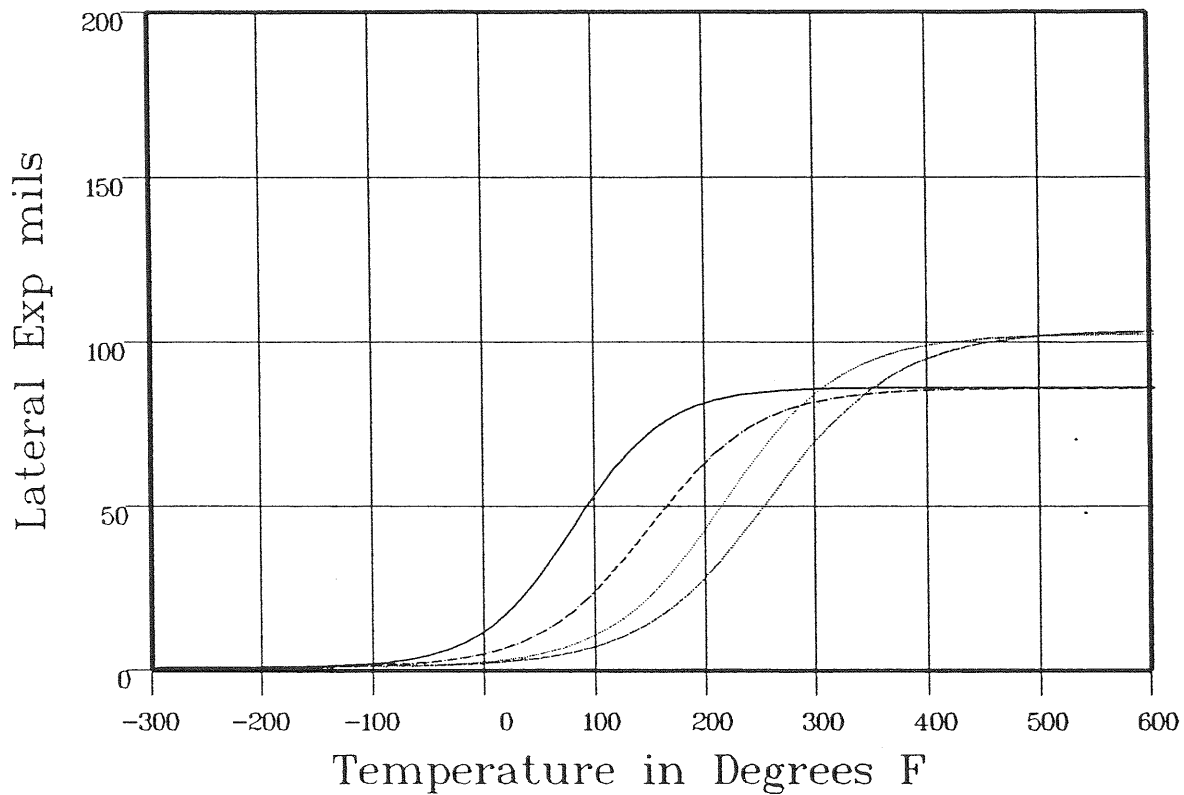
Figure 5-10 Charpy V-Notch Impact Energy vs. Temperature for Diablo Canyon Unit 1 Reactor Vessel Correlation Monitor Material

STANDARD REFERENCE MATERIAL

CVGRAPH 41 Hyperbolic Tangent Curve Printed at 11:09:33 on 09-06-2002

Results

Curve	Fluence	USE	d-USE	T @ LE35	d-T @ LE35
1	0	86.31	0	58.96	0
2	2.84E+18	85.97	-34	124.49	65.53
3	1.05E+19	102.39	16.07	178.01	119.05
4	1.37E+19	103.54	17.23	213.46	154.49



Curve Legend

1 \square ——— 2 \circ - - - - - 3 \diamond ——— 4 \triangle ———

Data Set(s) Plotted

Curve	Plant	Capsule	Material	Ori.	Heat#
1	DCI	UNIRR	SRM SA533B1	LT	
2	DCI	S	SRM SA533B1	LT	
3	DCI	Y	SRM SA533B1	LT	
4	DCI	V	SRM SA533B1	LT	

Figure 5-11 Charpy V-Notch Lateral Expansion vs. Temperature for Diablo Canyon Unit 1 Reactor Vessel Correlation Monitor Material

STANDARD REFERENCE MATERIAL

CVGRAPH 4.1 Hyperbolic Tangent Curve Printed at 11:15:09 on 09-06-2002

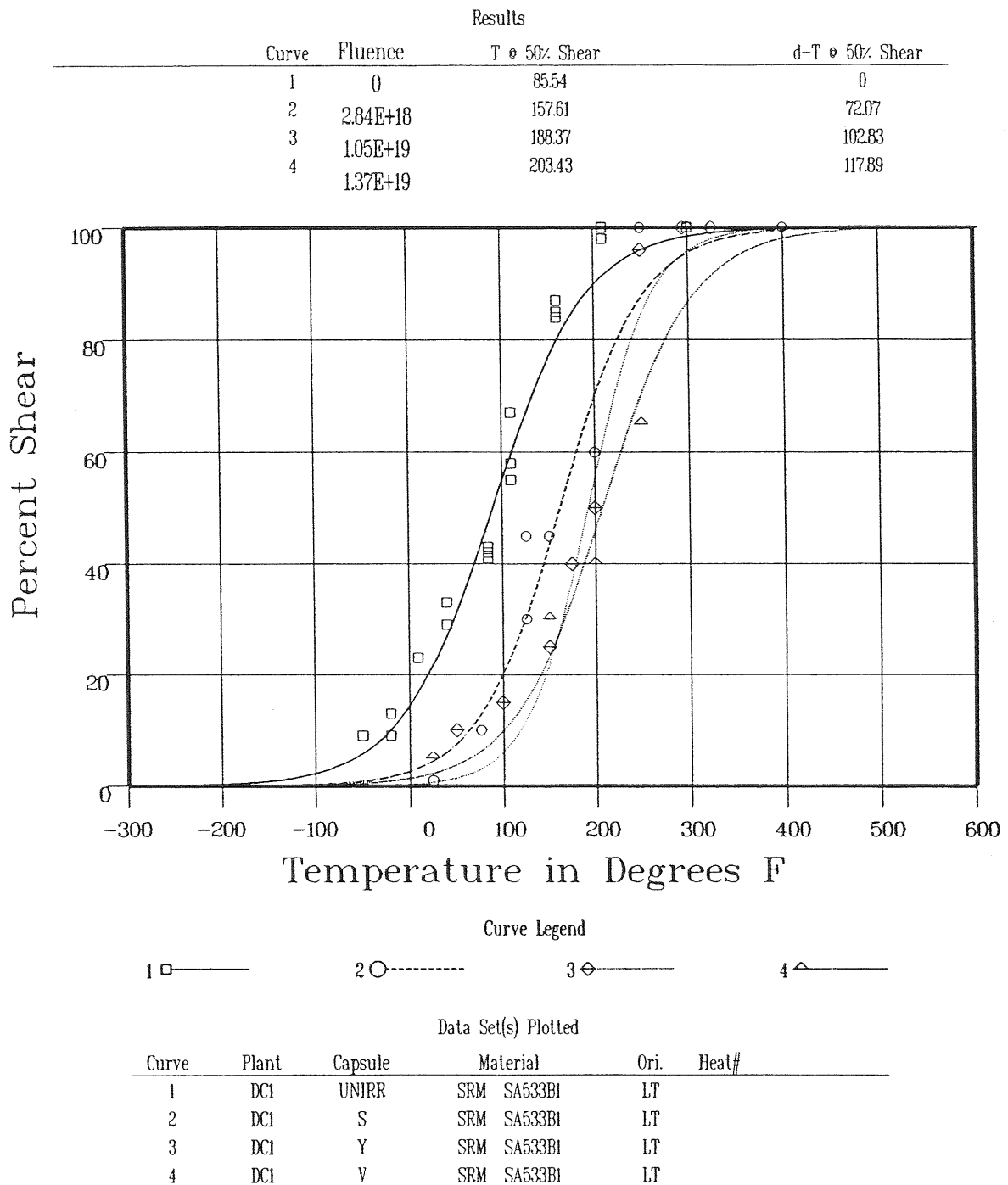


Figure 5-12 Charpy V-Notch Percent Shear vs. Temperature for Diablo Canyon Unit 1 Reactor Vessel Correlation Monitor Material

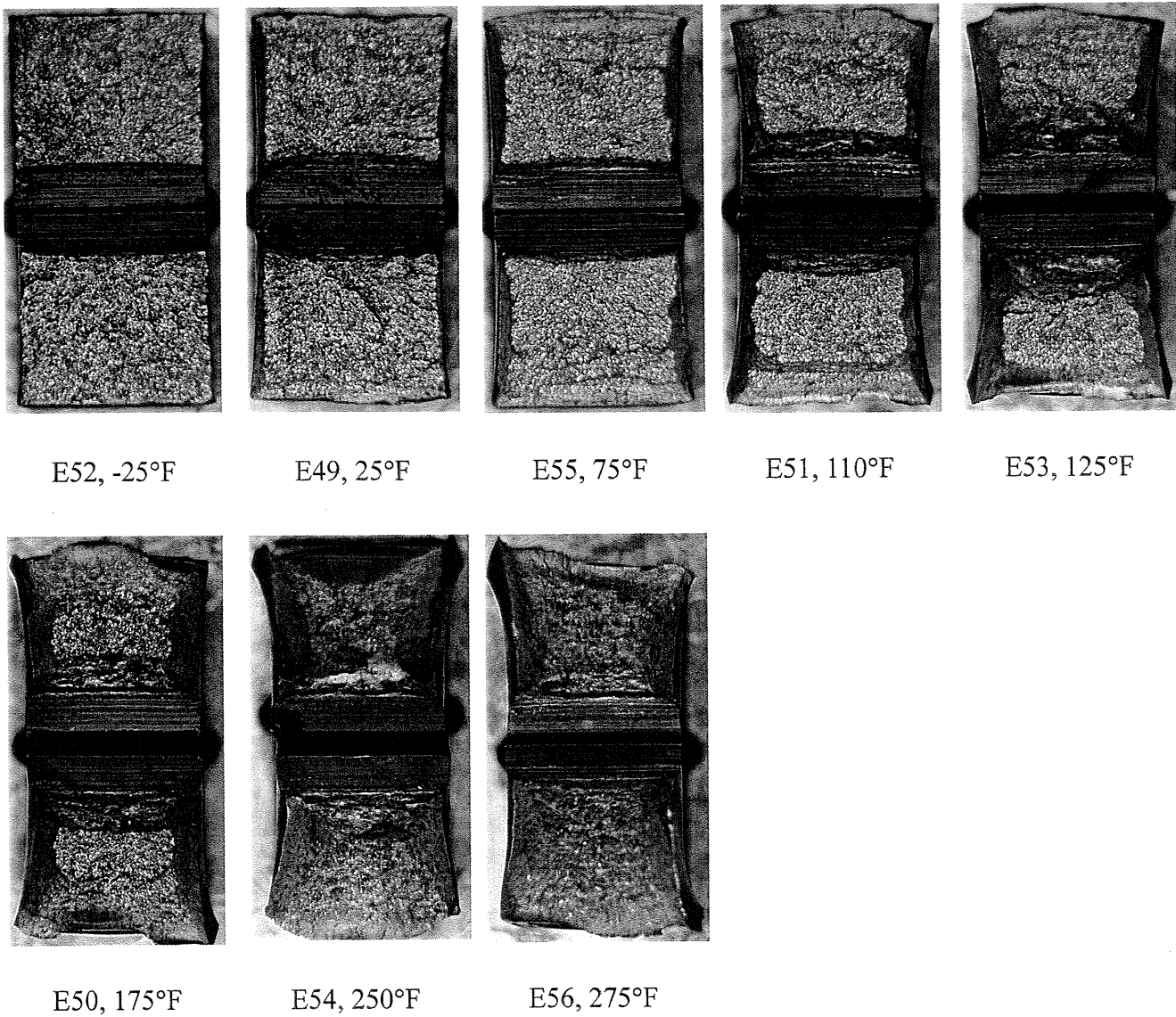


Figure 5-13 Charpy Impact Specimen Fracture Surfaces for Diablo Canyon Unit 1 Reactor Vessel Intermediate Shell Plate B4106-3 (Longitudinal Orientation)

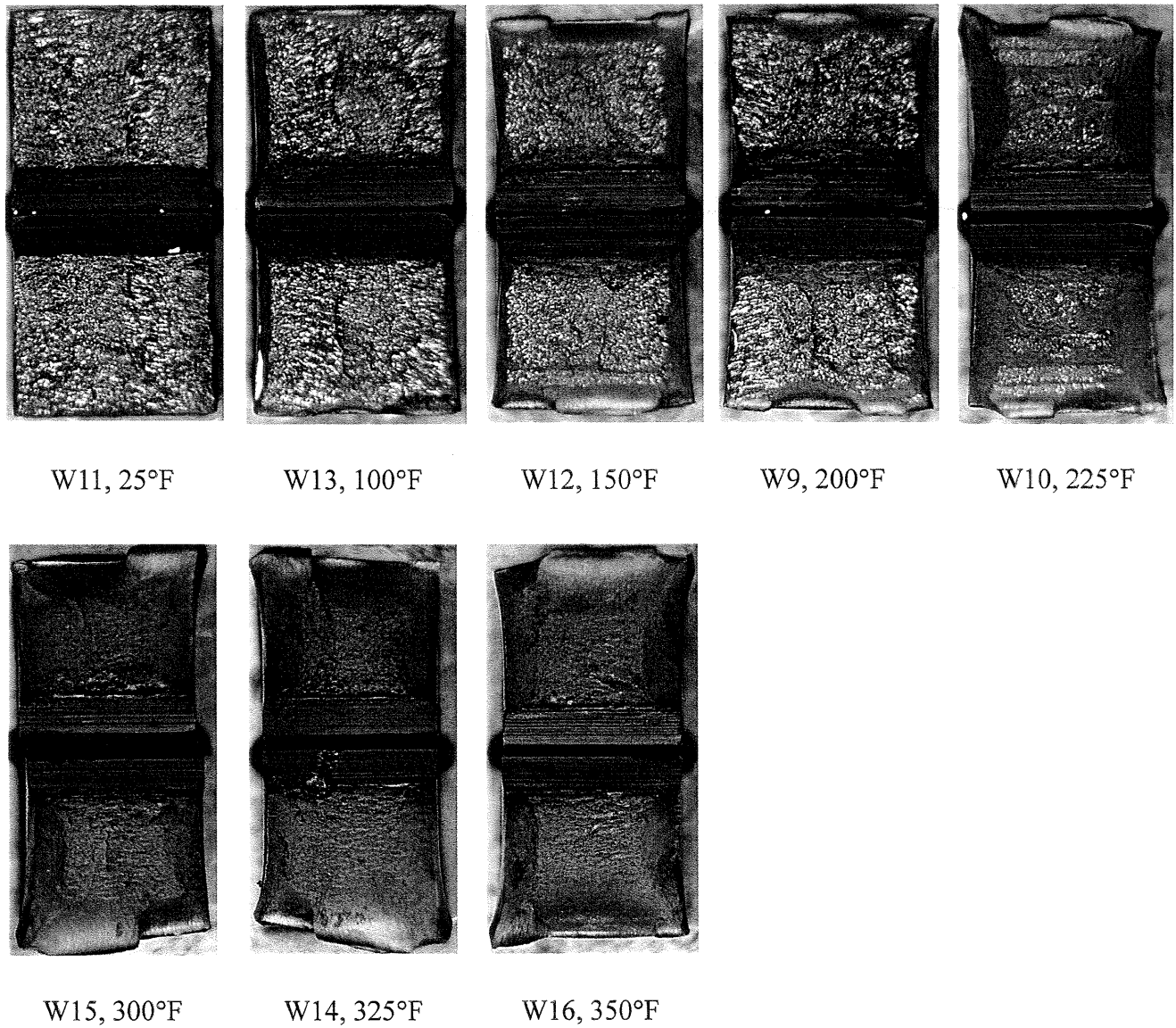
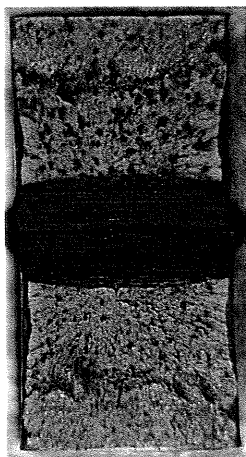
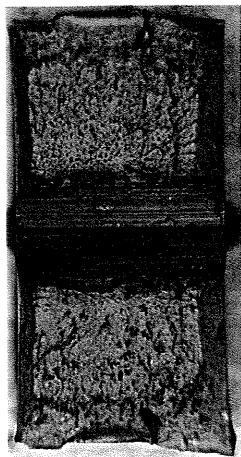


Figure 5-14 Charpy Impact Specimen Fracture Surfaces for Diablo Canyon Unit 1 Reactor Vessel Weld Metal



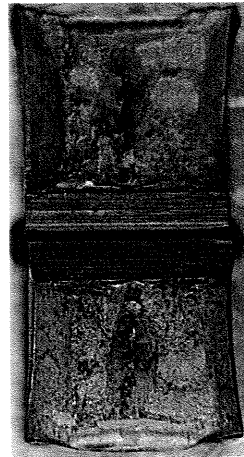
H14, -125°F



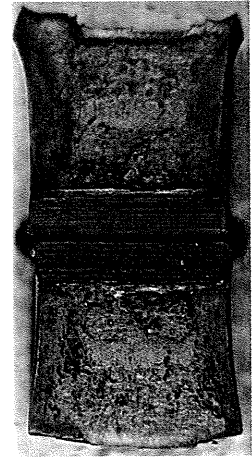
H12, -50°F



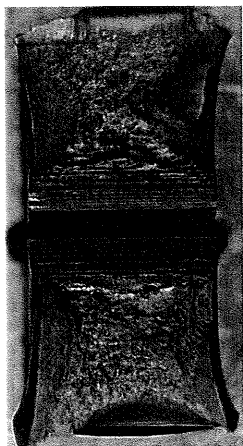
H11, 0°F



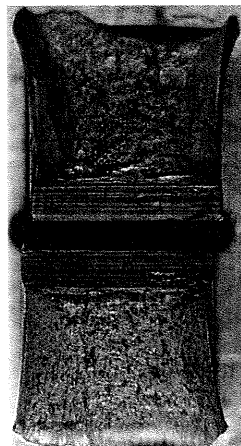
H10, 72°F



H9, 100°F



H15, 125°F



H16, 175°F



H13, 225°F

Figure 5-15 Charpy Impact Specimen Fracture Surfaces for Diablo Canyon Unit 1 Reactor Vessel Heat-Affected-Zone Metal

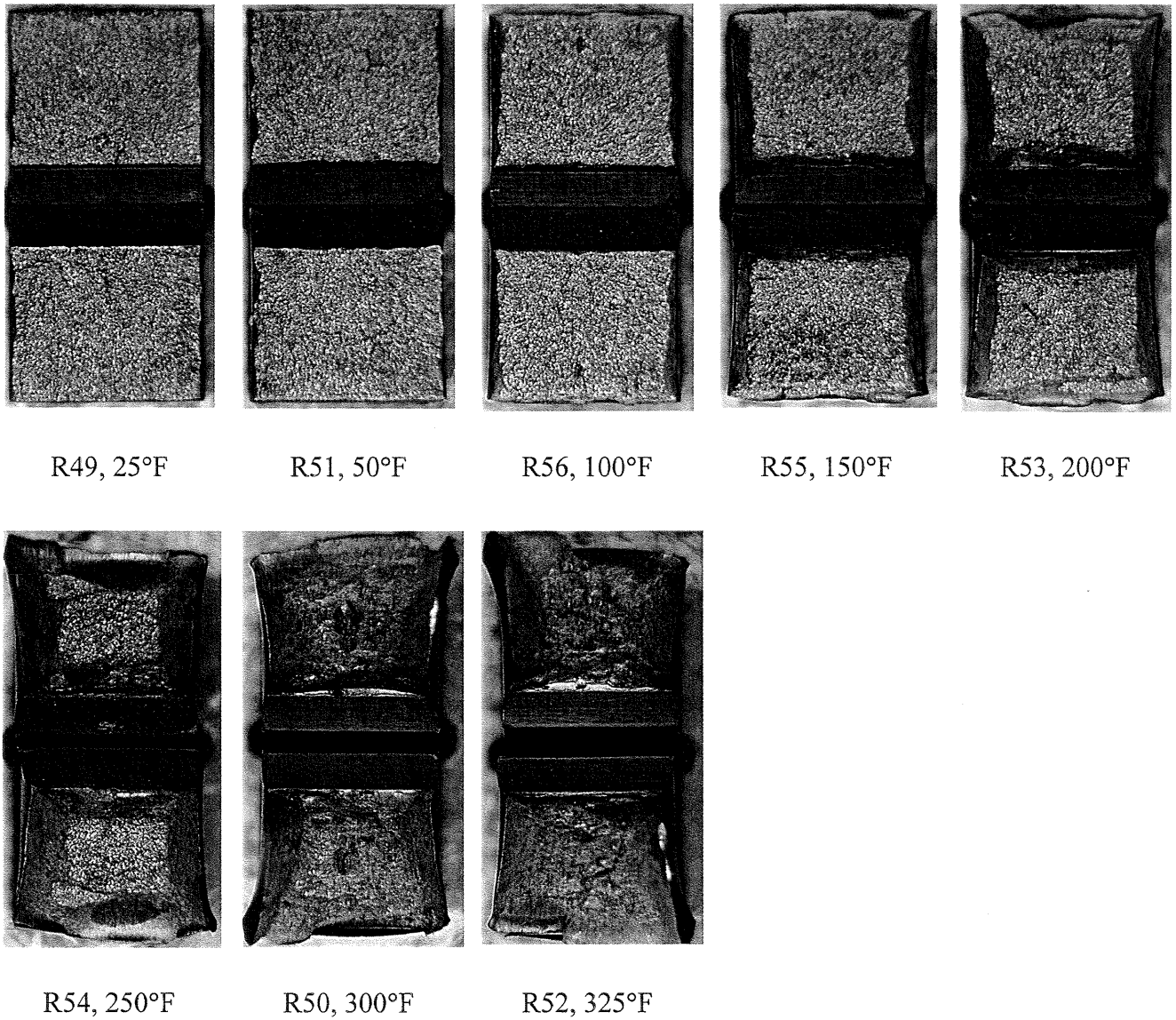


Figure 5-16 Charpy Impact Specimen Fracture Surfaces for Diablo Canyon Unit 1 Reactor Vessel Correlation Monitor Material

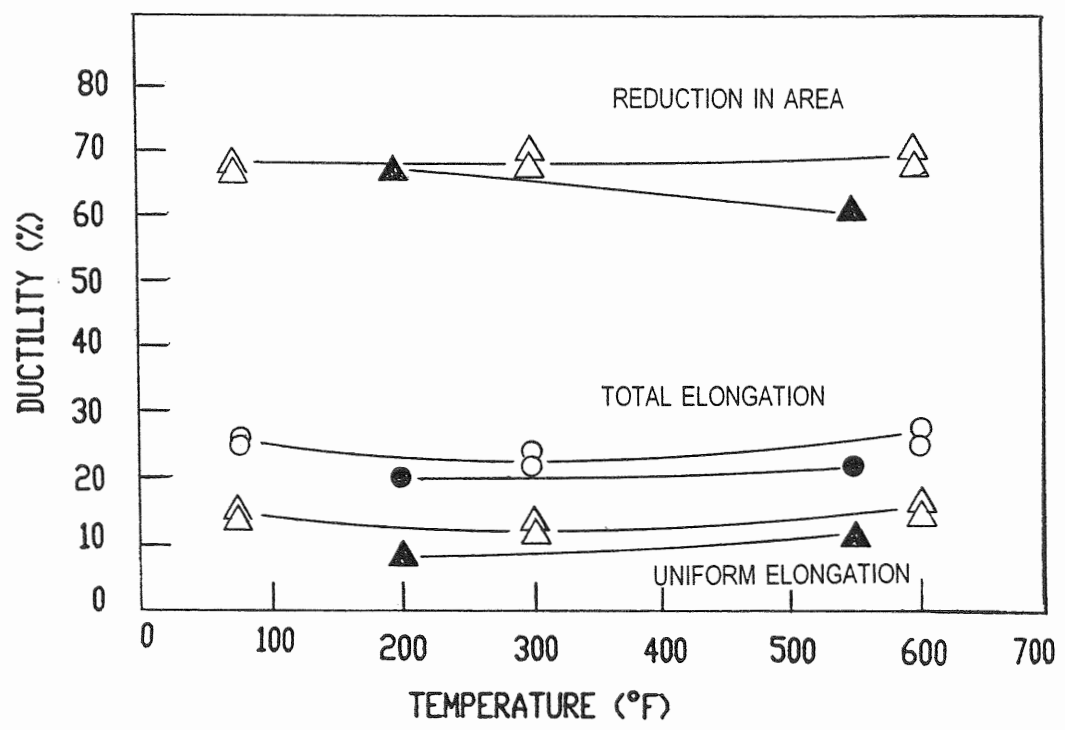
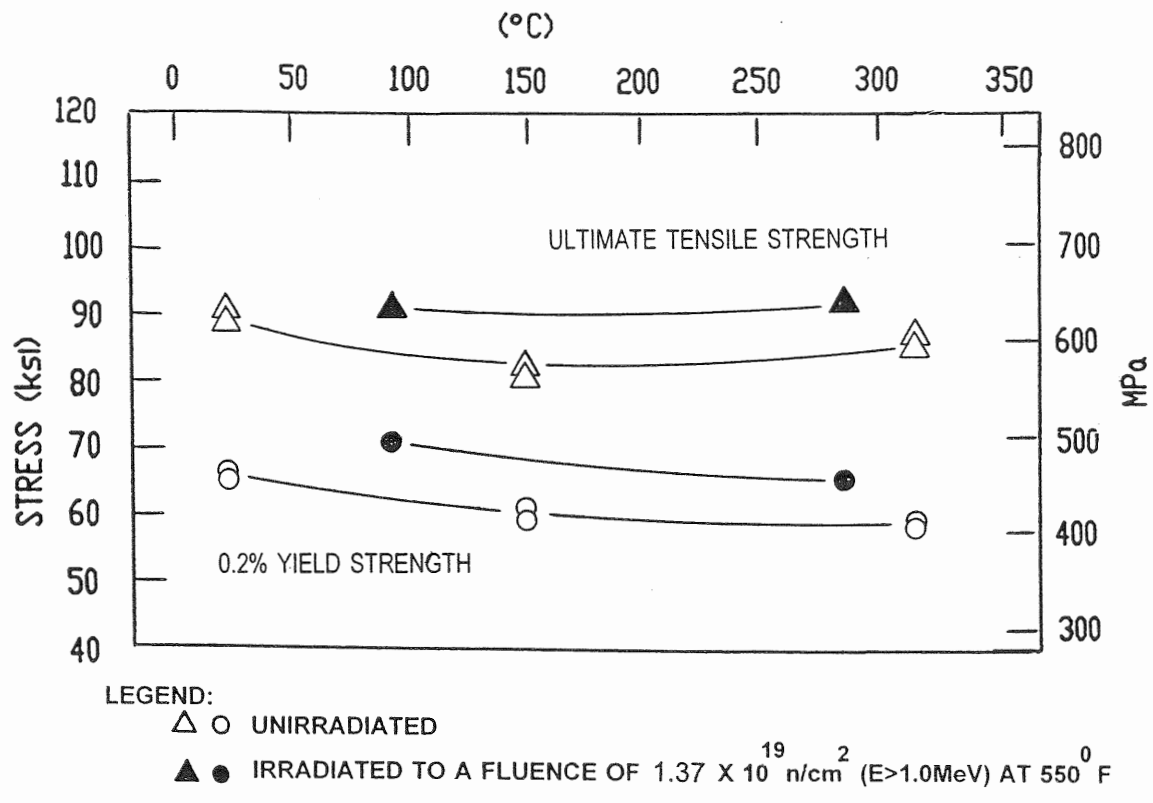


Figure 5-17 Tensile Properties for Diablo Canyon Unit 1 Reactor Vessel Intermediate Shell Plate B4106-3 (Longitudinal Orientation)

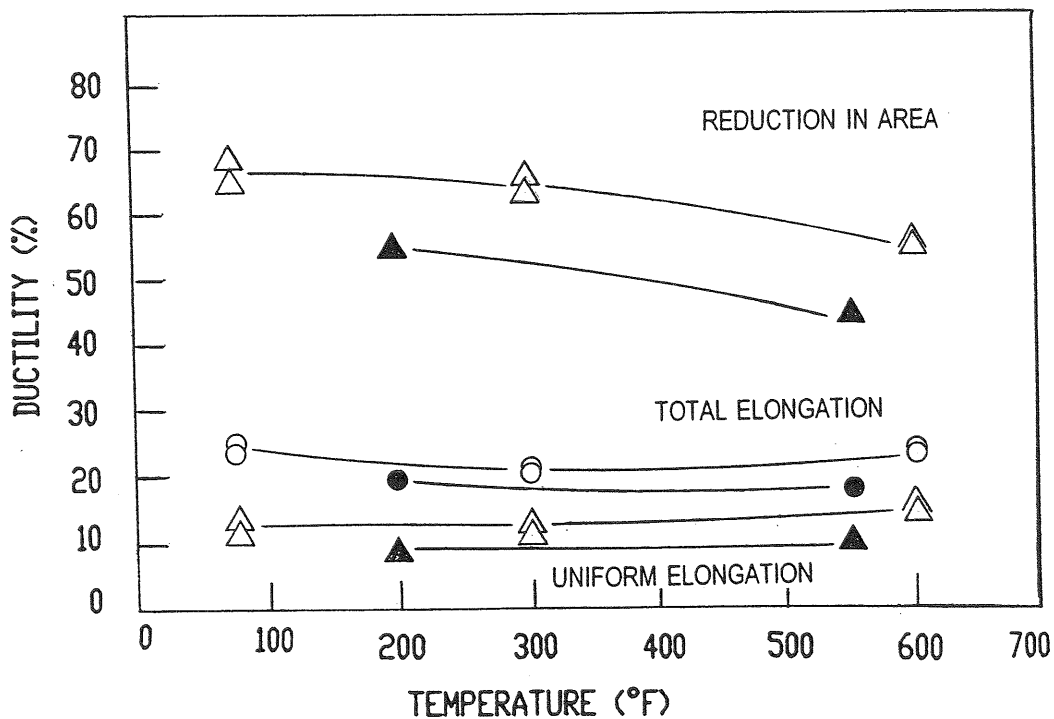
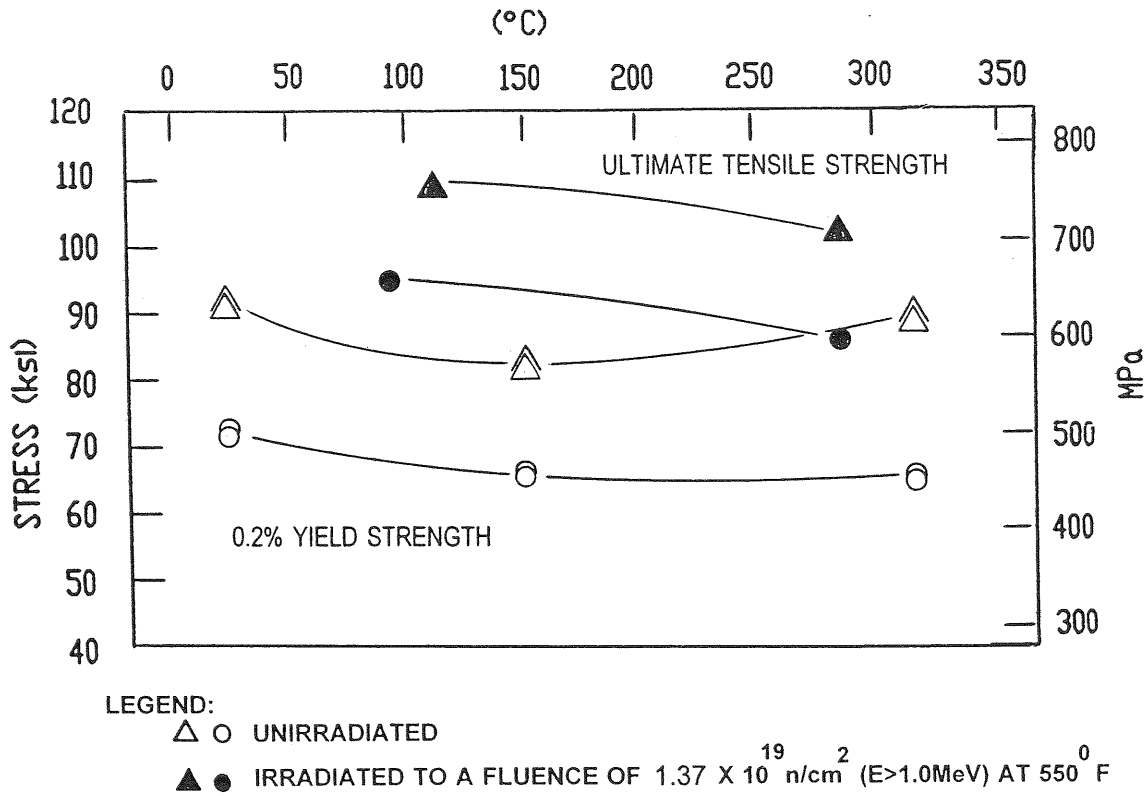
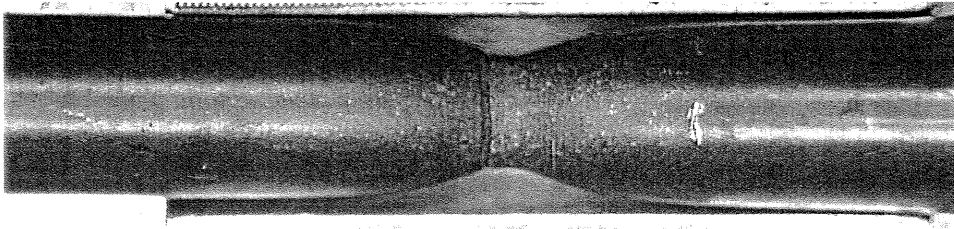
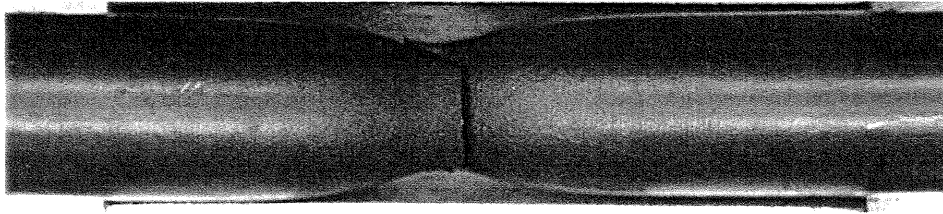


Figure 5-18 Tensile Properties for Diablo Canyon Unit 1 Reactor Vessel Weld Metal

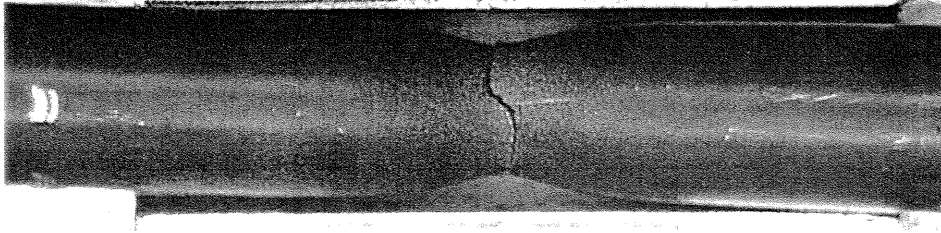


Specimen E8 Tested at 200°F



Specimen E9 Tested at 550°F

Figure 5-19 Fractured Tensile Specimens from Diablo Canyon Unit 1 Reactor Vessel Intermediate Shell Plate B4106-3 (Longitudinal Orientation)



Specimen W3 Tested at 200°F



Specimen W4 Tested at 550°F

Figure 5-20 Fractured Tensile Specimens from Diablo Canyon Unit 1 Reactor Vessel Weld Metal

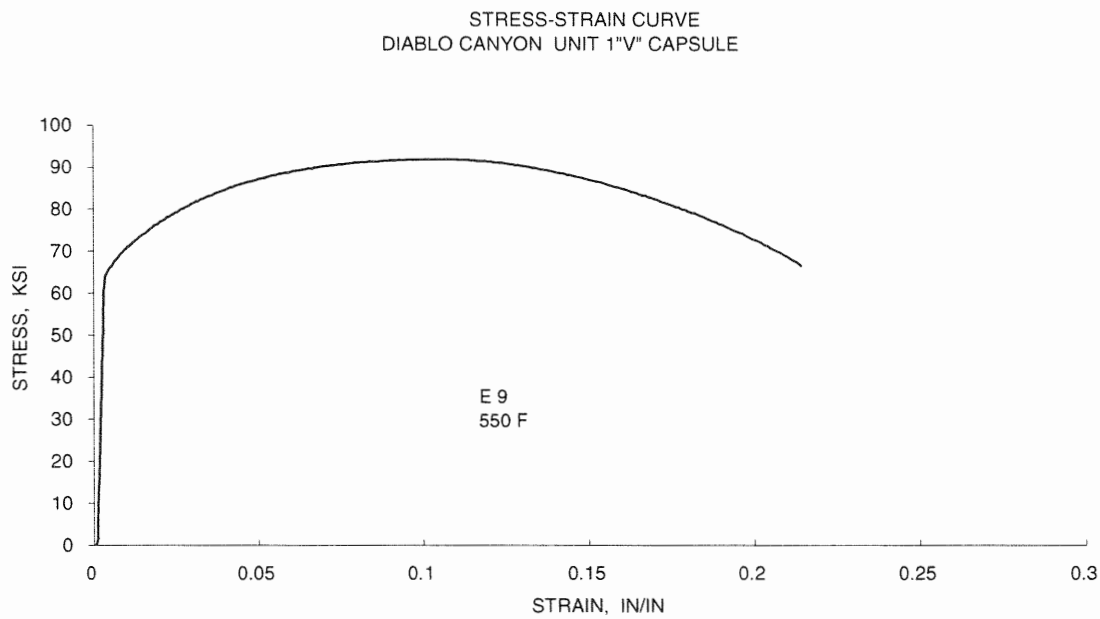
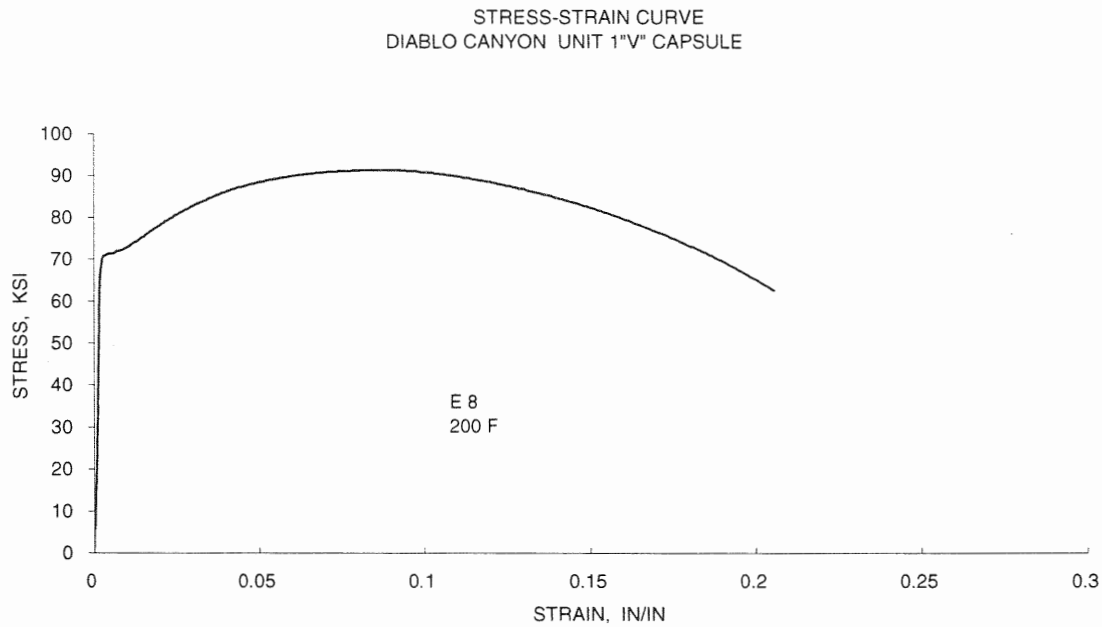


Figure 5-21 Engineering Stress-Strain Curves for Diablo Canyon Unit 1 Intermediate Shell Plate B4106-3 Tensile Specimens E8 and E9 (Longitudinal Orientation)

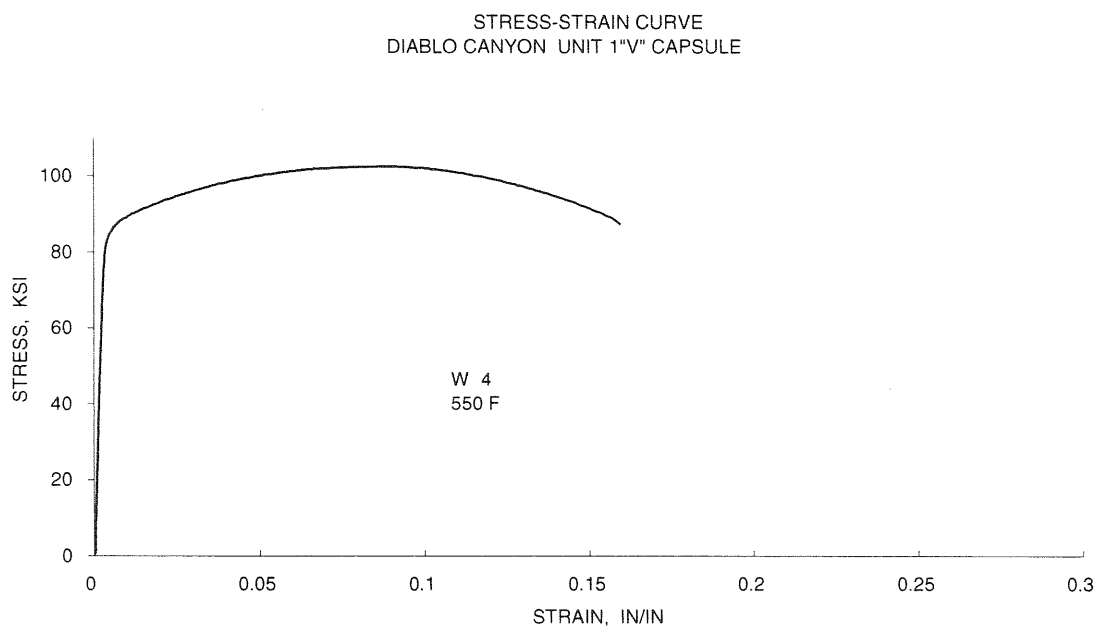
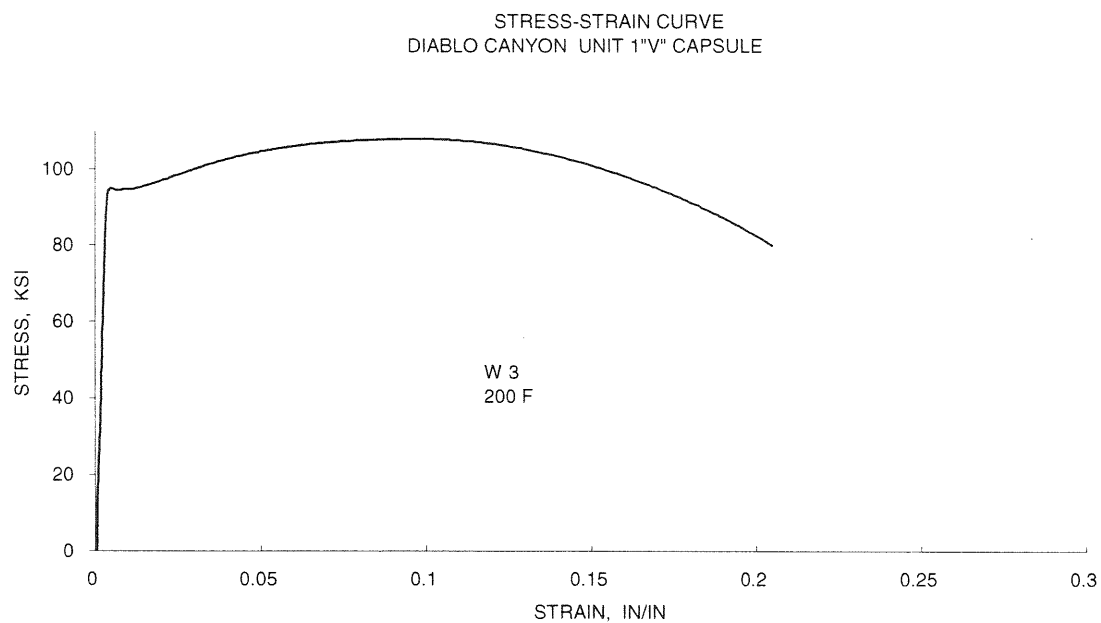


Figure 5-22 Engineering Stress-Strain Curves for Weld Metal Tensile Specimens W3 and W4

6 RADIATION ANALYSIS AND NEUTRON DOSIMETRY

6.1 INTRODUCTION

This section describes a discrete ordinates S_n transport analysis performed for the Diablo Canyon Unit 1 reactor to determine the neutron radiation environment within the reactor pressure vessel and surveillance capsules. In this analysis, fast neutron exposure parameters in terms of fast neutron fluence ($E > 1.0$ MeV) and iron atom displacements (dpa) were established on a plant and fuel cycle specific basis. An evaluation of the most recent dosimetry sensor set from Capsule V, withdrawn at the end of the eleventh plant operating cycle, is provided. In addition, in order to provide a complete measurement database applicable to Diablo Canyon Unit 1, results from prior in-vessel and ex-vessel irradiations are included in Appendix E to this report. The data included in Appendix E were previously documented in Reference 24. Comparisons of the results from these dosimetry evaluations with the analytical predictions served to validate the plant specific neutron transport calculations. These validated calculations subsequently formed the basis for providing projections of the neutron exposure of the reactor pressure vessel for operating periods extending to 54 Effective Full Power Years (EFPY). These projections also account for a plant uprating, from 3338 MWt to 3411 MWt, which began during the eleventh operating cycle.

The use of fast neutron fluence ($E > 1.0$ MeV) to correlate measured material property changes to the neutron exposure of the material has traditionally been accepted for the development of damage trend curves as well as for the implementation of trend curve data to assess the condition of the vessel. In recent years, however, it has been suggested that an exposure model that accounts for differences in neutron energy spectra between surveillance capsule locations and positions within the vessel wall could lead to an improvement in the uncertainties associated with damage trend curves and improved accuracy in the evaluation of damage gradients through the reactor vessel wall.

Because of this potential shift away from a threshold fluence toward an energy dependent damage function for data correlation, ASTM Standard Practice E853, "Analysis and Interpretation of Light-Water Reactor Surveillance Results," recommends reporting displacements per iron atom (dpa) along with fluence ($E > 1.0$ MeV) to provide a database for future reference. The energy dependent dpa function to be used for this evaluation is specified in ASTM Standard Practice E693, "Characterizing Neutron Exposures in Iron and Low Alloy Steels in Terms of Displacements per Atom." The application of the dpa parameter to the assessment of embrittlement gradients through the thickness of the reactor vessel wall has already been promulgated in Revision 2 to Regulatory Guide 1.99, "Radiation Embrittlement of Reactor Vessel Materials."

All of the calculations and dosimetry evaluations described in this section and in Appendix E were based on the latest available nuclear cross-section data derived from ENDF/B-VI and made use of the latest available calculational tools. Furthermore, the neutron transport and dosimetry evaluation methodologies follow the guidance and meet the requirements of Regulatory Guide 1.190, "Calculational and Dosimetry Methods for Determining Pressure Vessel Neutron Fluence."^[19] Additionally, the methods used to develop the calculated pressure vessel fluence are consistent with the NRC approved methodology described in WCAP-14040-NP-A, "Methodology Used to Develop Cold Overpressure Mitigating System Setpoints and RCS Heatup and Cooldown Limit Curves," January 1996.^[20] The specific calculational

methods applied are also consistent with those described in WCAP-15557, "Qualification of the Westinghouse Pressure Vessel Neutron Fluence Evaluation Methodology."^[21]

6.2 DISCRETE ORDINATES ANALYSIS

A plan view of the Diablo Canyon Unit 1 reactor geometry at the core midplane is shown in Figure 4-1. Eight irradiation capsules attached to the thermal shield are included in the reactor design that constitutes the reactor vessel surveillance program. The capsules are located at azimuthal angles of 4°, 176°, 184°, and 356° (4° from the core cardinal axes) and 40°, 140°, 220°, and 320° (40° from the core cardinal axes) as shown in Figure 4-1. The stainless steel specimen containers are 1-inch square by 56 inches in height. The containers are positioned axially such that the test specimens are centered on the core midplane, thus spanning the central 5 feet of the 12-foot high reactor core.

From a neutronic standpoint, the surveillance capsules and associated support structures are significant. The presence of these materials has a marked effect on both the spatial distribution of neutron flux and the neutron energy spectrum in the water annulus between the thermal shield and the reactor vessel. In order to determine the neutron environment at the test specimen location, the capsules themselves must be included in the analytical model.

In performing the fast neutron exposure evaluations for the Diablo Canyon Unit 1 reactor vessel and surveillance capsules, a series of fuel cycle specific forward transport calculations were carried out using the following three-dimensional flux synthesis technique:

$$\phi(r, \theta, z) = \phi(r, \theta) * \frac{\phi(r, z)}{\phi(r)}$$

where $\phi(r, \theta, z)$ is the synthesized three-dimensional neutron flux distribution, $\phi(r, \theta)$ is the transport solution in r, θ geometry, $\phi(r, z)$ is the two-dimensional solution for a cylindrical reactor model using the actual axial core power distribution, and $\phi(r)$ is the one-dimensional solution for a cylindrical reactor model using the same source per unit height as that used in the r, θ two-dimensional calculation. This synthesis procedure was carried out for each operating cycle at Diablo Canyon Unit 1.

For the Diablo Canyon Unit 1 transport calculations, the r, θ model depicted in Figure 6-1 was utilized since the reactor is octant symmetric. This r, θ model includes the core, the reactor internals, the thermal shield -- including explicit representations of the surveillance capsules at 4° and 40°, the pressure vessel cladding and vessel wall, the insulation external to the pressure vessel, and the primary biological shield wall. This model formed the basis for the calculated results and enabled making comparisons to the surveillance capsule dosimetry evaluations. In developing this analytical model, nominal design dimensions were employed for the various structural components. Likewise, water temperatures, and hence, coolant densities in the reactor core and downcomer regions of the reactor were taken to be representative of full power operating conditions. The coolant densities were treated on a fuel cycle specific basis. The reactor core itself was treated as a homogeneous mixture of fuel, cladding, water, and miscellaneous core structures such as fuel assembly grids, guide tubes, et cetera. The geometric mesh

description of the r,θ reactor model consisted of 170 radial by 67 azimuthal intervals. Mesh sizes were chosen to assure that proper convergence of the inner iterations was achieved on a pointwise basis. The pointwise inner iteration flux convergence criterion utilized in the r,θ calculations was set at a value of 0.001.

The r,z model used for the Diablo Canyon Unit 1 calculations that is shown in Figure 6-2 extended radially from the centerline of the reactor core out to a location interior to the primary biological shield and over an axial span from an elevation approximately 1-foot below the active fuel to approximately 1-foot above the active fuel. As in the case of the r,θ model, nominal design dimensions and full power coolant densities were employed in the calculations. In this case, the homogenous core region was treated as an equivalent cylinder with a volume equal to that of the active core zone. The stainless steel former plates located between the core baffle and core barrel regions were also explicitly included in the model. The r,z geometric mesh description of the reactor model consisted of 153 radial by 90 axial intervals. As in the case of the r,θ calculations, mesh sizes were chosen to assure that proper convergence of the inner iterations was achieved on a pointwise basis. The pointwise inner iteration flux convergence criterion utilized in the r,z calculations was also set at a value of 0.001.

The one-dimensional radial model used in the synthesis procedure consisted of the same 153 radial mesh intervals included in the r,z model. Thus, radial synthesis factors could be determined on a meshwise basis throughout the entire geometry.

The core power distributions used in the plant specific transport analysis were taken from the appropriate Diablo Canyon Unit 1 fuel cycle design reports. The data extracted from the design reports represented cycle dependent fuel assembly enrichments, burnups, and axial power distributions. This information was used to develop spatial and energy dependent core source distributions averaged over each individual fuel cycle. Therefore, the results from the neutron transport calculations provided data in terms of fuel cycle averaged neutron flux, which when multiplied by the appropriate fuel cycle length, generated the incremental fast neutron exposure for each fuel cycle. In constructing these core source distributions, the energy distribution of the source was based on an appropriate fission split for uranium and plutonium isotopes based on the initial enrichment and burnup history of individual fuel assemblies. From these assembly dependent fission splits, composite values of energy release per fission, neutron yield per fission, and fission spectrum were determined.

All of the transport calculations supporting this analysis were carried out using the DORT discrete ordinates code Version 3.1^[22] and the BUGLE-96 cross-section library.^[23] The BUGLE-96 library provides a 67 group coupled neutron-gamma ray cross-section data set produced specifically for light water reactor (LWR) applications. In these analyses, anisotropic scattering was treated with a P5 Legendre expansion and angular discretization was modeled with an S16 order of angular quadrature. Energy and space dependent core power distributions, as well as system operating temperatures, were treated on a fuel cycle specific basis.

Selected results from the neutron transport analyses are provided in Tables 6-1 through 6-6. In Table 6-1, the calculated exposure rates and integrated exposures, expressed in terms of both neutron fluence ($E > 1.0$ MeV) and dpa, are given at the radial and azimuthal center of the two azimuthally symmetric surveillance capsule positions (4° and 40°). Also note that Table 6-1 presents calculated exposure rates and integrated exposures for Capsule V, which was irradiated at a 4° location during Cycles 1 through 5,

and subsequently moved to a 40° location until it was removed from service at the end of Cycle 11. These results, representative of the axial midplane of the active core, establish the calculated exposure of the surveillance capsules withdrawn to date as well as projected into the future. Similar information is provided in Table 6-2 for the reactor vessel inner radius. The vessel data given in Table 6-2 are representative of the axial location of the maximum neutron exposure at each of the four azimuthal locations. It is also important to note that the data for the vessel inner radius were taken at the clad/base metal interface, and thus, represent the maximum calculated exposure levels of the vessel forgings and welds.

Both calculated fluence ($E > 1.0$ MeV) and dpa data are provided in Tables 6-1 and 6-2. These data tabulations include both plant and fuel cycle specific calculated neutron exposures at the end of the eleventh operating fuel cycle, as well as projections to 16, 24, 32, 40, 48, and 54 effective full power years (EFPY). The projections were based on the assumption that the radial power distribution averaged from fuel cycles 5-11 was representative of future plant operation. All remaining core parameters were obtained by averaging cycles 5-11. The future projections are also based on the current reactor power level of 3411 MWt.

Radial gradient information applicable to fast ($E > 1.0$ MeV) neutron fluence and dpa are given in Tables 6-3 and 6-4, respectively. The data, based on the cumulative integrated exposures from Cycles 1 through 11, are presented on a relative basis for each exposure parameter at several azimuthal locations. Exposure distributions through the vessel wall may be obtained by multiplying the calculated exposure at the vessel inner radius by the gradient data listed in Tables 6-3 and 6-4.

The calculated fast neutron exposures for the three surveillance capsules withdrawn from the Diablo Canyon Unit 1 reactor are provided in Table 6-5. These assigned neutron exposure levels are based on the plant and fuel cycle specific neutron transport calculations performed for the Diablo Canyon Unit 1 reactor.

Updated lead factors for the Diablo Canyon Unit 1 surveillance capsules are provided in Table 6-6. The capsule lead factor is defined as the ratio of the calculated fluence ($E > 1.0$ MeV) at the geometric center of the surveillance capsule to the corresponding maximum calculated fluence at the pressure vessel clad/base metal interface. In Table 6-6, the lead factors for capsules that have been withdrawn from the reactor (S, Y, and V) were based on the calculated fluence values for the irradiation period corresponding to the time of withdrawal for the individual capsules. For the capsules remaining in the reactor (U, W, X, A, B, C, and D), the lead factors correspond to the calculated fluence values at the end of 54 effective full power years (EFPY).

6.3 NEUTRON DOSIMETRY

The validity of the calculated neutron exposures previously reported in Section 6.2 is demonstrated by a direct comparison against the measured sensor reaction rates and via a least squares evaluation performed for each of the capsule dosimetry sets. However, since the neutron dosimetry measurement data merely serves to validate the calculated results, only the direct comparison of measured-to-calculated results for the most recent surveillance capsule removed from service is provided in this section of the report. For completeness, the assessment of all measured dosimetry removed to date, based on direct, best estimate, and least squares evaluation comparisons, is documented in Appendix E.

The direct comparison of measured versus calculated fast neutron threshold reaction rates for the sensors from Capsule V that was withdrawn from Diablo Canyon Unit 1 at the end of the eleventh fuel cycle, is summarized below.

Reaction	Reaction Rates (rps/atom)		M/C Ratio
	Measured	Calculated	
$^{63}\text{Cu}(n,\alpha)^{60}\text{Co}$	2.26E-17	2.32E-17	0.97
$^{54}\text{Fe}(n,p)^{54}\text{Mn}$	1.81E-15	2.32E-15	0.78
$^{58}\text{Ni}(n,p)^{58}\text{Co}$	2.85E-15	2.77E-15	0.90
$^{238}\text{U}(n,p)^{137}\text{Cs (Cd)}$	8.84E-15	9.24E-14	0.82
$^{237}\text{Np}(n,f)^{137}\text{Cs (Cd)}$	7.82E-14	7.39E-14	0.97
Average:			0.89
% Standard Deviation:			9.8

The measured-to-calculated (M/C) reaction rate ratios for the Capsule V threshold reactions range from 0.78 to 0.97, and the average M/C ratio is $0.89 \pm 9.8\%$ (1σ). This direct comparison falls well within the $\pm 20\%$ criterion specified in Regulatory Guide 1.190; furthermore, it is consistent with the full set of comparisons given in Appendix E for all measured dosimetry removed to date from the Diablo Canyon Unit 1 reactor. As a result, these comparisons validate the current analytical results described in Section 6.2 which are deemed applicable for Diablo Canyon Unit 1.

6.4 CALCULATIONAL UNCERTAINTIES

The uncertainty associated with the calculated neutron exposure of the Diablo Canyon Unit 1 surveillance capsule and reactor pressure vessel is based on the recommended approach provided in Regulatory Guide 1.190. In particular, the qualification of the methodology was carried out in the following four stages:

1. Comparison of calculations with benchmark measurements from the Pool Critical Assembly (PCA) simulator at the Oak Ridge National Laboratory (ORNL).
2. Comparisons of calculations with surveillance capsule and reactor cavity measurements from the H. B. Robinson power reactor benchmark experiment.
3. An analytical sensitivity study addressing the uncertainty components resulting important input parameters applicable to the plant specific transport calculations used in the neutron exposure assessments.
4. Comparisons of the plant specific calculations with all available dosimetry results from the Diablo Canyon Unit 1 surveillance program.

The first phase of the methods qualification (PCA comparisons) addressed the adequacy of basic transport calculation and dosimetry evaluation techniques and associated cross-sections. This phase, however, did not test the accuracy of commercial core neutron source calculations nor did it address uncertainties in operational or geometric variables that impact power reactor calculations. The second phase of the qualification (H. B. Robinson comparisons) addressed uncertainties in these additional areas that are primarily methods related and would tend to apply generically to all fast neutron exposure evaluations. The third phase of the qualification (analytical sensitivity study) identified the potential uncertainties introduced into the overall evaluation due to calculational methods approximations as well as to a lack of knowledge relative to various plant specific input parameters. The overall calculational uncertainty applicable to the Diablo Canyon Unit 1 analysis was established from results of these three phases of the methods qualification.

The fourth phase of the uncertainty assessment (comparisons with Diablo Canyon Unit 1 measurements) was used solely to demonstrate the validity of the transport calculations and to confirm the uncertainty estimates associated with the analytical results. The comparison was used only as a check and was not used in any way to modify the calculated surveillance capsule and pressure vessel neutron exposures previously described in Section 6.2. As such, the validation of the Diablo Canyon Unit 1 analytical model based on the measured plant dosimetry is completely described in Appendix E.

The following summarizes the uncertainties developed from the first three phases of the methodology qualification. Additional information pertinent to these evaluations is provided in Reference 21.

	Capsule	Vessel IR
PCA Comparisons	3%	3%
H. B. Robinson Comparisons	3%	3%
Analytical Sensitivity Studies	10%	11%
Additional Uncertainty for Factors not Explicitly Evaluated	5%	5%
Net Calculational Uncertainty	12%	13%

The net calculational uncertainty was determined by combining the individual components in quadrature. Therefore, the resultant uncertainty was random and no systematic bias was applied to the analytical results.

The plant specific measurement comparisons described in Appendix E support these uncertainty assessments for Diablo Canyon Unit 1.

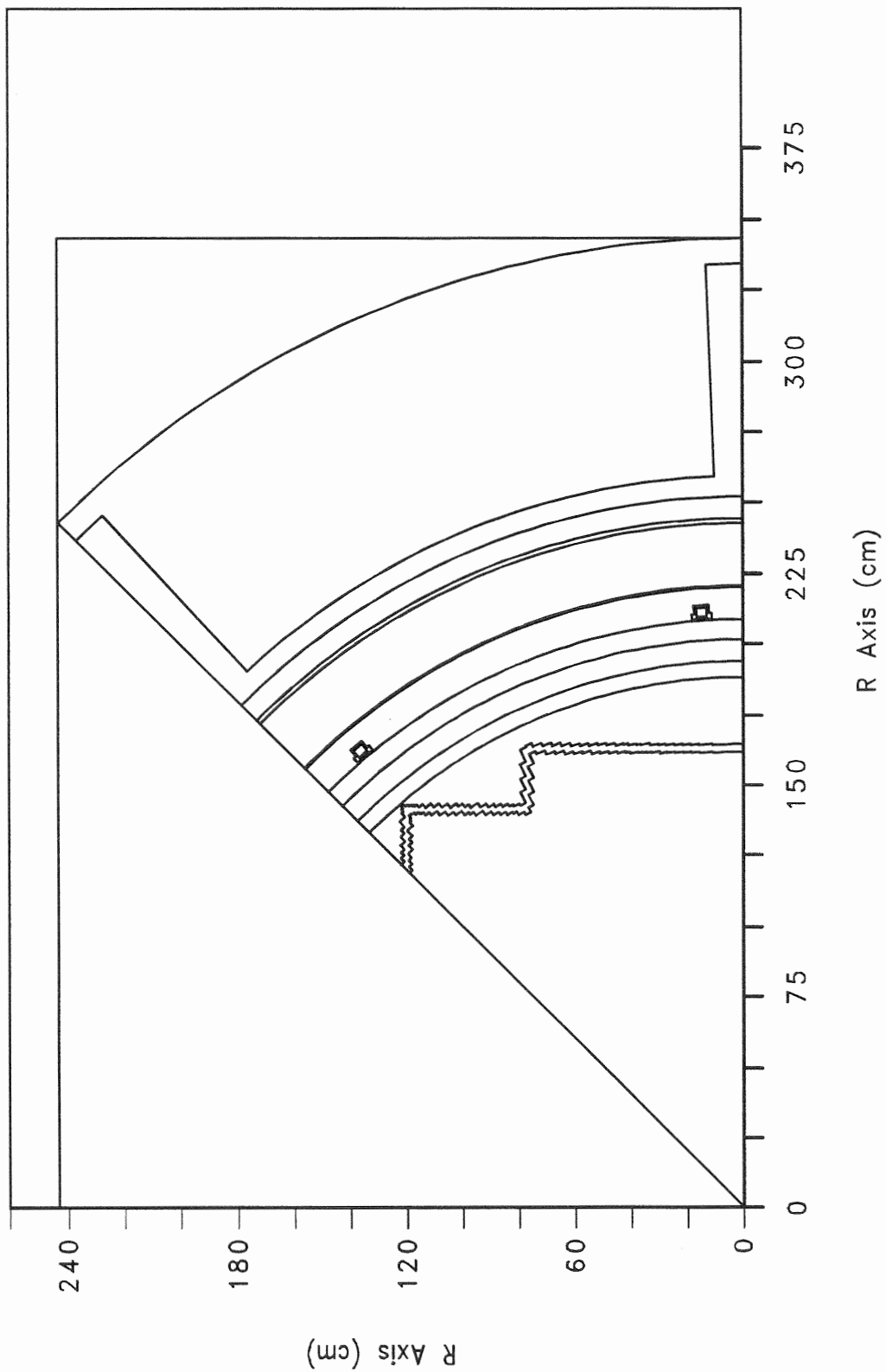


Figure 6-1 Diablo Canyon Unit 1 r,θ Reactor Geometry at the Core Midplane

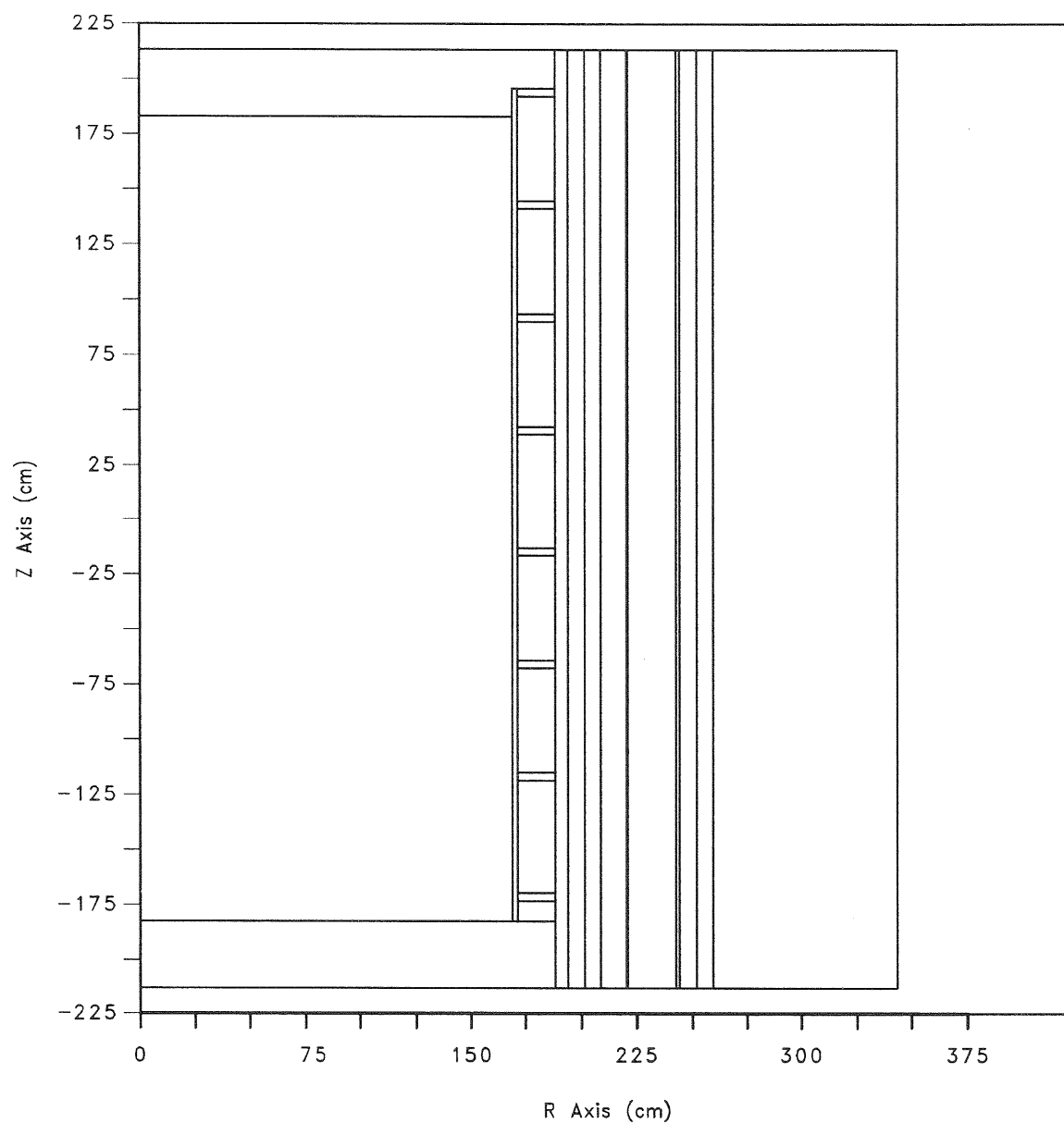


Figure 6-2 Diablo Canyon Unit 1 r,z Reactor Geometry

Table 6-1
Calculated Neutron Exposure Rates and Integrated Exposures
At The Surveillance Capsule Center

Neutrons ($E > 1.0$ MeV)

Cycle	Cycle Length [EFPS]	Cumulative Irradiation Time [EFPS]	Cumulative Irradiation Time [EFPY]	Neutron Flux ($E > 1.0$ MeV) [n/cm ² -s]		
				4°	40°	4° → 40° (Cap. V*)
1	3.94E+07	3.94E+07	1.25	2.24E+10	7.23E+10	2.24E+10
2	3.23E+07	7.16E+07	2.27	1.94E+10	6.03E+10	1.94E+10
3	3.72E+07	1.09E+08	3.45	1.60E+10	6.28E+10	1.60E+10
4	3.34E+07	1.42E+08	4.51	1.63E+10	4.85E+10	1.63E+10
5	4.31E+07	1.85E+08	5.87	1.54E+10	4.14E+10	1.54E+10
6	4.01E+07	2.25E+08	7.14	1.61E+10	4.16E+10	4.16E+10
7	4.18E+07	2.67 E+08	8.47	1.56E+10	4.11E+10	4.11E+10
8	4.04E+07	3.08 E+08	9.75	1.37E+10	3.69E+10	3.69E+10
9	5.13E+07	3.59 E+08	11.38	1.51E+10	3.87E+10	3.87E+10
10	4.72E+07	4.06 E+08	12.87	1.36E+10	3.80E+10	3.80E+10
11	4.58E+07	4.52 E+08	14.27	1.49E+10	3.84E+10	3.84E+10
Projection	5.29E+07	5.05 E+08	16.00	1.52E+10	4.02E+10	4.02E+10
Projection	2.53E+08	7.57 E+08	24.00	1.52E+10	4.02E+10	4.02E+10
Projection	2.53E+08	1.01E+09	32.00	1.52E+10	4.02E+10	4.02E+10
Projection	2.53E+08	1.26E+09	40.00	1.52E+10	4.02E+10	4.02E+10
Projection	2.53E+08	1.51E+09	48.00	1.52E+10	4.02E+10	4.02E+10
Projection	1.89E+08	1.70E+09	54.00	1.52E+10	4.02E+10	4.02E+10

Note: Neutron exposure values reported for the surveillance capsules are centered at the core midplane.

* Capsule V was irradiated at a 4° location during Cycles 1 through 5 followed by a 40° location during Cycles 6 through 11 when it was subsequently removed from service.

Table 6-1 cont'd

Calculated Neutron Exposure Rates and Integrated Exposures

At The Surveillance Capsule Center

Neutrons ($E > 1.0$ MeV)

Cycle	Cycle Length [EFPS]	Cumulative Irradiation Time [EFPS]	Cumulative Irradiation Time [EFPY]	Neutron Fluence ($E > 1.0$ MeV) [n/cm ²]		
				4°	40°	4° → 40° (Cap. V*)
1	3.94E+07	3.94E+07	1.25	8.82E+17	2.84E+18	8.82E+17
2	3.23E+07	7.16E+07	2.27	1.51E+18	4.79E+18	1.51E+18
3	3.72E+07	1.09E+08	3.45	2.10E+18	7.13E+18	2.10E+18
4	3.34E+07	1.42E+08	4.51	2.65E+18	8.75E+18	2.65E+18
5	4.31E+07	1.85E+08	5.87	3.31E+18	1.05E+19	3.31E+18
6	4.01E+07	2.25E+08	7.14	3.96E+18	1.22E+19	4.98E+18
7	4.18E+07	2.67E+08	8.47	4.61E+18	1.39E+19	6.69E+18
8	4.04E+07	3.08E+08	9.75	5.16E+18	1.54E+19	8.18E+18
9	5.13E+07	3.59E+08	11.38	5.93E+18	1.74E+19	1.02E+19
10	4.72E+07	4.06E+08	12.87	6.58E+18	1.92E+19	1.20E+19
11	4.58E+07	4.52E+08	14.27	7.26E+18	2.09E+19	1.37E+19
Projection	5.29E+07	5.05E+08	16.00	8.06E+18	2.31E+19	1.58E+19
Projection	2.53E+08	7.57E+08	24.00	1.19E+19	3.32E+19	2.60E+19
Projection	2.53E+08	1.01E+09	32.00	1.57E+19	4.33E+19	3.61E+19
Projection	2.53E+08	1.26E+09	40.00	1.96E+19	5.35E+19	4.63E+19
Projection	2.53E+08	1.51E+09	48.00	2.34E+19	6.36E+19	5.64E+19
Projection	1.89E+08	1.70E+09	54.00	2.63E+19	7.12E+19	6.40E+19

Note: Neutron exposure values reported for the surveillance capsules are centered at the core midplane.

* Capsule V was irradiated at a 4° location during Cycles 1 through 5 followed by a 40° location during Cycles 6 through 11 when it was subsequently removed from service.

Table 6-1 cont'd

Calculated Neutron Exposure Rates and Integrated Exposures

At The Surveillance Capsule Center

Iron Atom Displacements

Cycle	Cycle Length [EFPS]	Cumulative Irradiation Time [EFPS]	Cumulative Irradiation Time [EFY]	Displacement Rate [dpa/s]		
				4°	40°	4° → 40° (Cap. V*)
1	3.94E+07	3.94E+07	1.25	3.61E-11	1.22E-10	3.61E-11
2	3.23E+07	7.16E+07	2.27	3.12E-11	1.02E-10	3.12E-11
3	3.72E+07	1.09E+08	3.45	2.57E-11	1.06E-10	2.57E-11
4	3.34E+07	1.42E+08	4.51	2.63E-11	8.14E-11	2.63E-11
5	4.31E+07	1.85E+08	5.87	2.48E-11	6.95E-11	2.48E-11
6	4.01E+07	2.25E+08	7.14	2.60E-11	6.98E-11	6.98E-11
7	4.18E+07	2.67E+08	8.47	2.51E-11	6.90E-11	6.90E-11
8	4.04E+07	3.08E+08	9.75	2.20E-11	6.19E-11	6.19E-11
9	5.13E+07	3.59E+08	11.38	2.43E-11	6.50E-11	6.50E-11
10	4.72E+07	4.06E+08	12.87	2.20E-11	6.37E-11	6.37E-11
11	4.58E+07	4.52E+08	14.27	2.39E-11	6.45E-11	6.45E-11
Projection	5.29E+07	5.05E+08	16.00	2.45E-11	6.74E-11	6.74E-11
Projection	2.53E+08	7.57E+08	24.00	2.45E-11	6.74E-11	6.74E-11
Projection	2.53E+08	1.01E+09	32.00	2.45E-11	6.74E-11	6.74E-11
Projection	2.53E+08	1.26E+09	40.00	2.45E-11	6.74E-11	6.74E-11
Projection	2.53E+08	1.51E+09	48.00	2.45E-11	6.74E-11	6.74E-11
Projection	1.89E+08	1.70E+09	54.00	2.45E-11	6.74E-11	6.74E-11

Note: Neutron exposure values reported for the surveillance capsules are centered at the core midplane.

* Capsule V was irradiated at a 4° location during Cycles 1 through 5 followed by a 40° location during Cycles 6 through 11 when it was subsequently removed from service.

Table 6-1 cont'd

Calculated Neutron Exposure Rates and Integrated Exposures

At The Surveillance Capsule Center

Iron Atom Displacements

Cycle	Cycle Length [EFPS]	Cumulative Irradiation Time [EFPS]	Cumulative Irradiation Time [EFPY]	Displacements [dpa]		
				4°	40°	4° → 40° (Cap. V*)
1	3.94E+07	3.94E+07	1.25	1.42E-03	4.80E-03	1.42E-03
2	3.23E+07	7.16E+07	2.27	2.43E-03	8.08E-03	2.43E-03
3	3.72E+07	1.09E+08	3.45	3.39E-03	1.20E-02	3.39E-03
4	3.34E+07	1.42E+08	4.51	4.26E-03	1.47E-02	4.26E-03
5	4.31E+07	1.85E+08	5.87	5.33E-03	1.77E-02	5.33E-03
6	4.01E+07	2.25E+08	7.14	6.37E-03	2.05E-02	8.13E-03
7	4.18E+07	2.67 E+08	8.47	7.42E-03	2.34E-02	1.10E-02
8	4.04E+07	3.08 E+08	9.75	8.31E-03	2.59E-02	1.35E-02
9	5.13E+07	3.59 E+08	11.38	9.56E-03	2.92E-02	1.69E-02
10	4.72E+07	4.06 E+08	12.87	1.06E-02	3.23E-02	1.99E-02
11	4.58E+07	4.52 E+08	14.27	1.17E-02	3.52E-02	2.28E-02
Projection	5.29E+07	5.05 E+08	16.00	1.30E-02	3.88E-02	2.64E-02
Projection	2.53E+08	7.57 E+08	24.00	1.92E-02	5.58E-02	4.34E-02
Projection	2.53E+08	1.01E+09	32.00	2.54E-02	7.28E-02	6.04E-02
Projection	2.53E+08	1.26E+09	40.00	3.16E-02	8.99E-02	7.75E-02
Projection	2.53E+08	1.51E+09	48.00	3.77E-02	1.07E-01	9.45E-02
Projection	1.89E+08	1.70E+09	54.00	4.24E-02	1.20E-01	1.07E-01

Note: Neutron exposure values reported for the surveillance capsules are centered at the core midplane.

* Capsule V was irradiated at a 4° location during Cycles 1 through 5 followed by a 40° location during Cycles 6 through 11 when it was subsequently removed from service.

Table 6-2

Calculated Azimuthal Variation of Maximum Exposure Rates

And Integrated Exposures at the Reactor Vessel

Clad/Base Metal Interface

Cycle	Cycle Length [EFPS]	Cumulative Irradiation Time [EFPS]	Cumulative Irradiation Time [EFPY]	Neutron Flux ($E > 1.0$ MeV) [n/cm ² -s]			
				0°	15°	30°	45°
1	3.94E+07	3.94E+07	1.25	6.75E+09	1.07E+10	1.35E+10	2.08E+10
2	3.23E+07	7.16E+07	2.27	5.93E+09	8.45E+09	1.16E+10	1.75E+10
3	3.72E+07	1.09E+08	3.45	4.83E+09	7.87E+09	1.19E+10	1.82E+10
4	3.34E+07	1.42E+08	4.51	4.94E+09	7.57E+09	9.54E+09	1.43E+10
5	4.31E+07	1.85E+08	5.87	4.67E+09	7.06E+09	8.80E+09	1.20E+10
6	4.01E+07	2.25E+08	7.14	4.88E+09	7.65E+09	8.87E+09	1.21E+10
7	4.18E+07	2.67 E+08	8.47	4.70E+09	7.56E+09	8.99E+09	1.19E+10
8	4.04E+07	3.08 E+08	9.75	4.19E+09	6.86E+09	8.24E+09	1.08E+10
9	5.13E+07	3.59 E+08	11.38	4.58E+09	6.99E+09	8.40E+09	1.12E+10
10	4.72E+07	4.06 E+08	12.87	4.08E+09	7.26E+09	8.74E+09	1.10E+10
11	4.58E+07	4.52 E+08	14.27	4.42E+09	8.20E+09	9.48E+09	1.10E+10
Projection	5.29E+07	5.05 E+08	16.00	4.59E+09	7.52E+09	8.96E+09	1.16E+10
Projection	2.53E+08	7.57 E+08	24.00	4.59E+09	7.52E+09	8.96E+09	1.16E+10
Projection	2.53E+08	1.01E+09	32.00	4.59E+09	7.52E+09	8.96E+09	1.16E+10
Projection	2.53E+08	1.26E+09	40.00	4.59E+09	7.52E+09	8.96E+09	1.16E+10
Projection	2.53E+08	1.51E+09	48.00	4.59E+09	7.52E+09	8.96E+09	1.16E+10
Projection	1.89E+08	1.70E+09	54.00	4.59E+09	7.52E+09	8.96E+09	1.16E+10

Table 6-2 cont'd

Calculated Azimuthal Variation of Maximum Exposure Rates

And Integrated Exposures at the Reactor Vessel

Clad/Base Metal Interface

Cycle	Cycle Length [EFPS]	Cumulative Irradiation Time [EFPS]	Cumulative Irradiation Time [EFPY]	Neutron Fluence (E > 1.0 MeV) [n/cm ²]			
				0°	15°	30°	45°
1	3.94E+07	3.94E+07	1.25	2.66E+17	4.21E+17	5.33E+17	8.20E+17
2	3.23E+07	7.16E+07	2.27	4.57E+17	6.93E+17	9.07E+17	1.38 E+18
3	3.72E+07	1.09E+08	3.45	6.37E+17	9.86E+17	1.35 E+18	2.06 E+18
4	3.34E+07	1.42E+08	4.51	8.01E+17	1.24 E+18	1.67 E+18	2.54 E+18
5	4.31E+07	1.85E+08	5.87	1.00E+18	1.54 E+18	2.05 E+18	3.06 E+18
6	4.01E+07	2.25E+08	7.14	1.20 E+18	1.85 E+18	2.40 E+18	3.54 E+18
7	4.18E+07	2.67 E+08	8.47	1.39 E+18	2.17 E+18	2.78 E+18	4.04 E+18
8	4.04E+07	3.08 E+08	9.75	1.56 E+18	2.44 E+18	3.11 E+18	4.47 E+18
9	5.13E+07	3.59 E+08	11.38	1.80 E+18	2.80 E+18	3.54 E+18	5.05 E+18
10	4.72E+07	4.06 E+08	12.87	1.99 E+18	3.14 E+18	3.95 E+18	5.56 E+18
11	4.58E+07	4.52 E+08	14.27	2.19 E+18	3.52 E+18	4.39 E+18	6.07 E+18
Projection	5.29E+07	5.05 E+08	16.00	2.44 E+18	3.91 E+18	4.86 E+18	6.68 E+18
Projection	2.53E+08	7.57 E+08	24.00	3.59 E+18	5.81 E+18	7.12 E+18	9.62 E+18
Projection	2.53E+08	1.01E+09	32.00	4.75 E+18	7.71 E+18	9.39 E+18	1.26E+19
Projection	2.53E+08	1.26E+09	40.00	5.91 E+18	9.61 E+18	1.17E+19	1.55E+19
Projection	2.53E+08	1.51E+09	48.00	7.07 E+18	1.15E+19	1.39E+19	1.84E+19
Projection	1.89E+08	1.70E+09	54.00	7.94 E+18	1.29E+19	1.56E+19	2.06E+19

Table 6-2 cont'd

Calculated Azimuthal Variation of Fast Neutron Exposure Rates

And Iron Atom Displacement Rates At the Reactor Vessel

Clad/Base Metal Interface

Cycle	Cycle Length [EFPS]	Cumulative Irradiation Time [EFPS]	Cumulative Irradiation Time [EFPY]	Iron Atom Displacement Rate [dpa/s]			
				0°	15°	30°	45°
1	3.94E+07	3.94E+07	1.25	1.09E-11	1.71E-11	2.19E-11	3.37E-11
2	3.23E+07	7.16E+07	2.27	9.61E-12	1.36E-11	1.87E-11	2.83E-11
3	3.72E+07	1.09E+08	3.45	7.83E-12	1.26E-11	1.91E-11	2.94E-11
4	3.34E+07	1.42E+08	4.51	8.00E-12	1.21E-11	1.54E-11	2.31E-11
5	4.31E+07	1.85E+08	5.87	7.56E-12	1.13E-11	1.42E-11	1.94E-11
6	4.01E+07	2.25E+08	7.14	7.91E-12	1.23E-11	1.43E-11	1.95E-11
7	4.18E+07	2.67 E+08	8.47	7.63E-12	1.21E-11	1.45E-11	1.92E-11
8	4.04E+07	3.08 E+08	9.75	6.79E-12	1.10E-11	1.33E-11	1.75E-11
9	5.13E+07	3.59 E+08	11.38	7.43E-12	1.12E-11	1.35E-11	1.81E-11
10	4.72E+07	4.06 E+08	12.87	6.63E-12	1.16E-11	1.41E-11	1.77E-11
11	4.58E+07	4.52 E+08	14.27	7.19E-12	1.31E-11	1.53E-11	1.78E-11
Projection	5.29E+07	5.05 E+08	16.00	7.45E-12	1.20E-11	1.44E-11	1.88E-11
Projection	2.53E+08	7.57 E+08	24.00	7.45E-12	1.20E-11	1.44E-11	1.88E-11
Projection	2.53E+08	1.01E+09	32.00	7.45E-12	1.20E-11	1.44E-11	1.88E-11
Projection	2.53E+08	1.26E+09	40.00	7.45E-12	1.20E-11	1.44E-11	1.88E-11
Projection	2.53E+08	1.51E+09	48.00	7.45E-12	1.20E-11	1.44E-11	1.88E-11
Projection	1.89E+08	1.70E+09	54.00	7.45E-12	1.20E-11	1.44E-11	1.88E-11

Table 6-2 cont'd

Calculated Azimuthal Variation of Maximum Exposure Rates

And Integrated Exposures at the Reactor Vessel

Clad/Base Metal Interface

Cycle	Cycle Length [EFPS]	Cumulative Irradiation Time [EFPS]	Cumulative Irradiation Time [EFPY]	Iron Atom Displacements [dpa]			
				0°	15°	30°	45°
1	3.94E+07	3.94E+07	1.25	4.31E-04	6.74E-04	8.60E-04	1.33E-03
2	3.23E+07	7.16E+07	2.27	7.41E-04	1.11E-03	1.46E-03	2.24E-03
3	3.72E+07	1.09E+08	3.45	1.03E-03	1.58E-03	2.17E-03	3.33E-03
4	3.34E+07	1.42E+08	4.51	1.30E-03	1.99E-03	2.69E-03	4.10E-03
5	4.31E+07	1.85E+08	5.87	1.63E-03	2.47E-03	3.30E-03	4.94E-03
6	4.01E+07	2.25E+08	7.14	1.94E-03	2.96E-03	3.87E-03	5.72E-03
7	4.18E+07	2.67 E+08	8.47	2.26E-03	3.47E-03	4.47E-03	6.52E-03
8	4.04E+07	3.08 E+08	9.75	2.53E-03	3.91E-03	5.01E-03	7.22E-03
9	5.13E+07	3.59 E+08	11.38	2.91E-03	4.48E-03	5.70E-03	8.15E-03
10	4.72E+07	4.06 E+08	12.87	3.23E-03	5.03E-03	6.36E-03	8.99E-03
11	4.58E+07	4.52 E+08	14.27	3.56E-03	5.63E-03	7.06E-03	9.80E-03
Projection	5.29E+07	5.05 E+08	16.00	3.95E-03	6.27E-03	7.83E-03	1.08E-02
Projection	2.53E+08	7.57 E+08	24.00	5.83E-03	9.31E-03	1.15E-02	1.55E-02
Projection	2.53E+08	1.01E+09	32.00	7.71E-03	1.23E-02	1.51E-02	2.03E-02
Projection	2.53E+08	1.26E+09	40.00	9.59E-03	1.54E-02	1.88E-02	2.50E-02
Projection	2.53E+08	1.51E+09	48.00	1.15E-02	1.84E-02	2.24E-02	2.98E-02
Projection	1.89E+08	1.70E+09	54.00	1.29E-02	2.07E-02	2.51E-02	3.33E-02

Table 6-3

Relative Radial Distribution Of Neutron Fluence ($E > 1.0$ MeV)

Within The Reactor Vessel Wall

RADIUS (cm)	AZIMUTHAL ANGLE			
	0°	15°	30°	45°
220.35	1.000	1.000	1.000	1.000
225.87	0.545	0.546	0.550	0.540
231.39	0.263	0.263	0.266	0.256
236.90	0.122	0.121	0.123	0.116
242.42	0.056	0.054	0.056	0.050
Note: Base Metal Inner Radius = 220.35 cm Base Metal 1/4T = 225.87 cm Base Metal 1/2T = 231.39 cm Base Metal 3/4T = 236.90 cm Base Metal Outer Radius = 242.42 cm				

Table 6-4

Relative Radial Distribution of Iron Atom Displacements (dpa)

Within The Reactor Vessel Wall

RADIUS (cm)	AZIMUTHAL ANGLE			
	0°	15°	30°	45°
220.35	1.000	1.000	1.000	1.000
225.87	0.642	0.639	0.648	0.638
231.39	0.396	0.390	0.402	0.338
236.90	0.240	0.235	0.245	0.228
242.42	0.138	0.133	0.139	0.118
Note: Base Metal Inner Radius = 220.35 cm Base Metal 1/4T = 225.87 cm Base Metal 1/2T = 231.39 cm Base Metal 3/4T = 236.90 cm Base Metal Outer Radius = 242.42 cm				

Table 6-5

Calculated Fast Neutron Exposure of Surveillance Capsules

Withdrawn from Diablo Canyon Unit 1

Capsule	Irradiation Time [EFPY]	Fluence (E > 1.0 MeV) [n/cm ²]	Iron Displacements [dpa]
S	1.25	2.84E+18	4.80E-03
Y	5.87	1.05E+19	1.77E-02
V	14.27	1.37E+19	2.28E-02

Table 6-6

Calculated Surveillance Capsule Lead Factors

Capsule ID And Location	Status	Lead Factor
S (40°)	Withdrawn EOC 1 (for analysis)	3.46
Y (40°)	Withdrawn EOC 5 (for analysis)	3.44
T (40°)	Withdrawn EOC 5 (for storage)	3.44
Z (40°)	Withdrawn EOC 5 (for storage)	3.44
V (4° → 40°)	Withdrawn EOC 11 (for analysis)	2.26
U (4°)	In Reactor	1.28
W (4°)	In Reactor	1.28
X (4°)	In Reactor	1.28
A (4°)	In Reactor	1.31
B (40°)	In Reactor	3.46
C (40°)	In Reactor	3.46
D (40°)	In Reactor	3.46

Notes:

1. Capsule V was irradiated at a 4° location for Cycles 1 through 5, and at a 40° location during Cycles 6 through 11, after which it was removed from service.
2. Lead factors for capsules remaining in the reactor are based on projected exposure calculations through 54 EFPY.
3. Capsules A, B, C, and D were not inserted into position until the beginning of cycle 6.
4. Capsule C is estimated to be withdrawn at the end of cycle 12.

7 SURVEILLANCE CAPSULE REMOVAL SCHEDULE

The following surveillance capsule removal schedule was developed by PG&E and it meets the requirements of ASTM E185-82. This recommended removal schedule is applicable to 32 EFPY of operation.

Table 7-1 Diablo Canyon Unit 1 Reactor Vessel Surveillance Capsule Withdrawal Schedule				
Capsule	Location	Lead Factor^(a)	Removal Time (EFPY)^(b)	Fluence (n/cm², E > 1.0 MeV)^(a)
S	320°	3.46	1.25 (Tested, 1R1)	0.284
Y	40°	3.44	5.86 (Tested, 1R5)	1.05
T	140°	3.44	5.86 (Removed, 1R5)	1.05
Z	220°	3.44	5.86 (Removed, 1R5)	1.05
V	320°	2.26	14.27 (Tested, 1R11)	1.37
C ^(c)	140°	3.46	15.9 (Estimated)	2.31 ^(e)
D ^(c)	220°	3.46	20.7 ^(d) (Estimated)	2.91 ^(e)
B ^(c)	40°	3.46	20.7 (Estimated)	2.91 ^(e)
A ^(c)	184°	1.31	Standby	-
U	356°	1.28	Standby	-
X	176°	1.28	Standby	-
W	4°	1.28	Standby	-

Notes:

(a) Updated in Capsule V dosimetry analysis [$\times 10^{19}$ n/cm², E > 1.0 MeV], see Table 6-5.

(b) Effective Full Power Years (EFPY) from plant startup. Beginning with cycle 11, the rated full power changed from 3338 to 3411 MWt.

(c) Installed at 5.86 EFPY (EOC5).

(d) Anneal at 15.9 EFPY and reinsert.

(e) Projected fluence on capsule at proposed withdrawal date. Fluence on capsule equals fluence on the vessel at the given EFPY * Lead Factor.

8 REFERENCES

1. Regulatory Guide 1.99, Revision 2, *Radiation Embrittlement of Reactor Vessel Materials*, U.S. Nuclear Regulatory Commission, May, 1988.
2. Code of Federal Regulations, 10CFR50, Appendix G, *Fracture Toughness Requirements*, and Appendix H, *Reactor Vessel Material Surveillance Program Requirements*, U.S. Nuclear Regulatory Commission, Washington, D.C.
3. WCAP-8465, *Pacific Gas and Electric Co. Diablo Canyon Unit No. 1 Reactor Vessel Radiation Surveillance Program*, J.A. Davidson, et. al., dated January 1975.
4. WCAP-11567, *Analysis of Capsule S from the Pacific Gas and Electric Company Diablo Canyon Unit 1 Reactor Vessel Radiation Surveillance Program*, S.E. Yanichko, et. al., dated December 1987.
5. WCAP-13750, *Analysis of Capsule Y from the Pacific Gas and Electric Company Diablo Canyon Unit 1 Reactor Vessel Radiation Surveillance Program*, E. Terek, et. al., dated July 1993.
6. ASTM E185-82, *Standard Practice for Conducting Surveillance Tests for Light-Water Cooled Nuclear Power Reactor Vessels*.
7. ASTM E23-98, *Standard Test Method for Notched Bar Impact Testing of Metallic Materials*, ASTM, 1998.
8. ASTM A370-97a, *Standard Test Methods and Definitions for Mechanical Testing of Steel Products*, ASTM, 1997.
9. ASTM E8-99, *Standard Test Methods for Tension Testing of Metallic Materials*, ASTM, 1999.
10. ASTM E21-92 (1998), *Standard Test Methods for Elevated Temperature Tension Tests of Metallic Materials*, ASTM, 1998.
11. Procedure RMF 8402, *Surveillance Capsule Testing Program*, Revision 2.
12. Procedure RMF 8102, *Tensile Testing*, Revision 1.
13. Procedure RMF 8103, *Charpy Impact Testing*, Revision 1.
14. WCAP-14370, *Use of the Hyperbolic Tangent Function for Fitting Transition Temperature Toughness Data*, T. R. Mager, et al, May 1995.
15. ASTM E208, *Standard Test Method for Conducting Drop-Weight Test to Determine Nil-Ductility Transition Temperature of Ferritic Steels*, in ASTM Standards, Section 3, American Society for Testing and Materials, Philadelphia, PA.

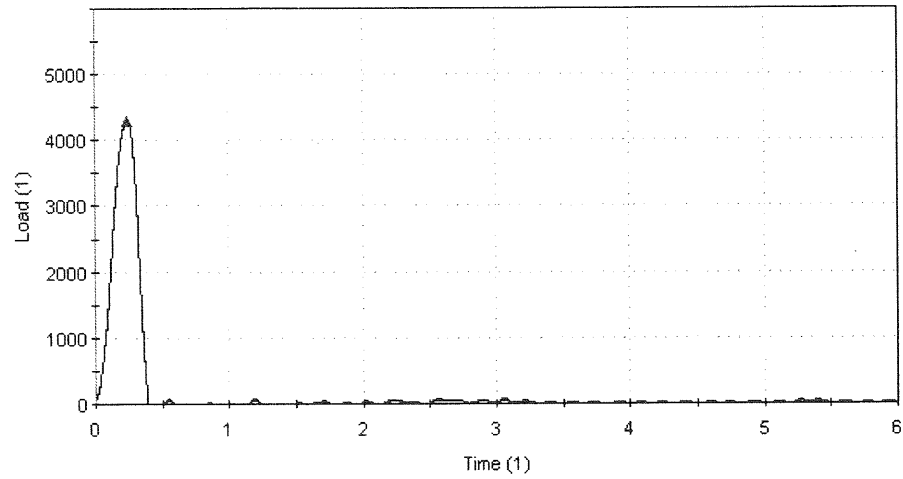
16. Section XI of the ASME Boiler and Pressure Vessel Code, Appendix G, *Fracture Toughness Criteria for Protection Against Failure*.
17. ASTM E185-70, *Recommended Practice for Surveillance Tests for Nuclear Reactor Vessels*.
18. ASTM E83-93, *Standard Practice for Verification and Classification of Extensometers*, in ASTM Standards, Section 3, American Society for Testing and Materials, Philadelphia, PA, 1993.
19. Regulatory Guide RG-1.190, *Calculational and Dosimetry Methods for Determining Pressure Vessel Neutron Fluence*, U. S. Nuclear Regulatory Commission, Office of Nuclear Regulatory Research, March 2001.
20. WCAP-14040-NP-A, Revision 2, *Methodology Used to Develop Cold Overpressure Mitigating System Setpoints and RCS Heatup and Cooldown Limit Curves*, January 1996.
21. WCAP-15557, Revision 0, *Qualification of the Westinghouse Pressure Vessel Neutron Fluence Evaluation Methodology*, August 2000.
22. RSICC Computer Code Collection CCC-650, *DOORS 3.1, One, Two- and Three-Dimensional Discrete Ordinates Neutron/Photon Transport Code System*, August 1996.
23. RSIC Data Library Collection DLC-185, *BUGLE-96, Coupled 47 Neutron, 20 Gamma-Ray Group Cross Section Library Derived from ENDF/B-VI for LWR Shielding and Pressure Vessel Dosimetry Applications*, March 1996.
24. WCAP-15780, *Fast Neutron Fluence and Neutron Dosimetry Evaluations for the Diablo Canyon Unit 1 Reactor Pressure Vessel*. December 2001.
25. PG&E Letter No. DCL-92-072, *Diablo Canyon Unit 1 Supplemental Reactor Vessel Radiation Surveillance Program*, March 1992.
26. WCAP-13440, Revision 0, *Supplemental Reactor Vessel Radiation Surveillance Program for the Pacific Gas and Electric Company Diablo Canyon Unit No. 1*, December 1992.
27. Combustion Engineering Report CE NPSD-1039, Revision 2, *Best Estimate Copper and Nickel Values in CE Fabricated Reactor Vessel Welds*, June 1997.

APPENDIX A

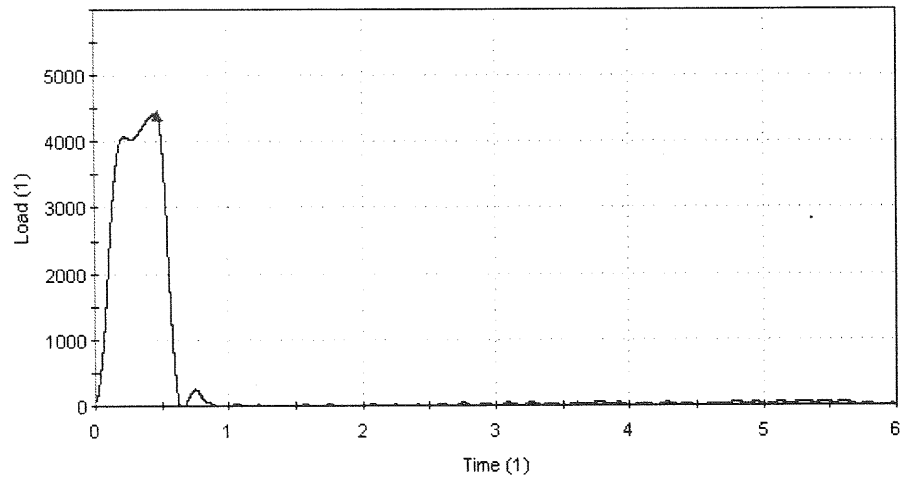
LOAD-TIME RECORDS FOR CHARPY SPECIMEN TESTS

- Specimen prefix “E” denotes Intermediate Plate, Longitudinal Orientation
- Specimen prefix “R” denotes Correlation Monitor Material
- Specimen prefix “W” denotes Weld Material
- Specimen prefix “H” denotes Heat-Affected Zone material
- Load (1) is in units of lbs
- Time (1) is in units of milli seconds

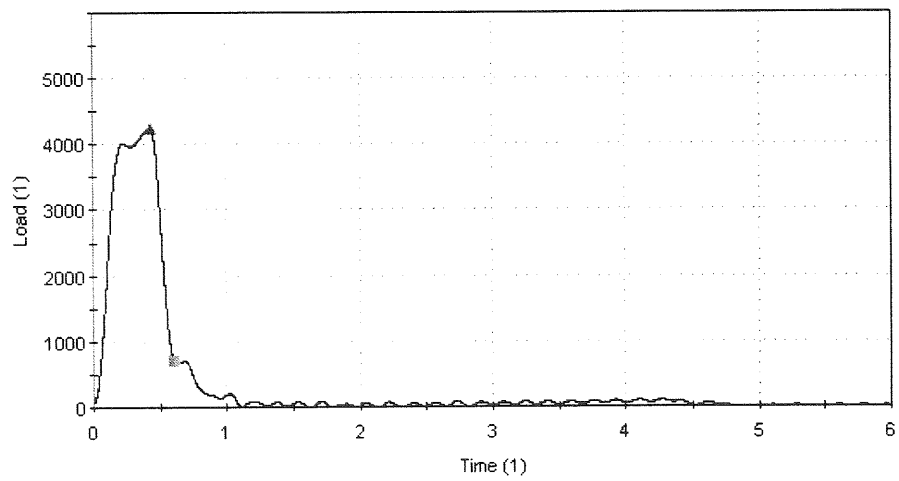
PC0340



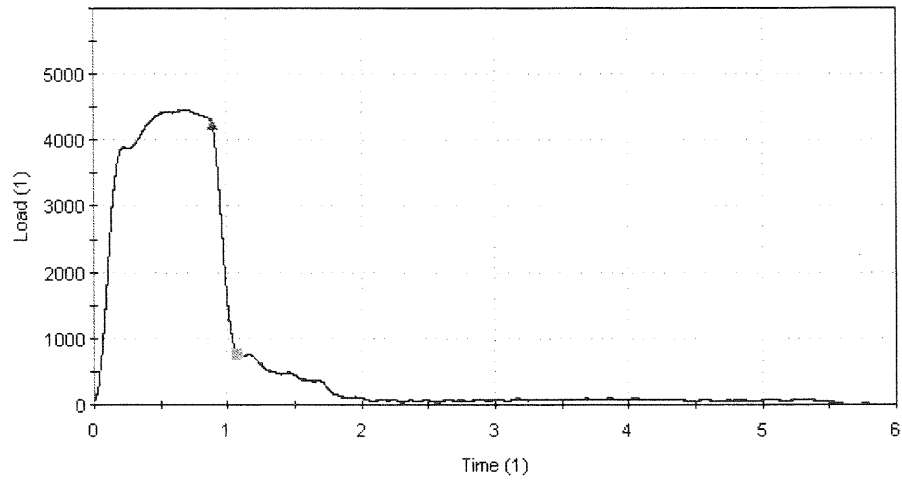
E52, -25°F



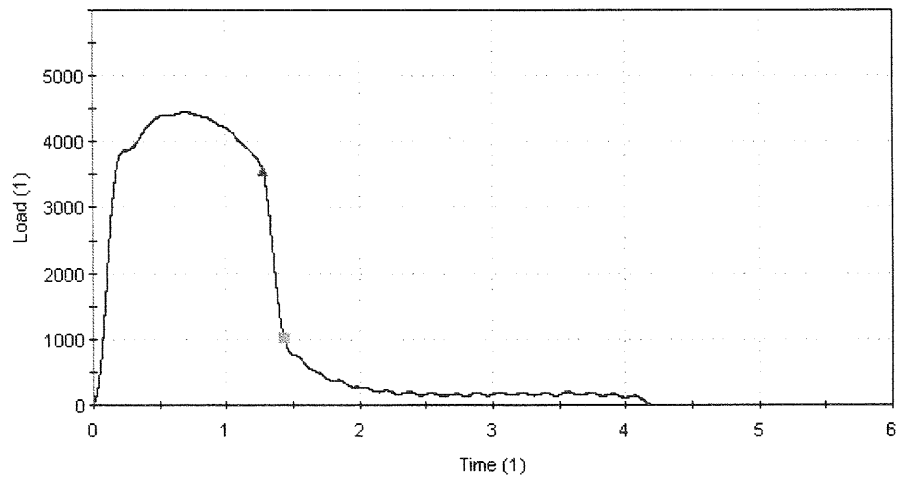
E49, 25°F



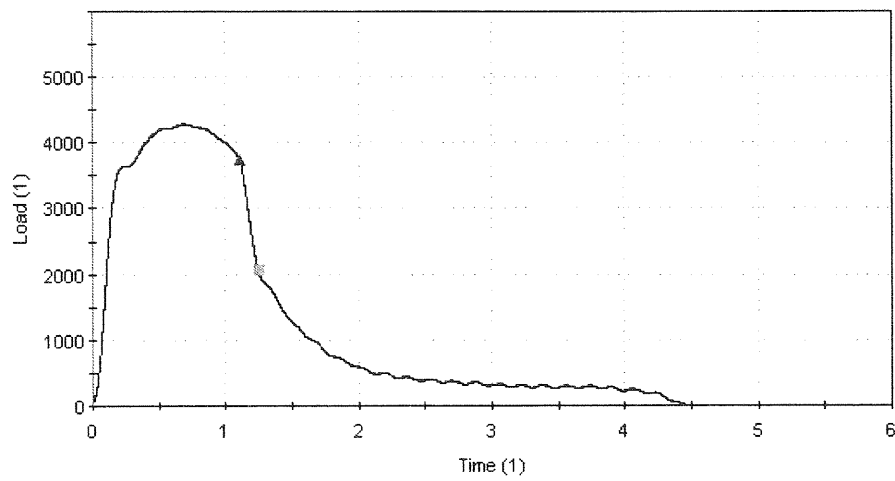
E55, 75°F



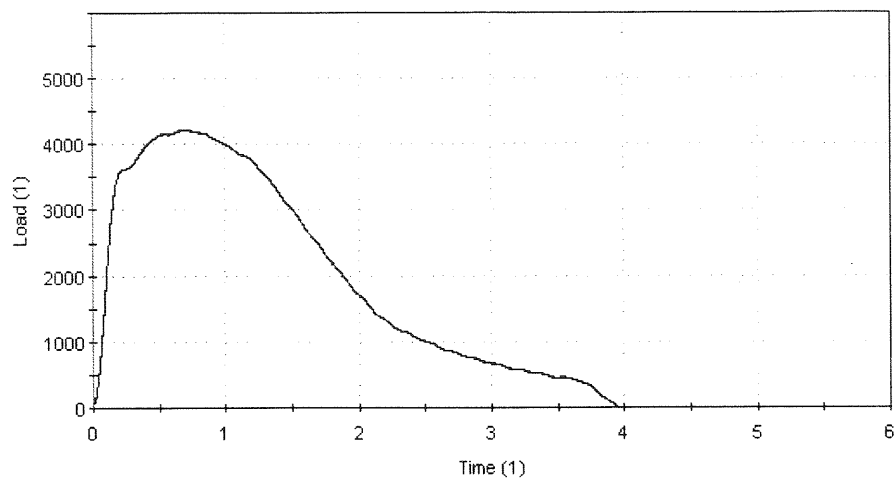
E51, 110°F



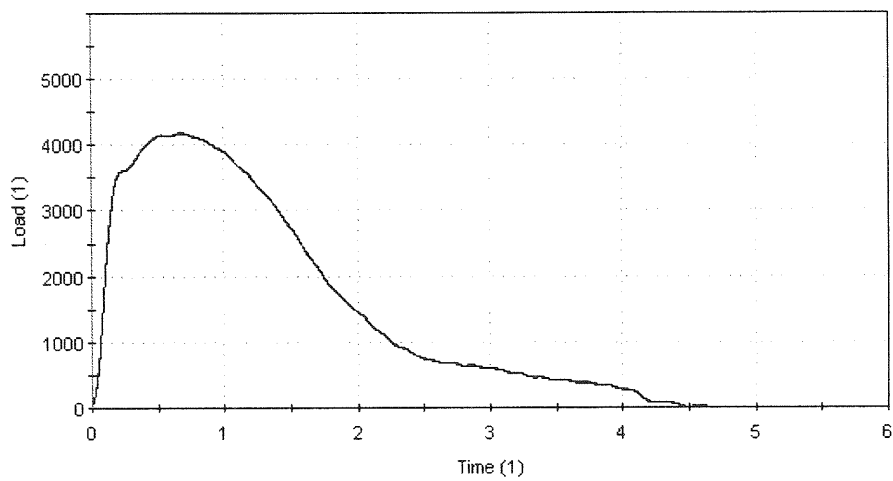
E53, 125°F



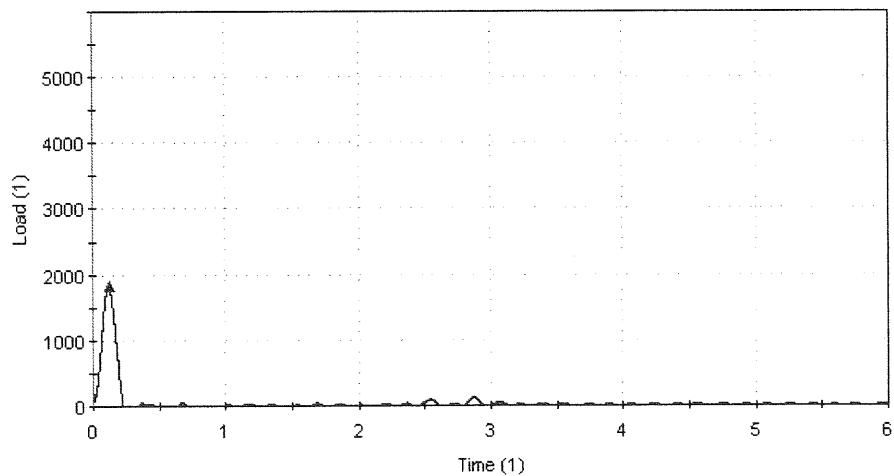
E50, 175°F



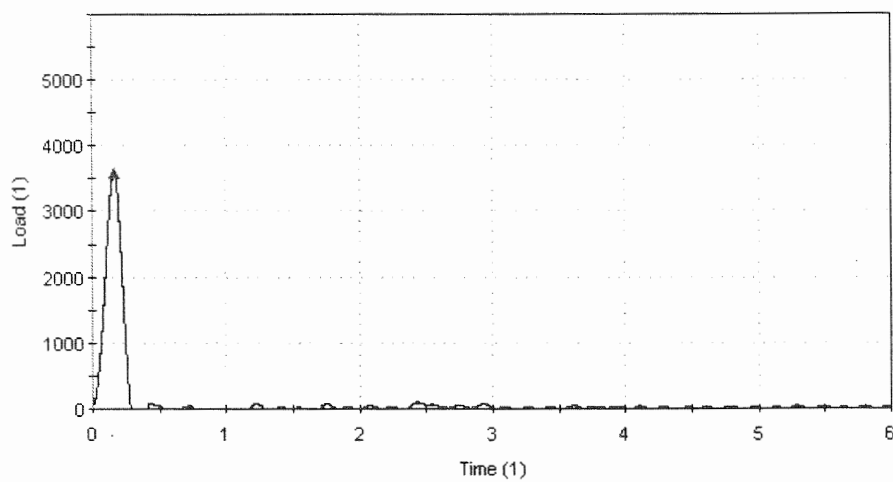
E54, 250°F



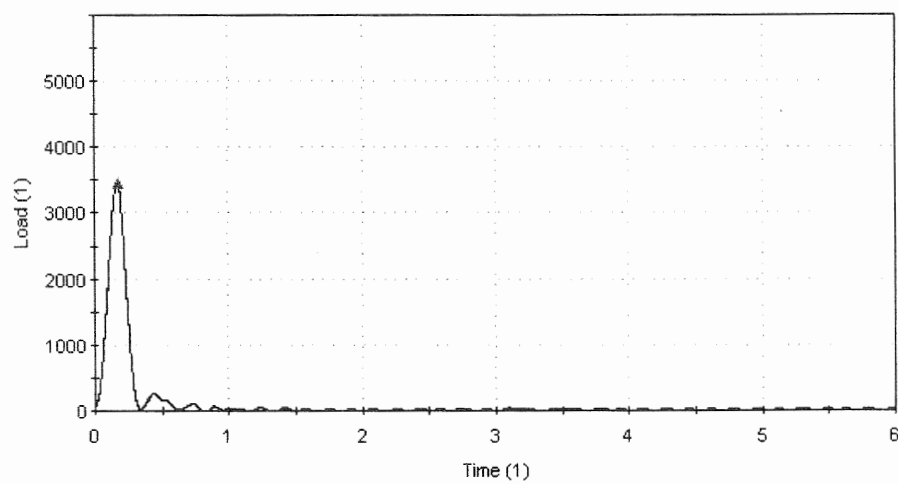
E56, 275°F



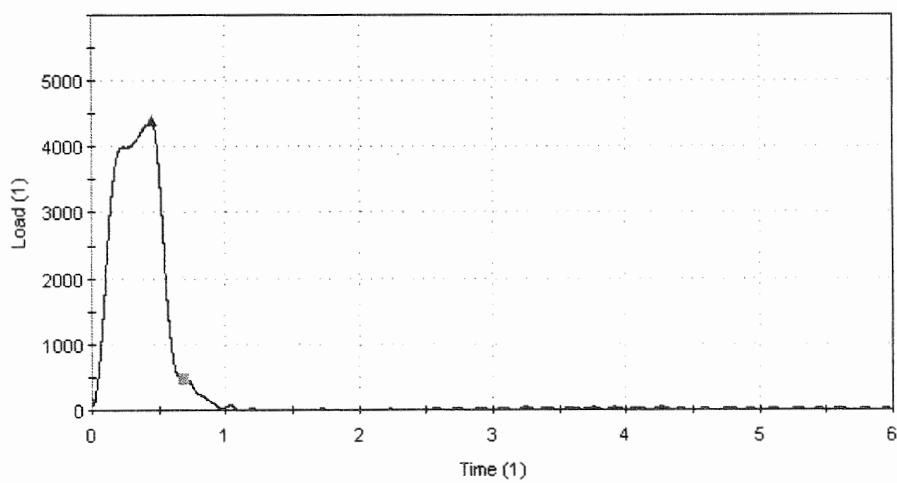
R49, 25°F



R51, 50°F

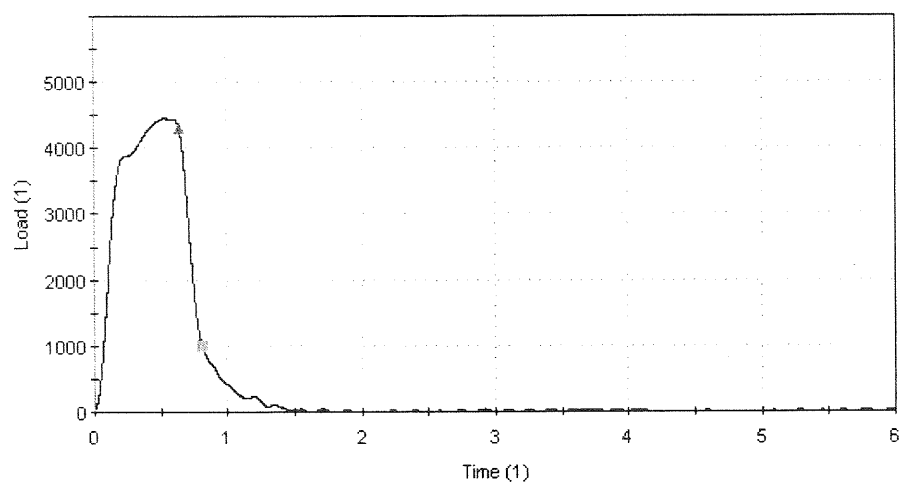


R56, 100°F

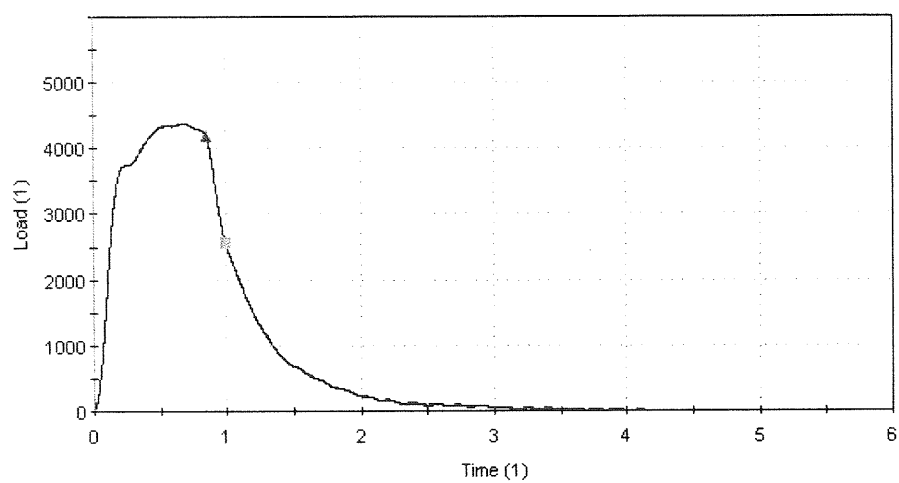


R55, 150°F

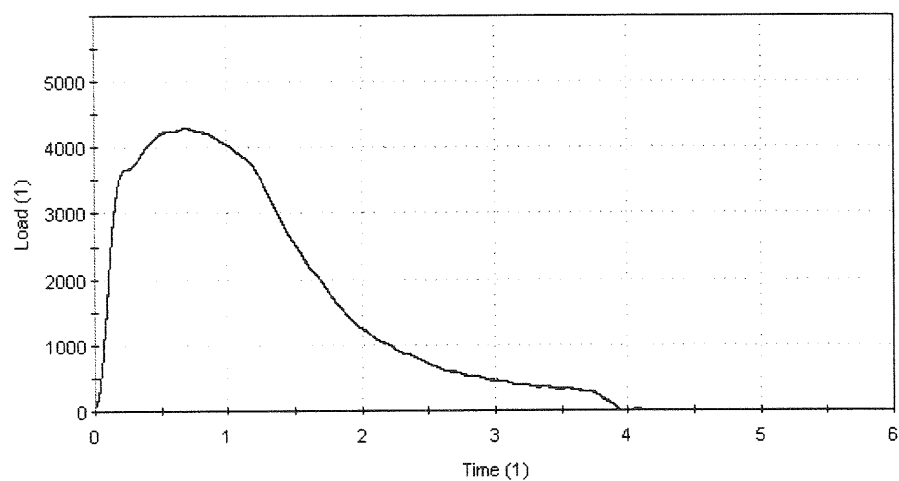
236940



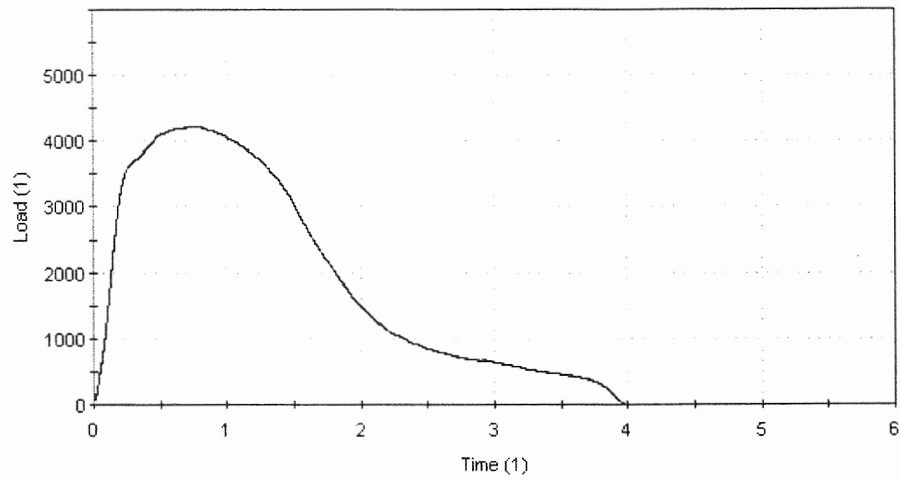
R53, 200°F



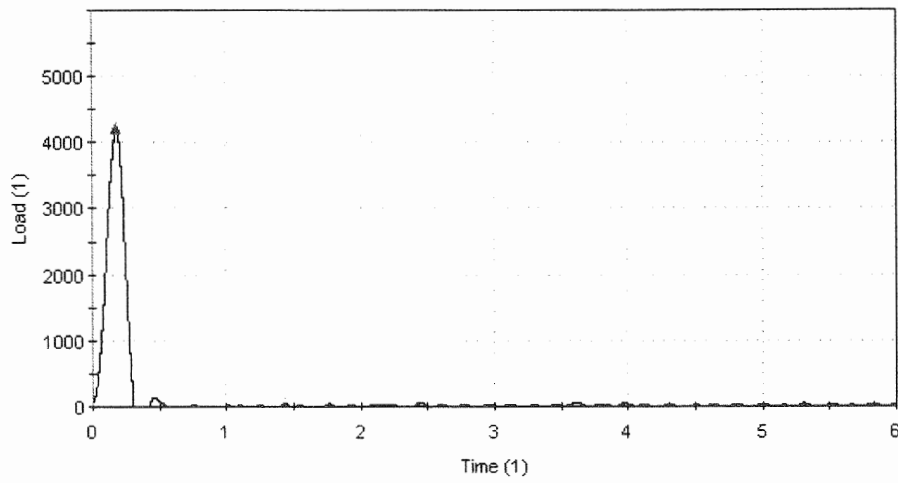
R54, 250°F



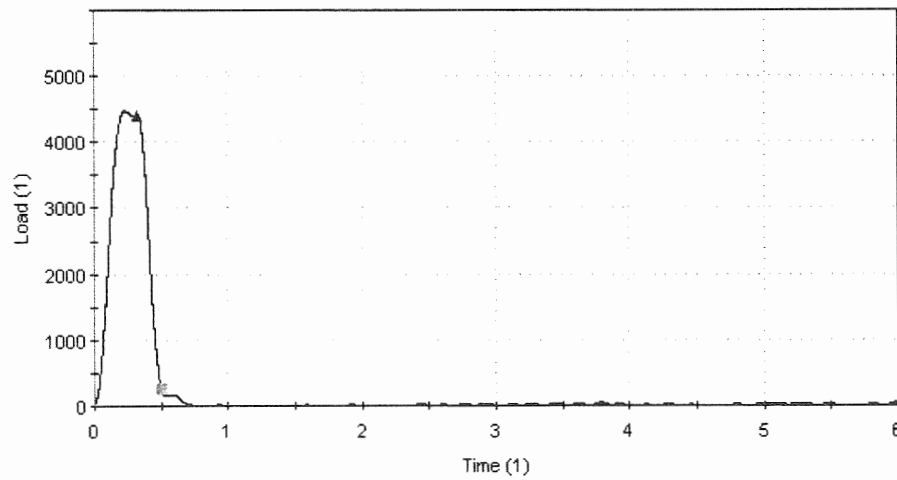
R50, 300°F



R52, 325°F

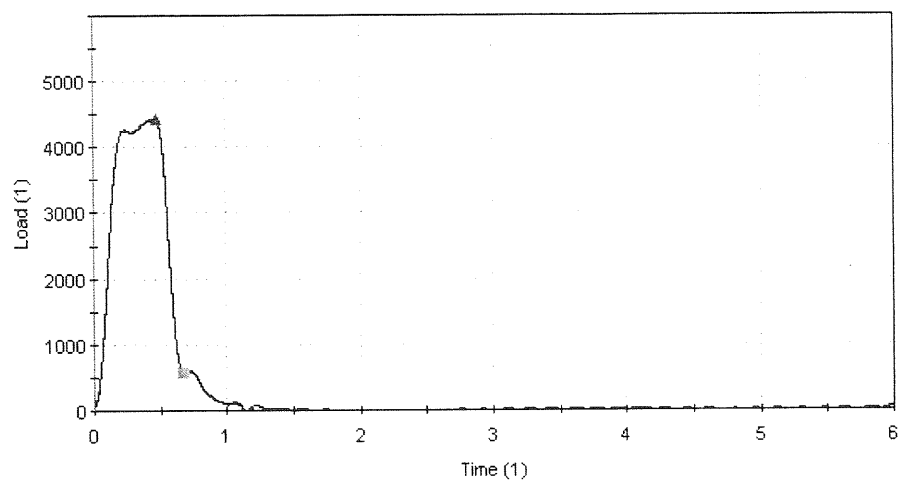


W11, 25°F

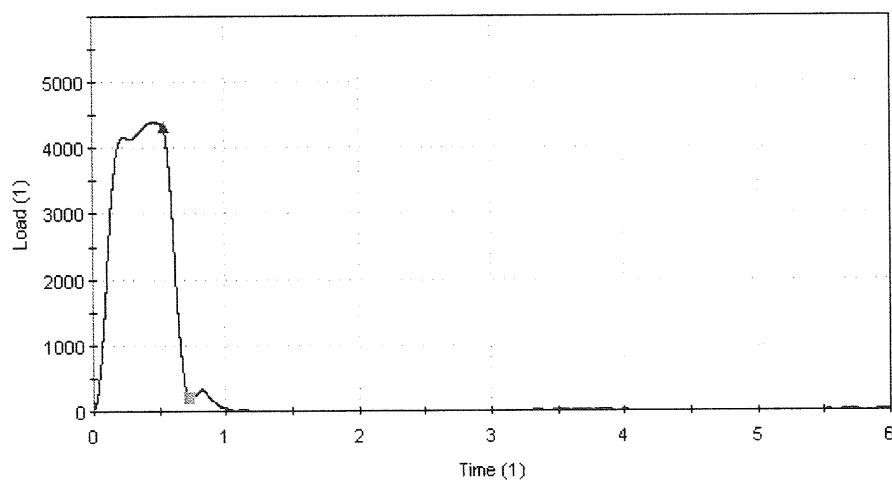


W13, 100°F

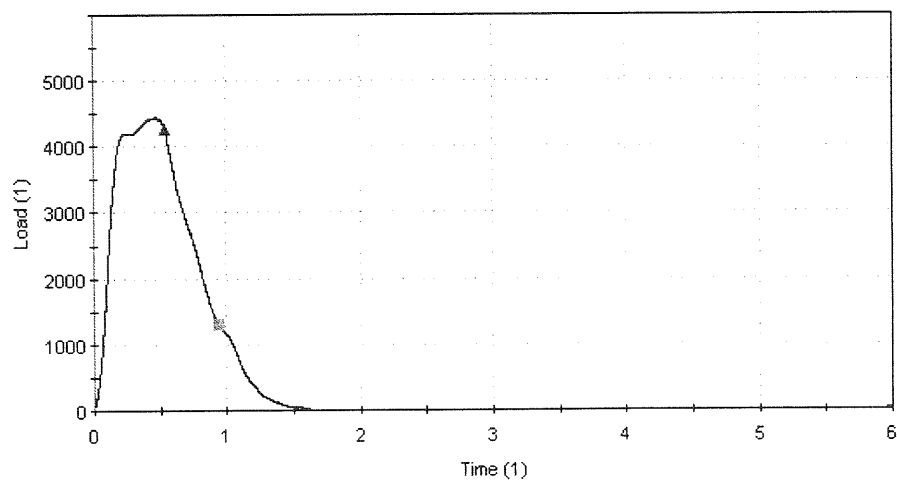
236940



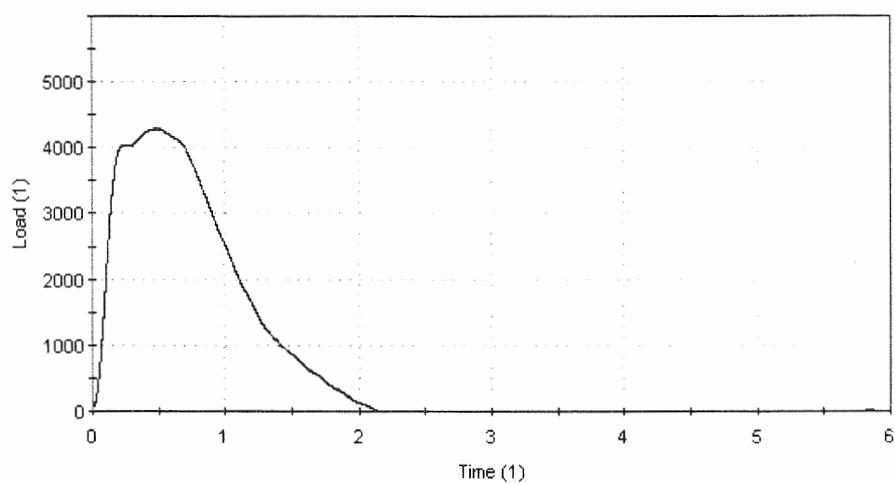
W12, 150°F



W9, 200°F

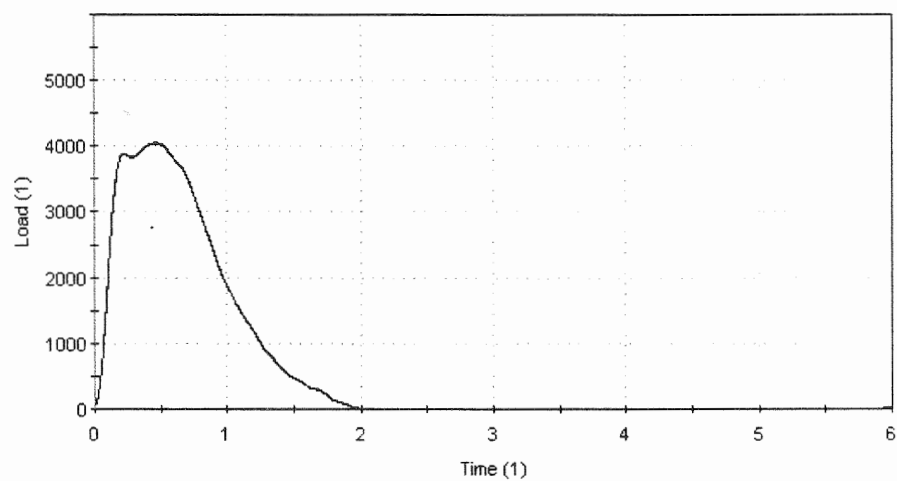


W10, 225°F

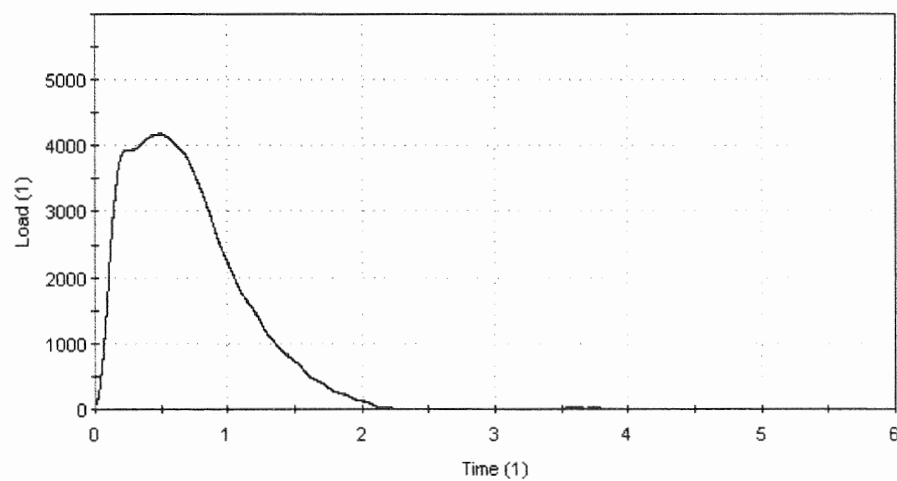


236940

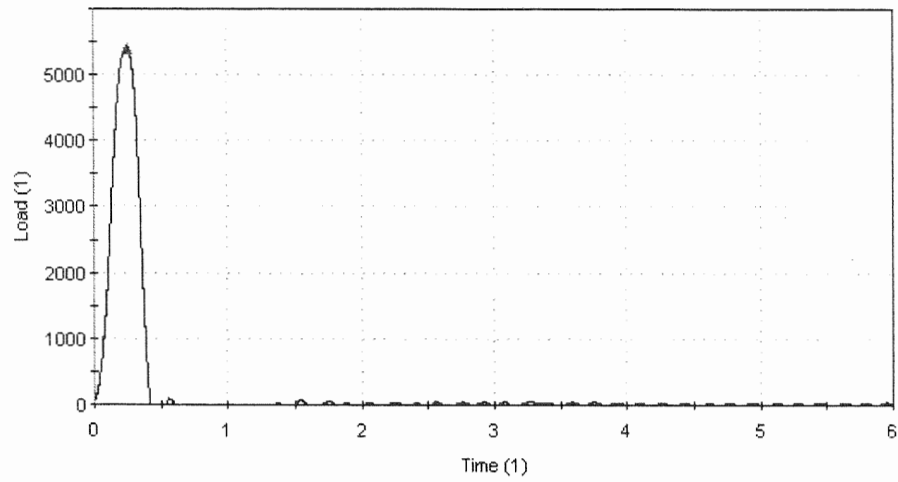
W15, 300°F



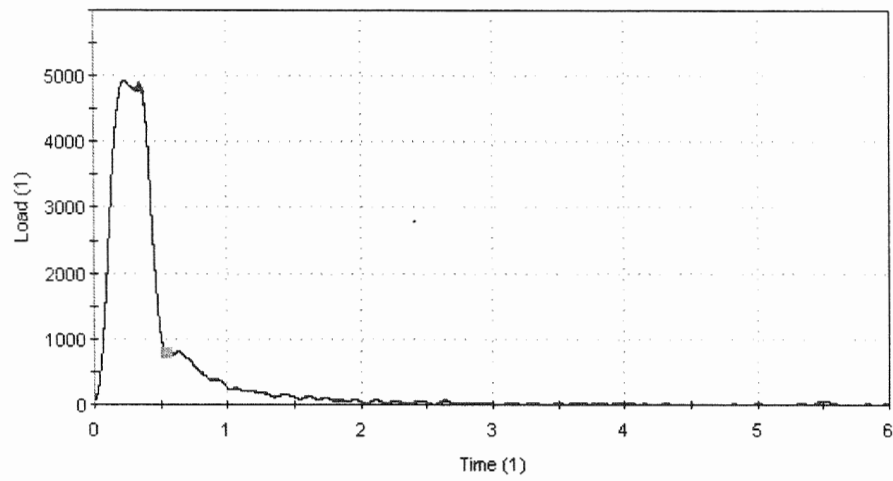
W14, 325°F



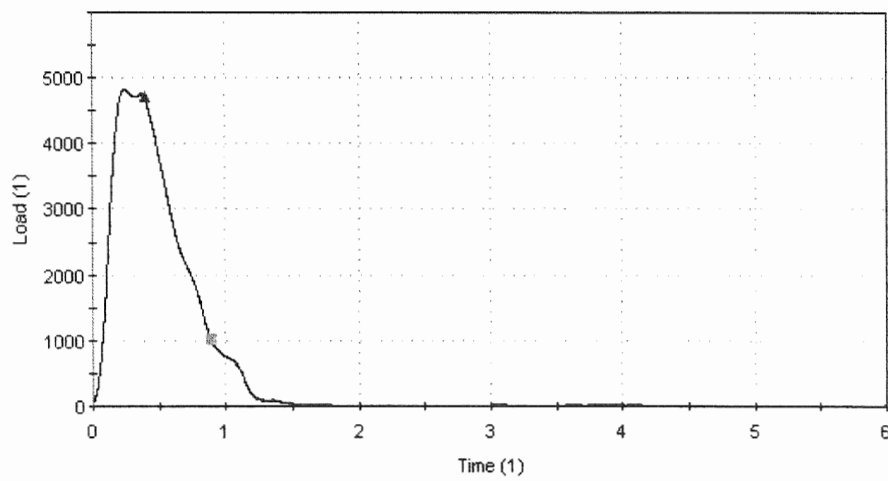
W16, 350°F



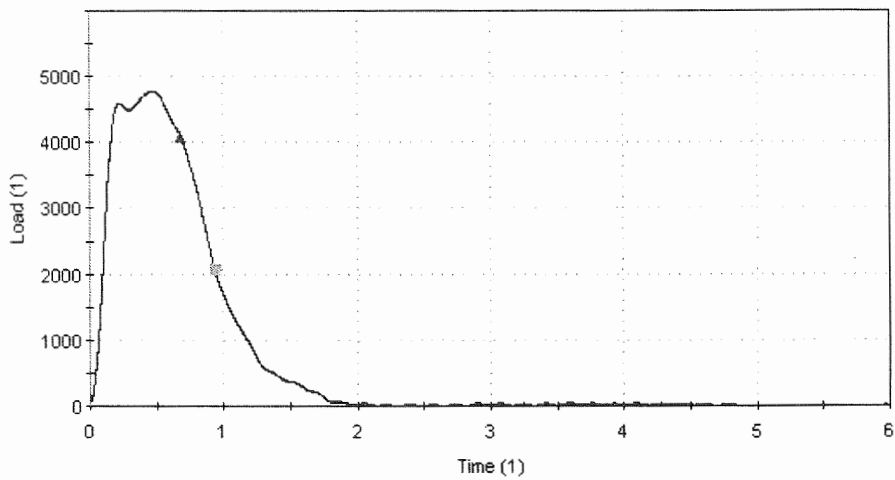
H14, -125°F



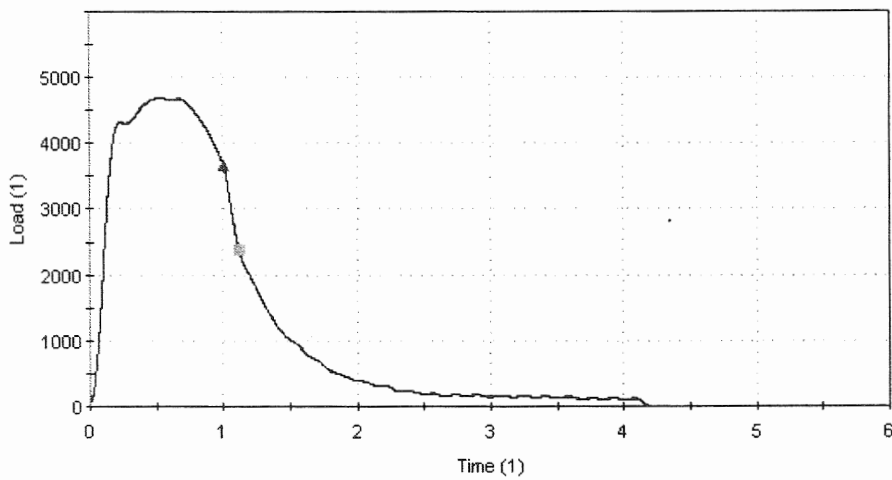
H12, -50°F



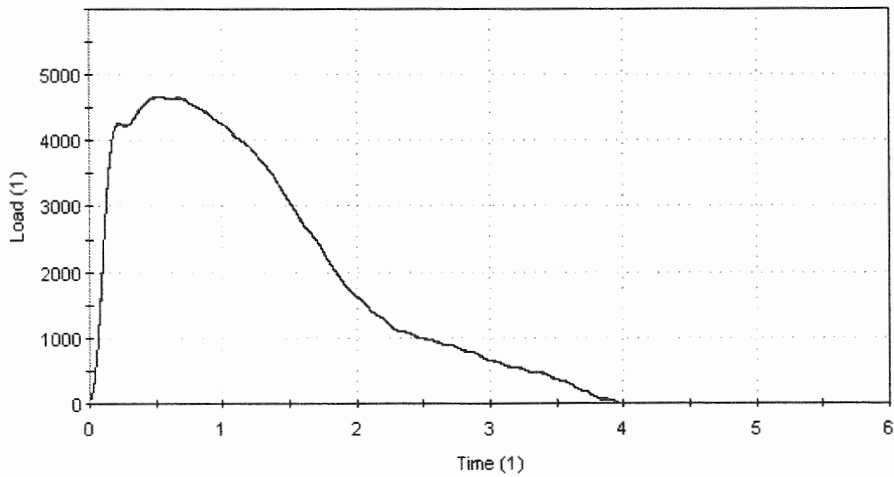
H11, 0°F



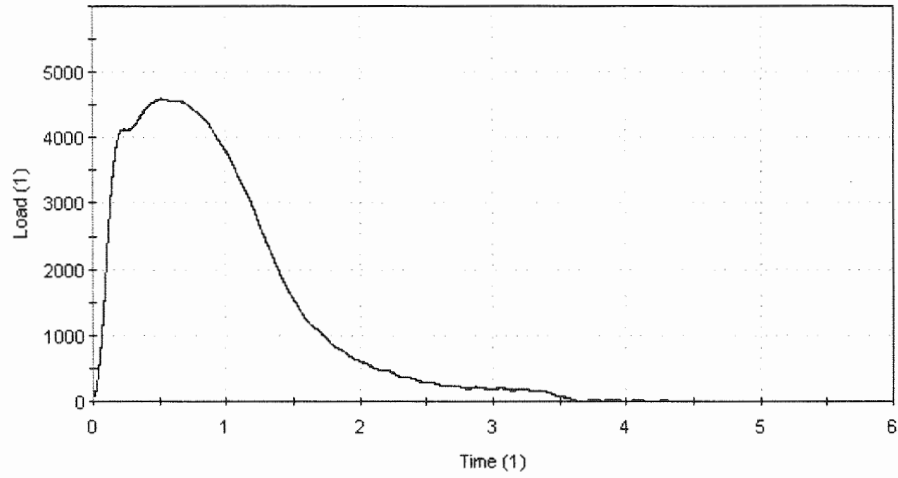
H10, 72°F



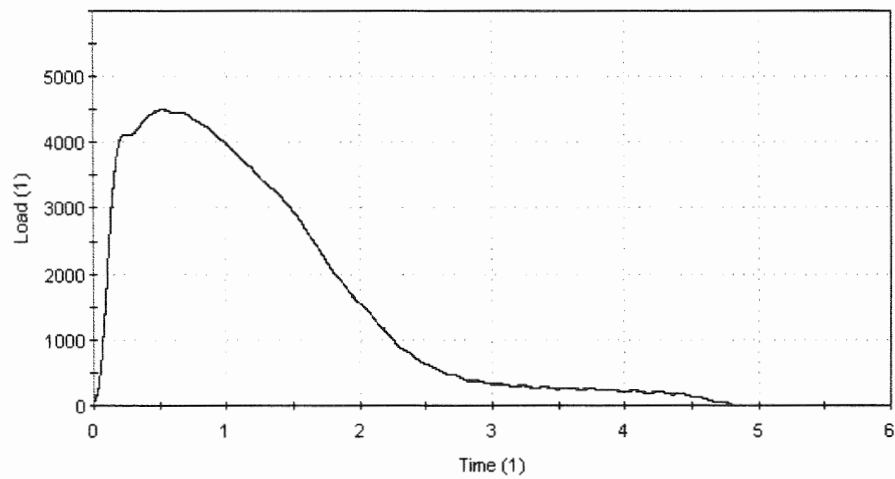
H9, 100°F



H15, 125°F



H16, 175°F



H13, 225°F

APPENDIX B

**CHARPY V-NOTCH SHIFT RESULTS FOR EACH
CAPSULE PREVIOUS FIT* VS. SYMMETRIC
HYPERBOLIC TANGENT CURVE-FITTING METHOD
(CVGRAPH VERSION 4.1)**

*The previous fit was plotted by PG&E using the EPRI Hyperbolic Tangent Curve Fitting Routine.

TABLE B-1
Changes in Average 30 ft-lb Temperatures for Intermediate Shell
Forging B4106-3 (Longitudinal Orientation)
Previous Fit vs. CVGRAPH 4.1 [°F]

Capsule	Previous Fit			CVGRAPH 4.1 Fit		
	Unirradiated	Irradiated	ΔT_{30}	Unirradiated	Irradiated	ΔT_{30}
S	5	3	-2	5.14	3.36	-1.78
Y	5	52	47	5.14	53.81	48.66
V	-	-	-	5.14	39.46	34.32

TABLE B-2
Changes in Average 50 ft-lb Temperatures for Intermediate Shell
Forging B4106-3 (Longitudinal Orientation)
Previous Fit vs. CVGRAPH 4.1 [°F]

Capsule	Previous Fit			CVGRAPH 4.1 Fit		
	Unirradiated	Irradiated	ΔT_{50}	Unirradiated	CVGRAPH Fit	ΔT_{50}
S	41	45	4	39.31	45.43	6.11
Y	41	94	53	39.31	91.82	52.51
V	-	-	-	39.31	77.51	38.19

TABLE B-3
Changes in Average 35 mil Lateral Expansion Temperatures for Intermediate Shell
Forging B4106-3 (Longitudinal Orientation)
Previous Fit vs. CVGRAPH 4.1 [°F]

Capsule	Previous Fit			CVGRAPH 4.1 Fit		
	Unirradiated	Irradiated	ΔT_{35}	Unirradiated	Irradiated	ΔT_{35}
S	29	29	0	28.65	28.92	0.27
Y	29	75	46	28.65	74.89	46.24
V	-	-	-	28.65	89.72	61.07

TABLE B-4
Changes in Average Energy Absorption at Full Shear for Intermediate Shell
Forging B4106-3 (Longitudinal Orientation)
Previous Fit vs. CVGRAPH 4.1 [ft-lb]

Capsule	Previous Fit*			CVGRAPH 4.1 Fit		
	Unirradiated	Irradiated	ΔE	Unirradiated	Irradiated	ΔE
S	122	126	4	118	126	8
Y	122	119 (110)	-3 (-12)	118	110	-8
V	-	-	-	118	121	3

*Values in parenthesis were calculated per the definition of Upper Shelf Energy given in ASTM E185-82. Note that the CVGRAPH USE values were also defined by ASTM E185-82.

TABLE B-5
Changes in Average 30 ft-lb Temperatures for Surveillance Weld Material
Previous Fit vs. CVGRAPH 4.1 [°F]

Capsule	Previous Fit			CVGRAPH 4.1 Fit		
	Unirradiated	Irradiated	ΔT_{30}	Unirradiated	Irradiated	ΔT_{30}
S	-67	43	110	-65.62	45.17	110.79
Y	-67	167	234	-65.62	166.97	232.59
V	-	-	-	-65.62	135.45	201.07

TABLE B-6
Changes in Average 50 ft-lb Temperatures for Surveillance Weld Material
Previous Fit vs. CVGRAPH 4.1 [°F]

Capsule	Previous Fit			CVGRAPH 4.1 Fit		
	Unirradiated	Irradiated	ΔT_{50}	Unirradiated	Irradiated	ΔT_{50}
S	-23	125	148	-24.16	120.38	144.54
Y	-23	253	276	-24.16	255.73	279.9
V	-	-	-	-24.16	219.26	243.43

TABLE B-7
Changes in Average 35 mil Lateral Expansion Temperatures for Surveillance Weld Material
Previous Fit vs. CVGRAPH 4.1 [°F]

Capsule	Previous Fit			CVGRAPH 4.1 Fit		
	Unirradiated	Irradiated	ΔT_{35}	Unirradiated	Irradiated	ΔT_{35}
S	-46	96	142	-46.52	95.28	141.81
Y	-46	195	241	-46.52	194.25	240.77
V	-	-	-	-46.52	220.66	267.19

TABLE B-8
Changes in Average Energy Absorption at Full Shear for Surveillance Weld Material
Previous Fit vs. CVGRAPH 4.1 [ft-lb]

Capsule	Previous Fit*			CVGRAPH 4.1 Fit		
	Unirradiated	Irradiated	ΔE	Unirradiated	Irradiated	ΔE
S	98	87	-11	91	81	-10
Y	98	66 (60)	-32 (-38)	91	60	-31
V	-	-	-	91	66	-25

*Values in parenthesis were calculated per the definition of Upper Shelf Energy given in ASTM E185-82. Note that the CVGRAPH USE values were also defined by ASTM E185-82.

TABLE B-9
Changes in Average 30 ft-lb Temperatures for the Weld Heat-Affected-Zone Material
Previous Fit vs. CVGRAPH 4.1 [°F]

Capsule	Previous Fit			CVGRAPH 4.1 Fit		
	Unirradiated	Irradiated	ΔT_{30}	Unirradiated	Irradiated	ΔT_{30}
S	-168	-91	77	-163.55	-91.24	72.31
Y	-168	-84	84	-163.55	-83.77	79.77
V	-	-	-	-163.55	-52.65	110.9

TABLE B-10
Changes in Average 50 ft-lb Temperatures for the Weld Heat-Affected-Zone Material
Previous Fit vs. CVGRAPH 4.1 [°F]

Capsule	Previous Fit			CVGRAPH 4.1 Fit		
	Unirradiated	Irradiated	ΔT_{50}	Unirradiated	Irradiated	ΔT_{50}
S	-111	-55	56	-111.75	-55.29	56.46
Y	-111	-36	75	-111.75	-35.96	75.78
V	-	-	-	-111.75	-1.98	109.77

TABLE B-11
Changes in Average 35 mil Lateral Expansion Temperatures for the Weld Heat-Affected-Zone Material
Previous Fit vs. CVGRAPH 4.1 [°F]

Capsule	Previous Fit			CVGRAPH 4.1 Fit		
	Unirradiated	Irradiated	ΔT_{35}	Unirradiated	Irradiated	ΔT_{35}
S	-107	-64	43	-107.5	-64.26	43.24
Y	-107	-36	71	-107.5	-36.47	71.03
V	-	-	-	-107.5	18.76	126.27

TABLE B-12
Changes in Average Energy Absorption at Full Shear for the Weld Heat-Affected-Zone Material
Previous Fit vs. CVGRAPH 4.1 [ft-lb]

Capsule	Previous Fit*			CVGRAPH 4.1 Fit		
	Unirradiated	Irradiated	ΔE	Unirradiated	Irradiated	ΔE
S	147	125	-22	136	125	-11
Y	147	110 (109)	-37 (-38)	136	109	-27
V	-	-	-	136	116	-20

*Values in parenthesis were calculated per the definition of Upper Shelf Energy given in ASTM E185-82.
Note that the CVGRAPH USE values were also defined by ASTM E185-82.

TABLE B-13
Changes in Average 30 ft-lb Temperatures for the Correlation Monitor Material
Previous Fit vs. CVGRAPH 4.1 [°F]

Capsule	Previous Fit			CVGRAPH 4.1 Fit		
	Unirradiated	Irradiated	ΔT_{30}	Unirradiated	Irradiated	ΔT_{30}
S	46	112	66	46.44	112.06	65.62
Y	46	158	112	46.44	162.23	115.79
V	-	-	-	46.44	163.05	116.61

TABLE B-14
Changes in Average 50 ft-lb Temperatures for the Correlation Monitor Material
Previous Fit vs. CVGRAPH 4.1 [°F]

Capsule	Previous Fit			CVGRAPH 4.1 Fit		
	Unirradiated	Irradiated	ΔT_{50}	Unirradiated	Irradiated	ΔT_{50}
S	78	146	68	78.3	143.42	65.11
Y	78	190	112	78.3	188.9	110.59
V	-	-	-	78.3	197.42	119.12

TABLE B-15
Changes in Average 35 mil Lateral Expansion Temperatures for the Correlation Monitor Material
Previous Fit vs. CVGRAPH 4.1 [°F]

Capsule	Previous Fit			CVGRAPH 4.1 Fit		
	Unirradiated	Irradiated	ΔT_{35}	Unirradiated	Irradiated	ΔT_{35}
S	59	124	65	58.96	124.49	65.53
Y	59	178	119	58.96	178.01	119.05
V	-	-	-	58.96	213.46	154.49

TABLE B-16
Changes in Average Energy Absorption at Full Shear for the Correlation Monitor Material
Previous Fit vs. CVGRAPH 4.1 [ft-lb]

Capsule	Previous Fit*			CVGRAPH 4.1 Fit		
	Unirradiated	Irradiated	ΔE	Unirradiated	Irradiated	ΔE
S	124	123	-1	123	120	-3
Y	124	122 (112)	-2 (-12)	123	112	-11
V	-	-	-	123	117	-6

*Values in parenthesis were calculated per the definition of Upper Shelf Energy given in ASTM E185-82.
Note that the CVGRAPH USE values were also defined by ASTM E185-82.

APPENDIX C

CHARPY V-NOTCH PLOTS FOR EACH CAPSULE
USING SYMMETRIC HYPERBOLIC TANGENT
CURVE-FITTING METHOD

Contained in Table C-1 are the upper shelf energy values used as input for the generation of the Charpy V-notch plots using CVGRAPH, Version 4.1. The definition for Upper Shelf Energy (USE) is given in ASTM E185-82, Section 4.18, and reads as follows:

“upper shelf energy level – the average energy value for all Charpy specimens (normally three) whose test temperature is above the upper end of the transition region. For specimens tested in sets of three at each test temperature, the set having the highest average may be regarded as defining the upper shelf energy.”

If there are specimens tested in set of three at each temperature Westinghouse reports the set having the highest average energy as the USE (usually unirradiated material). If the specimens were not tested in sets of three at each temperature Westinghouse reports the average of all 100% shear Charpy data as the USE. Hence, the USE values reported in Table C-1 and used to generate the Charpy V-notch curves were determined utilizing this methodology.

The lower shelf energy values were fixed at 2.2* ft-lb for all cases.

Table C-1 Upper Shelf Energy Values Fixed in CVGRAPH [ft-lb]				
Material	Unirradiated	Capsule S	Capsule Y	Capsule V
Intermediate Shell Plate B4106-3 (Longitudinal Orientation)	118	126	110	121
Weld Metal (heat # 27204)	91	81	60	66
HAZ Material	136	125	109	116
Correlation Monitor Material	123	120	112	117

*The Charpy V-notch curves show a value of 2.19 ft-lb, rather than 2.2. This is an inconsistency with the CVGraph program; the value of 2.2 is entered into the program, however, the value of 2.19 appears on the plot. This inconsistency is not expected to alter the results.

INTER SHELL PLATE B4106-3 UNIRR (LONG)

236940

CVGRAPH 4.1 Hyperbolic Tangent Curve Printed at 11:11:43 on 08-19-2002

Page 1

Coefficients of Curve 1

A = 60.09

B = 57.9

C = 85.44

T0 = 54.37

Equation is: $CVN = A + B * [\tanh((T - T0)/C)]$

Upper Shelf Energy: 118 Fixed Temp. at 30 ft-lbs: 5.1 Temp. at 50 ft-lbs: 39.3 Lower Shelf Energy: 2.19 Fixed

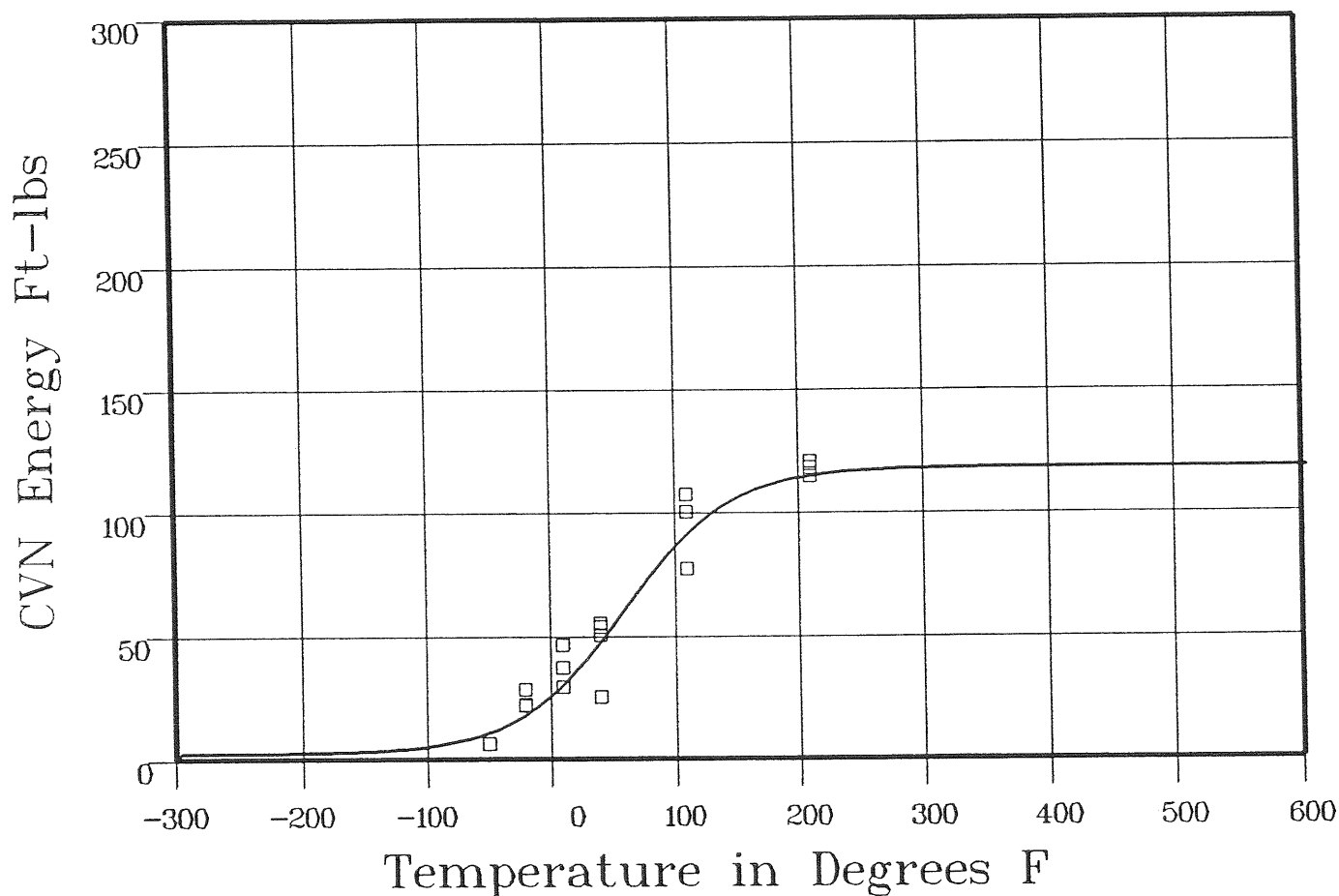
Material: PLATE SA533B1

Heat Number: B4106-3

Orientation: LT

Capsule: UNIRR

Total Fluence:



Plant: DC1 Cap: UNIRR Data Set(s) Plotted Material: PLATE SA533B1 Ori: LT Heat #: B4106-3

Charpy V-Notch Data

Temperature	Input CVN Energy	Computed CVN Energy	Differential
-50	6	11.45	-5.45
-50	6	11.45	-5.45
-50	6	11.45	-5.45
-20	21.5	19.47	2.02
-20	28	19.47	8.52
-20	22	19.47	2.52
10	37	32.46	4.53
10	46	32.46	13.53
10	29	32.46	-3.46

**** Data continued on next page ****

236940

INTER SHELL PLATE B4106-3 UNIRR (LONG)

Page 2

Material: PLATE SA533B1

Heat Number: B4106-3

Orientation: LT

Capsule: UNIRR

Total Fluence:

Charpy V-Notch Data (Continued)

Temperature	Input CVN Energy	Computed CVN Energy	Differential
40	55	50.44	4.55
40	25	50.44	-25.44
40	53.5	50.44	3.05
40	50	50.44	-.44
110	77	93.23	-16.23
110	100	93.23	6.76
110	107	93.23	13.76
210	120.5	115.04	5.45
210	118	115.04	2.95
210	114.5	115.04	-.54
			SUM of RESIDUALS = 5.13

INTER SHELL PLATE B4106-3 CAPSULE S (LONG)

CVGRAPH 4.1 Hyperbolic Tangent Curve Printed at 11:11:43 on 08-19-2002

Page 1

Coefficients of Curve 2

A = 64.09

B = 61.9

C = 108.49

T0 = 70.58

Equation is: $CVN = A + B * [\tanh((T - T0)/C)]$

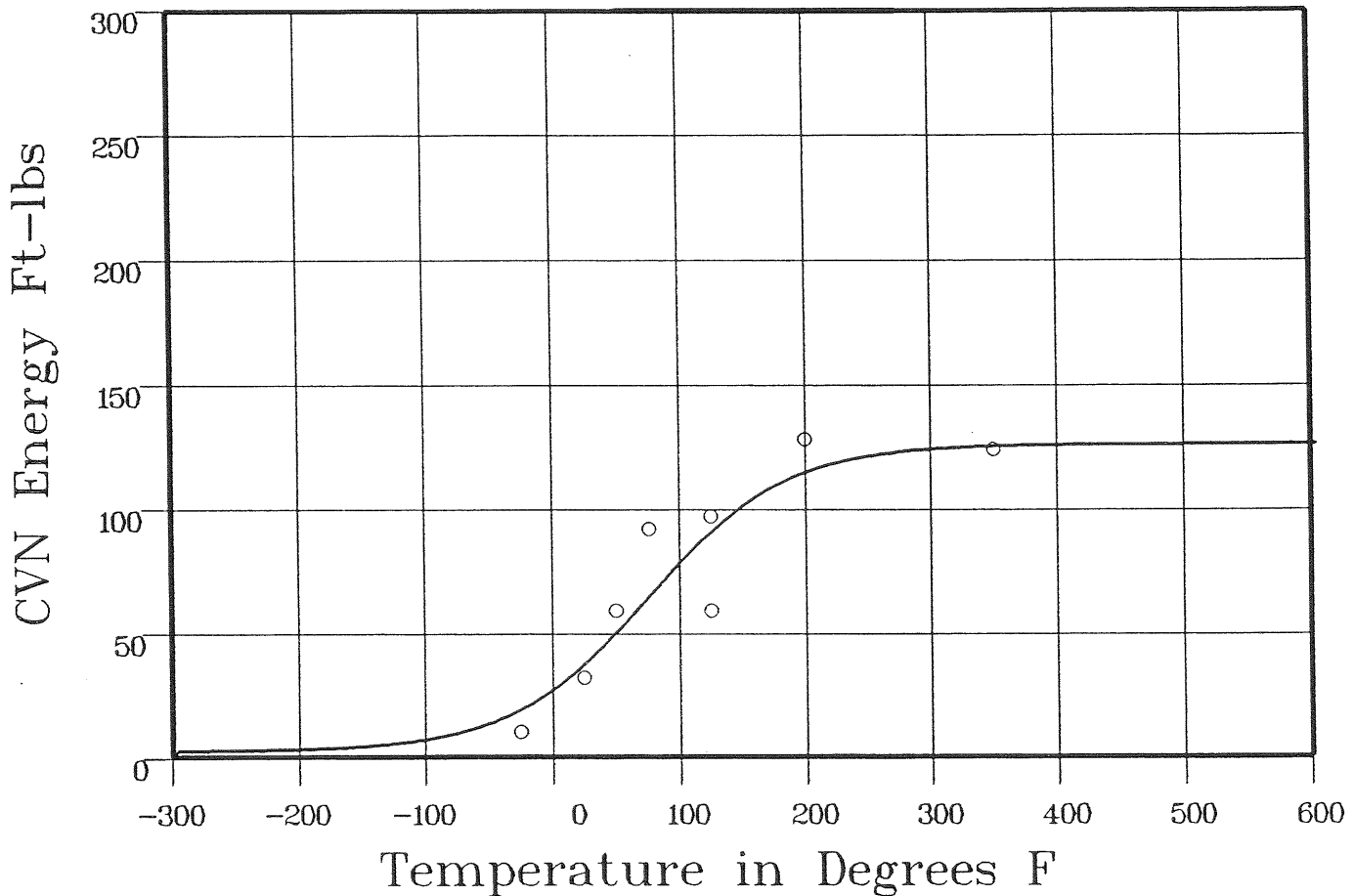
Upper Shelf Energy: 126 Fixed Temp. at 30 ft-lbs: 3.3 Temp. at 50 ft-lbs: 45.4 Lower Shelf Energy: 2.19 Fixed

Material: PLATE SA533B1

Heat Number: B4106-3

Orientation: LT

Capsule: Total Fluence: 2.84E+18



Data Set(s) Plotted

Plant: DCI

Cap: S

Material: PLATE SA533B1

Ori: LT

Heat #: B4106-3

Charpy V-Notch Data

Temperature	Input CVN Energy	Computed CVN Energy	Differential
-25	10	20.33	-10.33
25	32	39.51	-7.51
50	59	52.49	6.5
76	92	67.18	24.81
125	97	92.78	4.21
125	59	92.78	-33.78
200	128	115.56	12.43
350	124	125.28	-1.28

SUM of RESIDUALS = -4.95

INTER SHELL PLATE B4106-3 CAPSULE Y (LONG)

236940

CVGRAPH 4.1 Hyperbolic Tangent Curve Printed at 11:11:43 on 08-19-2002

Page 1

Coefficients of Curve 3

A = 56.09

B = 53.9

C = 91.63

T0 = 102.24

Equation is: $CVN = A + B * [\tanh((T - T0)/C)]$

Upper Shelf Energy: 110 Fixed Temp. at 30 ft-lbs: 53.8 Temp. at 50 ft-lbs: 91.8 Lower Shelf Energy: 2.19 Fixed

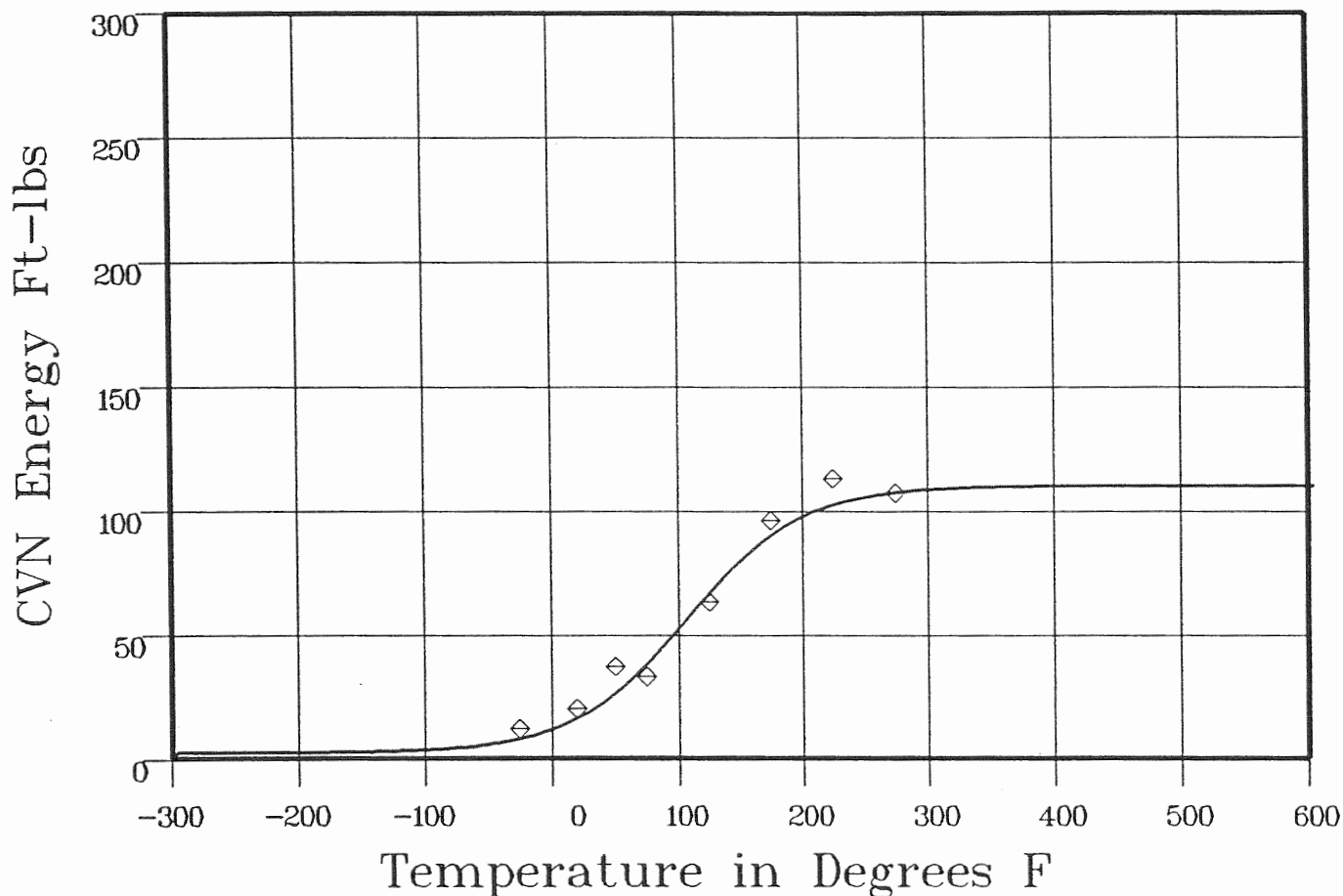
Material: PLATE SA533B1

Heat Number: B4106-3

Orientation: LT

Capsule: Y

Total Fluence: 1.05E+19



Data Set(s) Plotted
Plant: DCI Cap: Y Material: PLATE SA533B1 Ori: LT Heat #: B4106-3

Charpy V-Notch Data

Temperature	Input CVN Energy	Computed CVN Energy	Differential
-25	12	8.51	3.48
20	20	17.55	2.44
50	37	28.31	8.68
75	33	40.53	-7.53
125	63	69.21	-6.21
175	96	91.7	4.29
225	113	103.07	9.92
275	107	107.57	-5.7

SUM of RESIDUALS = 14.5

INTER SHELL PLATE B4106-3 CAPSULE V (LONG)

236940

CVGRAPH 4.1 Hyperbolic Tangent Curve Printed at 11:11:43 on 08-19-2002

Page 1

Coefficients of Curve 4

A = 61.59	B = 59.4	C = 96.29	T0 = 96.56
-----------	----------	-----------	------------

$$\text{Equation is: } \text{CVN} = A + B * [\tanh((T - T0)/C)]$$

Upper Shelf Energy: 121 Fixed Temp. at 30 ft-lbs: 39.4 Temp. at 50 ft-lbs: 77.5 Lower Shelf Energy: 2.19 Fixed

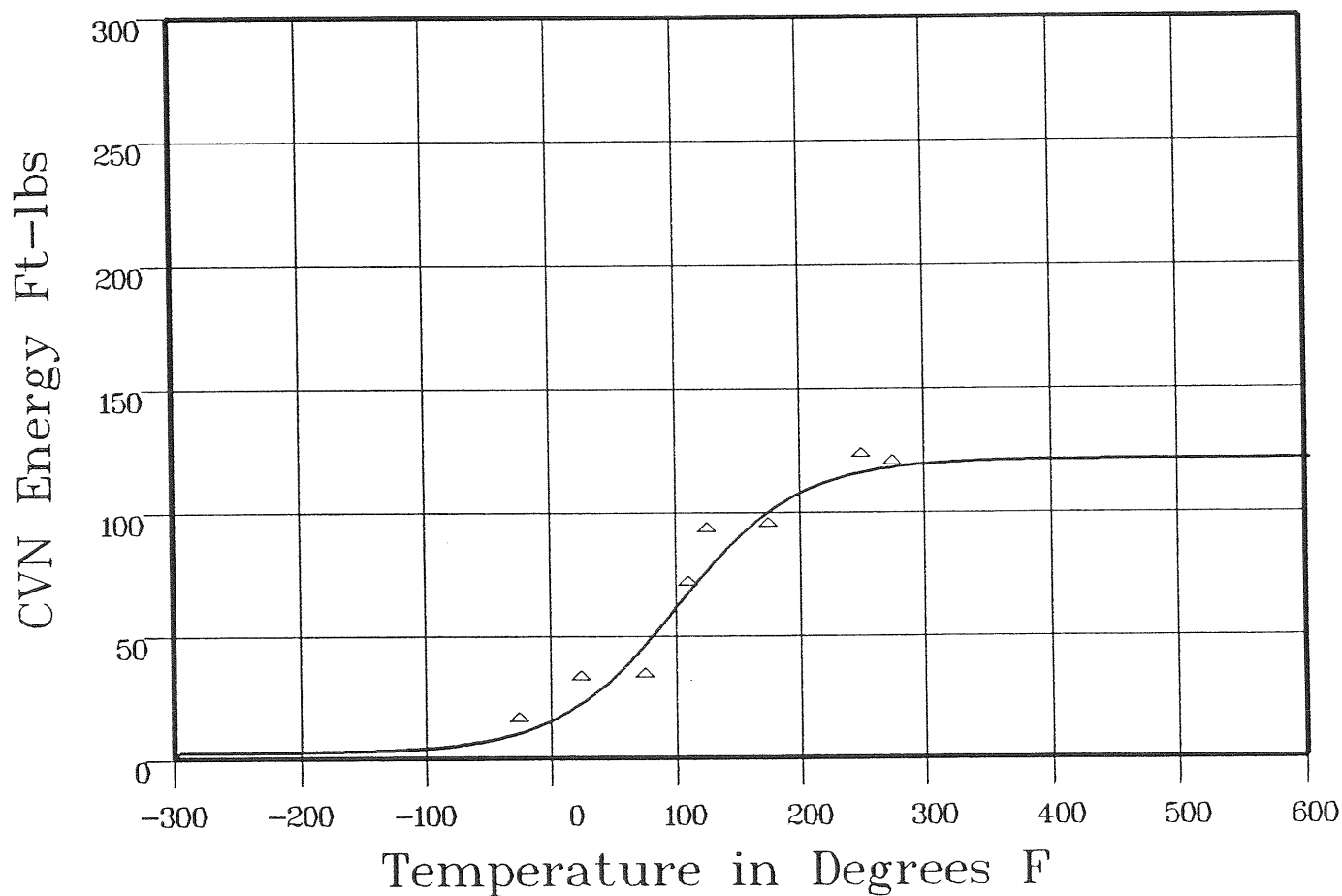
Material: PLATE SA533B1

Heat Number: B4106-3

Orientation: LT

Capsule: V

Total Fluence: 1.37E+19



Plant: DCI Cap: V Data Set(s) Plotted Material: PLATE SA533B1 Ori: LT Heat #: B4106-3

Charpy V-Notch Data

Temperature	Input CVN Energy	Computed CVN Energy	Differential
-25	15	11	3.99
25	32	24.11	7.88
75	33	48.51	-15.51
110	70	69.83	.16
125	92	78.64	13.35
175	94	101.52	-7.52
250	122	116.28	5.71

**** Data continued on next page ****

INTER SHELL PLATE B4106-3 CAPSULE V (LONG)

Page 2

236940

Material: PLATE SA533B1

Heat Number: B4106-3

Orientation: LT

Capsule: V

Total Fluence: 1.37E+19

Charpy V-Notch Data (Continued)

Temperature
275

Input CVN Energy
119

Computed CVN Energy
118.15

Differential
.84

SUM of RESIDUALS = 8.91

INTER SHELL PLATE B4106-3 UNIRR (LONG) 236940

CVGRAPH 4.1 Hyperbolic Tangent Curve Printed at 11:38:29 on 08-19-2002

Page 1

Coefficients of Curve 1

A = 45.01

B = 44.01

C = 88.8

T0 = 49.21

Equation is: $LE = A + B * [\tanh((T - T0)/C)]$

Upper Shelf LE: 89.02

Temperature at LE 35: 28.6

Lower Shelf LE: 1 Fixed

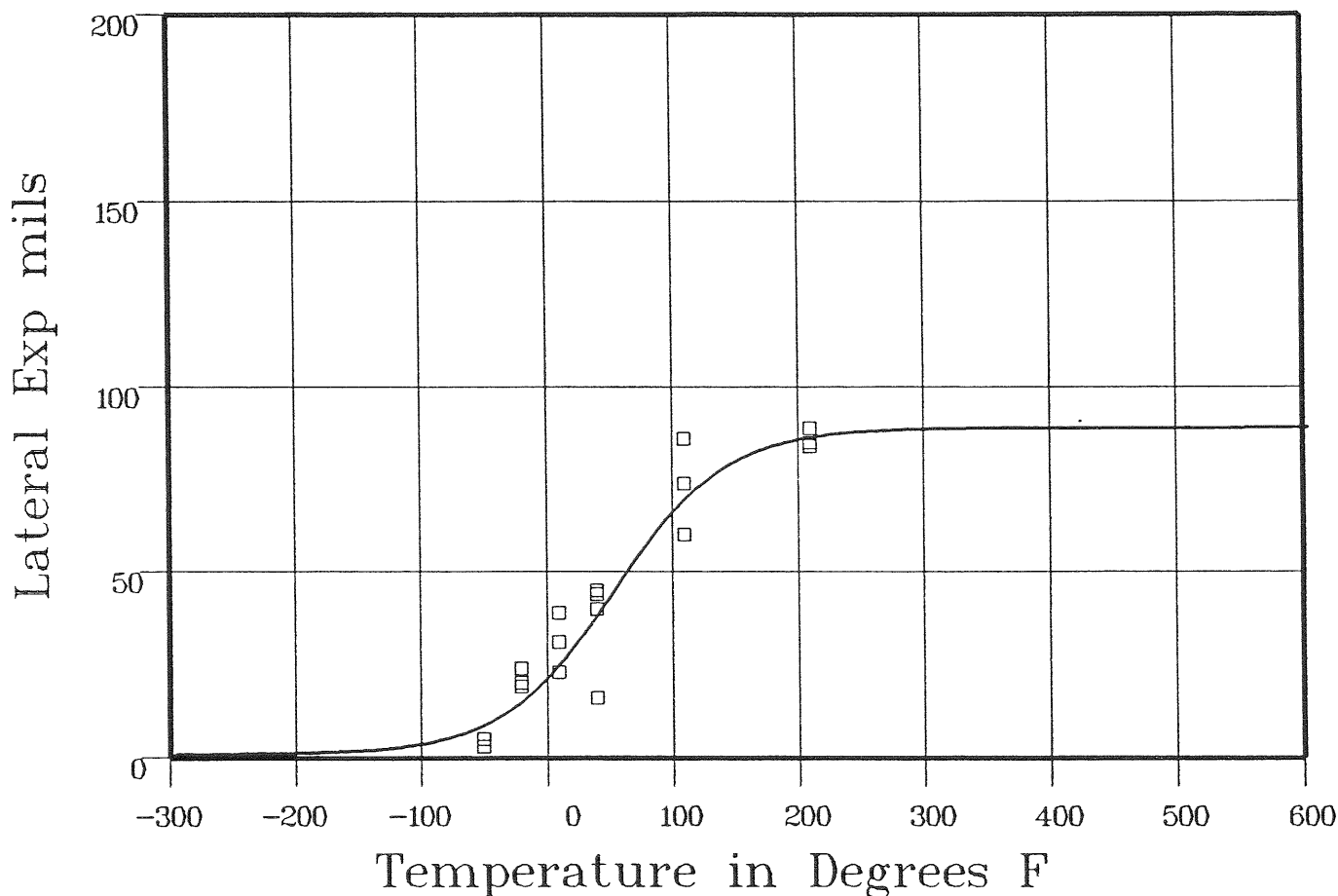
Material: PLATE SA533B1

Heat Number: B4106-3

Orientation: LT

Capsule: UNIRR

Total Fluence:



Plant: DCI Cap: UNIRR Material: PLATE SA533B1 Ori: LT Heat #: B4106-3

Charpy V-Notch Data

Temperature	Input Lateral Expansion	Computed LE	Differential
-50	3	9.51	-6.51
-50	3	9.51	-6.51
-50	5	9.51	-4.51
-20	19	16.3	2.69
-20	24	16.3	7.69
-20	20	16.3	3.69
10	31	26.74	4.25
10	39	26.74	12.25
10	23	26.74	-3.74

**** Data continued on next page ****

236940 INTER SHELL PLATE B4106-3 UNIRR (LONG)

Page 2

Material: PLATE SA533B1

Heat Number: B4106-3

Orientation: LT

Capsule: UNIRR

Total Fluence:

Charpy V-Notch Data (Continued)

Temperature	Input Lateral Expansion	Computed L.E.	Differential
40	44	40.46	3.53
40	16	40.46	-24.46
40	45	40.46	4.53
40	40	40.46	-.46
110	60	71.17	-11.17
110	74	71.17	2.82
110	86	71.17	14.82
210	84	86.73	-2.73
210	85	86.73	-1.73
210	89	86.73	2.26
			SUM of RESIDUALS = -3.27

INTER SHELL PLATE B4106-3 CAPSULE S (LONG)

CVGRAPH 4.1 Hyperbolic Tangent Curve Printed at 11:38:29 on 08-19-2002

236940

Page 1

Coefficients of Curve 2

A = 36.86

B = 35.86

C = 75.79

T0 = 32.87

Equation is: $LE = A + B * [\tanh((T - T0)/C)]$

Upper Shelf LE: 72.72

Temperature at LE 35: 28.9

Lower Shelf LE: 1 Fixed

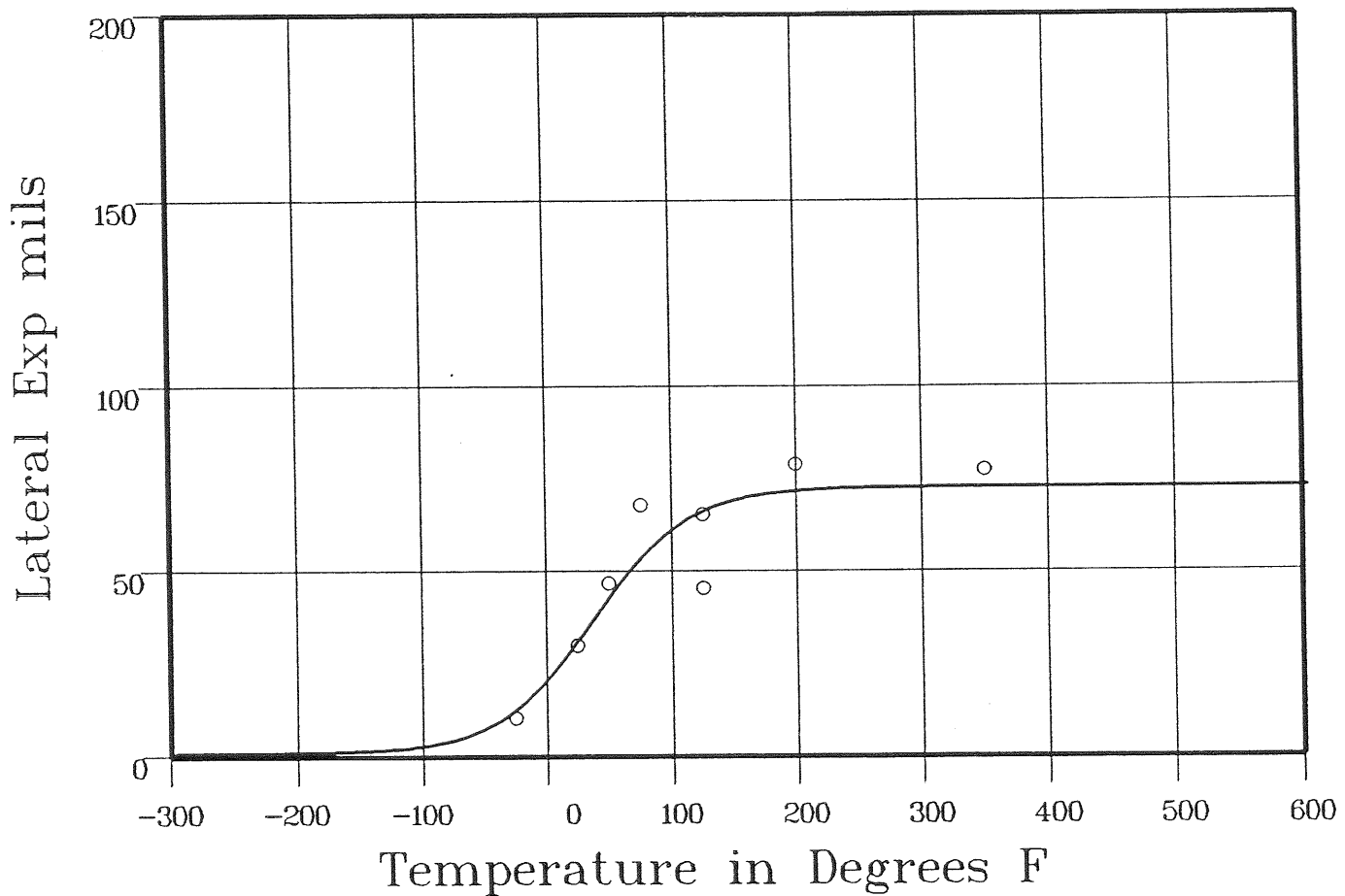
Material: PLATE SA533B1

Heat Number: B4106-3

Orientation: LT

Capsule: S

Total Fluence: 2.84E+18



Data Set(s) Plotted
Plant: DC1 Cap: S Material: PLATE SA533B1 Ori: LT Heat #: B4106-3

Charpy V-Notch Data

Temperature	Input Lateral Expansion	Computed LE	Differential
-25	10.5	13.79	-3.29
25	30	33.15	-3.15
50	47	44.83	2.16
76	68	55.32	12.67
125	65.5	66.92	-1.42
125	45.5	66.92	-21.42
200	79	71.86	7.13
350	77.5	72.71	4.78

SUM of RESIDUALS = -2.54

INTER SHELL PLATE B4106-3 CAPSULE Y (LONG)

236940

CVGRAPH 4.1 Hyperbolic Tangent Curve Printed at 11:38:29 on 08-19-2002

Page 1

Coefficients of Curve 3

A = 43.76

B = 42.76

C = 110.43

T0 = 97.85

Equation is: $LE = A + B * [\tanh((T - T0)/C)]$

Upper Shelf LE: 86.52

Temperature at LE 35: 74.8

Lower Shelf LE: 1 Fixed

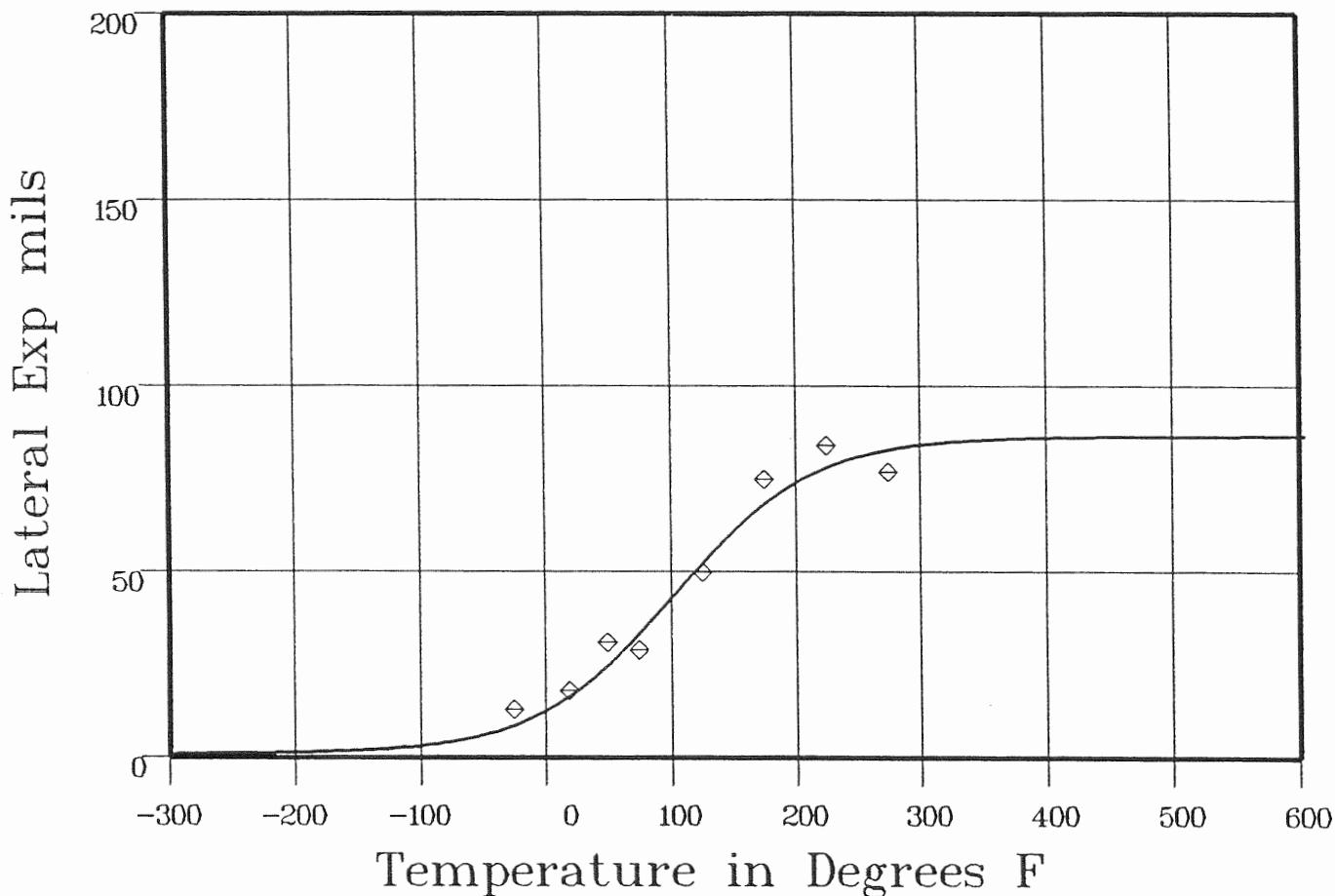
Material: PLATE SA533B1

Heat Number: B4106-3

Orientation: LT

Capsule: Y

Total Fluence: 1.05E+19



Data Set(s) Plotted

Plant: DC1

Cap: Y

Material: PLATE SA533B1

Ori: LT

Heat #: B4106-3

Charpy V-Notch Data

Temperature	Input Lateral Expansion	Computed LE	Differential
-25	13	9.34	3.65
20	18	17.78	21
50	31	26.31	4.68
75	29	35.03	-6.03
125	50	54.06	-4.06
175	75	69.56	5.43
225	84	78.74	5.25
275	77	83.19	-6.19

SUM of RESIDUALS = 2.94

INTER SHELL PLATE B4106-3 CAPSULE V (LONG)

CVGRAPH 4.1 Hyperbolic Tangent Curve Printed at 11:38:29 on 08-19-2002

Page 1

236940

Coefficients of Curve 4

A = 41.48

B = 40.48

C = 106.09

T0 = 106.87

Equation is: $LE = A + B * [\tanh((T - T0)/C)]$

Upper Shelf LE: 81.97

Temperature at LE 35: 89.7

Lower Shelf LE: 1 Fixed

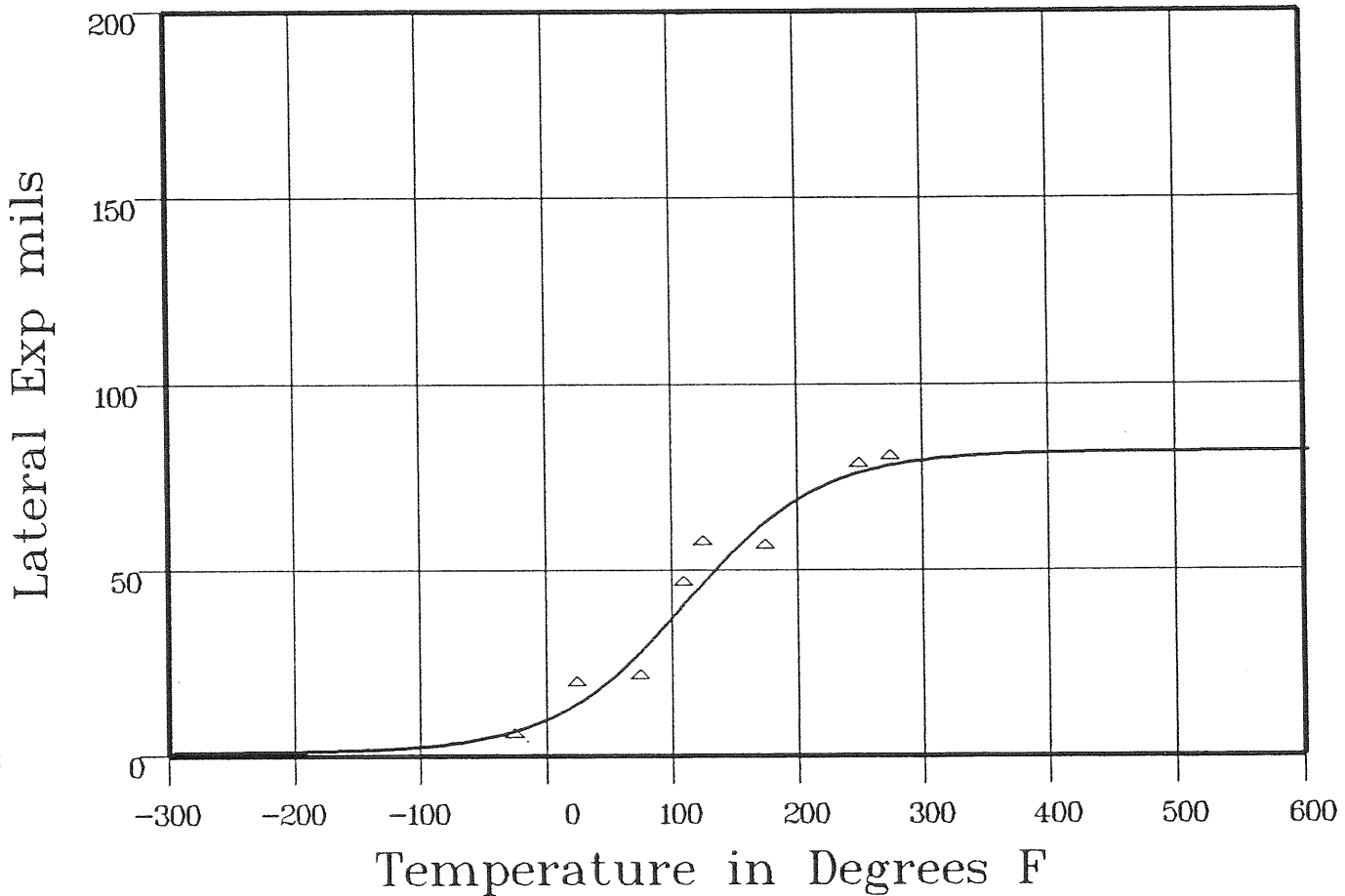
Material: PLATE SA533B1

Heat Number: B4106-3

Orientation: LT

Capsule: V

Total Fluence: 137E+19



Data Set(s) Plotted
 Plant: DCI Cap: V Material: PLATE SA533B1 Ori: LT Heat #: B4106-3

Charpy V-Notch Data

Temperature	Input Lateral Expansion	Computed LE	Differential
-25	5	7.22	-2.22
25	19	15.25	3.74
75	21	29.67	-8.67
110	46	42.68	3.31
125	57	48.33	8.66
175	56	64.41	-8.41
250	78	76.86	1.13

**** Data continued on next page ****

INTER SHELL PLATE B4106-3 CAPSULE V (LONG)

Page 2

236940

Material: PLATE SA533B1

Heat Number: B4106-3

Orientation: LT

Capsule: V

Total Fluence: 1.37E+19

Charpy V-Notch Data (Continued)

Temperature
275

Input Lateral Expansion
80

Computed L.E.
78.71

Differential
128

SUM of RESIDUALS = -1.18

INTER SHELL PLATE B4106-3 UNIRR (LONG)

CVGRAPH 4.1 Hyperbolic Tangent Curve Printed at 11:49:00 on 08-19-2002

236940

Page 1

Coefficients of Curve 1

A = 50

B = 50

C = 102.68

T0 = 77.35

Equation is: $\text{Shear}\% = A + B * [\tanh((T - T_0)/C)]$

Temperature at 50% Shear: 77.3

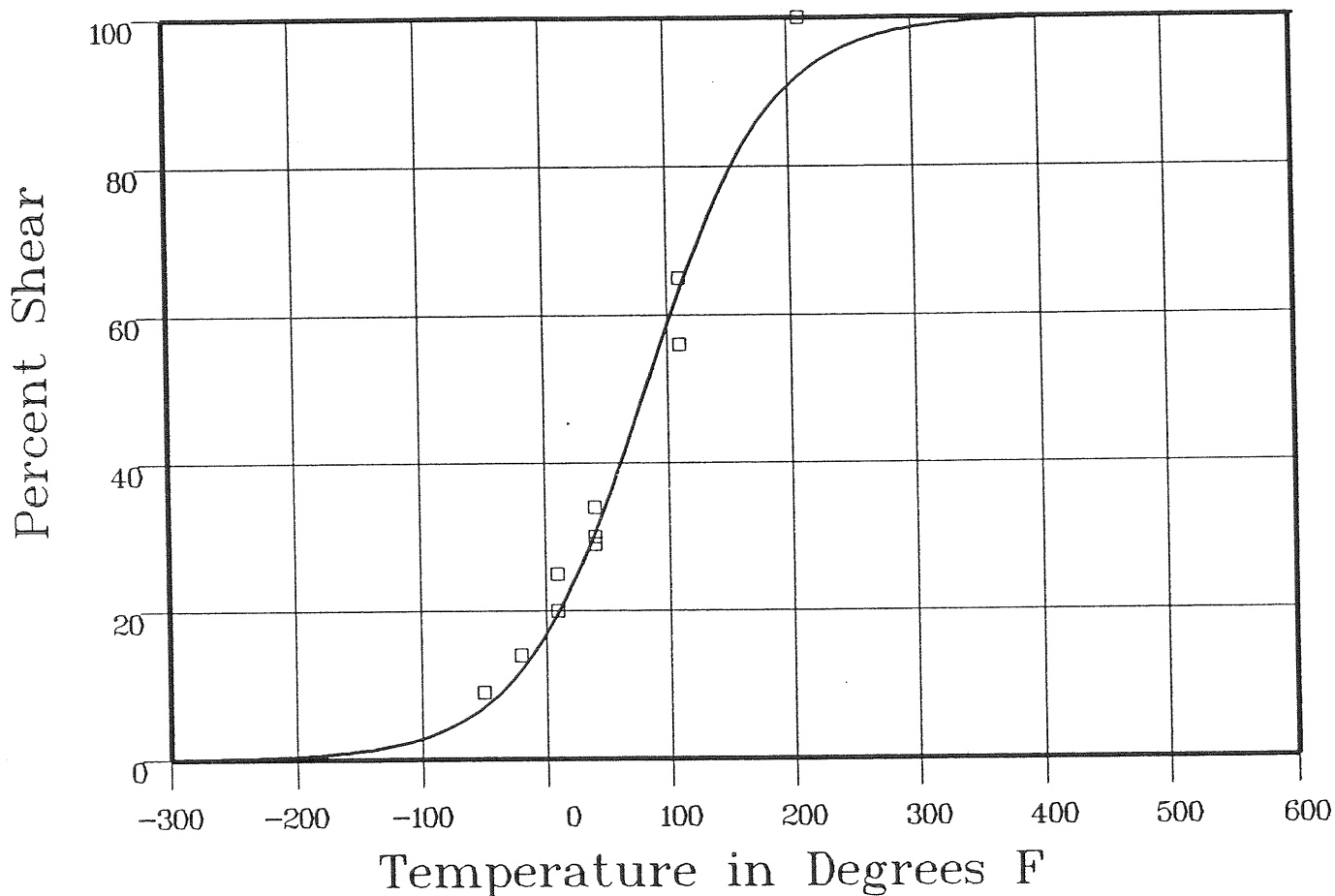
Material: PLATE SA533B1

Heat Number: B4106-3

Orientation: LT

Capsule: UNIRR

Total Fluence:



Data Set(s) Plotted
 Plant: DCI Cap: UNIRR Material: PLATE SA533B1 Ori: LT Heat #: B4106-3

Charpy V-Notch Data

Temperature	Input Percent Shear	Computed Percent Shear	Differential
-50	9	7.72	1.27
-50	9	7.72	1.27
-50	9	7.72	1.27
-20	14	13.05	.94
-20	14	13.05	.94
-20	14	13.05	.94
10	25	21.21	3.78
10	20	21.21	-1.21
10	25	21.21	3.78

**** Data continued on next page ****

INTER SHELL PLATE B4106-3 UNIRR (LONG)

Page 2

236940

Material: PLATE SA533B1

Heat Number: B4106-3

Orientation: LT

Capsule: UNIRR

Total Fluence:

Charpy V-Notch Data (Continued)

Temperature	Input Percent Shear	Computed Percent Shear	Differential
40	34	32.57	1.42
40	29	32.57	-3.57
40	34	32.57	1.42
40	30	32.57	-2.57
110	56	65.38	-9.38
110	65	65.38	-38
110	65	65.38	-38
210	100	92.98	7.01
210	100	92.98	7.01
210	100	92.98	7.01
			SUM of RESIDUALS = 20.62

INTER SHELL PLATE B4106-3 CAPSULE S (LONG)

CVGRAPH 4.1 Hyperbolic Tangent Curve Printed at 11:49:00 on 08-19-2002

236940

Page 1

Coefficients of Curve 2

A = 50

B = 50

C = 97

T0 = 87.89

Equation is: Shear% = A + B * [tanh((T - T0)/C)]

Temperature at 50% Shear: 87.8

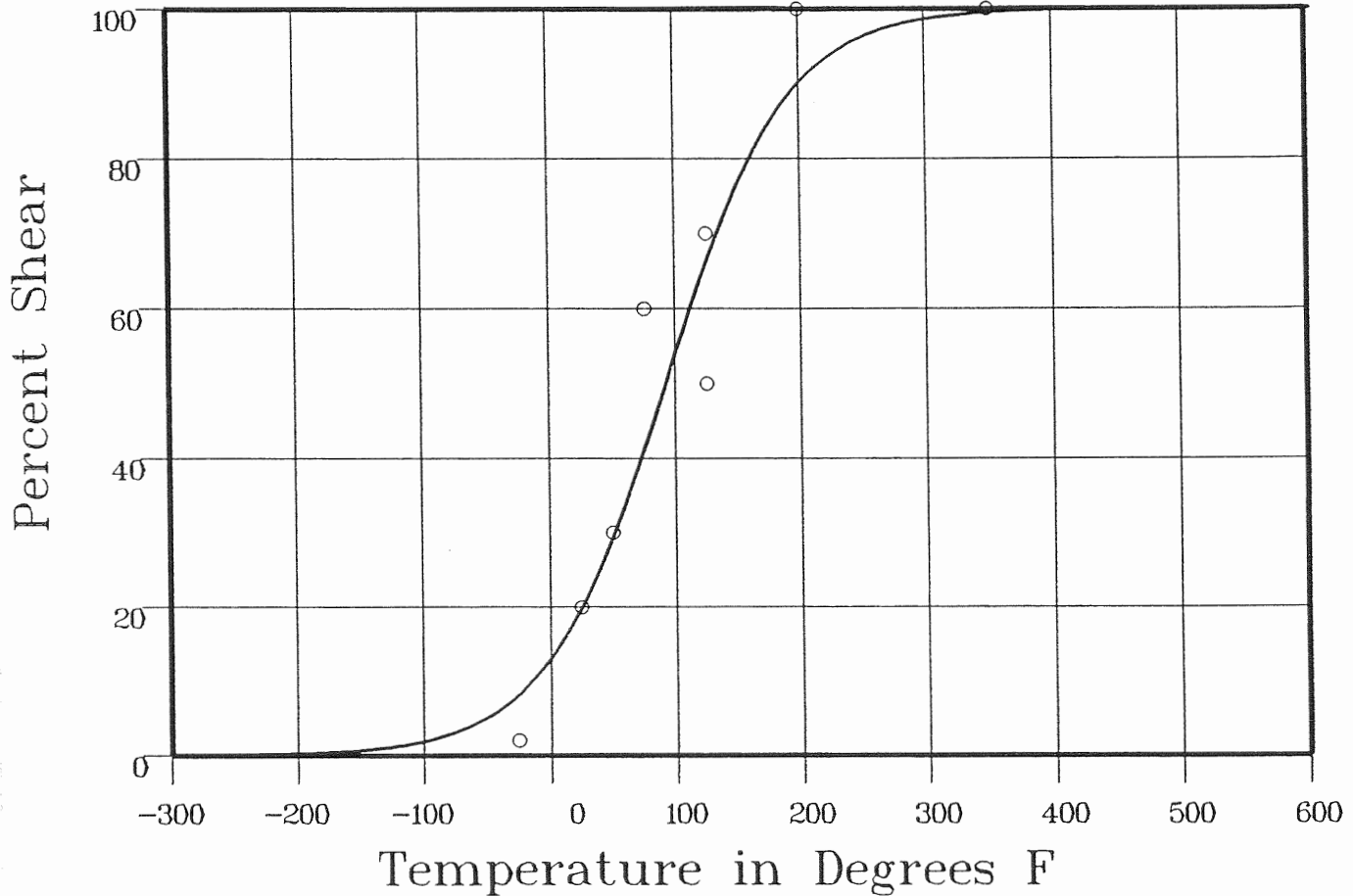
Material: PLATE SA533B1

Heat Number: B4106-3

Orientation: LT

Capsule: S

Total Fluence: 2.84E+18



Data Set(s) Plotted

Plant: DCI

Cap: S

Material: PLATE SA533B1

Ori: LT

Heat #: B4106-3

Charpy V-Notch Data

Temperature	Input Percent Shear	Computed Percent Shear	Differential
-25	2	8.88	-6.88
25	20	21.47	-1.47
50	30	31.4	-1.4
76	60	43.9	16.09
125	70	68.24	1.75
125	50	68.24	-18.24
200	100	90.98	9.01
350	100	99.55	.44

SUM of RESIDUALS = -.69

INTER SHELL PLATE B4106-3 CAPSULE Y (LONG)

236940

CVGRAPH 4.1 Hyperbolic Tangent Curve Printed at 11:49:00 on 08-19-2002

Page 1

Coefficients of Curve 3

A = 50	B = 50	C = 8724	T0 = 99.6
--------	--------	----------	-----------

Equation is: $\text{Shear}\% = A + B * [\tanh((T - T0)/C)]$

Temperature at 50% Shear: 99.6

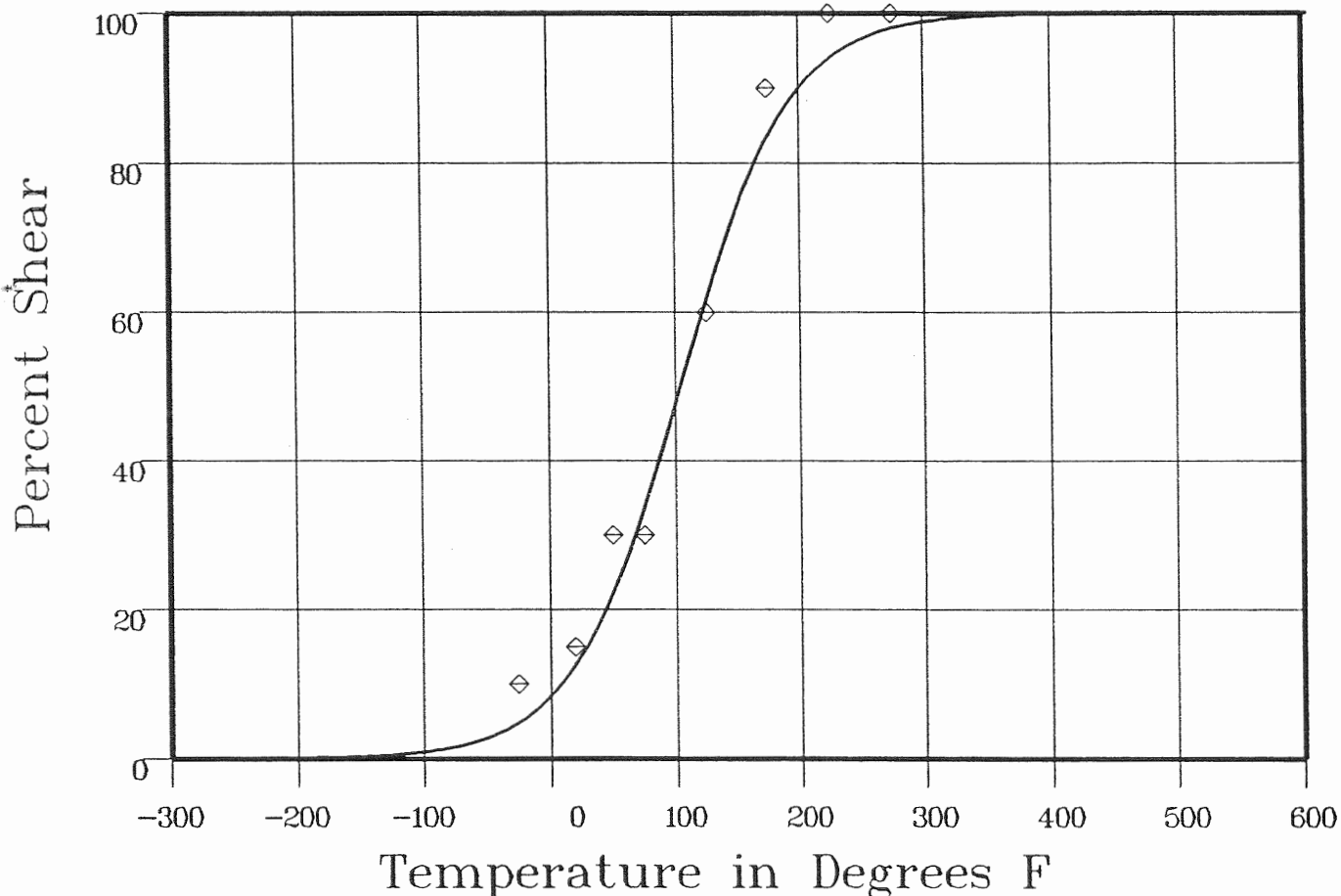
Material: PLATE SA533B1

Heat Number: B4106-3

Orientation: LT

Capsule: Y

Total Fluence: 1.05E+19



Data Set(s) Plotted

Plant: DCI

Cap: Y

Material: PLATE SA533B1

Ori: LT

Heat #: B4106-3

Charpy V-Notch Data

Temperature	Input Percent Shear	Computed Percent Shear	Differential
-25	10	5.43	4.56
20	15	13.88	1.11
50	30	24.28	5.71
75	30	36.25	-6.25
125	60	64.15	-4.15
175	90	84.91	5.08
225	100	94.65	5.34
275	100	98.23	1.76

SUM of RESIDUALS = 13.17

INTER SHELL PLATE B4106-3 CAPSULE V (LONG)

236940

CVGRAPH 4.1 Hyperbolic Tangent Curve Printed at 11:49:00 on 08-19-2002

Page 1

Coefficients of Curve 4

A = 50

B = 50

C = 72.05

T0 = 117.18

Equation is: $\text{Shear}\% = A + B * [\tanh((T - T0)/C)]$

Temperature at 50% Shear: 117.1

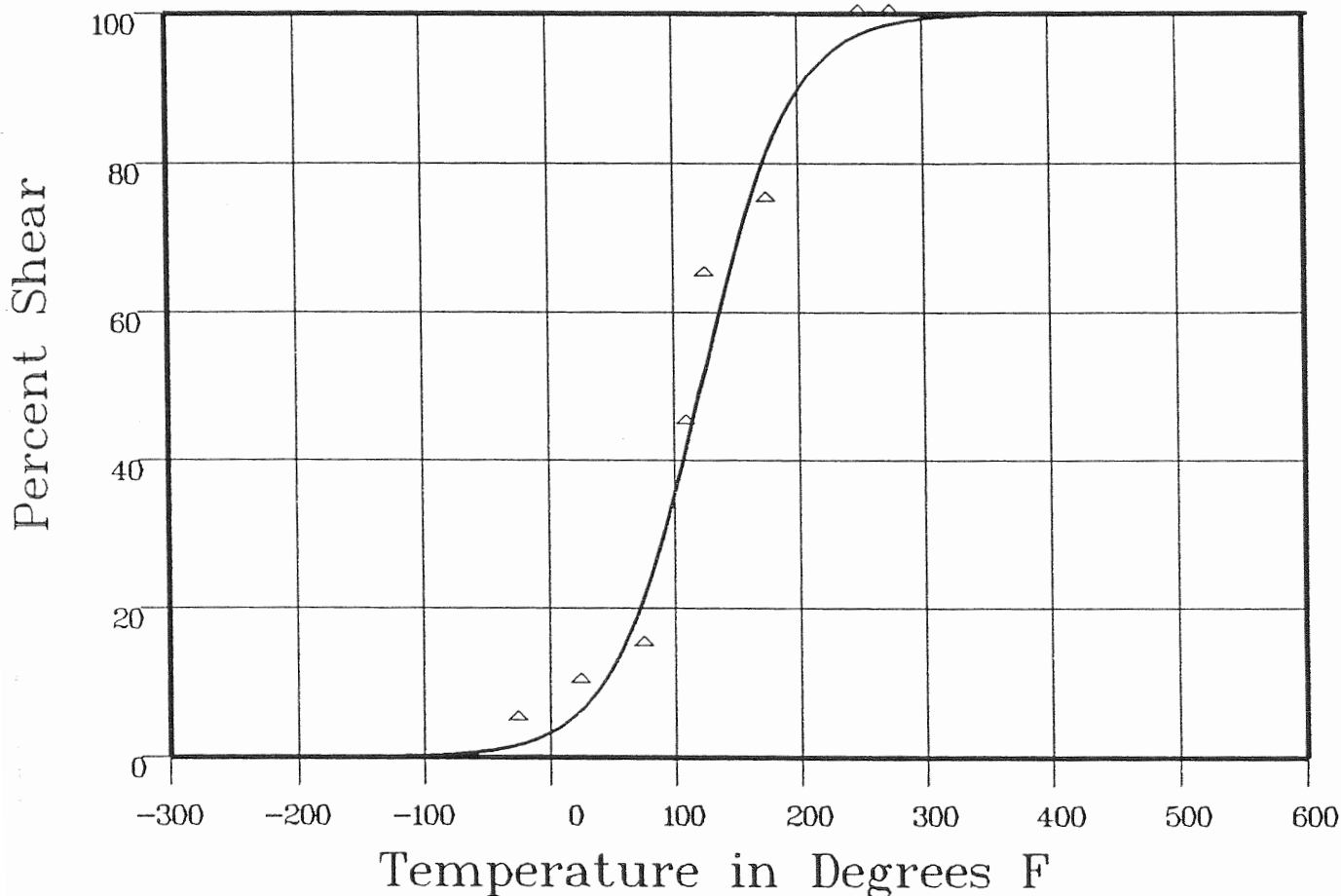
Material: PLATE SA533B1

Heat Number: B4106-3

Orientation: LT

Capsule: V

Total Fluence: 1.37E+19



Plant: DCI Cap: V Material: PLATE SA533B1 Ori: LT Heat #: B4106-3

Charpy V-Notch Data

Temperature	Input Percent Shear	Computed Percent Shear	Differential
-25	5	1.89	3.1
25	10	7.18	2.81
75	15	23.66	-8.66
110	45	45.02	-.02
125	65	55.39	9.6
175	75	83.26	-8.26
250	100	97.55	2.44

**** Data continued on next page ****

INTER SHELL PLATE B4106-3 CAPSULE V (LONG)

Page 2

236940

Material: PLATE SA533B1

Heat Number: B4106-3

Orientation: LT

Capsule: V

Total Fluence: 1.37E+19

Charpy V-Notch Data (Continued)

Temperature
275

Input Percent Shear
100

Computed Percent Shear
98.76

Differential
123

SUM of RESIDUALS = 223

WELD METAL UNIRRADIATED

236840

CVGRAPH 4.1 Hyperbolic Tangent Curve Printed at 12:20:17 on 08-19-2002

Page 1

Coefficients of Curve 1

A = 46.59

B = 44.4

C = 88.27

T0 = -30.93

Equation is: $CVN = A + B * [\tanh((T - T0)/C)]$

Upper Shelf Energy: 91 Fixed Temp. at 30 ft-lbs: -65.6 Temp. at 50 ft-lbs: -24.1 Lower Shelf Energy: 2.19 Fixed

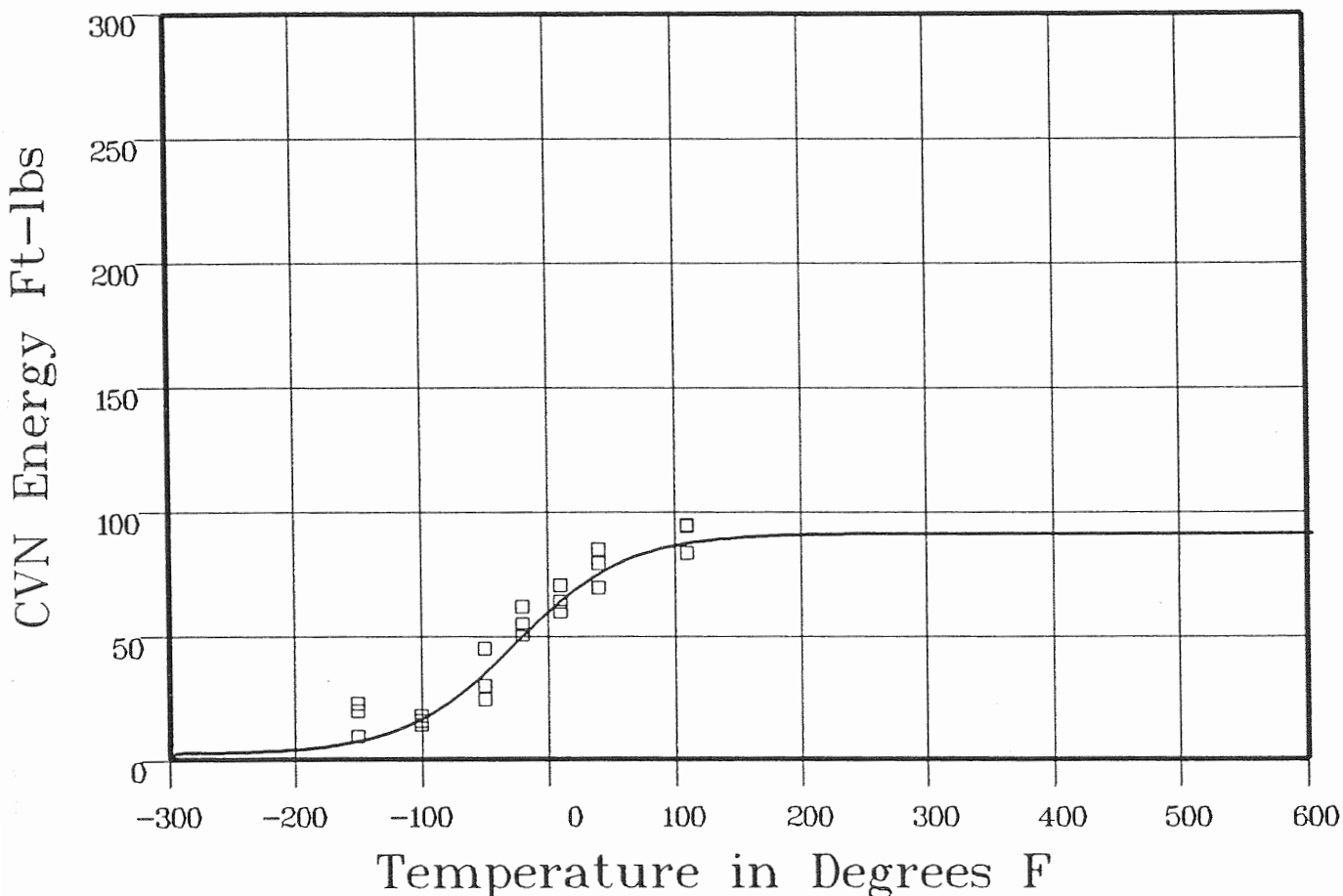
Material: WELD LINDE 1092

Heat Number: 27204 FLUX LOT 3714

Orientation:

Capsule: UNIRR

Total Fluence:



Data Set(s) Plotted

Plant: DCI

Cap: UNIRR

Material: WELD LINDE 1092

Ori:

Heat #: 27204 FLUX LOT 3714

Charpy V-Notch Data

Temperature	Input CVN Energy	Computed CVN Energy	Differential
-150	19.5	7.8	11.69
-150	9	7.8	1.19
-150	22.5	7.8	14.69
-100	15.5	17.55	-2.05
-100	17.5	17.55	-.05
-100	14	17.55	-3.55
-50	44.5	37.15	7.34
-50	24	37.15	-13.15
-50	29.5	37.15	-7.65

**** Data continued on next page ****

236940

WELD METAL UNIRRADIATED

Page 2

Material: WELD LINDE 1092

Heat Number: 27204 FLUX LOT 3714

Orientation:

Capsule: UNIRR

Total Fluence:

Charpy V-Notch Data (Continued)

Temperature	Input CVN Energy	Computed CVN Energy	Differential
-20	50	52.07	-2.07
-20	61.5	52.07	9.42
-20	54.5	52.07	2.42
10	63.5	65.83	-2.33
10	59.5	65.83	-6.33
10	70	65.83	4.16
40	84.5	76.17	8.32
40	79	76.17	2.82
40	69	76.17	-7.17
110	83	87.49	-4.49
110	94.5	87.49	7
110	94	87.49	6.5
			SUM of RESIDUALS = 26.7

WELD METAL CAPSULE S

CVGRAPH 4.1 Hyperbolic Tangent Curve Printed at 12:20:17 on 08-19-2002

Page 1

Coefficients of Curve 2

A = 41.59

B = 39.4

C = 144.65

T0 = 89.06

Equation is: $CVN = A + B * [\tanh((T - T0)/C)]$

Upper Shelf Energy: 81 Fixed Temp. at 30 ft-lbs: 45.1 Temp. at 50 ft-lbs: 120.3 Lower Shelf Energy: 2.19 Fixed

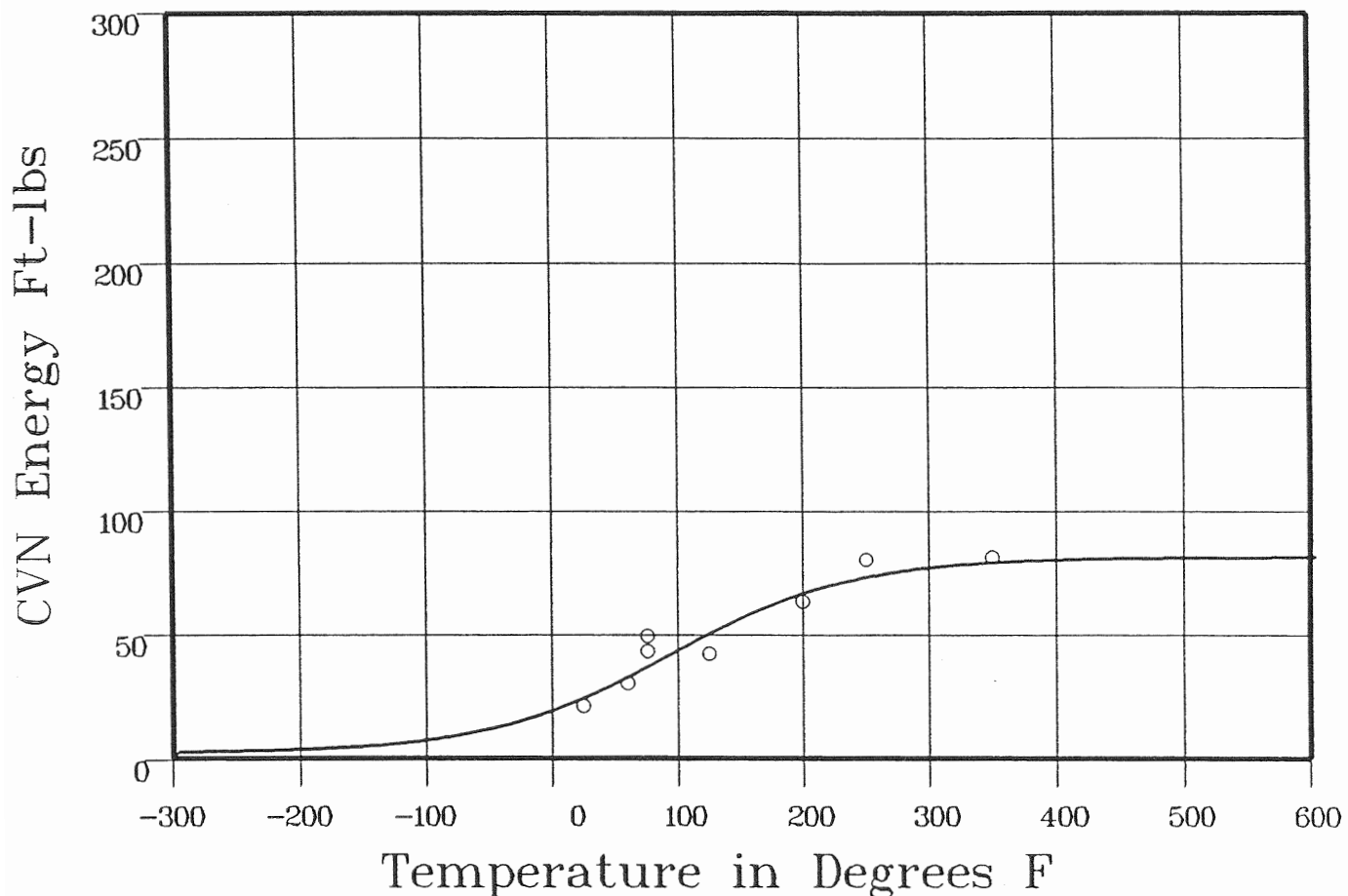
Material: WELD LINDE 1092

Heat Number: 27204 FLUX LOT 3714

Orientation:

Capsule: S

Total Fluence: 2.84E+18



Data Set(s) Plotted

Plant: DCI

Cap: S

Material: WELD LINDE 1092

Ori:

Heat #: 27204 FLUX LOT 3714

Charpy V-Notch Data

Temperature	Input CVN Energy	Computed CVN Energy	Differential
25	21	25.2	-4.2
60	30	33.78	-3.78
76	49	38.05	10.94
76	43	38.05	4.94
125	42	51.19	-9.19
200	63	67.01	-4.01
250	80	73.31	6.68
350	81	78.91	2.08

SUM of RESIDUALS = 3.45

236940

WELD METAL CAPSULE Y

CVGRAPH 4.1 Hyperbolic Tangent Curve Printed at 12:20:17 on 08-19-2002

Page 1

Coefficients of Curve 3

A = 31.1

B = 28.89

C = 108.21

T0 = 171.09

Equation is: $CVN = A + B * [\tanh((T - T0)/C)]$

Upper Shelf Energy: 60 Fixed

Temp. at 30 ft-lbs: 166.9

Temp. at 50 ft-lbs: 255.7

Lower Shelf Energy: 2.2 Fixed

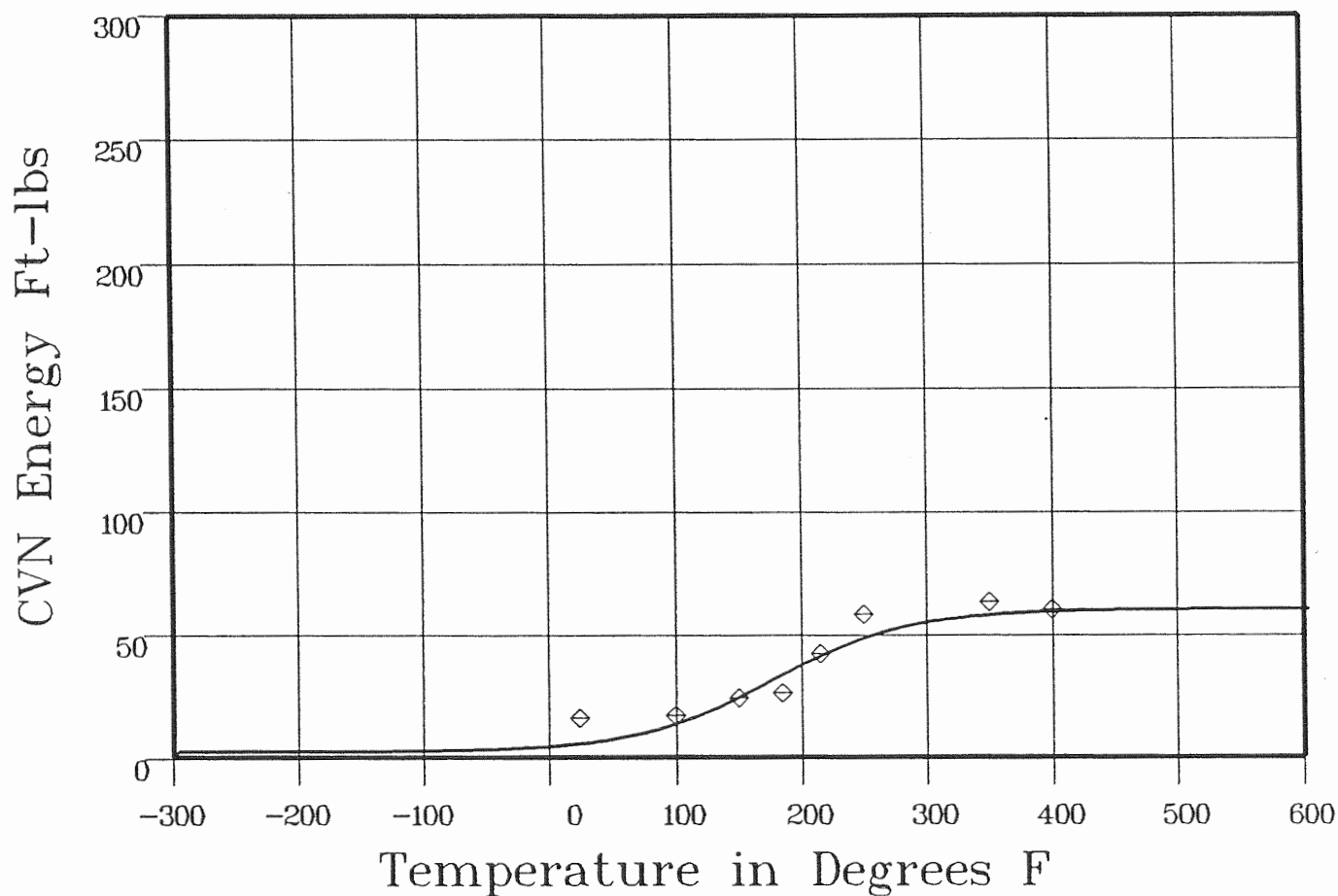
Material: WELD LINDE 1092

Heat Number: 27204 FLUX LOT 3714

Orientation:

Capsule: Y

Total Fluence: 1.05E+19



Data Set(s) Plotted

Plant: DCI

Cap: Y

Material: WELD LINDE 1092

Ori:

Heat #: 27204 FLUX LOT 3714

Charpy V-Notch Data

Temperature	Input CVN Energy	Computed CVN Energy	Differential
25	16	5.83	10.16
100	17	14.44	2.55
150	24	25.53	-1.53
185	26	34.79	-8.79
215	42	42.22	-22
250	58	49.09	8.9
350	63	57.95	5.04
400	60	59.17	.82

SUM of RESIDUALS = 16.94

WELD METAL CAPSULE V

236340

CVGRAPH 4.1 Hyperbolic Tangent Curve Printed at 12:20:17 on 08-19-2002

Page 1

Coefficients of Curve 4

A = 34.09

B = 31.89

C = 123.9

T0 = 151.46

Equation is: $CVN = A + B * [\tanh((T - T0)/C)]$

Upper Shelf Energy: 65.99 Fixed

Temp. at 30 ft-lbs: 135.4

Temp. at 50 ft-lbs: 219.2

Lower Shelf Energy: 2.19 Fixed

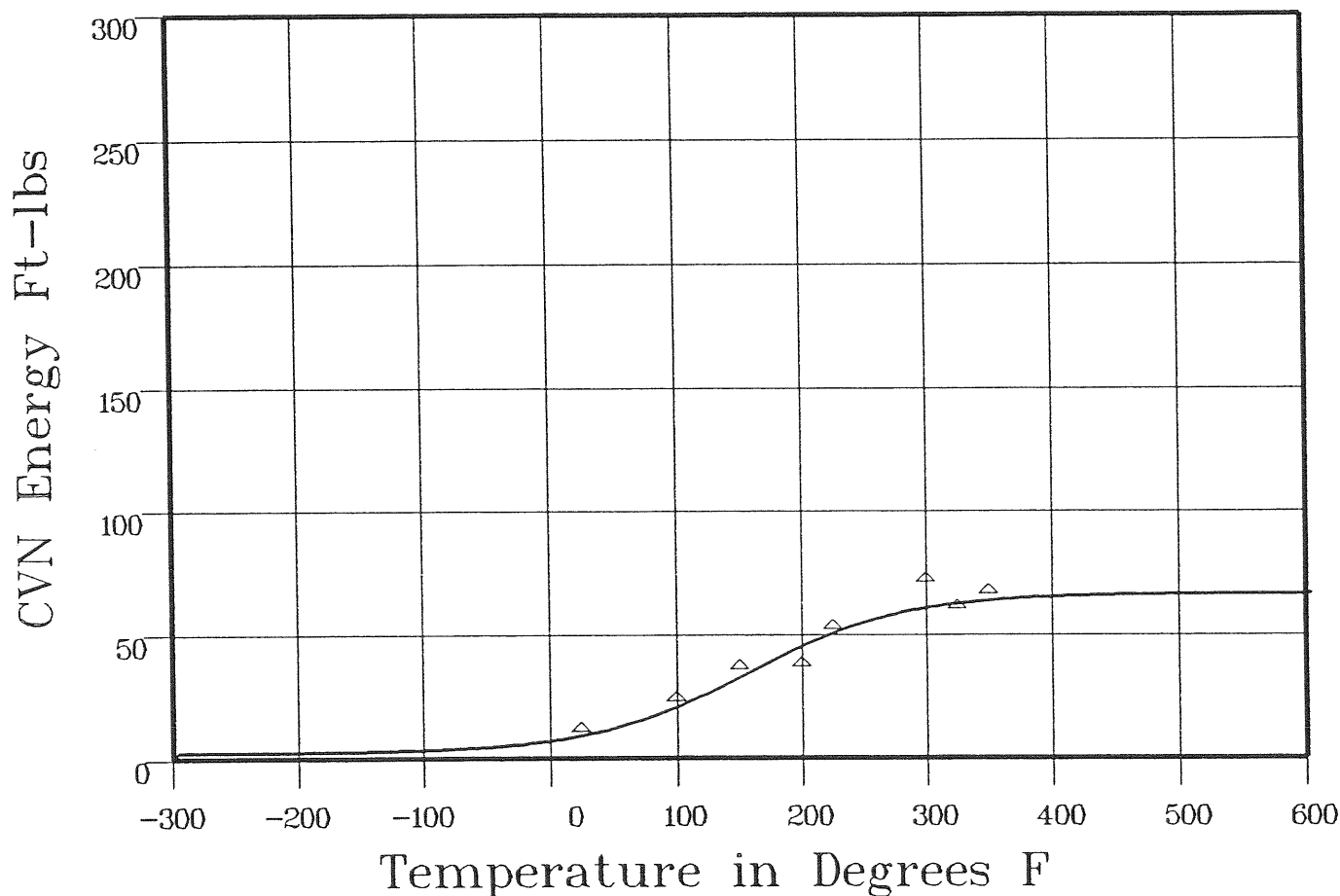
Material: WELD LINDE 1092

Heat Number: 27204 FLUX LOT 3714

Orientation:

Capsule: V

Total Fluence: 1.37E+19



Data Set(s) Plotted

Plant: DC1

Cap: V

Material: WELD LINDE 1092

Ori:

Heat #: 27204 FLUX LOT 3714

Charpy V-Notch Data

Temperature	Input CVN Energy	Computed CVN Energy	Differential
25	11	9.53	1.46
100	23	21.56	1.43
150	36	33.72	2.27
200	37	45.99	-8.99
225	52	51.08	.91
300	71	60.68	10.31
325	60	62.34	-2.34

**** Data continued on next page ****

236940

WELD METAL CAPSULE V

Page 2

Material: WELD LINDE 1092

Heat Number: 27204 FLUX LOT 3714

Orientation:

Capsule: V

Total Fluence: 1.37E+19

Charpy V-Notch Data (Continued)

Temperature
350

Input CVN Energy
66

Computed CVN Energy
63.51

Differential
2.48

SUM of RESIDUALS = 7.56

WELD METAL UNIRADIATED

236940

CVGRAPH 4.1 Hyperbolic Tangent Curve Printed at 12:30:39 on 08-19-2002

Page 1

Coefficients of Curve 1

A = 44.58

B = 43.58

C = 94.87

T0 = -25.31

Equation is: $LE = A + B * | \tanh((T - T0)/C) |$

Upper Shelf LE: 88.17

Temperature at LE 35: -46.5

Lower Shelf LE: 1 Fixed

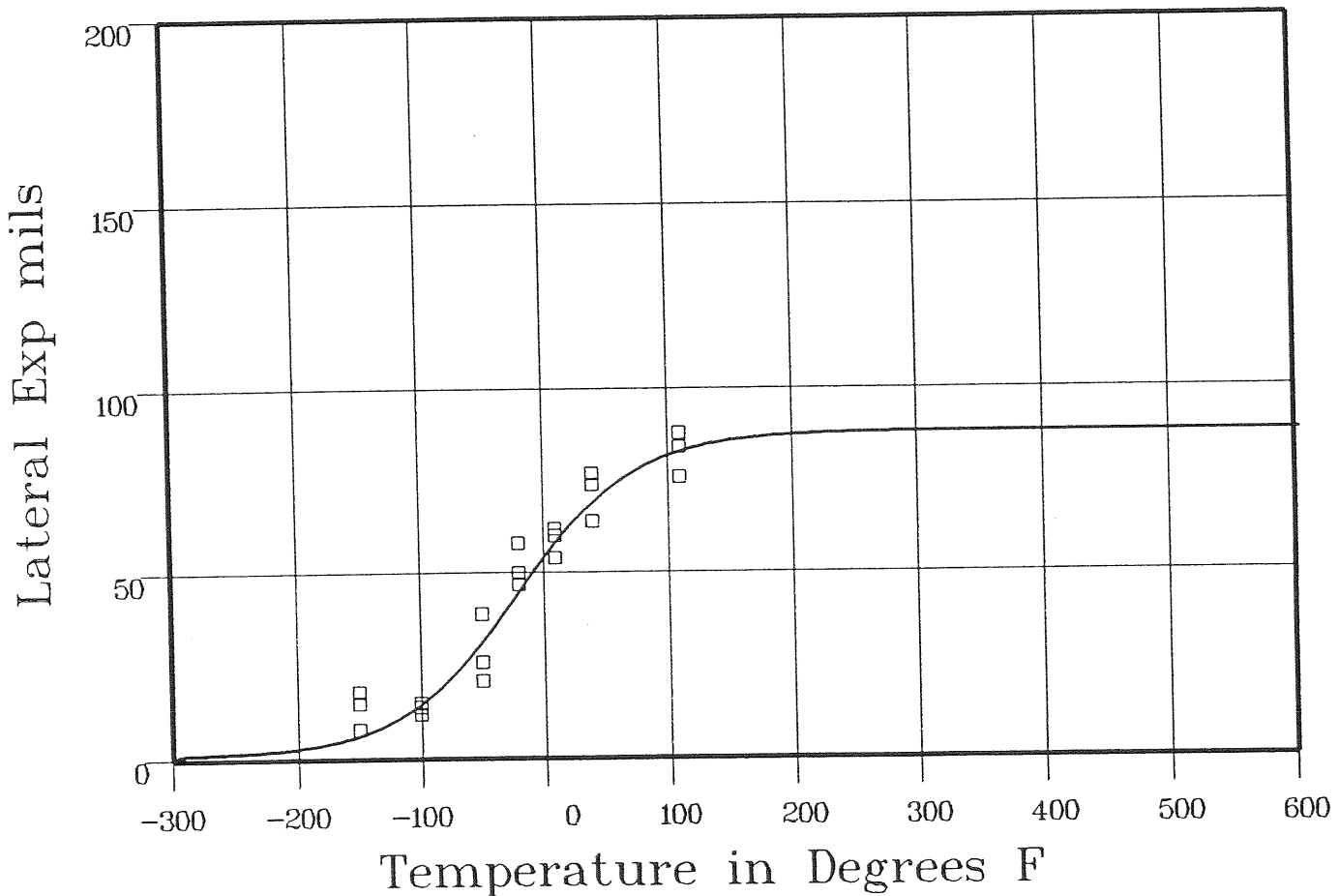
Material: WELD LINDE 1092

Heat Number: 27204 FLUX LOT 3714

Orientation:

Capsule: UNIRR

Total Fluence:



Plant: DCI Cap: UNIRR Material: WELD LINDE 1092 Ori: Heat #: 27204 FLUX LOT 3714

Charpy V-Notch Data

Temperature	Input Lateral Expansion	Computed L.E.	Differential
-150	15	6.86	8.13
-150	8	6.86	1.13
-150	18	6.86	11.13
-100	12	15.95	-3.95
-100	15	15.95	-.95
-100	14	15.95	-1.95
-50	39	33.49	5.5
-50	21	33.49	-12.49
-50	26	33.49	-7.49

**** Data continued on next page ****

236340

WELD METAL UNIRADIATED

Page 2

Material: WELD LINDE 1092

Heat Number: 27204 FLUX LOT 3714

Orientation:

Capsule: UNIRR

Total Fluence:

Charpy V-Notch Data (Continued)

Temperature	Input Lateral Expansion	Computed L.E.	Differential
-20	47	47.02	-.02
-20	58	47.02	10.97
-20	50	47.02	2.97
10	60	60.1	-.1
10	54	60.1	-6.1
10	62	60.1	1.89
40	77	70.6	6.39
40	74	70.6	3.39
40	64	70.6	-6.6
110	76	83.42	-7.42
110	88	83.42	4.57
110	84	83.42	.57
			SUM of RESIDUALS = 9.55

WELD METAL CAPSULE S

236340

CVGRAPH 4.1 Hyperbolic Tangent Curve Printed at 12:30:39 on 08-19-2002

Page 1

Coefficients of Curve 2

A = 37.45

B = 36.45

C = 152.02

T0 = 105.55

Equation is: $LE = A + B * [\tanh((T - T0)/C)]$

Upper Shelf LE: 73.91

Temperature at LE 35: 95.2

Lower Shelf LE: 1 Fixed

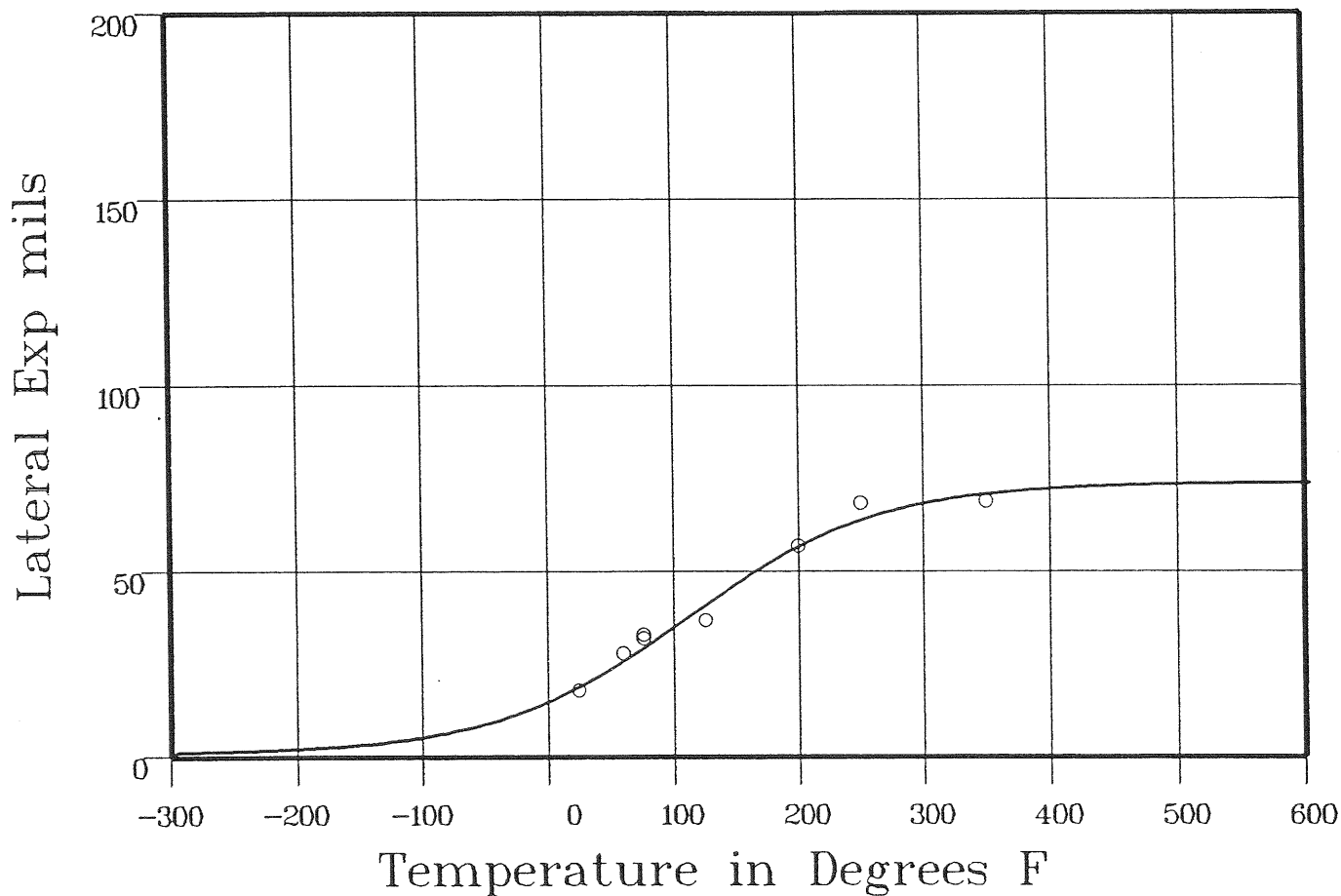
Material: WELD LINDE 1092

Heat Number: 27204 FLUX LOT 3714

Orientation:

Capsule: S

Total Fluence: 2.84E+18



Data Set(s) Plotted

Plant: DCI

Cap: S

Material: WELD LINDE 1092

Ori:

Heat #: 27204 FLUX LOT 3714

Charpy V-Notch Data

Temperature	Input Lateral Expansion	Computed LE	Differential
25	18	19.76	-1.76
60	28	26.85	1.14
76	33	30.45	2.54
76	32	30.45	1.54
125	37	42.09	-5.09
200	57	57.58	-5.58
250	68.5	64.43	4.06
350	69	71.1	-2.1

SUM of RESIDUALS = -2.5

236940

WELD METAL CAPSULE Y

CVGRAPH 4.1 Hyperbolic Tangent Curve Printed at 12:30:39 on 08-19-2002

Page 1

Coefficients of Curve 3

A = 31.12

B = 30.12

C = 115.87

T0 = 179.24

Equation is: $LE = A + B * [\tanh((T - T0)/C)]$

Upper Shelf LE: 61.24

Temperature at L.E. 35: 194.2

Lower Shelf LE: 1 Fixed

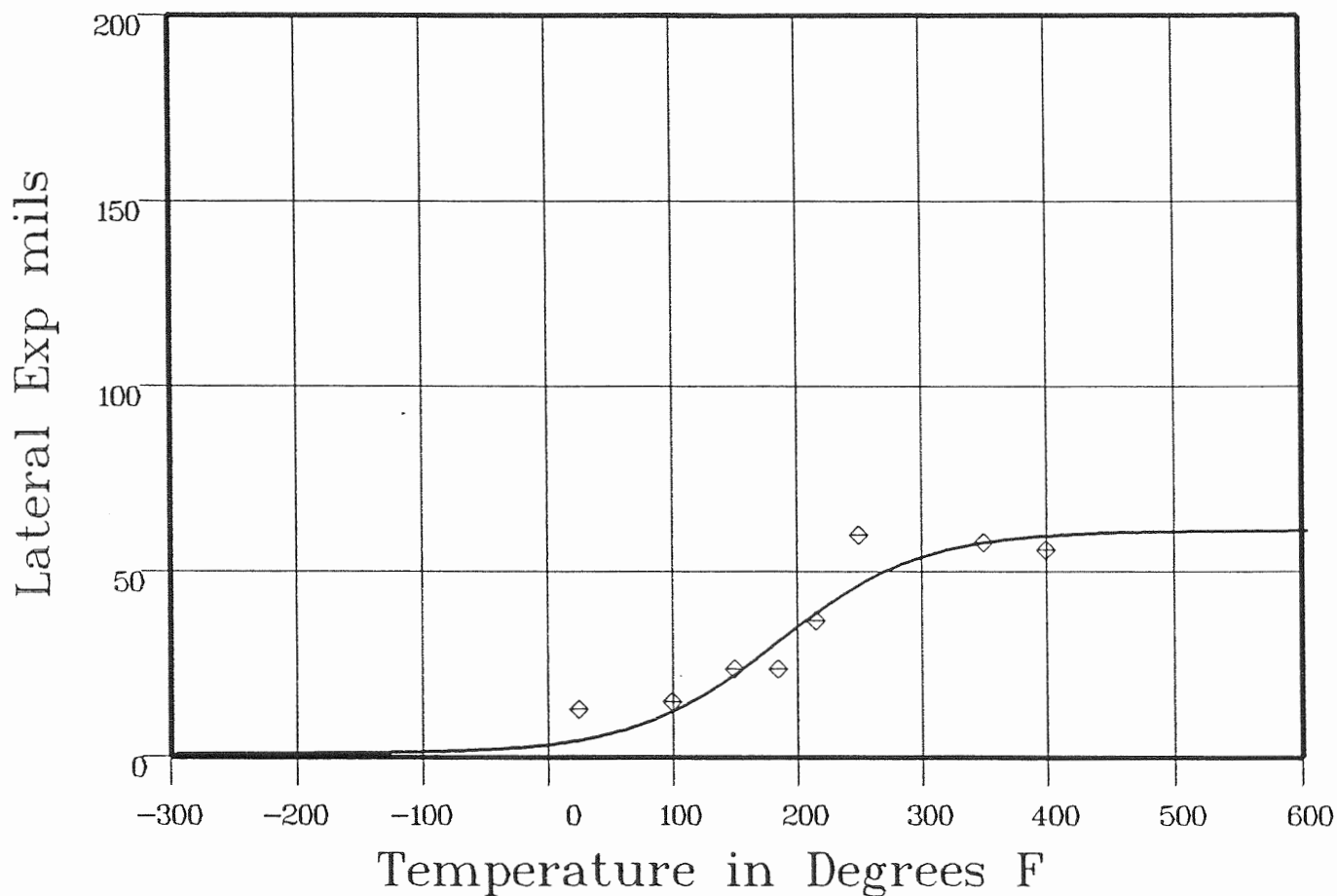
Material: WELD LINDE 1092

Heat Number: 27204 FLUX LOT 3714

Orientation:

Capsule: Y

Total Fluence: 1.05E+19



Data Set(s) Plotted

Plant: DCI

Cap: Y

Material: WELD LINDE 1092

Ori:

Heat #: 27204 FLUX LOT 3714

Charpy V-Notch Data

Temperature	Input Lateral Expansion	Computed L.E.	Differential
25	13	4.93	8.06
100	15	13.22	1.77
150	24	23.67	.32
185	24	32.61	-8.61
215	37	40.13	-3.13
250	60	47.52	12.47
350	58	58.23	-.23
400	56	59.93	-3.93

SUM of RESIDUALS = 6.72

WELD METAL CAPSULE V

236340

CVGRAPH 4.1 Hyperbolic Tangent Curve Printed at 12:30:39 on 08-19-2002

Page 1

Coefficients of Curve 4

A = 27.73

B = 26.73

C = 124.44

T0 = 185.98

Equation is: $LE = A + B * [\tanh((T - T0)/C)]$

Upper Shelf LE: 54.47

Temperature at LE 35: 220.6

Lower Shelf LE: 1 Fixed

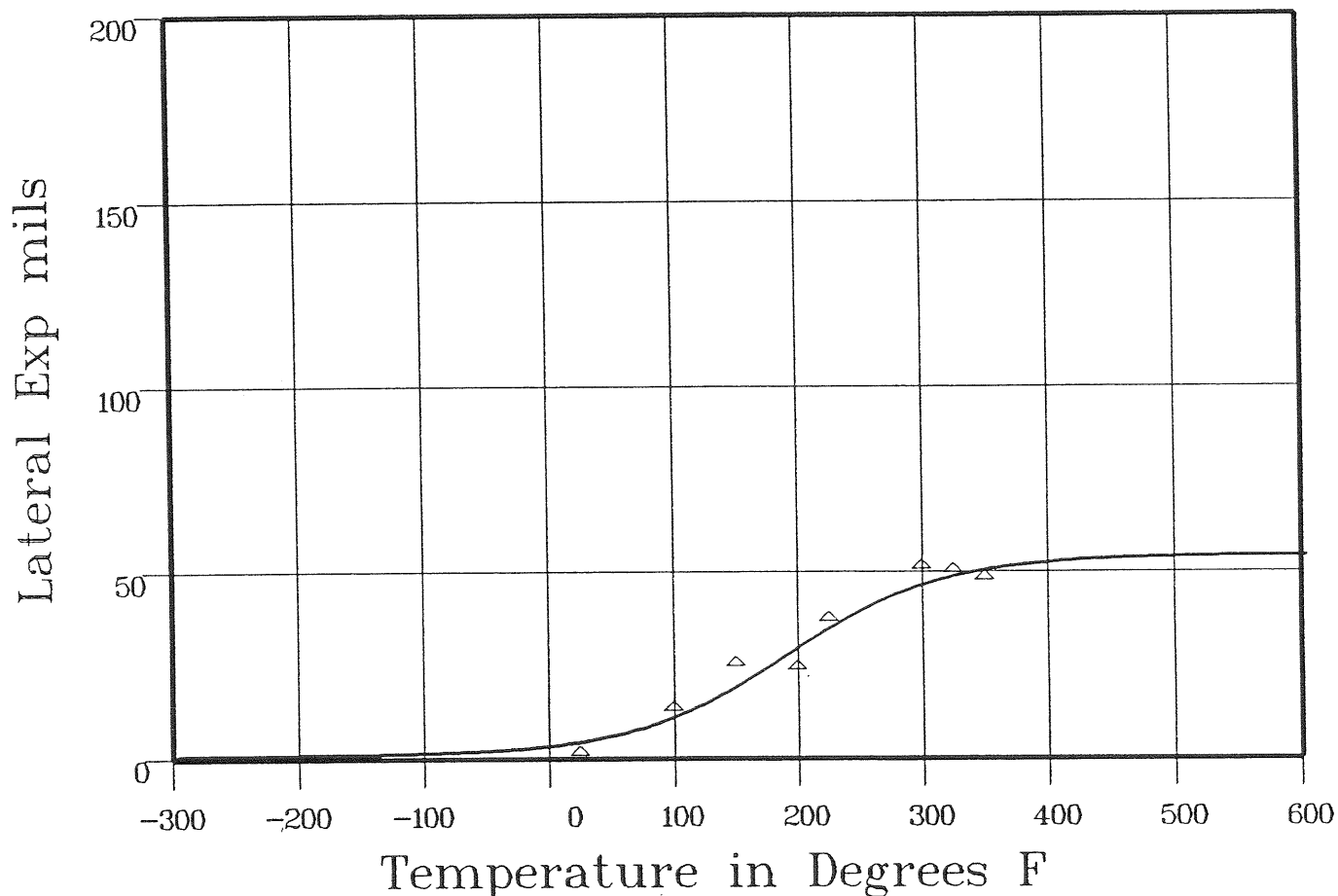
Material: WELD LINDE 1092

Heat Number: 27204 FLUX LOT 3714

Orientation:

Capsule: V

Total Fluence: 1.37E+19



Plant: DC1 Cap: V Material: WELD LINDE 1092 Ori.: Heat #: 27204 FLUX LOT 3714

Charpy V-Notch Data

Temperature	Input Lateral Expansion	Computed LE	Differential
25	1	4.74	-3.74
100	13	11.73	1.26
150	25	20.21	4.78
200	24	30.73	-6.73
225	37	35.85	1.14
300	51	47.09	3.9
325	50	49.3	.69

**** Data continued on next page ****

236340

WELD METAL CAPSULE V

Page 2

Material: WELD LINDE 1092

Heat Number: 27204 FLUX LOT 3714

Orientation:

Capsule: V

Total Fluence: 1.37E+19

Charpy V-Notch Data (Continued)

Temperature
350

Input Lateral Expansion
48

Computed L.E.
50.89

Differential
-2.89

SUM of RESIDUALS = -1.56

WELD METAL UNIRRADIATED

CVGRAPH 4.1 Hyperbolic Tangent Curve Printed at 12:44:50 on 08-19-2002

236340

Page 1

Coefficients of Curve 1

A = 50

B = 50

C = 75.76

T0 = -15.93

Equation is: $\text{Shear}\% = A + B * [\tanh((T - T_0)/C)]$

Temperature at 50% Shear: -15.9

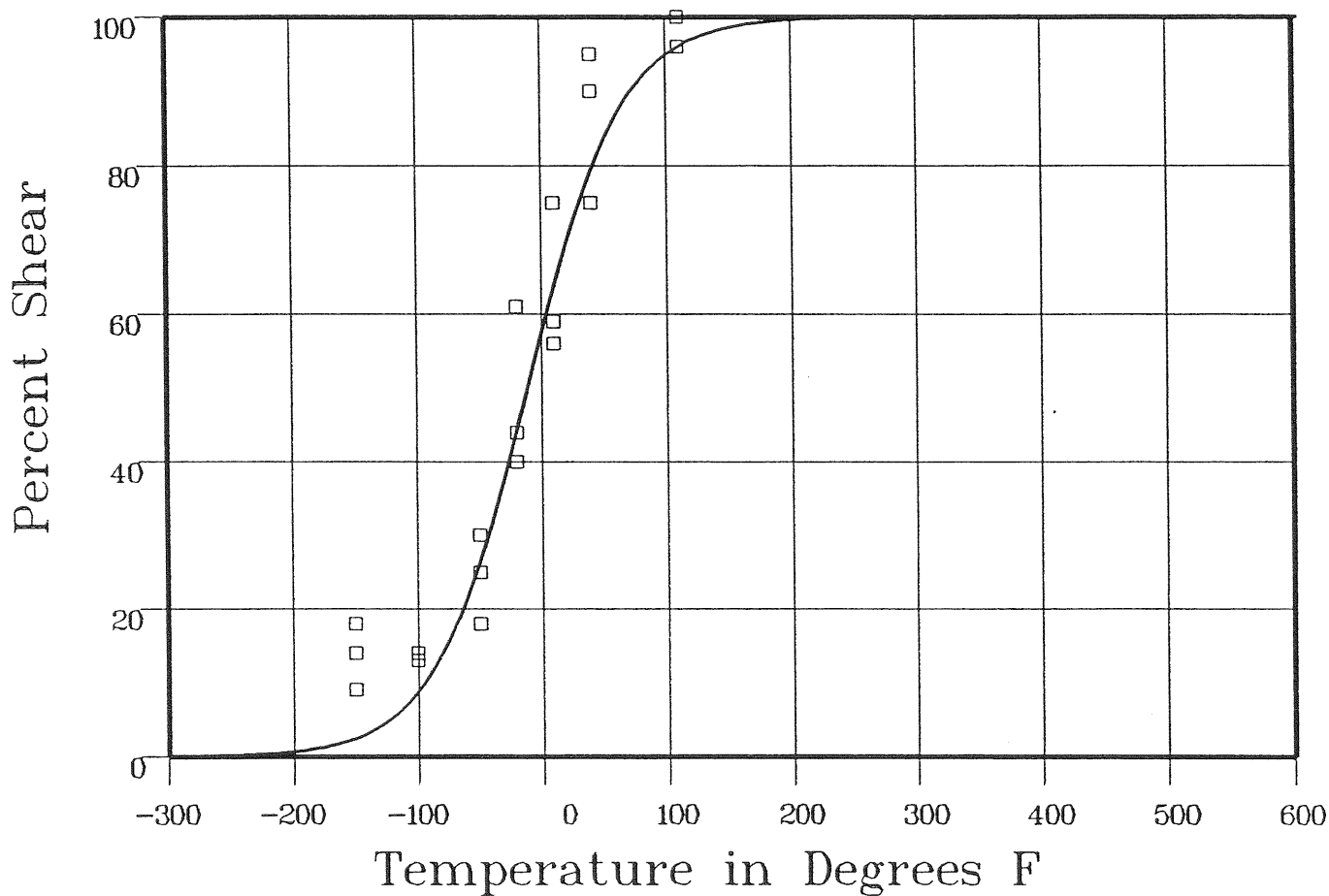
Material: WELD LINDE 1092

Heat Number: 27204 FLUX LOT 3714

Orientation:

Capsule: UNIRR

Total Fluence:



Data Set(s) Plotted

Plant: DCI

Cap.: UNIRR

Material: WELD LINDE 1092

Ori:

Heat #: 27204 FLUX LOT 3714

Charpy V-Notch Data

Temperature	Input Percent Shear	Computed Percent Shear	Differential
-150	18	2.82	15.17
-150	9	2.82	6.17
-150	14	2.82	11.17
-100	14	9.8	4.19
-100	13	9.8	3.19
-100	13	9.8	3.19
-50	30	28.92	1.07
-50	18	28.92	-10.92
-50	25	28.92	-3.92

**** Data continued on next page ****

236940

WELD METAL UNIRRADIATED

Page 2

Material: WELD LINDE 1092

Heat Number: 27204 FLUX LOT 3714

Orientation:

Capsule: UNIRR

Total Fluence:

Charpy V-Notch Data (Continued)

Temperature	Input Percent Shear	Computed Percent Shear	Differential
-20	40	47.32	-7.32
-20	61	47.32	13.67
-20	44	47.32	-3.32
10	56	66.47	-10.47
10	59	66.47	-7.47
10	75	66.47	8.52
40	90	81.4	8.59
40	95	81.4	13.59
40	75	81.4	-6.4
110	96	96.52	-.52
110	100	96.52	3.47
110	100	96.52	3.47
			SUM of RESIDUALS = 45.15

WELD METAL CAPSULE S

236940

CVGRAPH 4.1 Hyperbolic Tangent Curve Printed at 12:44:50 on 08-19-2002

Page 1

Coefficients of Curve 2

A = 50

B = 50

C = 109.59

T0 = 110.74

Equation is: $\text{Shear}\% = A + B * [\tanh((T - T0)/C)]$

Temperature at 50% Shear: 110.7

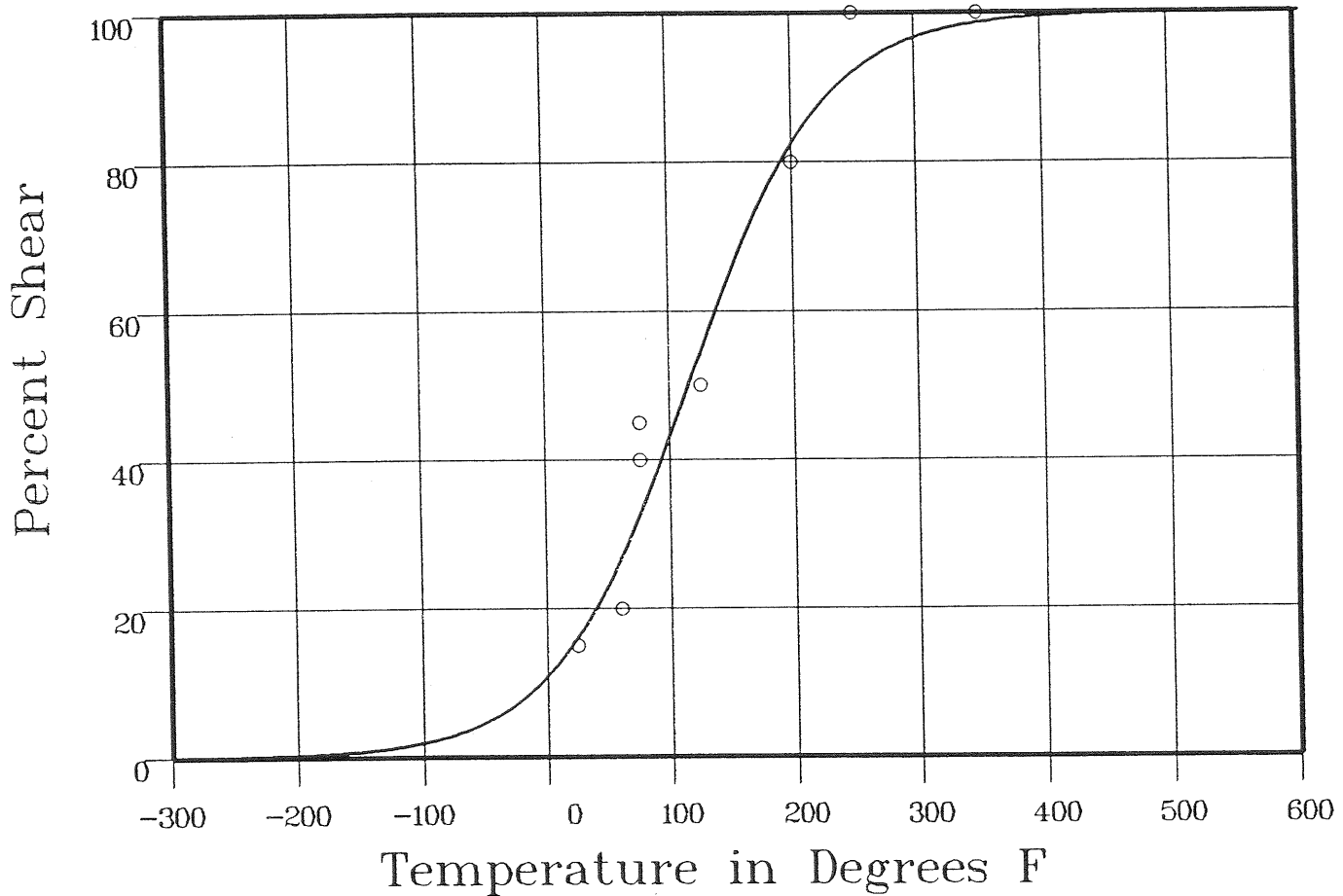
Material: WELD LINDE 1092

Heat Number: 27204 FLUX LOT 3714

Orientation:

Capsule: S

Total Fluence: 2.84E+18



Data Set(s) Plotted

Plant: DC1

Cap: S

Material: WELD LINDE 1092

Ori:

Heat #: 27204 FLUX LOT 3714

Charpy V-Notch Data

Temperature	Input Percent Shear	Computed Percent Shear	Differential
25	15	17.29	-2.29
60	20	28.37	-8.37
76	45	34.66	10.33
76	40	34.66	5.33
125	50	56.46	-6.46
200	80	83.6	-3.6
250	100	92.69	7.3
350	100	98.74	1.25

SUM of RESIDUALS = 3.49

226940

WELD METAL CAPSULE Y

CVGRAPH 4.1 Hyperbolic Tangent Curve Printed at 12:44:50 on 08-19-2002

Page 1

Coefficients of Curve 3

A = 50

B = 50

C = 87.67

T0 = 168.75

Equation is: $\text{Shear}\% = A + B * [\tanh((T - T0)/C)]$

Temperature at 50% Shear: 168.7

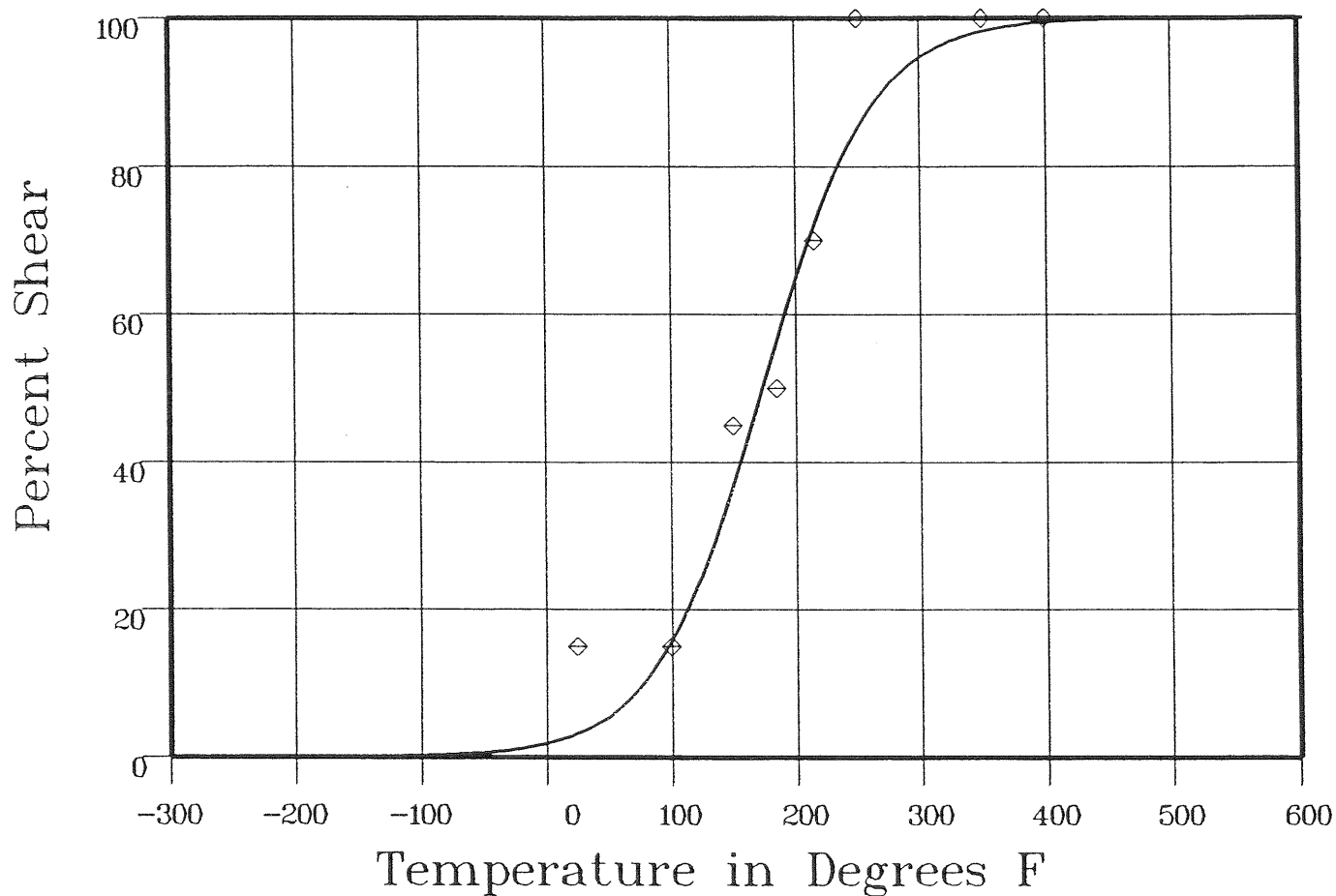
Material: WELD LINDE 1092

Heat Number: 27204 FLUX LOT 3714

Orientation:

Capsule: Y

Total Fluence: 1.05E+19



Data Set(s) Plotted

Plant: DCI

Cap: Y

Material: WELD LINDE 1092

Ori:

Heat #: 27204 FLUX LOT 3714

Charpy V-Notch Data

Temperature	Input Percent Shear	Computed Percent Shear	Differential
25	15	3.62	11.37
100	15	17.24	-2.24
150	45	39.46	5.53
185	50	59.16	-9.16
215	70	74.17	-4.17
250	100	86.45	13.54
350	100	98.42	1.57
400	100	99.49	.5

SUM of RESIDUALS = 16.95

WELD METAL CAPSULE V

CVGRAPH 4.1 Hyperbolic Tangent Curve Printed at 12:44:50 on 08-19-2002

Page 1

Coefficients of Curve 4

A = 50

B = 50

C = 66.4

T0 = 201.56

Equation is: $\text{Shear}\% = A + B * [\tanh((T - T0)/C)]$

Temperature at 50% Shear: 201.5

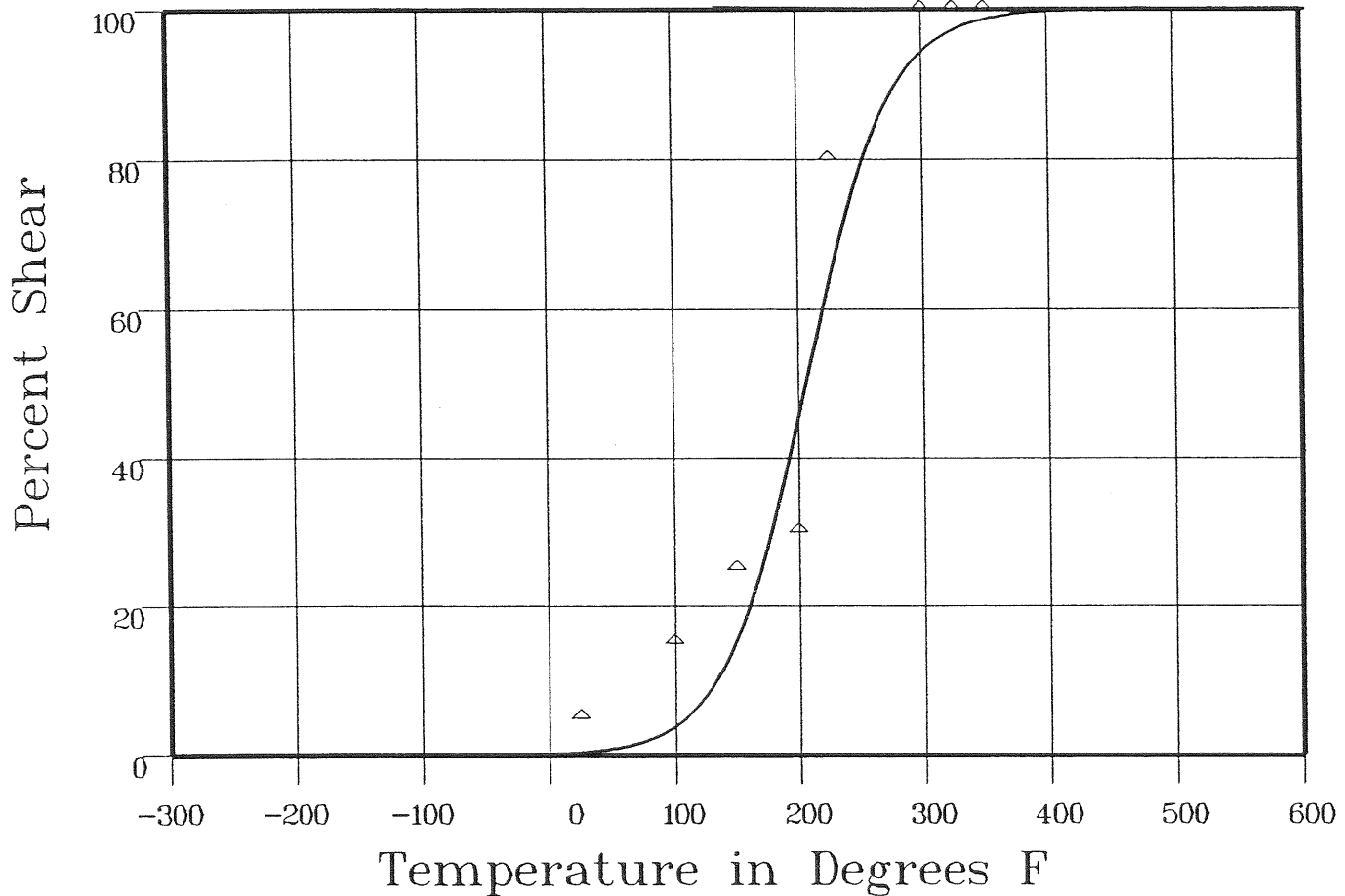
Material: WELD LINDE 1092

Heat Number: 27204 FLUX LOT 3714

Orientation:

Capsule: V

Total Fluence: 1.37E+19



Plant: DCI Cap: V Material: WELD LINDE 1092 Ori: Heat #: 27204 FLUX LOT 3714

Charpy V-Notch Data

Temperature	Input Percent Shear	Computed Percent Shear	Differential
25	5	.48	4.51
100	15	4.48	10.51
150	25	17.46	7.53
200	30	48.82	-18.82
225	80	66.94	13.05
300	100	95.09	4.9
325	100	97.62	2.37

**** Data continued on next page ****

236940

WELD METAL CAPSULE V

Page 2

Material: WELD LINDE 1092

Heat Number: 27204 FLUX LOT 3714

Orientation:

Capsule: V

Total Fluence: 1.37E+19

Charpy V-Notch Data (Continued)

Temperature
350

Input Percent Shear
100

Computed Percent Shear
98.86

Differential
113

SUM of RESIDUALS = 25.19

HEAT AFFECTED ZONE UNIRRADIATED

236940

CVGRAPH 4.1 Hyperbolic Tangent Curve Printed at 13:33:29 on 08-19-2002

Page 1

Coefficients of Curve 1

A = 69.09

B = 66.9

C = 137.93

T0 = -71.25

$$\text{Equation is: } \text{CVN} = A + B * [\tanh((T - T_0)/C)]$$

Upper Shelf Energy: 136 Fixed Temp. at 30 ft-lbs: -163.5 Temp. at 50 ft-lbs: -111.7 Lower Shelf Energy: 2.19 Fixed

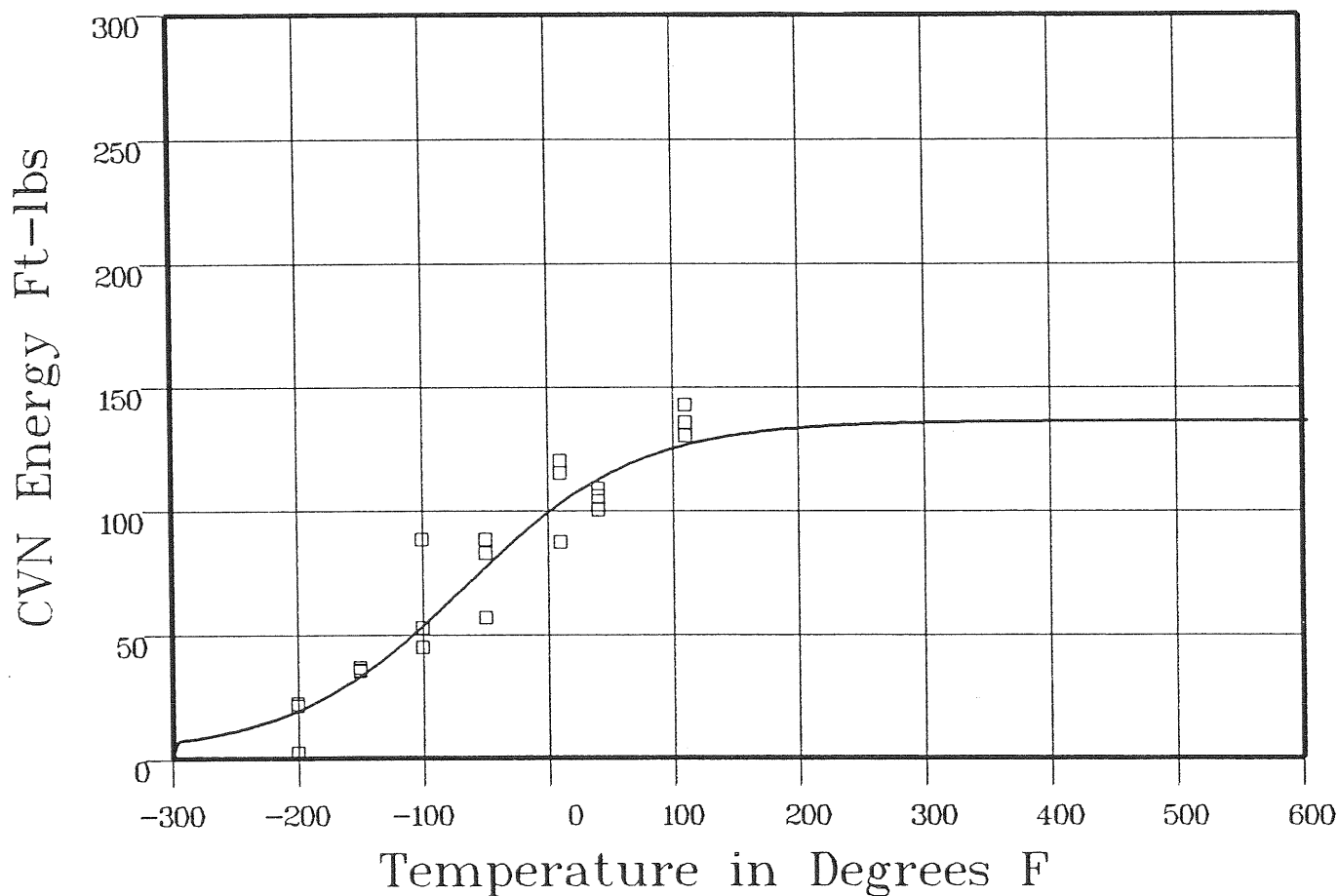
Material: HEAT AFFECTED ZONE

Heat Number:

Orientation:

Capsule: UNIRR

Total Fluence: 2.84E+18



Plant: DC1 Cap: UNIRR Data Set(s) Plotted Material: HEAT AFFECTED ZONE Ori: Heat #:

Charpy V-Notch Data

Temperature	Input CVN Energy	Computed CVN Energy	Differential
-200	22	20.11	1.88
-200	21	20.11	.88
-200	2	20.11	-18.11
-150	35	34.57	.42
-150	35.5	34.57	.92
-150	36.5	34.57	1.92
-100	44.5	55.35	-10.85
-100	52.5	55.35	-2.85
-100	88	55.35	32.64

**** Data continued on next page ****

236940

HEAT AFFECTED ZONE UNIRRADIATED

Page 2

Material: HEAT AFFD ZONE

Heat Number:

Orientation:

Capsule: UNIRR

Total Fluence:

Charpy V-Notch Data (Continued)

Temperature	Input CVN Energy	Computed CVN Energy	Differential
-50	88	79.32	8.67
-50	82.5	79.32	3.17
-50	56.5	79.32	-22.82
10	115	104.5	10.49
10	120	104.5	15.49
10	87	104.5	-17.5
40	105.5	113.76	-8.26
40	100	113.76	-13.76
40	108.5	113.76	-5.26
110	130	126.98	3.01
110	135.5	126.98	8.51
110	142.5	126.98	15.51

SUM of RESIDUALS = 4.09

HEAT AFFECTED ZONE CAPSULE S

236840

CVGRAPH 4.1 Hyperbolic Tangent Curve Printed at 13:53:38 on 09-03-2002

Page 1

Coefficients of Curve 1

A = 63.59

B = 61.4

C = 92.37

T0 = -34.48

Equation is: $CVN = A + B * | \tanh((T - T0)/C) |$

Upper Shelf Energy: 125 Fixed

Temp. at 30 ft-lbs: -91.2

Temp. at 50 ft-lbs: -55.2

Lower Shelf Energy: 2.19 Fixed

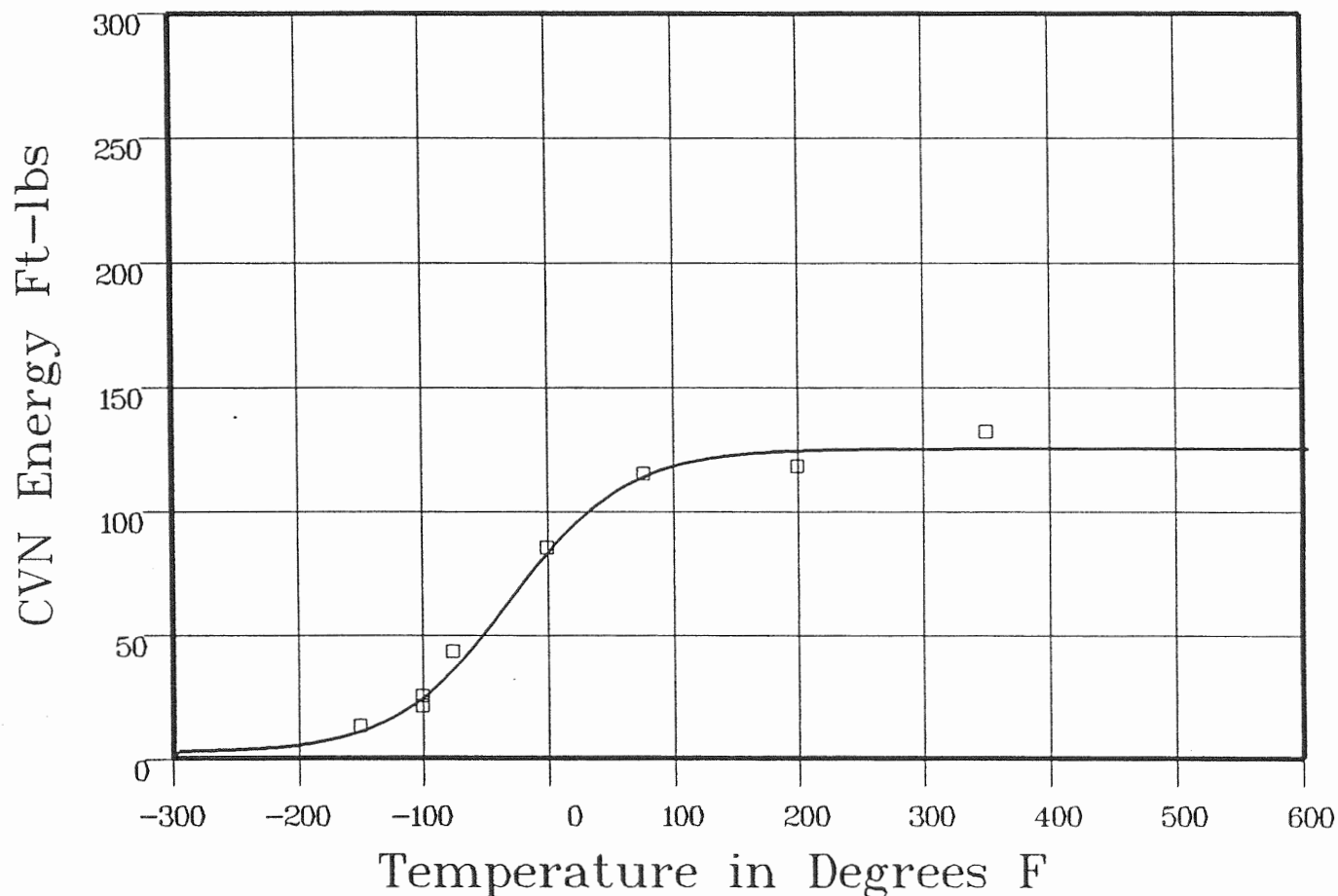
Material: HEAT AFFECTED ZONE

Heat Number:

Orientation:

Capsule: S

Total Fluence: 2.84E+18



Data Set(s) Plotted

Plant: DCI

Cap: S

Material: HEAT AFFECTED ZONE

Ori:

Heat #:

Charpy V-Notch Data

Temperature	Input CVN Energy	Computed CVN Energy	Differential
-150	13	11.5	1.49
-100	21	26.13	-5.13
-100	25	26.13	-1.13
-75	43	38.27	4.72
0	85	85.51	-0.51
76	115	114.71	0.28
200	118	124.23	-6.23
350	132	124.97	7.02

SUM of RESIDUALS = 51

HEAT AFFECTED ZONE CAPSULE Y

238940

CVGRAPH 4.1 Hyperbolic Tangent Curve Printed at 13:33:29 on 08-19-2002

Page 1

Coefficients of Curve 3

A = 55.59

B = 53.4

C = 114.66

T0 = -23.9

Equation is: $CVN = A + B * | \tanh((T - T0)/C) |$

Upper Shelf Energy: 109 Fixed Temp. at 30 ft-lbs: -83.7 Temp. at 50 ft-lbs: -35.9 Lower Shelf Energy: 2.19 Fixed

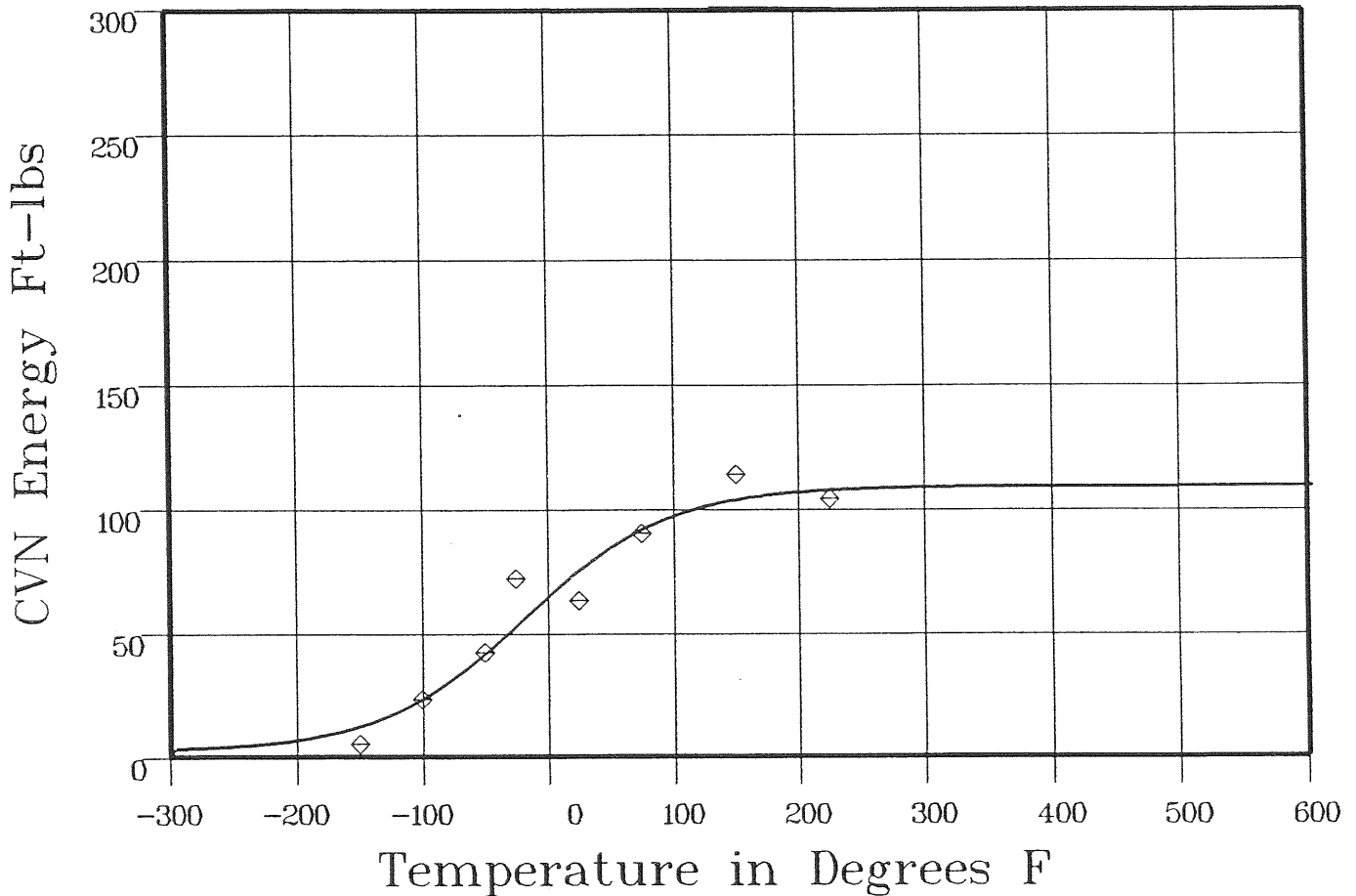
Material: HEAT AFFD ZONE

Heat Number:

Orientation:

Capsule: Y

Total Fluence: 1.05E+19



Data Set(s) Plotted

Plant: DCI

Cap: Y

Material: HEAT AFFD ZONE

Ori:

Heat #:

Charpy V-Notch Data

Temperature	Input CVN Energy	Computed CVN Energy	Differential
-150	5	12.85	-7.85
-100	23	24.58	-1.58
-50	42	43.65	-1.65
-25	72	55.08	16.91
25	63	77.08	-14.08
75	90	92.84	-2.84
150	114	104.09	9.9
225	104	107.62	-3.62

SUM of RESIDUALS = -4.83

HEAT AFFECTED ZONE CAPSULE V

236940

CVGRAPH 4.1 Hyperbolic Tangent Curve Printed at 13:33:29 on 08-19-2002

Page 1

Coefficients of Curve 4

A = 59.09

B = 56.9

C = 125.62

T0 = 18.28

Equation is: $CVN = A + B * [\tanh((T - T0)/C)]$

Upper Shelf Energy: 116 Fixed

Temp. at 30 ft-lbs: -52.6

Temp. at 50 ft-lbs: -1.9

Lower Shelf Energy: 2.19 Fixed

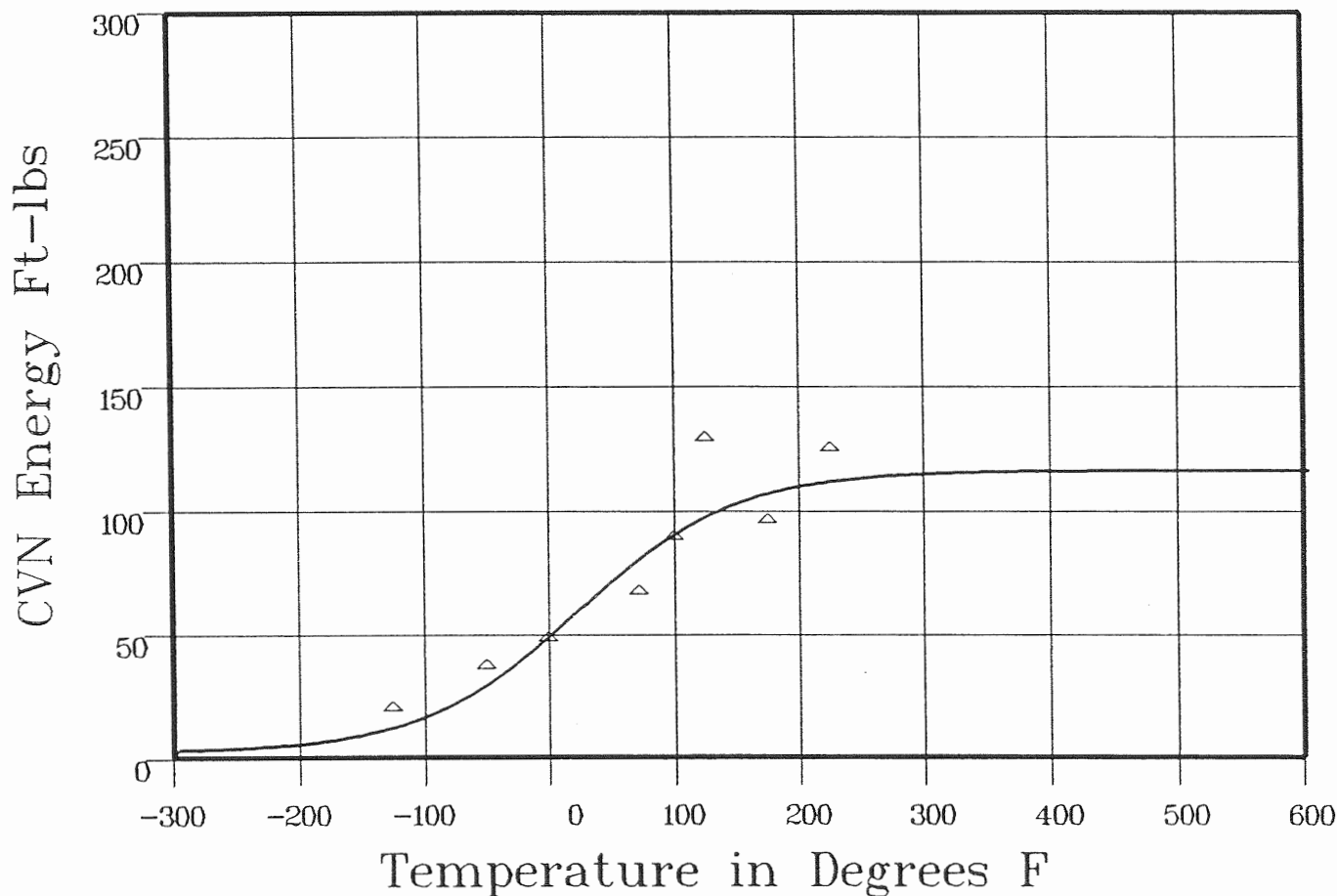
Material: HEAT AFFECTED ZONE

Heat Number:

Orientation:

Capsule: V

Total Fluence: 1.37E+19



Plant: DC1 Cap: V Data Set(s) Plotted Material: HEAT AFFECTED ZONE Ori: Heat #:

Charpy V-Notch Data

Temperature	Input CVN Energy	Computed CVN Energy	Differential
-125	19	12.75	6.24
-50	36	30.89	5.1
0	47	50.87	-3.87
72	66	82.04	-16.04
100	88	91.64	-3.64
125	128	98.4	29.59
175	95	107.32	-12.32

**** Data continued on next page ****

236340

HEAT AFFECTED ZONE CAPSULE V

Page 2

Material: HEAT AFFD ZONE

Heat Number:

Orientation:

Capsule: V

Total Fluence: 1.37E+19

Charpy V-Notch Data (Continued)

Temperature
225

Input CVN Energy
124

Computed CVN Energy
111.91

Differential
12.08

SUM of RESIDUALS = 17.12

HEAT AFFECTED ZONE UNIRRADIATED

238340

CVGRAPH 4.1 Hyperbolic Tangent Curve Printed at 14:27:03 on 08-19-2002

Page 1

Coefficients of Curve 1

A = 44.65

B = 43.65

C = 127.88

T0 = -78.75

Equation is: $LE = A + B * [\tanh((T - T0)/C)]$

Upper Shelf LE: 88.3

Temperature at LE 35: -107.5

Lower Shelf LE: 1 Fixed

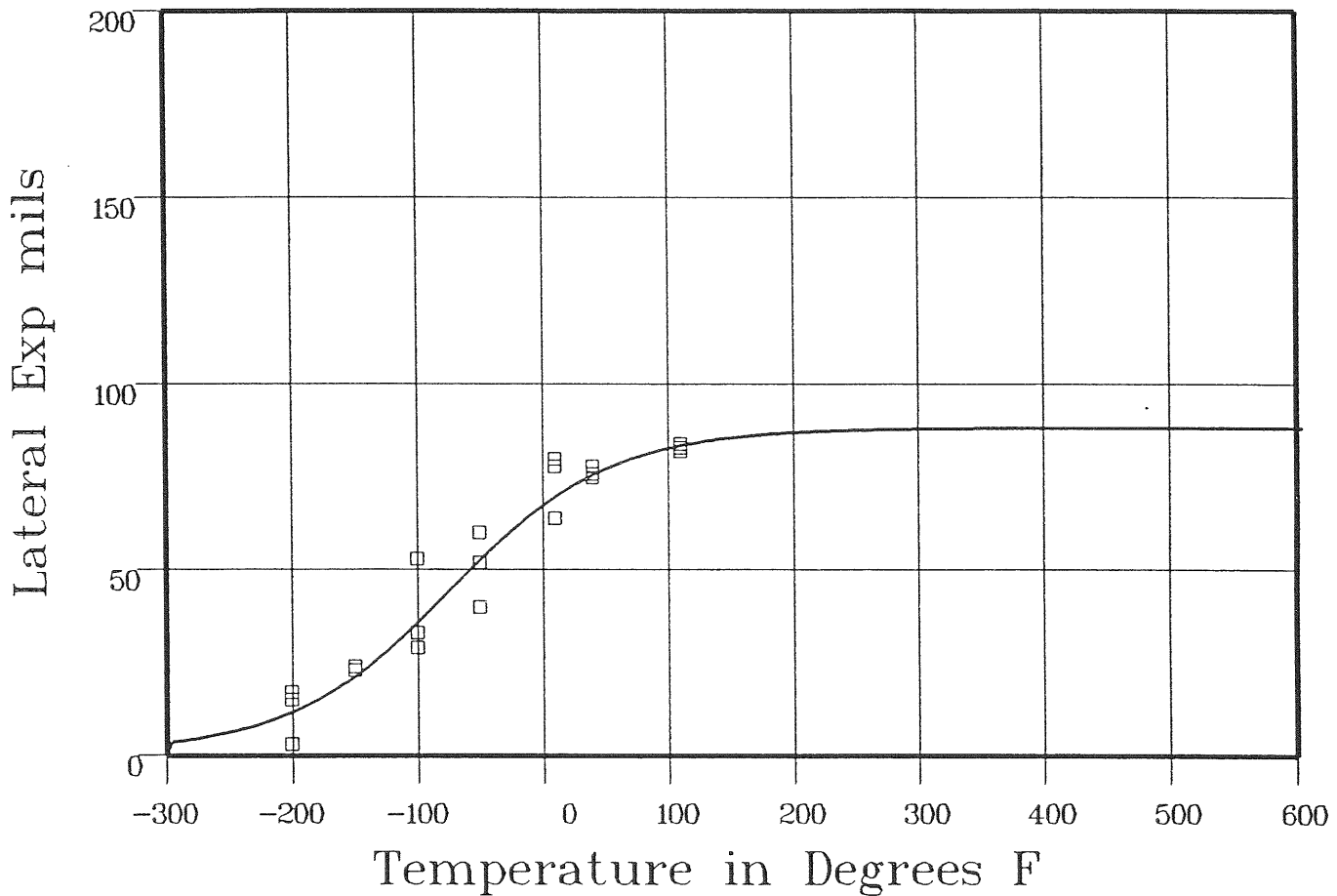
Material: HEAT AFFD ZONE

Heat Number:

Orientation:

Capsule: UNIRR

Total Fluence:



Plant: DCI Cap: UNIRR Data Set(s) Plotted Material: HEAT AFFD ZONE Ori: Heat #:

Charpy V-Notch Data

Temperature	Input Lateral Expansion	Computed LE	Differential
-200	15	12.39	2.6
-200	17	12.39	4.6
-200	3	12.39	-9.39
-150	23	22.57	.42
-150	23	22.57	.42
-150	24	22.57	1.42
-100	29	37.46	-8.46
-100	33	37.46	-4.46
-100	53	37.46	15.53

**** Data continued on next page ****

HEAT AFFECTED ZONE UNIRRADIATED

Page 2

235940

Material: HEAT AFFD ZONE

Heat Number:

Orientation:

Capsule: UNIRR

Total Fluence:

Charpy V-Notch Data (Continued)

Temperature	Input Lateral Expansion	Computed L.E.	Differential
-50	60	54.3	5.69
-50	52	54.3	-2.3
-50	40	54.3	-14.3
10	78	70.87	7.12
10	80	70.87	9.12
10	64	70.87	-6.87
40	76	76.51	-.51
40	78	76.51	1.48
40	75	76.51	-1.51
110	82	83.97	-1.97
110	84	83.97	.02
110	83	83.97	-.97

SUM of RESIDUALS = -2.32

HEAT AFFECTED ZONE CAPSULE S

CVGRAPH 4.1 Hyperbolic Tangent Curve Printed at 14:27:03 on 08-19-2002

Page 1

Coefficients of Curve 2

A = 41.37

B = 40.37

C = 94.53

T0 = -49.21

Equation is: $LE = A + B * [\tanh((T - T0)/C)]$

Upper Shelf LE: 81.74

Temperature at L.E. 35: -64.2

Lower Shelf LE: 1 Fixed

Material: HEAT AFFD ZONE

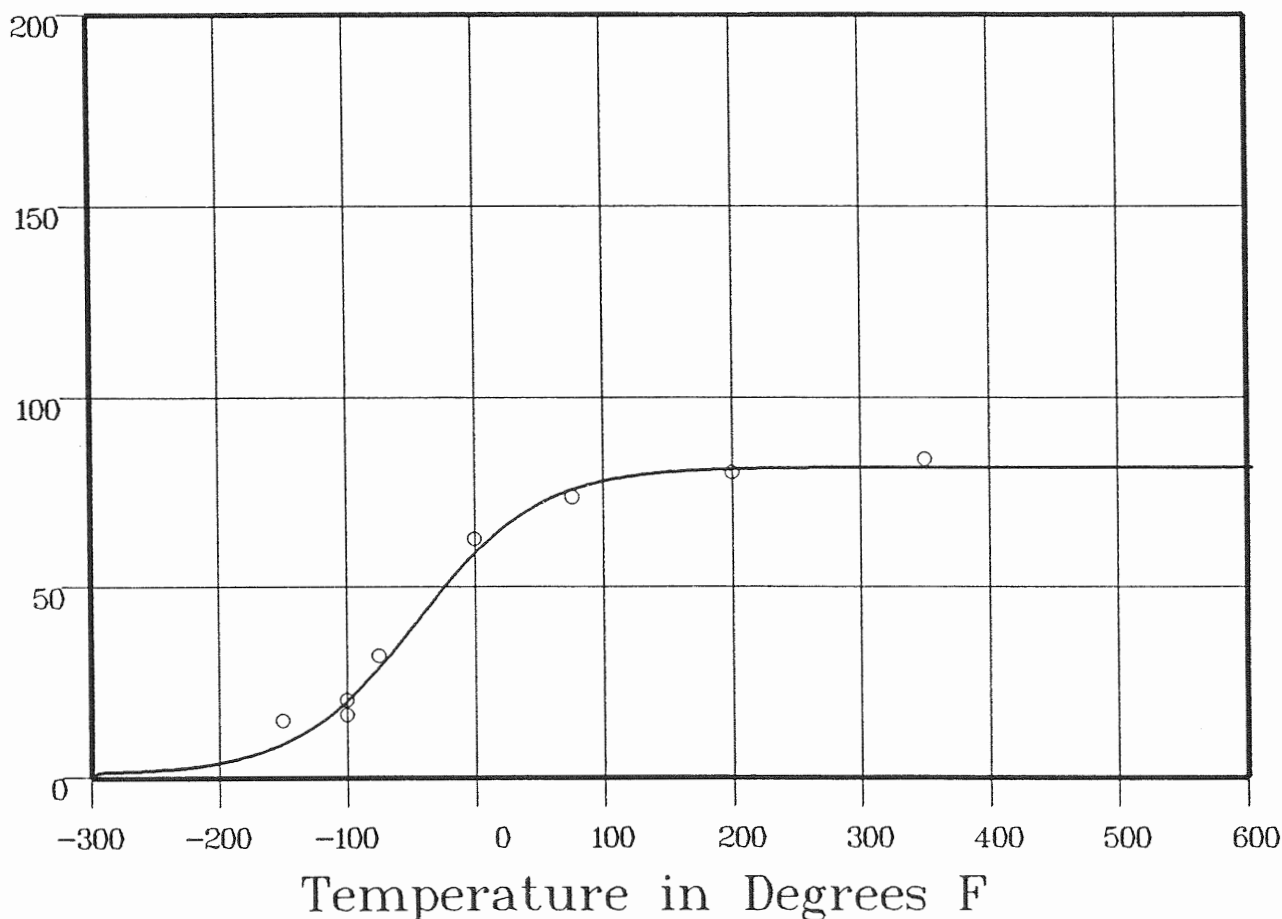
Heat Number:

Orientation:

Capsule: S

Total Fluence: 2.84E+18

Lateral Exp mils



Data Set(s) Plotted

Plant: DC1

Cap: S

Material: HEAT AFFD ZONE

Ori:

Heat #:

Charpy V-Notch Data

Temperature	Input Lateral Expansion	Computed L.E.	Differential
-150	15	9.55	5.44
-100	20.5	21.55	-1.05
-100	16.5	21.55	-5.05
-75	32	30.62	1.37
0	63	60.67	2.32
76	74	76.41	-2.41
200	80.5	81.33	-83
350	84	81.72	2.27

SUM of RESIDUALS = 2.05

236940

HEAT AFFECTED ZONE CAPSULE Y

CVGRAPH 4.1 Hyperbolic Tangent Curve Printed at 14:27:03 on 08-19-2002

Page 1

Coefficients of Curve 3

A = 41.72

B = 40.72

C = 134.42

T0 = -14.06

Equation is: $LE = A + B * [\tanh((T - T0)/C)]$

Upper Shelf LE: 82.45

Temperature at LE 35: -36.4

Lower Shelf LE: 1 Fixed

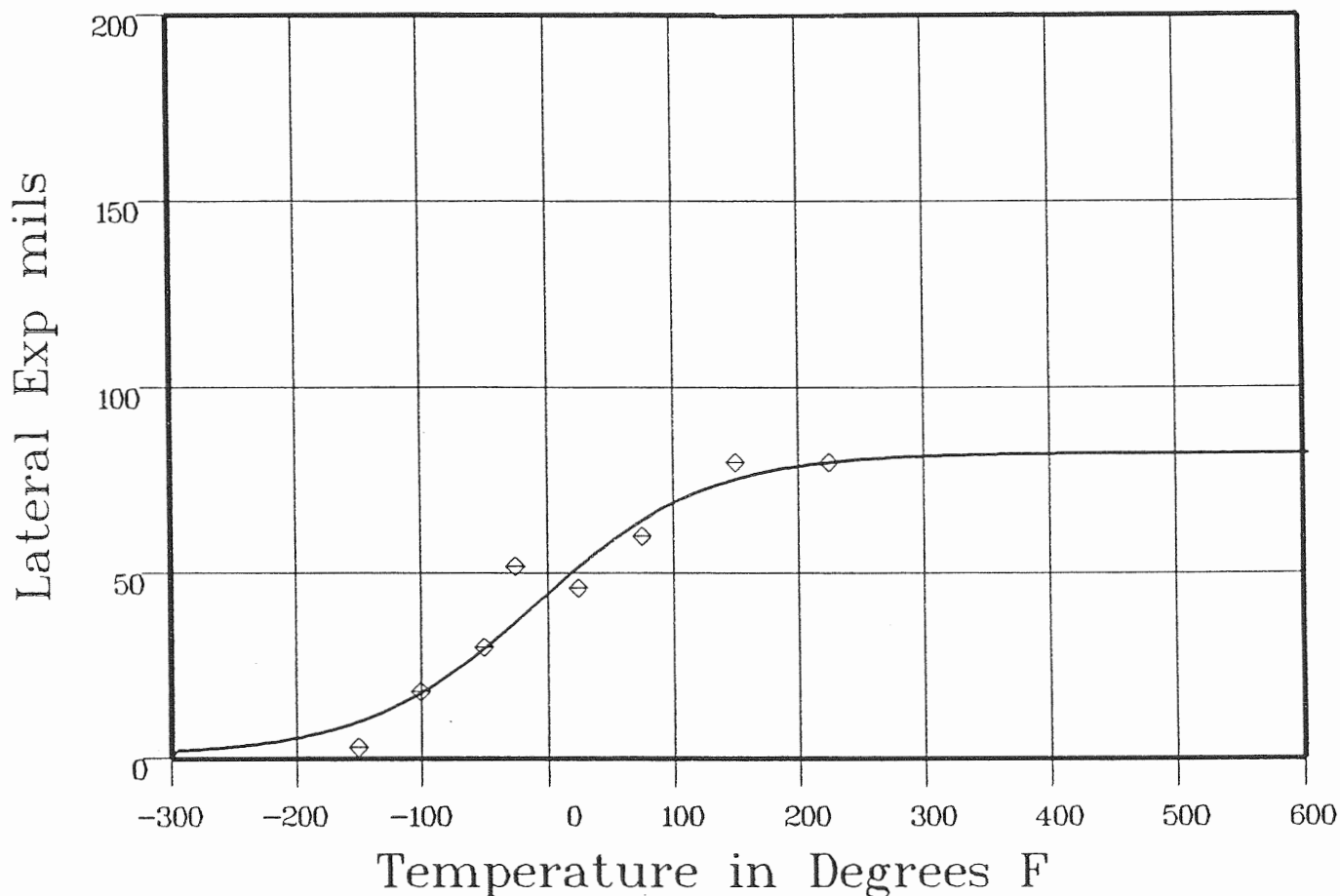
Material: HEAT AFFD ZONE

Heat Number:

Orientation:

Capsule: Y

Total Fluence: 1.05E+19



Plant: DCI Cap: Y Data Set(s) Plotted Material: HEAT AFFD ZONE Ori: Heat #:

Charpy V-Notch Data

Temperature	Input Lateral Expansion	Computed L.E.	Differential
-150	3	10.51	-7.51
-100	18	18.74	-7.4
-50	30	31.09	-1.09
-25	52	38.42	13.57
25	46	53.23	-7.23
75	60	65.34	-5.34
150	80	75.92	4.07
225	80	80.19	-1.19

SUM of RESIDUALS = -4.47

HEAT AFFECTED ZONE CAPSULE V

236940

CVGRAPH 4.1 Hyperbolic Tangent Curve Printed at 14:27:03 on 08-19-2002

Page 1

Coefficients of Curve 4

A = 41.84

B = 40.84

C = 143.96

T0 = 43.12

Equation is: $LE = A + B * | \tanh((T - T0)/C) |$

Upper Shelf LE: 82.69

Temperature at LE 35: 18.7

Lower Shelf LE: 1 Fixed

Material: HEAT AFFECTED ZONE

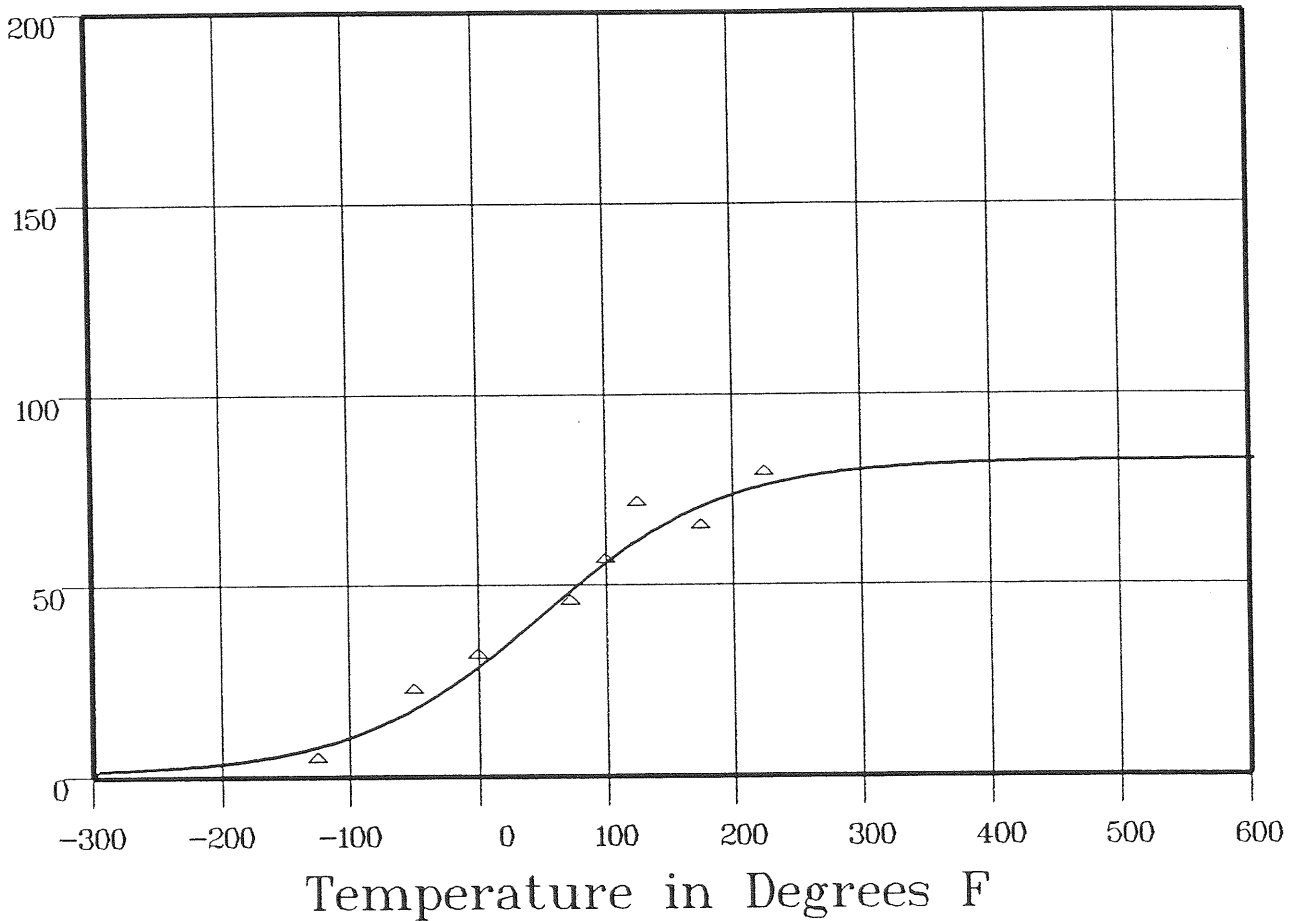
Heat Number:

Orientation:

Capsule: V

Total Fluence: 1.37E+19

Lateral Exp mils



Plant: DCI Cap: V Data Set(s) Plotted Material: HEAT AFFECTED ZONE Ori: Heat #:

Charpy V-Notch Data

Temperature	Input Lateral Expansion	Computed LE	Differential
-125	4	82	-4.2
-50	22	18.58	3.41
0	31	29.96	1.03
72	45	49.93	-4.93
100	56	57.19	-1.19
125	71	62.85	8.14
175	65	71.41	-6.41

**** Data continued on next page ****

236940

HEAT AFFECTED ZONE CAPSULE V

Page 2

Material: HEAT AFFD ZONE

Heat Number:

Orientation:

Capsule: V

Total Fluence: 1.37E+19

Charpy V-Notch Data (Continued)

Temperature
225

Input Lateral Expansion
79

Computed LE
76.64

Differential
2.35

SUM of RESIDUALS = -1.8

HEAT AFFECTED ZONE UNIRRADIATED

226940

CVGRAPH 4.1 Hyperbolic Tangent Curve Printed at 14:01:24 on 09-03-2002

Page 1

Coefficients of Curve 1

A = 50

B = 50

C = 109.44

T0 = -72.94

Equation is: $\text{Shear\%} = A + B * [\tanh((T - T0)/C)]$

Temperature at 50% Shear: -72.9

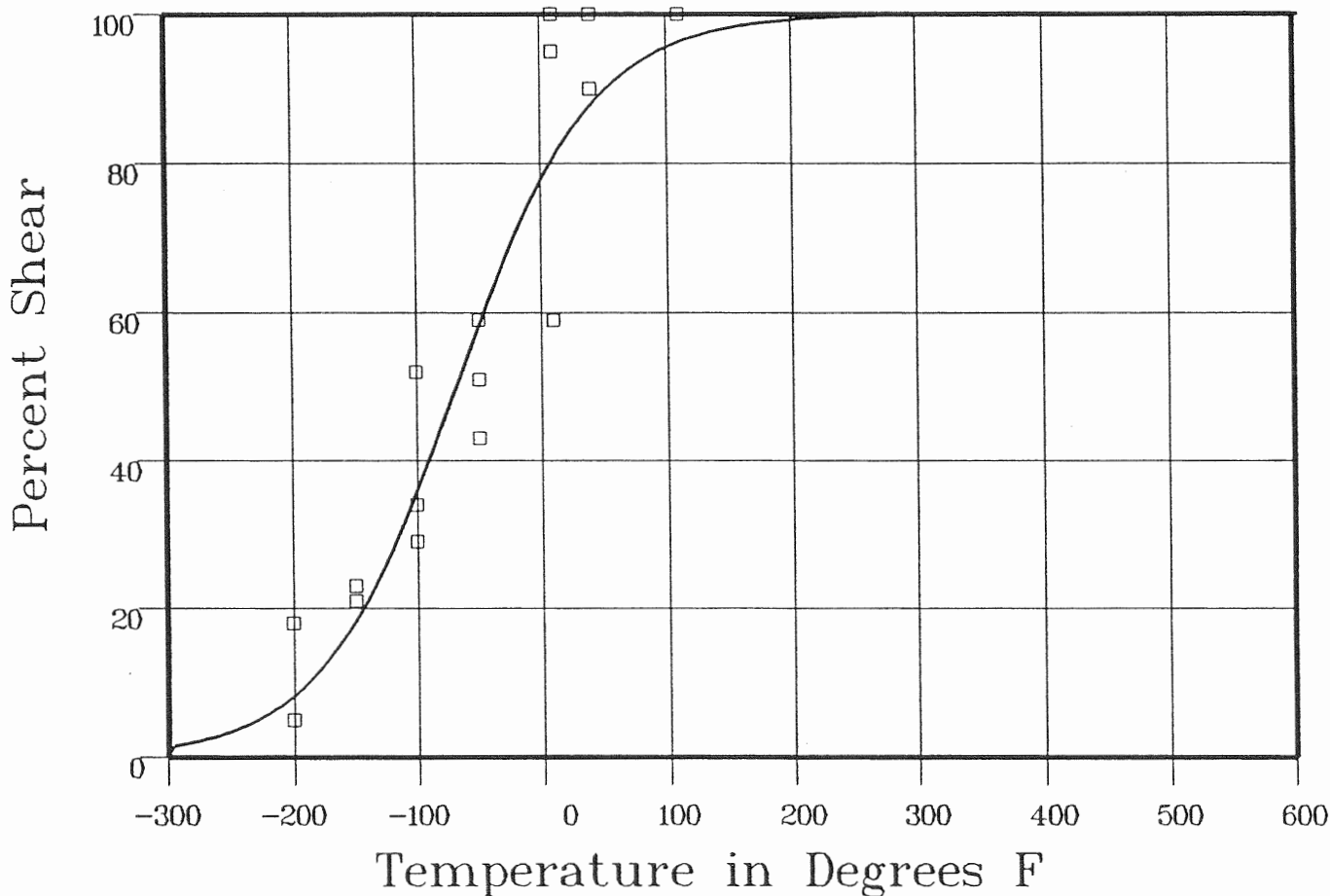
Material: HEAT AFFD ZONE

Heat Number:

Orientation:

Capsule: UNIRR

Total Fluence:



Plant: DCI Cap: UNIRR Material: HEAT AFFD ZONE Ori: Heat #:

Charpy V-Notch Data

Temperature	Input Percent Shear	Computed Percent Shear	Differential
-200	18	8.93	9.06
-200	18	8.93	9.06
-200	5	8.93	-3.93
-150	23	19.65	3.34
-150	21	19.65	1.34
-150	23	19.65	3.34
-100	29	37.88	-8.88
-100	34	37.88	-3.88
-100	52	37.88	14.11

**** Data continued on next page ****

HEAT AFFECTED ZONE UNIRRADIATED

Page 2

236940

Material: HEAT AFFECTED ZONE

Heat Number:

Orientation:

Capsule: UNIRR

Total Fluence:

Charpy V-Notch Data (Continued)

Temperature	Input Percent Shear	Computed Percent Shear	Differential
-50	59	60.32	-1.32
-50	51	60.32	-9.32
-50	43	60.32	-17.32
10	95	81.99	13
10	100	81.99	18
10	59	81.99	-22.99
40	90	88.73	126
40	100	88.73	11.26
40	100	88.73	11.26
110	100	96.58	3.41
110	100	96.58	3.41
110	100	96.58	3.41

SUM of RESIDUALS = 37.67

HEAT AFFECTED ZONE CAPSULE S

CVGRAPH 4.1 Hyperbolic Tangent Curve Printed at 14:01:24 on 09-03-2002

Page 1

Coefficients of Curve 2

A = 50

B = 50

C = 101.74

T0 = -15.46

Equation is: $\text{Shear\%} = A + B * [\tanh((T - T0)/C)]$

Temperature at 50% Shear: -15.4

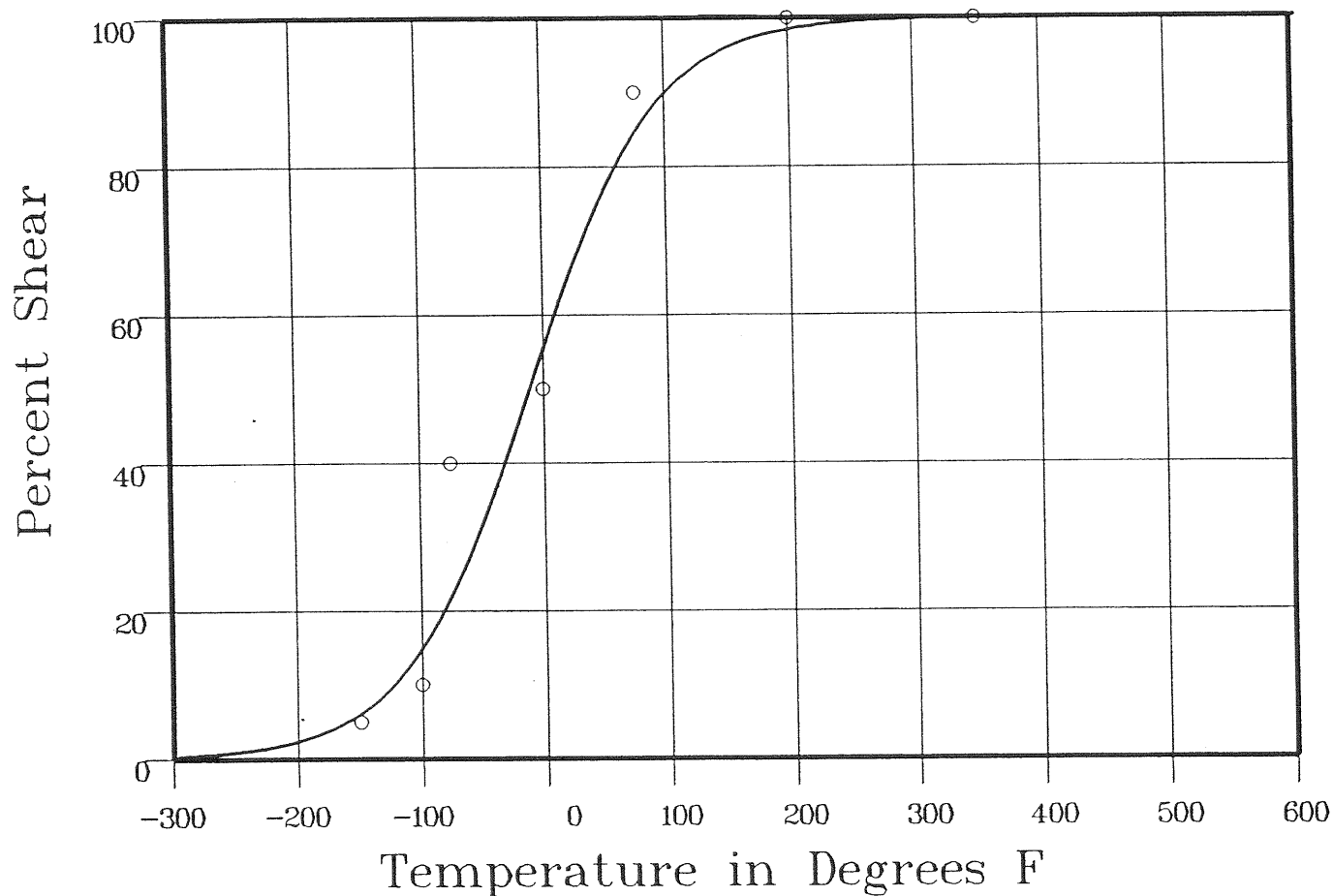
Material: HEAT AFFD ZONE

Heat Number:

Orientation:

Capsule: S

Total Fluence: 2.84E+18



Data Set(s) Plotted
Plant: DCI Cap: S Material: HEAT AFFD ZONE Ori: Heat #:

Charpy V-Notch Data

Temperature	Input Percent Shear	Computed Percent Shear	Differential
-150	5	6.63	-1.63
-100	10	15.95	-5.95
-100	10	15.95	-5.95
-75	40	23.68	16.31
0	50	57.54	-7.54
76	90	85.79	4.2
200	100	98.57	1.42
350	100	99.92	.07

SUM of RESIDUALS = .94

HEAT AFFECTED ZONE CAPSULE Y

236940

CVGRAPH 4.1 Hyperbolic Tangent Curve Printed at 14:01:24 on 09-03-2002

Page 1

Coefficients of Curve 3

A = 50

B = 50

C = 113.01

T0 = -36.27

Equation is $\text{Shear}\% = A + B * [\tanh((T - T0)/C)]$

Temperature at 50% Shear: -36.2

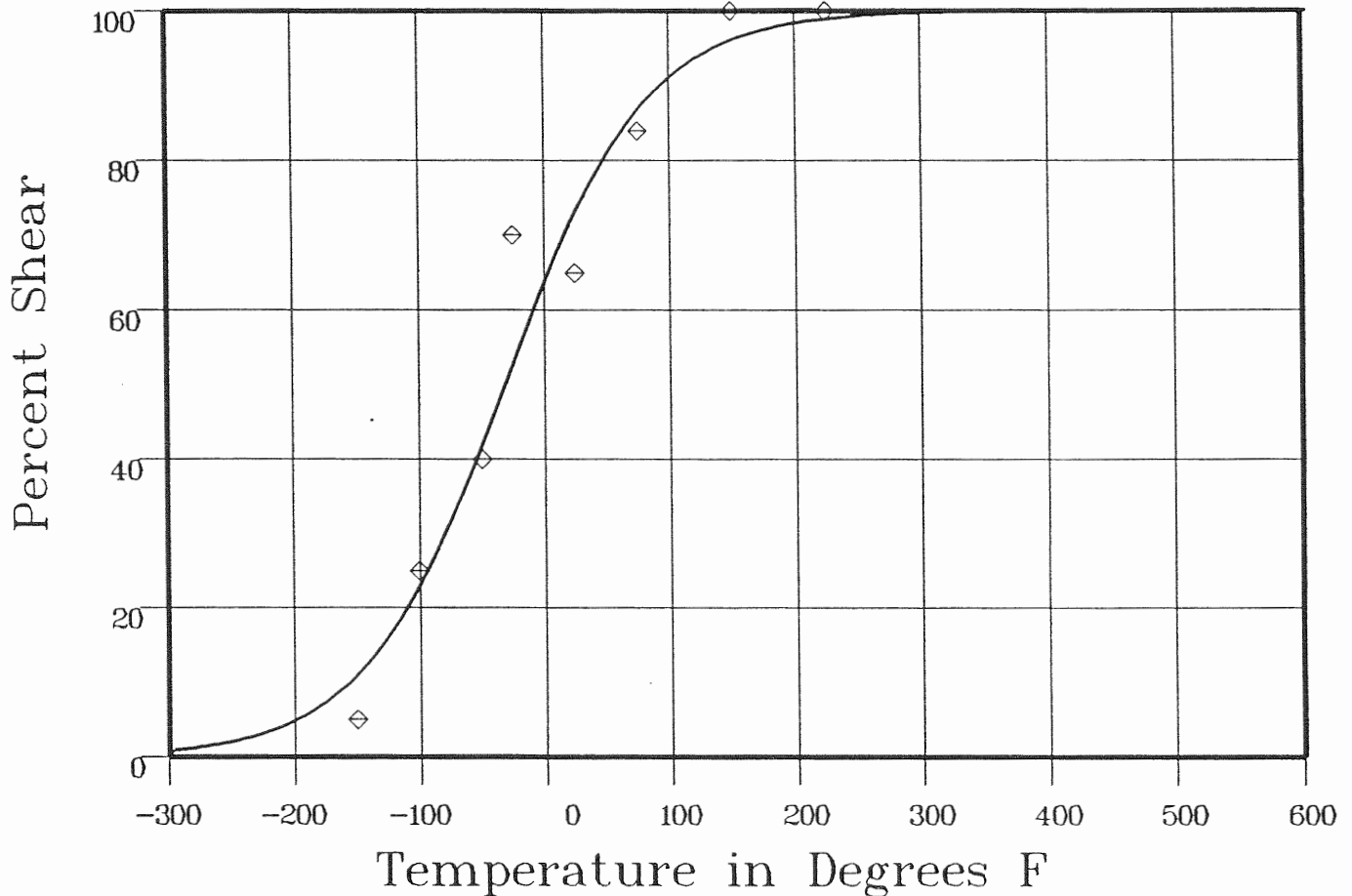
Material: HEAT AFFD ZONE

Heat Number:

Orientation:

Capsule: Y

Total Fluence: 1.05E+19



Data Set(s) Plotted
Plant: DCI Cap: Y Material: HEAT AFFD ZONE Ori: Heat #:

Charpy V-Notch Data

Temperature	Input Percent Shear	Computed Percent Shear	Differential
-150	5	11.79	-6.79
-100	25	24.45	.54
-50	40	43.95	-3.95
-25	70	54.97	15.02
25	65	74.73	-9.73
75	84	87.75	-3.75
150	100	96.43	3.56
225	100	99.02	.97

SUM of RESIDUALS = -4.12

HEAT AFFECTED ZONE CAPSULE V

CVGRAPH 4.1 Hyperbolic Tangent Curve Printed at 14:01:24 on 09-03-2002

Page 1

Coefficients of Curve 4

A = 50

B = 50

C = 116.82

T0 = -15.93

Equation is: $\text{Shear\%} = A + B * [\tanh((T - T0)/C)]$

Temperature at 50% Shear: -15.9

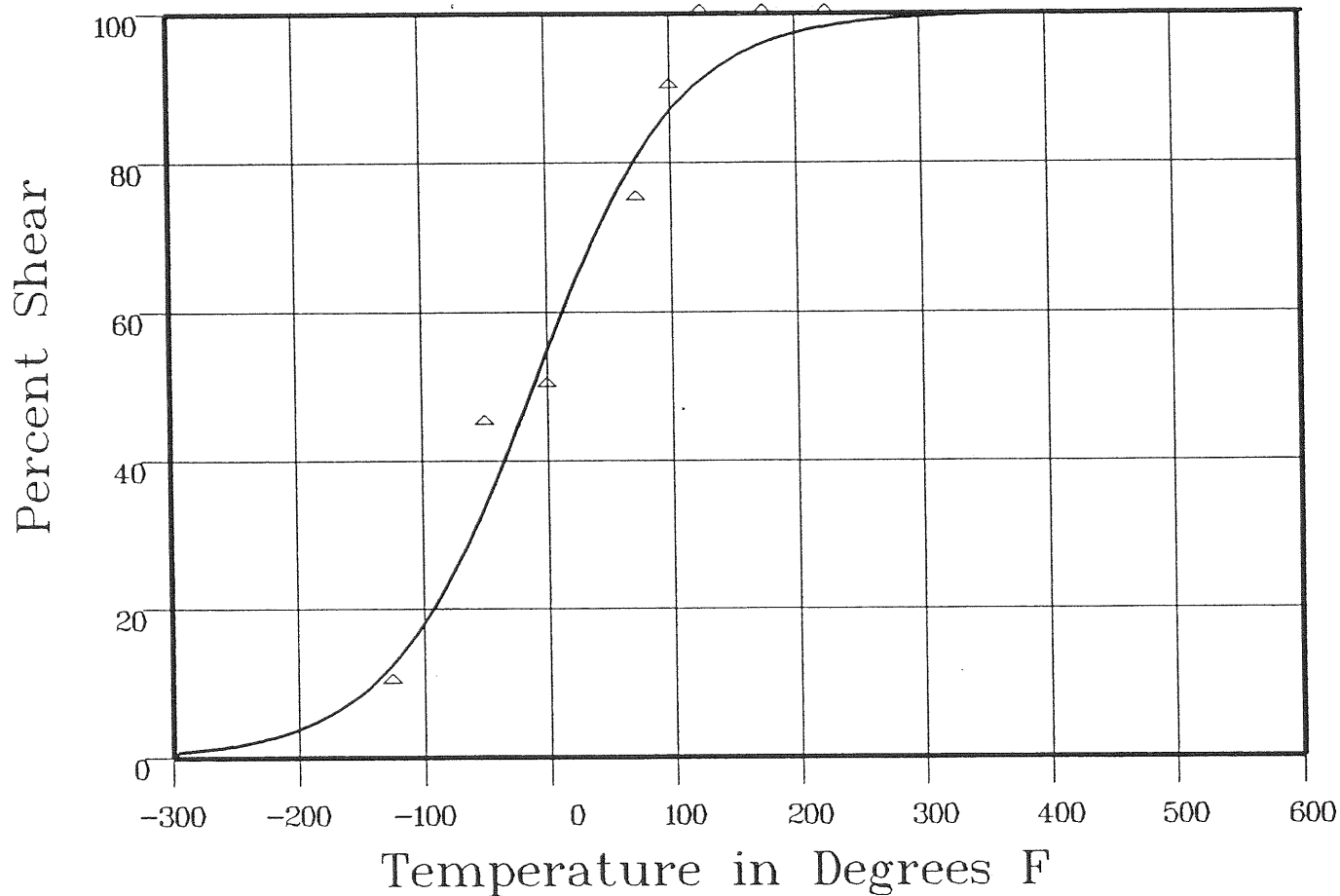
Material: HEAT AFFD ZONE

Heat Number:

Orientation:

Capsule: V

Total Fluence: 1.37E+19



Data Set(s) Plotted
Plant: DCI Cap: V Material: HEAT AFFD ZONE Ori: Heat #:

Charpy V-Notch Data

Temperature	Input Percent Shear	Computed Percent Shear	Differential
-125	10	13.38	-3.38
-50	45	35.82	9.17
0	50	56.77	-6.77
72	75	81.83	-6.83
100	90	87.91	2.08
125	100	91.77	8.22
175	100	96.33	3.66

**** Data continued on next page ****

HEAT AFFECTED ZONE CAPSULE V

Page 2

236940

Material: HEAT AFFD ZONE

Heat Number:

Orientation:

Capsule: V

Total Fluence: 1.37E+19

Charpy V-Notch Data (Continued)

Temperature
225

Input Percent Shear
100

Computed Percent Shear
98.4

Differential
159

SUM of RESIDUALS = 7.73

STANDARD REFERENCE MATERIAL UNIRRADIATED

CVGRAPH 4.1 Hyperbolic Tangent Curve Printed at 11:05:06 on 09-06-2002

Page 1

Coefficients of Curve 1

A = 62.59

B = 60.4

C = 81.25

T0 = 95.5

$$\text{Equation is: } \text{CVN} = A + B * [\tanh((T - T_0)/C)]$$

Upper Shelf Energy: 123 Fixed Temp. at 30 ft-lbs: 46.4 Temp. at 50 ft-lbs: 78.3 Lower Shelf Energy: 2.19 Fixed

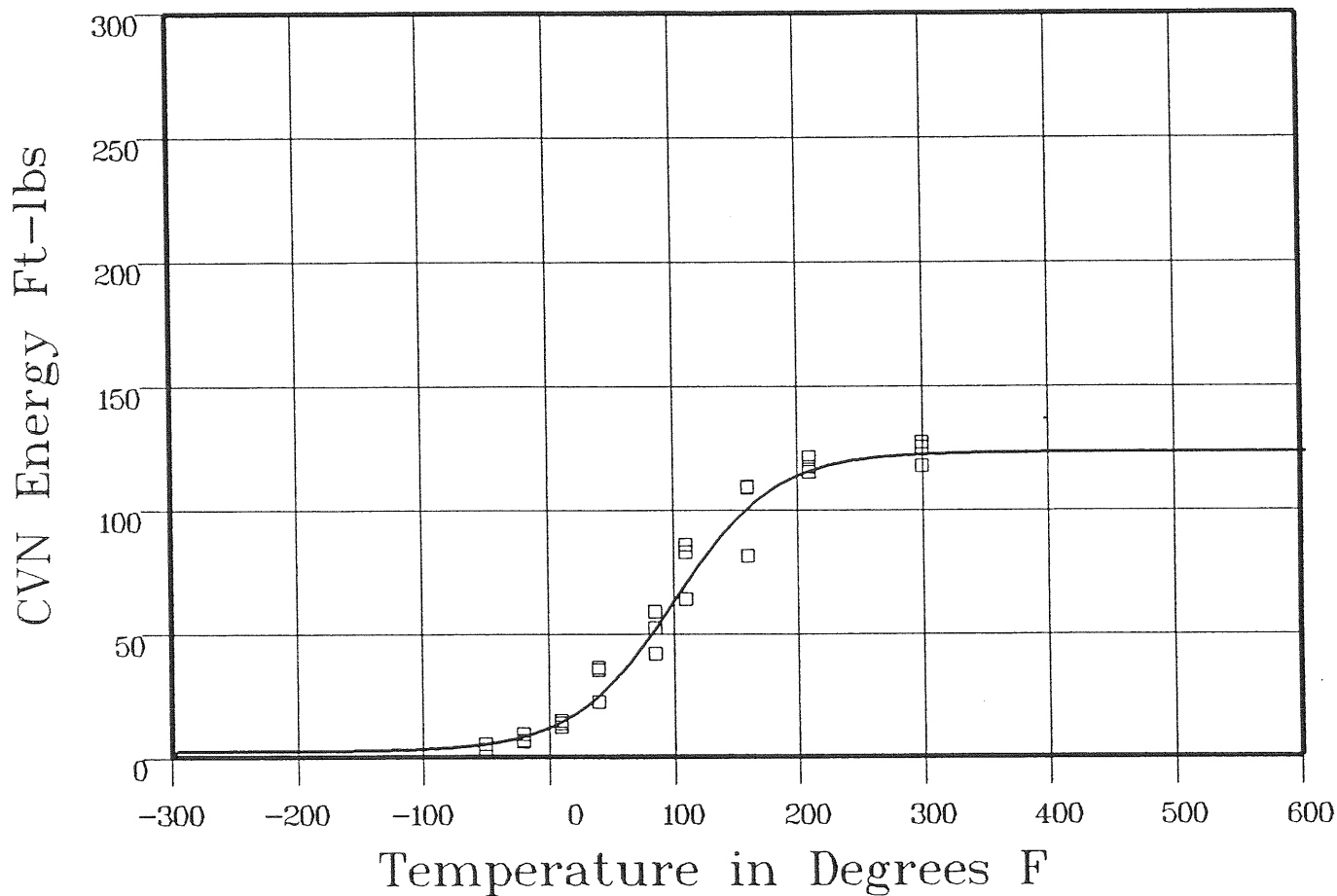
Material: SRM SA533B1

Heat Number:

Orientation: LT

Capsule: UNIRR

Total Fluence:



Data Set(s) Plotted

Plant: DCI

Cap: UNIRR

Material: SRM SA533B1

Ori: LT

Heat #:

Charpy V-Notch Data

Temperature	Input CVN Energy	Computed CVN Energy	Differential
-50	3	5.47	-2.47
-50	5	5.47	-4.7
-50	5	5.47	-4.7
-20	6	8.84	-2.84
-20	6.5	8.84	-2.34
-20	9	8.84	.15
10	13.5	15.32	-1.82
10	12	15.32	-3.32
10	14.5	15.32	-.82

**** Data continued on next page ****

STANDARD REFERENCE MATERIAL UNIRRADIATED

Page 2

236940

Material: SRM SA533B1

Heat Number:

Orientation: LT

Capsule: UNIRR

Total Fluence:

Charpy V-Notch Data (Continued)

Temperature	Input CVN Energy	Computed CVN Energy	Differential
40	22	26.74	-4.74
40	36	26.74	9.25
40	35	26.74	8.25
85	52	54.83	-2.83
85	58.5	54.83	3.66
85	41.5	54.83	-13.33
110	63.5	73.25	-9.75
110	82.5	73.25	9.24
110	85.5	73.25	12.24
160	109	102.49	6.5
160	108.5	102.49	6
160	81	102.49	-21.49
210	121	116.19	4.8
210	117	116.19	.8
210	115	116.19	-1.19
300	117.5	122.21	-4.71
300	125	122.21	2.78
300	127	122.21	4.78

SUM of RESIDUALS = -4.17

STANDARD REFERENCE MATERIAL CAPSULE S

CVGRAPH 4.1 Hyperbolic Tangent Curve Printed at 11:05:06 on 09-06-2002

Page 1

Coefficients of Curve 2

A = 61.09

B = 58.9

C = 79.04

T0 = 158.49

Equation is: $CVN = A + B * [\tanh((T - T0)/C)]$

Upper Shelf Energy: 120 Fixed Temp. at 30 ft-lbs: 112 Temp. at 50 ft-lbs: 143.4 Lower Shelf Energy: 219 Fixed

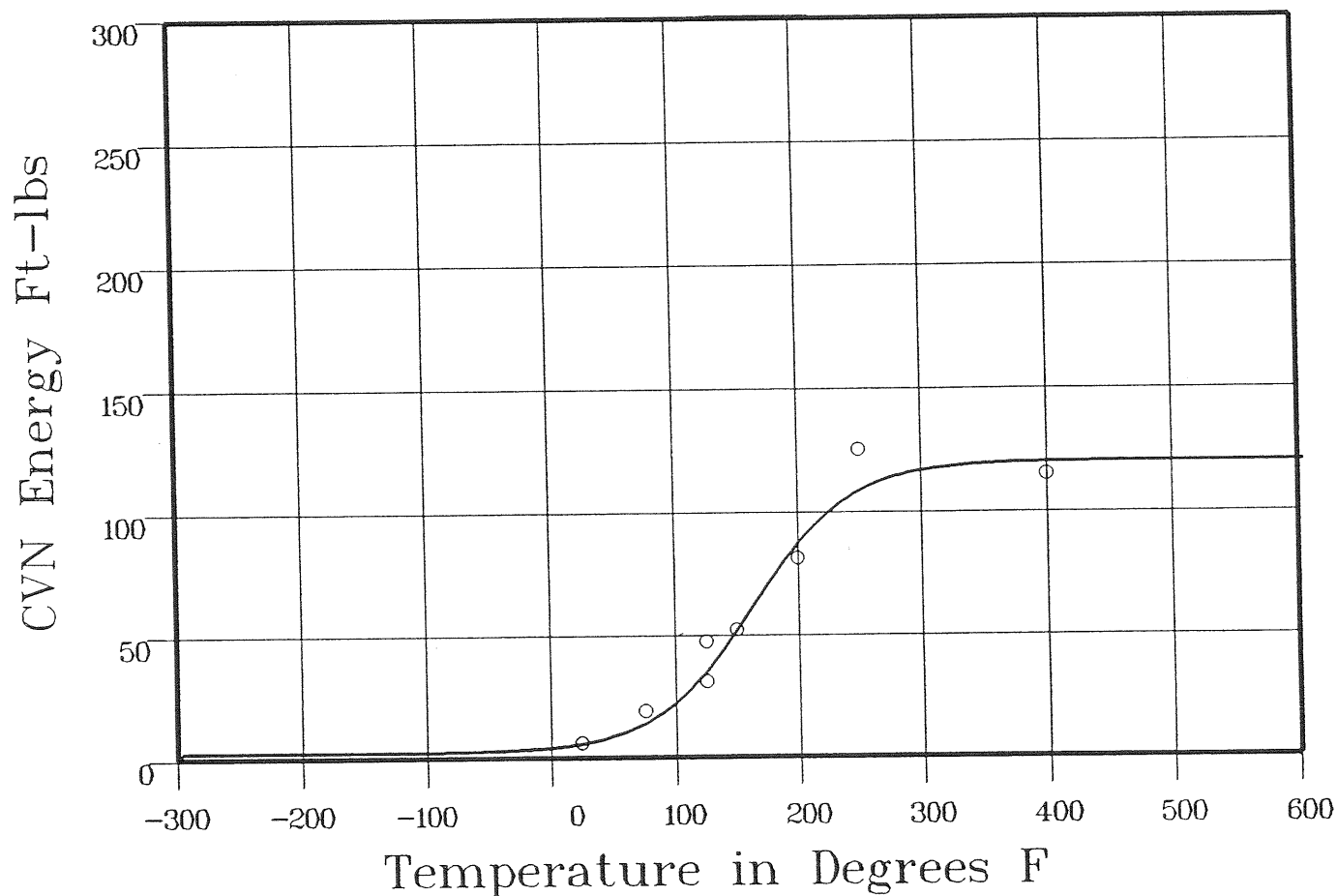
Material: SRM SA533B1

Heat Number:

Orientation: LT

Capsule: S

Total Fluence: 2.84E+18



Data Set(s) Plotted
Plant: DCI Cap: S Material: SRM SA533B1 Ori: LT Heat #:

Charpy V-Notch Data

Temperature	Input CVN Energy	Computed CVN Energy	Differential
25	6	6.08	-.08
76	19	15.19	3.8
125	47	37.53	9.46
125	31	37.53	-6.53
150	52	54.79	-2.79
200	81	89.46	-8.46
250	125	109.41	15.58
400	115	119.73	-4.73

SUM of RESIDUALS = 6.23

STANDARD REFERENCE MATERIAL CAPSULE Y

236940

CVGRAPH 4.1 Hyperbolic Tangent Curve Printed at 11:05:06 on 09-06-2002

Page 1

Coefficients of Curve 3

A = 57.09

B = 54.9

C = 64.9

T0 = 197.34

Equation is: $CVN = A + B * | \tanh((T - T0)/C) |$

Upper Shelf Energy: 112 Fixed Temp. at 30 ft-lbs: 162.2 Temp. at 50 ft-lbs: 188.9 Lower Shelf Energy: 2.19 Fixed

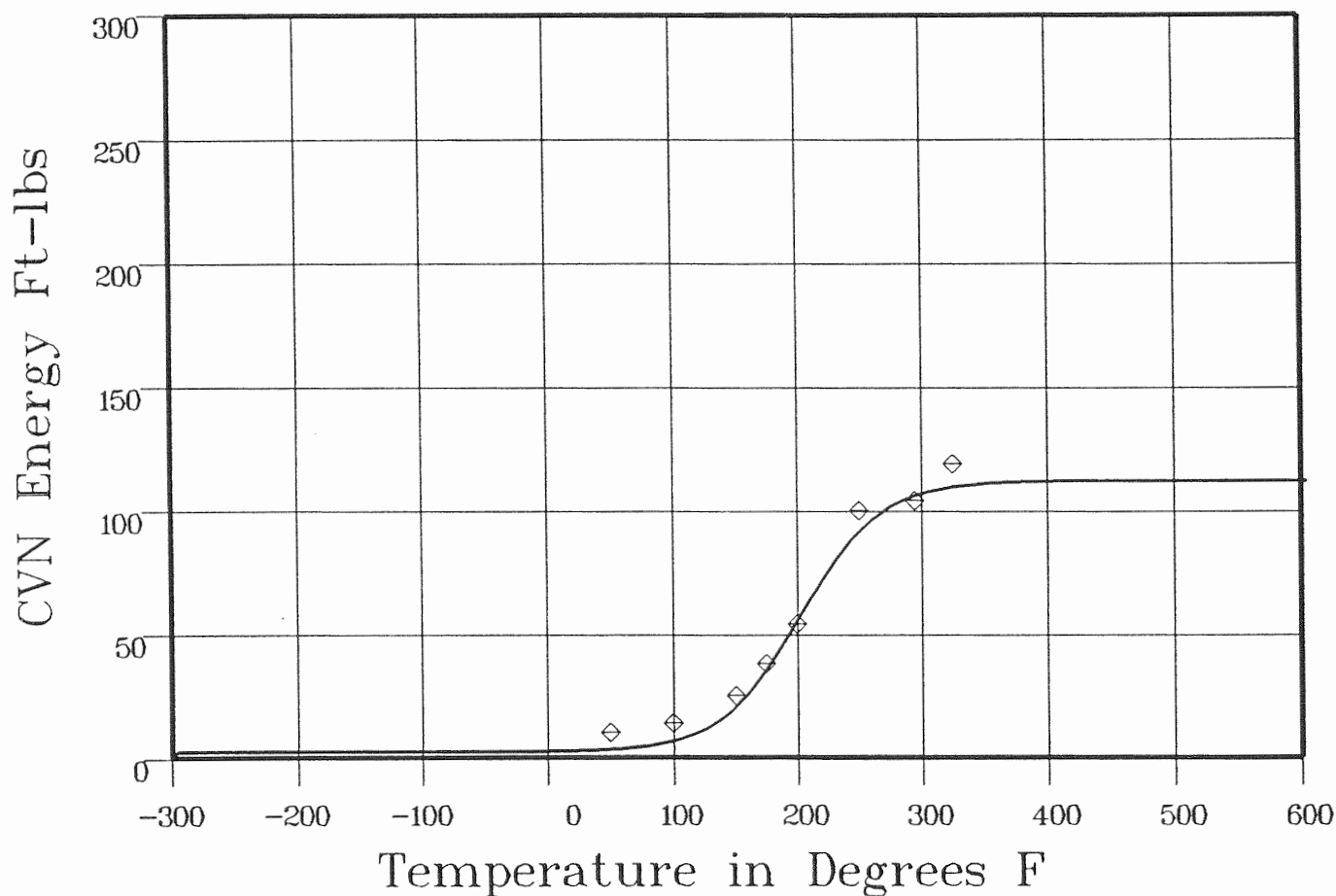
Material: SRM SA533B1

Heat Number:

Orientation: LT

Capsule: Y

Total Fluence: 1.05E+19



Data Set(s) Plotted

Plant: DCI

Cap: Y

Material: SRM SA533B1

Ori: LT

Heat #:

Charpy V-Notch Data

Temperature	Input CVN Energy	Computed CVN Energy	Differential
50	10	3.35	6.64
100	14	7.41	6.58
150	25	22.91	2.08
175	38	38.91	-.91
200	54	59.34	-5.34
250	100	93.89	6.1
295	104	106.83	-2.83
325	119	109.89	9.1

SUM of RESIDUALS = 21.42

STANDARD REFERENCE MATERIAL CAPSULE V

CVGRAPH 4.1 Hyperbolic Tangent Curve Printed at 11:05:06 on 09-06-2002

Page 1

Coefficients of Curve 4

A = 59.59

B = 57.4

C = 85.57

T0 = 211.87

$$\text{Equation is: } \text{CVN} = A + B * [\tanh((T - T0)/C)]$$

Upper Shelf Energy: 117 Fixed Temp. at 30 ft-lbs: 163 Temp. at 50 ft-lbs: 197.4 Lower Shelf Energy: 2.19 Fixed

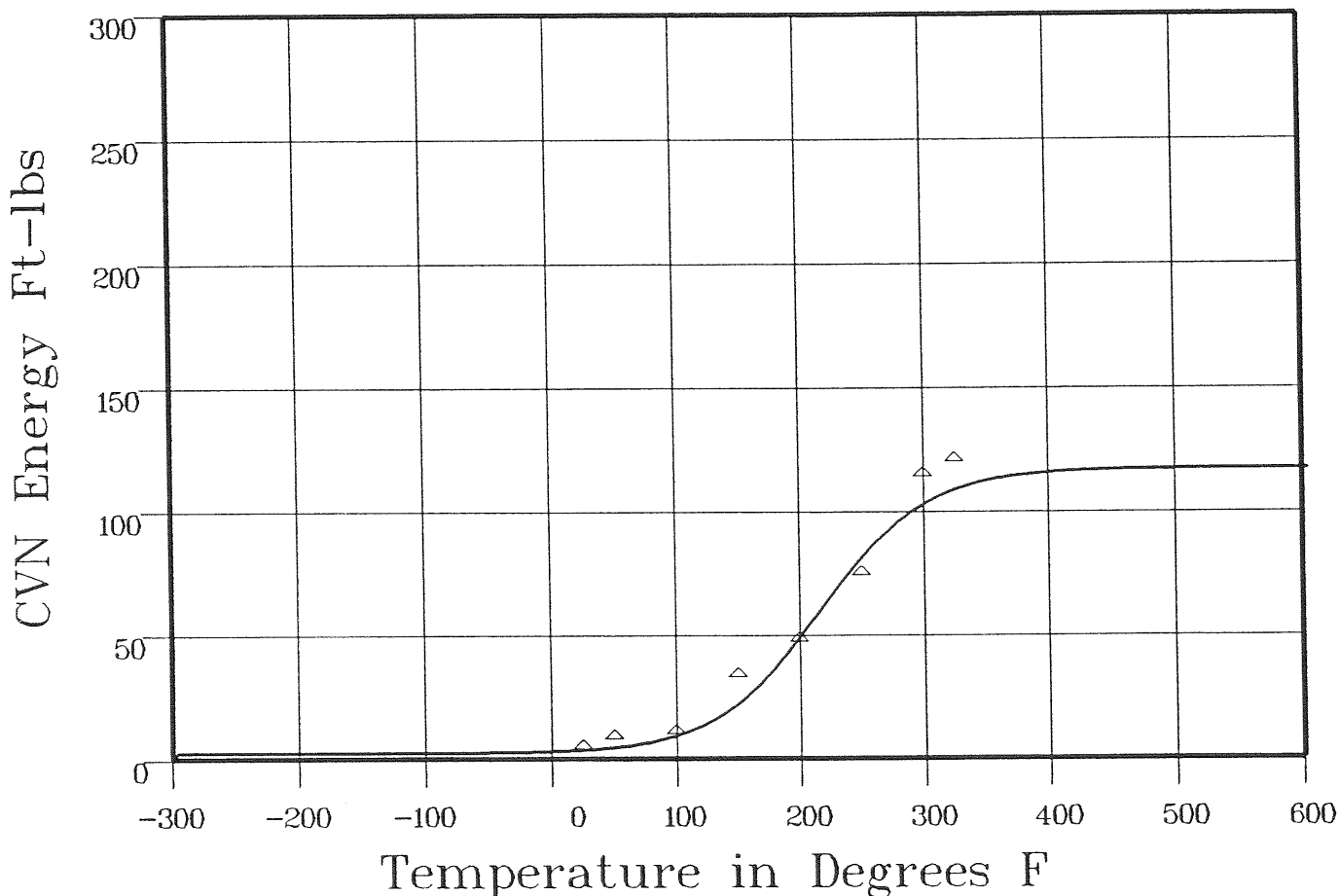
Material: SRM SA533B1

Heat Number:

Orientation: LT

Capsule: V

Total Fluence: 1.37E+19



Data Set(s) Plotted

Plant: DCI

Cap: V

Material: SRM SA533B1

Ori: LT

Heat #:

Charpy V-Notch Data

Temperature	Input CVN Energy	Computed CVN Energy	Differential
25	4	3.63	.36
50	8	4.75	3.24
100	10	10.03	-.03
150	33	24.08	8.91
200	47	51.68	-4.68
250	74	83.6	-9.6
300	114	104.01	9.98

**** Data continued on next page ****

236940

STANDARD REFERENCE MATERIAL CAPSULE V

Page 2

Material: SRM SA533B1

Heat Number:

Orientation: LT

Capsule: V

Total Fluence: 1.37E+19

Charpy V-Notch Data (Continued)

Temperature
325

Input CVN Energy
120

Computed CVN Energy
109.38

Differential
10.61

SUM of RESIDUALS = 18.8

STANDARD REFERENCE MATERIAL UNIRRADIATED

236940

CVGRAPH 4.1 Hyperbolic Tangent Curve Printed at 11:09:33 on 09-06-2002

Page 1

Coefficients of Curve 1

A = 43.65

B = 42.65

C = 84.08

T0 = 76.27

Equation is: $LE = A + B * | \tanh((T - T0)/C) |$

Upper Shelf LE: 86.31

Temperature at LE 35: 58.9

Lower Shelf LE: 1 Fixed

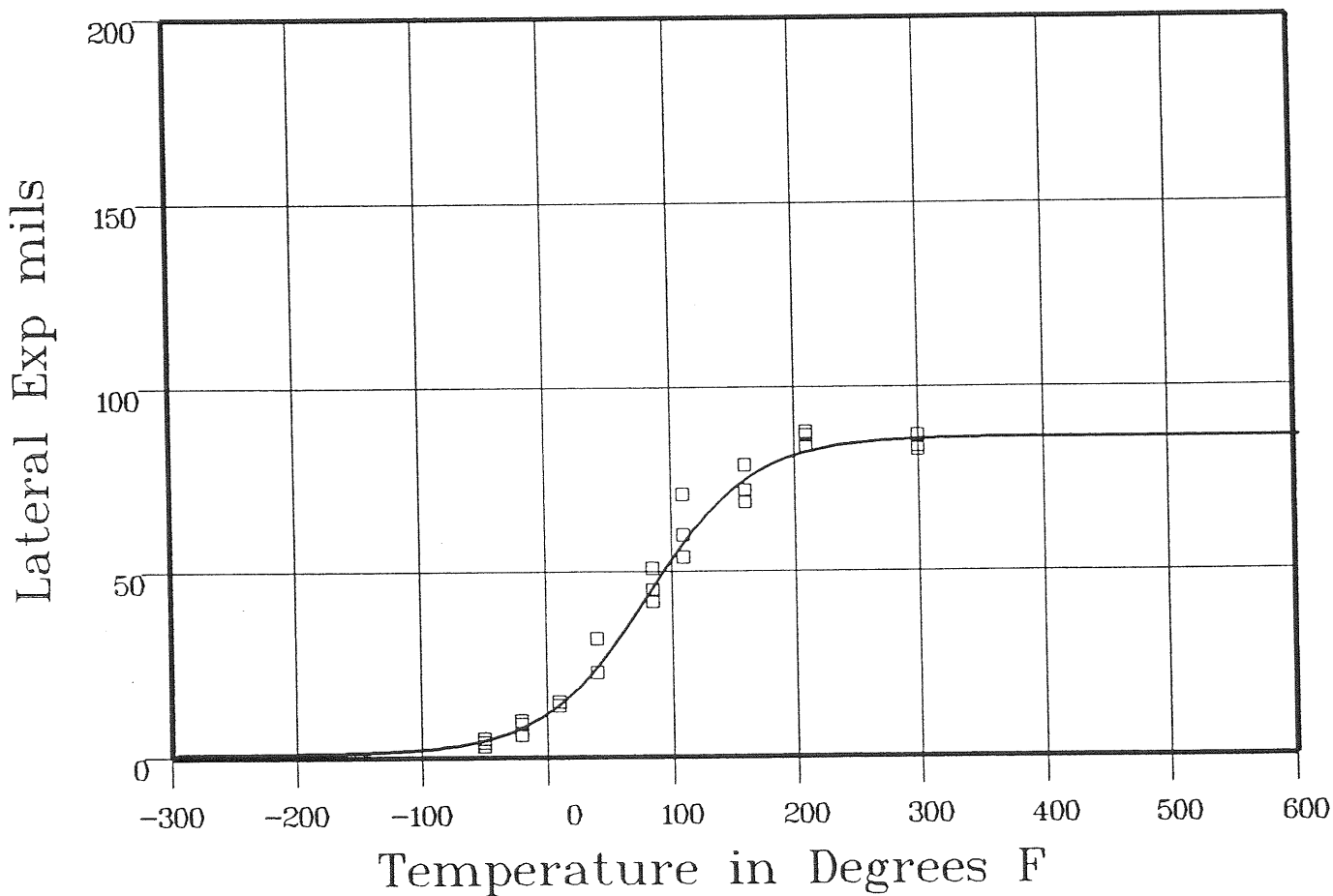
Material: SRM SA533B1

Heat Number:

Orientation: LT

Capsule: UNIRR

Total Fluence:



Data Set(s) Plotted

Plant: DCI

Cap: UNIRR

Material: SRM SA533B1

Ori: LT

Heat #:

Charpy V-Notch Data

Temperature	Input Lateral Expansion	Computed LE	Differential
-50	4	5.03	-1.03
-50	3	5.03	-2.03
-50	5	5.03	-.03
-20	9	8.84	.15
-20	6	8.84	-2.84
-20	10	8.84	1.15
10	14	15.61	-1.61
10	15	15.61	-.61
10	14	15.61	-1.61

**** Data continued on next page ****

STANDARD REFERENCE MATERIAL UNIRRADIATED

226940

Page 2

Material: SRM SA533B1

Heat Number:

Orientation: LT

Capsule: UNIRR

Total Fluence:

Charpy V-Notch Data (Continued)

Temperature	Input Lateral Expansion	Computed L.E.	Differential
40	23	26.31	-3.31
40	32	26.31	5.68
40	32	26.31	5.68
85	45	48.06	-3.06
85	51	48.06	2.93
85	42	48.06	-6.06
110	54	59.9	-5.9
110	60	59.9	.09
110	71	59.9	11.09
160	79	76.07	2.92
160	72	76.07	-4.07
160	69	76.07	-7.07
210	87	82.91	4.08
210	84	82.91	1.08
210	88	82.91	5.08
300	83	85.9	-2.9
300	87	85.9	1.09
300	84	85.9	-1.9

SUM of RESIDUALS = -3.03

STANDARD REFERENCE MATERIAL CAPSULE S

235840

CVGRAPH 4.1 Hyperbolic Tangent Curve Printed at 11:09:33 on 09-06-2002

Page 1

Coefficients of Curve 2

A = 43.48

B = 42.48

C = 100.49

T0 = 144.84

Equation is: $LE = A + B * [\tanh((T - T0)/C)]$

Upper Shelf LE: 85.97

Temperature at LE 35: 124.4

Lower Shelf LE: 1 Fixed

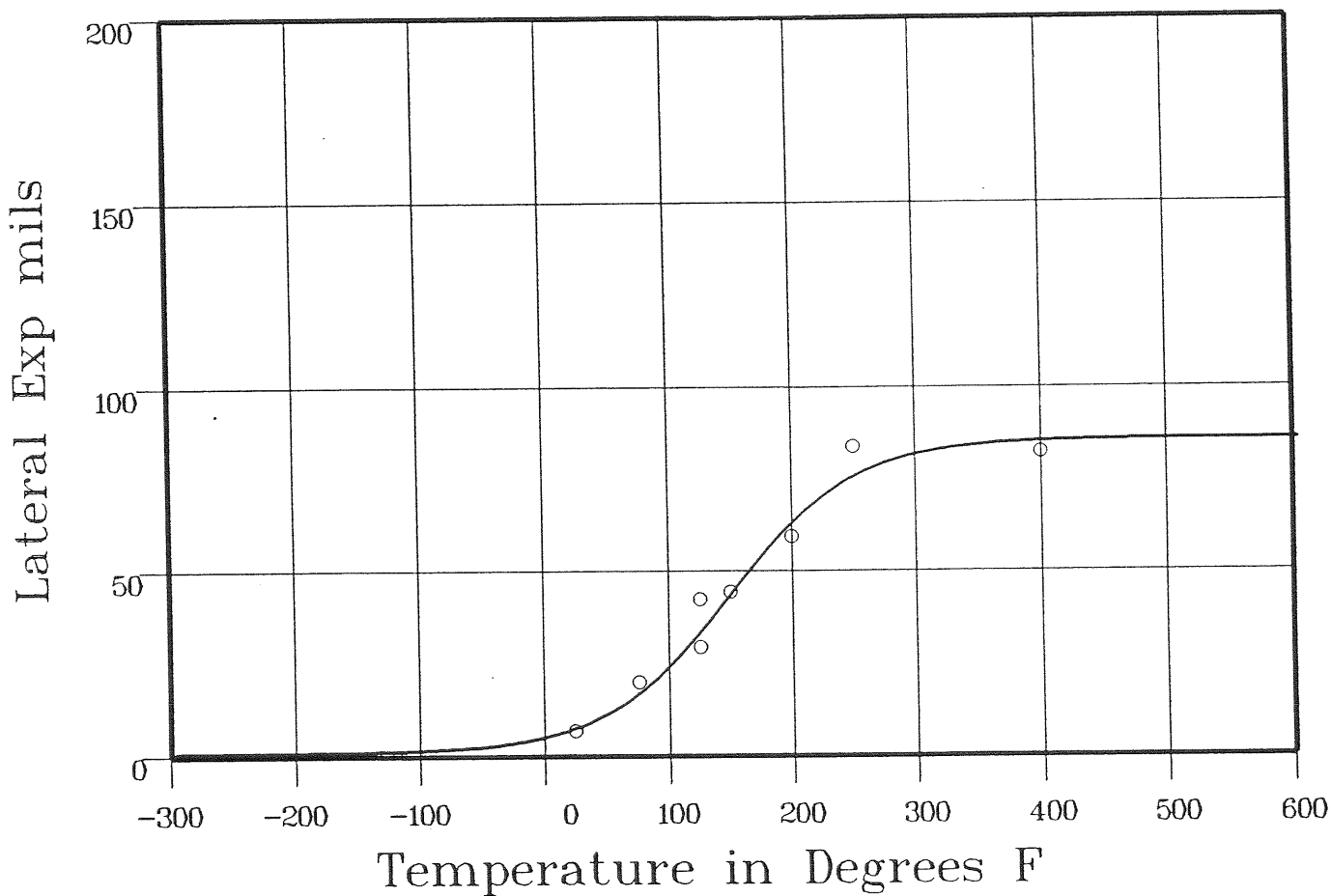
Material: SRM SA533B1

Heat Number:

Orientation: LT

Capsule: S

Total Fluence: 2.84E+18



Data Set(s) Plotted

Plant: DC1

Cap: S

Material: SRM SA533B1

Ori: LT

Heat #:

Charpy V-Notch Data

Temperature	Input Lateral Expansion	Computed LE	Differential
25	7	8.16	-1.16
76	20	18.21	1.78
125	42.5	35.2	7.29
125	29.5	35.2	-5.7
150	44.5	45.66	-1.16
200	59.5	64.71	-5.21
250	84	76.64	7.35
400	82.5	85.44	-2.94

SUM of RESIDUALS = 24

STANDARD REFERENCE MATERIAL CAPSULE Y

236940

CVGRAPH 4.1 Hyperbolic Tangent Curve Printed at 11:09:33 on 09-06-2002

Page 1

Coefficients of Curve 3

A = 51.69

B = 50.69

C = 106.44

T0 = 214.43

Equation is: $LE = A + B * | \tanh((T - T0)/C) |$

Upper Shelf LE: 102.39

Temperature at L.E. 35: 178

Lower Shelf LE: 1 Fixed

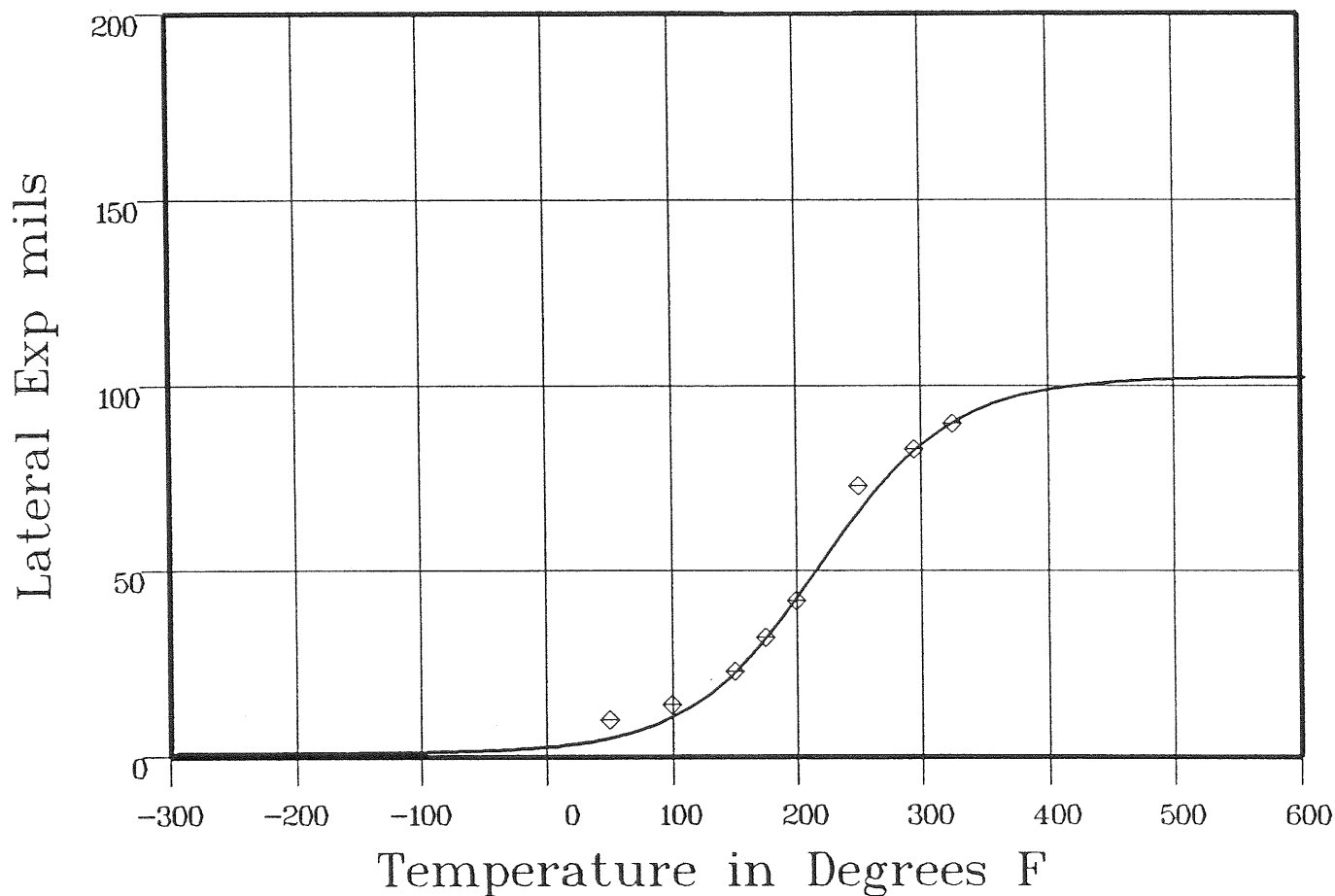
Material: SRM SA533B1

Heat Number:

Orientation: LT

Capsule: Y

Total Fluence: 1.05E+19



Data Set(s) Plotted

Plant: DC1

Cap: Y

Material: SRM SA533B1

Ori: LT

Heat #:

Charpy V-Notch Data

Temperature	Input Lateral Expansion	Computed L.E.	Differential
50	10	5.41	4.58
100	14	11.57	2.42
150	23	24.27	-1.27
175	32	33.73	-1.73
200	42	44.86	-2.86
250	73	68.03	4.96
295	83	84.1	-1.1
325	90	91.1	-1.1

SUM of RESIDUALS = 3.88

STANDARD REFERENCE MATERIAL CAPSULE V

CVGRAPH 4.1 Hyperbolic Tangent Curve Printed at 11:09:33 on 09-06-2002

Page 1

Coefficients of Curve 4

A = 52.27

B = 51.27

C = 117

T0 = 254.48

Equation is: $LE = A + B * [\tanh((T - T0)/C)]$

Upper Shelf LE: 103.54

Temperature at LE 35: 213.4

Lower Shelf LE: 1 Fixed

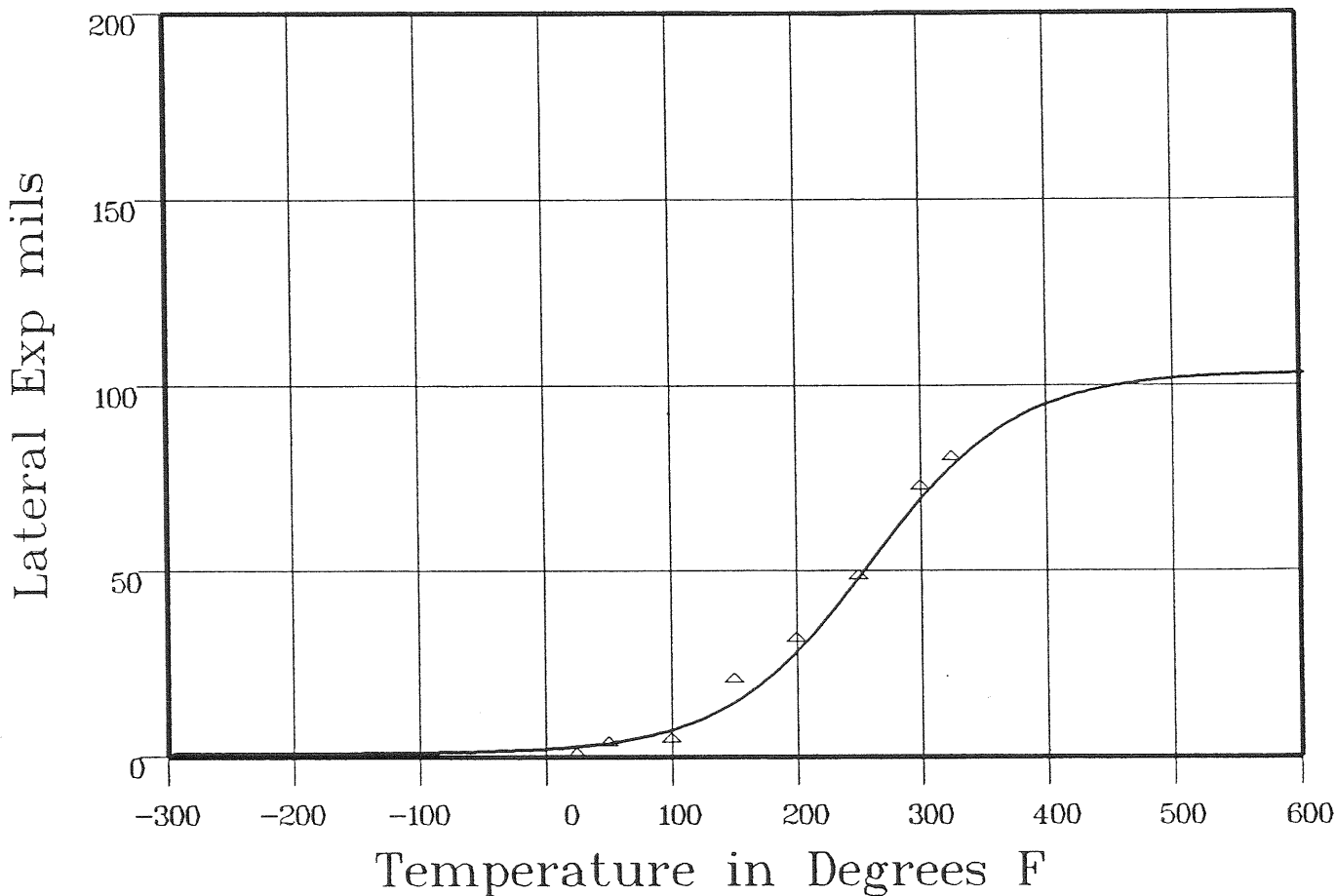
Material: SRM SA533B1

Heat Number:

Orientation: LT

Capsule: V

Total Fluence: 1.37E+19



Data Set(s) Plotted
Plant: DCI Cap: V Material: SRM SA533B1 Ori: LT Heat #:

Charpy V-Notch Data

Temperature	Input Lateral Expansion	Computed LE	Differential
25	0	2.99	-2.99
50	3	4.01	-1.01
100	4	7.82	-3.82
150	20	15.72	4.27
200	31	29.98	1.01
250	48	50.3	-2.3
300	72	71.27	.72

**** Data continued on next page ****

STANDARD REFERENCE MATERIAL CAPSULE V

236940

Page 2

Material: SRM SA533B1

Heat Number:

Orientation: LT

Capsule: V

Total Fluence: 1.37E+19

Charpy V-Notch Data (Continued)

Temperature
325

Input Lateral Expansion
80

Computed LE
79.9

Differential
.09

SUM of RESIDUALS = -4.03

STANDARD REFERENCE MATERIAL UNIRRADIATED

CVGRAPH 4.1 Hyperbolic Tangent Curve Printed at 11:15:09 on 09-06-2002

Page 1

Coefficients of Curve 1

A = 50

B = 50

C = 100.89

T0 = 85.54

Equation is: $\text{Shear\%} = A + B * [\tanh((T - T0)/C)]$

Temperature at 50% Shear: 85.5

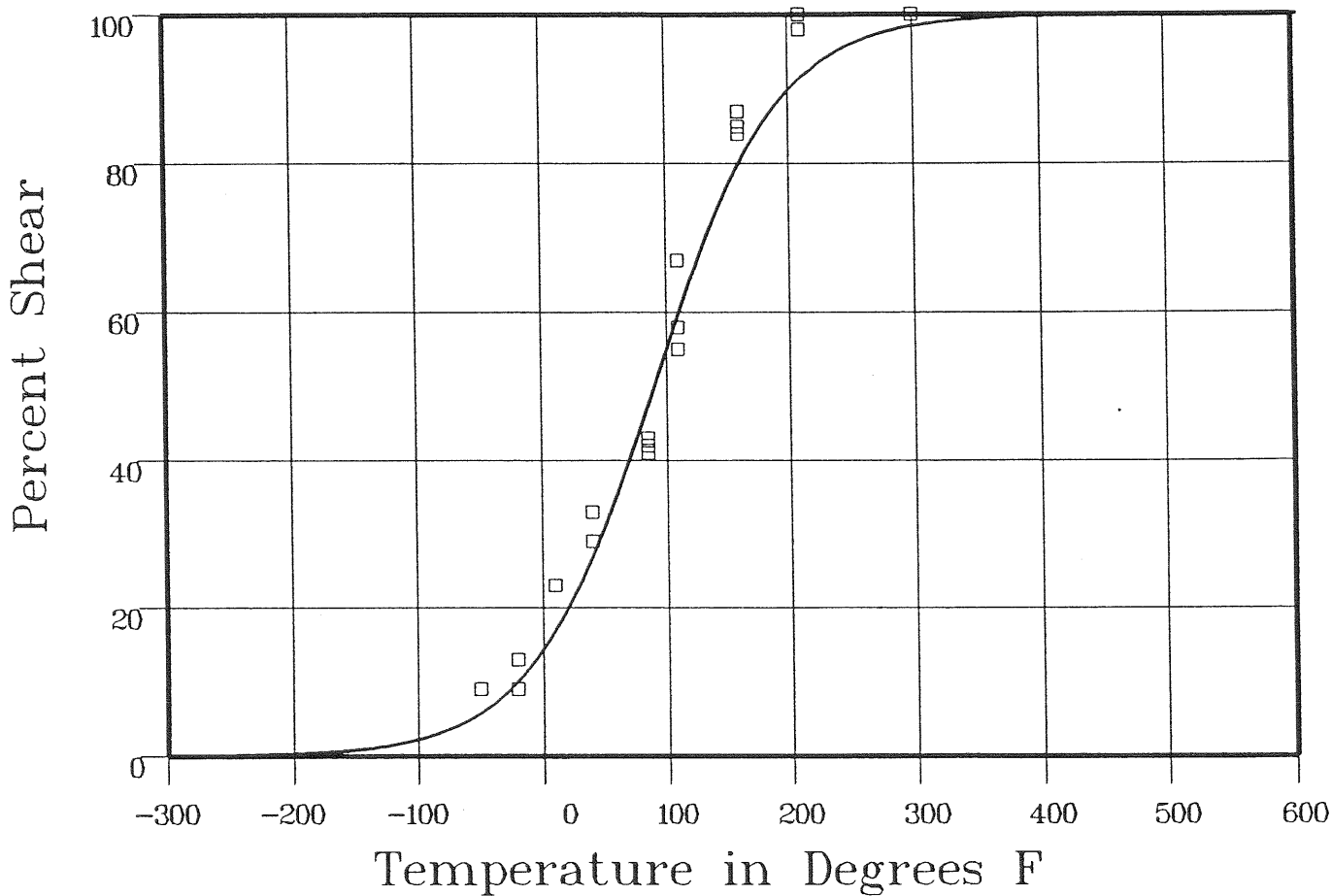
Material: SRM SA533B1

Heat Number:

Orientation: LT

Capsule: UNIRR

Total Fluence:



Data Set(s) Plotted

Plant: DCI

Cap: UNIRR

Material: SRM SA533B1

Ori: LT

Heat #:

Charpy V-Notch Data

Temperature	Input Percent Shear	Computed Percent Shear	Differential
-50	9	6.37	2.62
-50	9	6.37	2.62
-50	9	6.37	2.62
-20	13	10.98	2.01
-20	9	10.98	-1.98
-20	13	10.98	2.01
10	23	18.27	4.72
10	23	18.27	4.72
10	23	18.27	4.72

**** Data continued on next page ****

STANDARD REFERENCE MATERIAL UNIRRADIATED

236940

Page 2

Material: SRM SA533B1

Heat Number:

Orientation: LT

Capsule: UNIRR

Total Fluence:

Charpy V-Notch Data (Continued)

Temperature	Input Percent Shear	Computed Percent Shear	Differential
40	33	28.84	4.15
40	29	28.84	.15
40	29	28.84	.15
85	42	49.72	-7.72
85	43	49.72	-6.72
85	41	49.72	-8.72
110	55	61.88	-6.88
110	58	61.88	-3.88
110	67	61.88	5.11
160	87	81.39	5.6
160	84	81.39	2.6
160	85	81.39	3.6
210	100	92.17	7.82
210	98	92.17	5.82
210	98	92.17	5.82
300	100	98.59	1.4
300	100	98.59	1.4
300	100	98.59	1.4

SUM of RESIDUALS = 35.18

STANDARD REFERENCE MATERIAL CAPSULE S

CVGRAPH 4.1 Hyperbolic Tangent Curve Printed at 11:15:09 on 09-06-2002

236940

Page 1

Coefficients of Curve 2

A = 50

B = 50

C = 90.18

T0 = 157.61

Equation is: $\text{Shear}\% = A + B * | \tanh((T - T0)/C) |$

Temperature at 50% Shear: 157.6

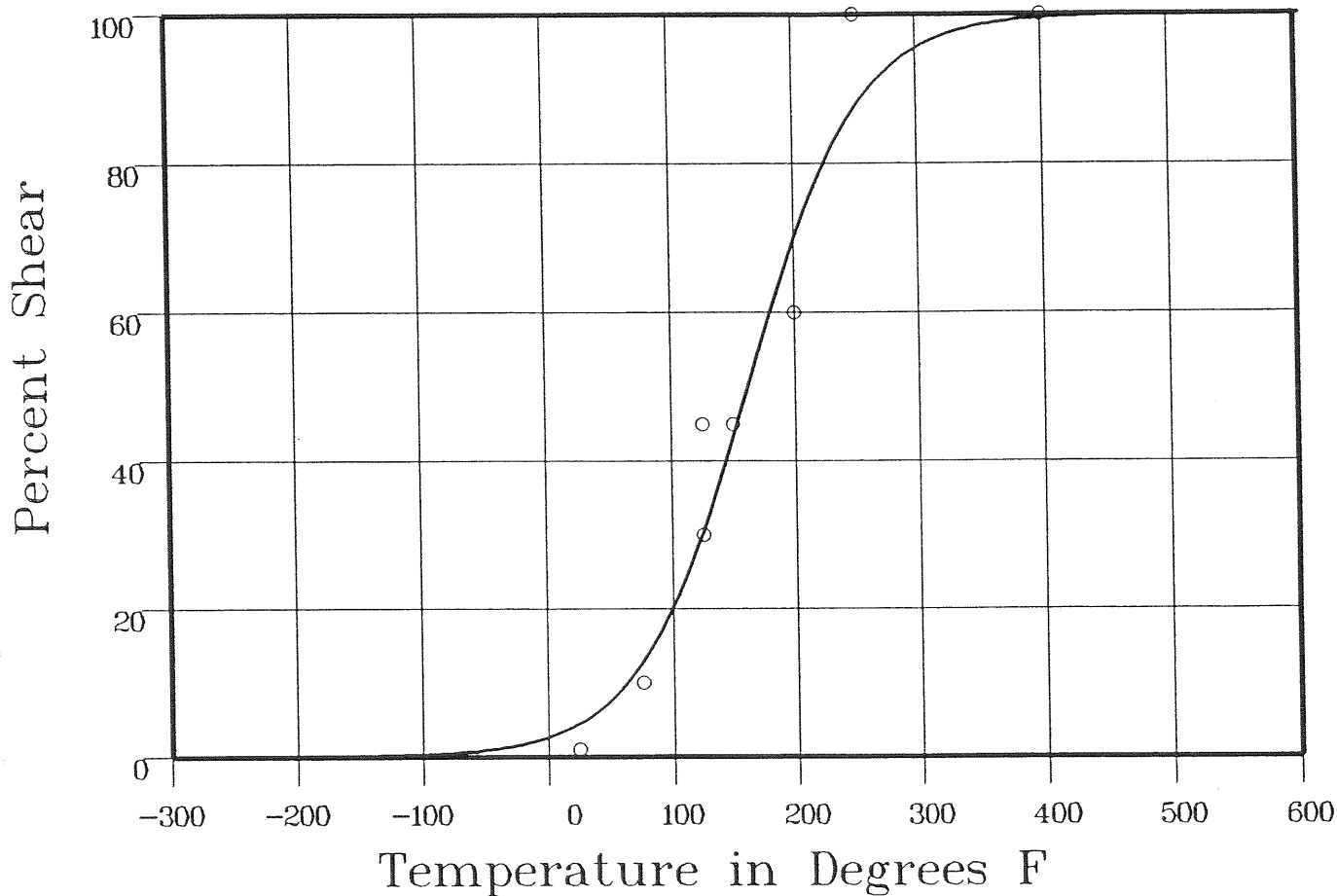
Material: SRM SA533B1

Heat Number:

Orientation: LT

Capsule: S

Total Fluence: 2.84E+18



Data Set(s) Plotted

Plant: DC1

Cap: S

Material: SRM SA533B1

Ori: LT

Heat #:

Charpy V-Notch Data

Temperature	Input Percent Shear	Computed Percent Shear	Differential
25	1	5.01	-4.01
76	10	14.06	-4.06
125	45	32.66	12.33
125	30	32.66	-2.66
150	45	45.78	-7.8
200	60	71.9	-11.9
250	100	88.58	11.41
400	100	99.53	.46

SUM of RESIDUALS = .77

STANDARD REFERENCE MATERIAL CAPSULE Y

236940

CVGRAPH 4.1 Hyperbolic Tangent Curve Printed at 11:15:09 on 09-06-2002

Page 1

Coefficients of Curve 3

A = 50

B = 50

C = 67.9

T0 = 188.37

Equation is: $\text{Shear}\% = A + B * [\tanh((T - T0)/C)]$

Temperature at 50% Shear: 188.3

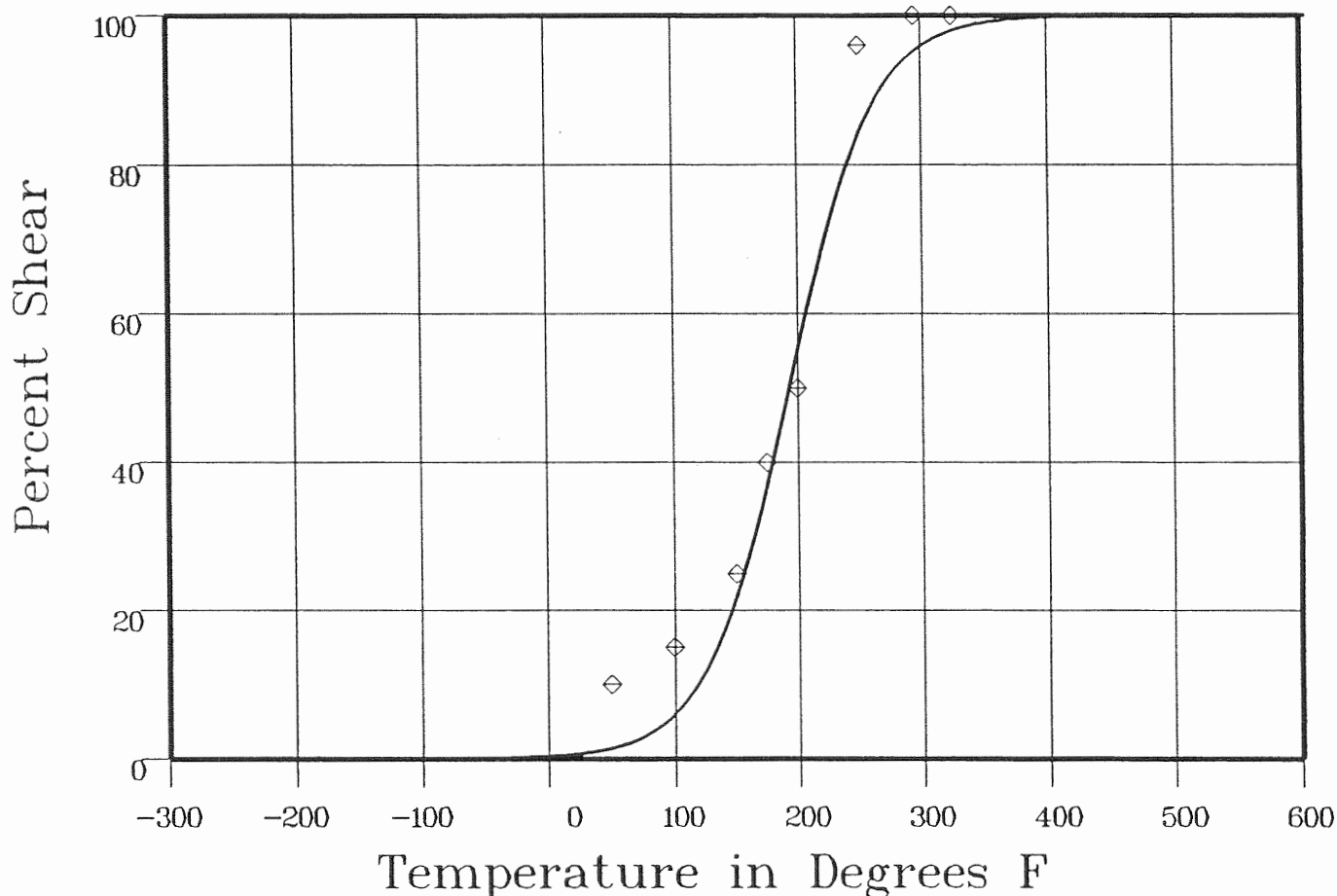
Material: SRM SA533B1

Heat Number:

Orientation: LT

Capsule: Y

Total Fluence: 1.05E+19



Data Set(s) Plotted
Plant: DCI Cap: Y Material: SRM SA533B1 Ori: LT Heat #:

Charpy V-Notch Data

Temperature	Input Percent Shear	Computed Percent Shear	Differential
50	10	166	8.33
100	15	6.89	8.1
150	25	24.41	.58
175	40	40.27	-27
200	50	58.47	-8.47
250	96	85.99	10
295	100	95.85	4.14
325	100	98.24	1.75

SUM of RESIDUALS = 24.18

STANDARD REFERENCE MATERIAL CAPSULE V

CVGRAPH 4.1 Hyperbolic Tangent Curve Printed at 11:15:09 on 09-06-2002

Page 1

Coefficients of Curve 4

A = 50

B = 50

C = 98.01

T0 = 203.43

Equation is: $\text{Shear}\% = A + B * [\tanh((T - T0)/C)]$

Temperature at 50% Shear: 203.4

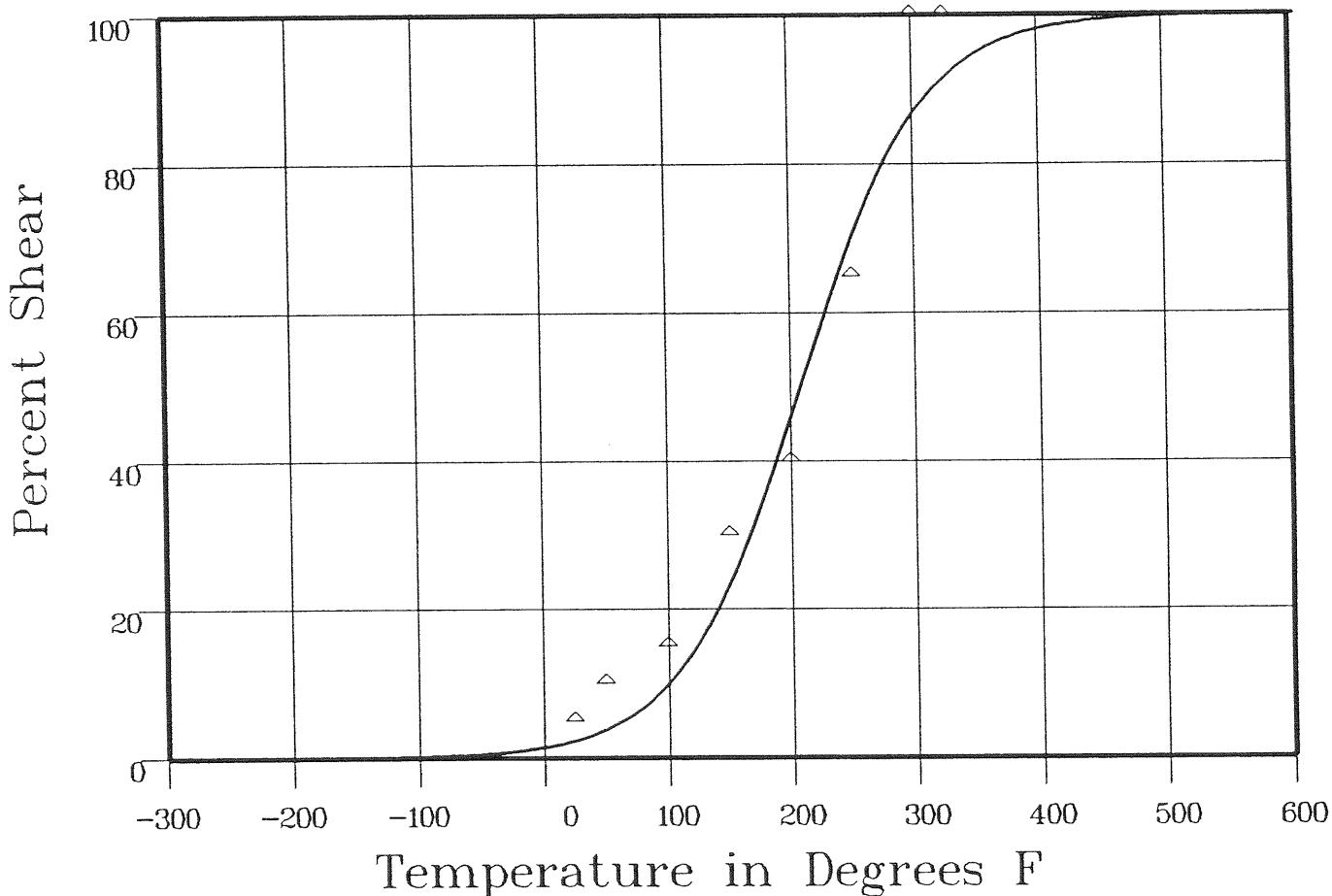
Material: SRM SA533B1

Heat Number:

Orientation: LT

Capsule: V

Total Fluence: 1.37E+19



Data Set(s) Plotted
Plant: DCI Cap: V Material: SRM SA533B1 Ori: LT Heat #:

Charpy V-Notch Data

Temperature	Input Percent Shear	Computed Percent Shear	Differential
25	5	2.55	2.44
50	10	4.18	5.81
100	15	10.8	4.19
150	30	25.15	4.84
200	40	48.24	-8.24
250	65	72.11	-7.11
300	100	87.76	12.23

**** Data continued on next page ****

STANDARD REFERENCE MATERIAL CAPSULE V

Page 2

236940

Material: SRM SA533B1

Heat Number:

Orientation: LT

Capsule: V

Total Fluence: 1.37E+19

Charpy V-Notch Data (Continued)

Temperature
325

Input Percent Shear
100

Computed Percent Shear
92.27

Differential
7.72

SUM of RESIDUALS = 21.89

236940

APPENDIX D

DIABLO CANYON UNIT 1 SURVEILLANCE PROGRAM

CREDIBILITY ANALYSIS

INTRODUCTION:

Regulatory Guide 1.99, Revision 2, describes general procedures acceptable to the NRC staff for calculating the effects of neutron radiation embrittlement of the low-alloy steels currently used for light-water-cooled reactor vessels. Position C.2 of Regulatory Guide 1.99, Revision 2, describes the method for calculating the adjusted reference temperature and Charpy upper-shelf energy of reactor vessel beltline materials using surveillance capsule data. The methods of Position C.2 can only be applied when two or more credible surveillance data sets become available from the reactor in question.

To date there have been three surveillance capsules removed from the Diablo Canyon Unit 1 reactor vessel. To use these surveillance data sets, they must be shown to be credible. In accordance with the discussion of Regulatory Guide 1.99, Revision 2, there are five requirements that must be met for the surveillance data to be judged credible.

The purpose of this evaluation is to apply the credibility requirements of Regulatory Guide 1.99, Revision 2, to the Diablo Canyon Unit 1 reactor vessel surveillance data and determine if the Diablo Canyon Unit 1 surveillance data is credible.

EVALUATION:

Criterion 1: Materials in the capsules should be those judged most likely to be controlling with regard to radiation embrittlement.

The beltline region of the reactor vessel is defined in Appendix G to 10 CFR Part 50, "Fracture Toughness Requirements", as follows:

"the reactor vessel (shell material including welds, heat affected zones, and plates or forgings) that directly surrounds the effective height of the active core and adjacent regions of the reactor vessel that are predicted to experience sufficient neutron radiation damage to be considered in the selection of the most limiting material with regard to radiation damage."

The Diablo Canyon Unit 1 reactor vessel consists of the following beltline region materials:

236940

- Intermediate Shell Plate B4106-1 (Heat Number C2884-1)
- Intermediate Shell Plate B4106-2 (Heat Number C2854-2)
- Intermediate Shell Plate B4106-3 (Heat Number C2793-1)
- Lower Shell Plate B4107-1 (Heat C3121-1)
- Lower Shell Plate B4107-2 (Heat Number C3131-2)
- Lower Shell Plate B4107-3 (Heat Number C3131-1)
- Intermediate Shell Plate Longitudinal Weld Seams 2-442 A, B, C (Heat # 27204, Linde 1092)
- Lower Shell Plate Longitudinal Weld Seams 3-442 A, B, C (Heat # 27204, Linde 1092)
- Intermediate to Lower Shell Plate Circumferential Weld Seam 9-442 (Heat # 21935, Linde 1092)

Per WCAP-8465, the Diablo Canyon Unit 1 surveillance program was based on ASTM E185, "Recommended Practice for Surveillance Tests on Nuclear Reactor Vessels". Per Section 3.1 of ASTM E185-70, "Sample shall represent one heat of the base metal and one butt weld if a weld occurs in the irradiated region."

At the time the Diablo Canyon Unit 1 surveillance capsule program was developed, intermediate shell plates were judged to be most limiting based on the lowest initial upper shelf energy values and higher initial copper values. Hence, all the intermediate shell plates were therefore utilized in the surveillance program.

The weld material in the Diablo Canyon Unit 1 surveillance program was made of the same wire heat as the reactor vessel upper to intermediate and lower shell longitudinal weld seams (Wire Heat No. 27204, Flux Type Linde 1092). This represents six of the seven welds in the beltline area. The seventh weld, the intermediate to lower shell girth welds, was made from heat 21935. This weld had a higher initial USE and lower copper content than heat 27204. Thus, heat 27204 was chosen as the surveillance weld. ASTM E185-70 only requires that the surveillance material represent a weld in the irradiated region. Since the surveillance weld heat # 27204 is the same as the intermediate and lower shell longitudinal welds, then this criterion is true.

Hence, Criterion 1 is met for the Diablo Canyon Unit 1 reactor vessel.

Criterion 2: Scatter in the plots of Charpy energy versus temperature for the irradiated and unirradiated conditions should be small enough to permit the determination of the 30 ft-lb temperature and upper shelf energy unambiguously.

236940

Plots of Charpy energy versus temperature for the unirradiated and irradiated condition are presented in Appendix C. Based on engineering judgment, the scatter in the data presented in these plots is small enough to permit the determination of the 30 ft-lb temperature and the upper shelf energy of the Diablo Canyon Unit 1 surveillance materials unambiguously. Hence, the Diablo Canyon Unit 1 surveillance program meets this criterion.

Criterion 3: When there are two or more sets of surveillance data from one reactor, the scatter of ΔRT_{NDT} values about a best-fit line drawn as described in Regulatory Position 2.1 normally should be less than 28°F for welds and 17°F for base metal. Even if the fluence range is large (two or more orders of magnitude), the scatter should not exceed twice those values. Even if the data fail this criterion for use in shift calculations, they may be credible for determining decrease in upper shelf energy if the upper shelf can be clearly determined, following the definition given in ASTM E185-82.

The functional form of the least squares method as described in Regulatory Position 2.1 will be utilized to determine a best-fit line for this data and to determine if the scatter of these ΔRT_{NDT} values about this line is less than 28°F for welds and less than 17°F for the plate.

Following is the calculation of the best fit line as described in Regulatory Position 2.1 of Regulatory Guide 1.99, Revision 2. In addition, the recommended NRC methods for determining credibility will be followed. The NRC methods were presented to industry at a meeting held by the NRC on February 12 and 13, 1998. At this meeting the NRC presented five cases. Of the five cases Case 1 ("Surveillance data available from plant but no other source") most closely represents the situation listed above for Diablo Canyon Unit 1 surveillance weld metal. Note, for the plate materials, the straight forward method of Regulatory Guide 1.99, Revision 2 will be followed.

236940

TABLE D-1
Diablo Canyon Unit 1 Surveillance Capsule Data

Material	Capsule	F ⁽¹⁾	FF ⁽²⁾	ΔRT_{NDT} ⁽³⁾	FF x ΔRT_{NDT}	FF ²
Intermediate Shell Plate B4106-3 (Longitudinal)	S	0.284	0.656	0 ⁽⁴⁾	0	0.430
	Y	1.05	1.014	48.66	49.34	1.028
	V	1.37	1.087	34.32	37.31	1.182
	SUM				86.65	2.64
	$CF_{Plate} = \sum(FF \times \Delta RT_{NDT}) \div \sum(FF^2) = 86.65 \div 2.64 = 32.8^\circ F$					
Weld Metal (Heat # 27204)	S	0.284	0.656	110.79	72.68	0.430
	Y	1.05	1.014	232.59	235.85	1.028
	V	1.37	1.087	201.07	218.56	1.182
	SUM				527.09	2.64
	$CF_{Weld} = \sum(FF \times \Delta RT_{NDT}) \div \sum(FF^2) = 527.09 \div 2.64 = 199.7^\circ F$					

Notes:

1. F = Calculated fluence from Section 6 of this report, [$\times 10^{19}$ n/cm², E > 1.0 MeV].
2. FF = fluence factor = $F^{(0.28 - 0.1 \log F)}$
3. ΔRT_{NDT} values are the measured 30 ft-lb shift values, [$^\circ F$].
4. Actual value for Capsule S is -1.78. However, a negative shift in RT_{NDT} should not physically occur. Thus, a value of zero is conservatively assumed.

The scatter of ΔRT_{NDT} values about the functional form of a best-fit line drawn as described in Regulatory Position 2.1 is presented in Table D-2.

200940

TABLE D-2
Best Fit Evaluation for Diablo Canyon Unit 1 Surveillance Materials

Material	Capsule	CF (°F)	FF	Measured ΔRT_{NDT} (30 ft-lb) (°F)	Best Fit ΔRT_{NDT} (°F)	Scatter of ΔRT_{NDT} (°F)	< 17°F (Base Metals) < 28°F (Weld Metal)
Inter. Shell Plate B4106-3 (Longitudinal)	S	32.8	0.656	-1.78	21.52	-23.3	No
	Y	32.8	1.014	48.66	33.26	15.4	Yes
	V	32.8	1.087	34.32	35.65	-1.33	Yes
Weld Metal (Heat # 27204)	S	199.7	0.656	110.79	131.00	-20.21	Yes
	Y	199.7	1.014	232.59	202.50	30.09	No
	V	199.7	1.087	201.07	217.07	-16.0	Yes

Table D-2 indicates that one of the plate data points and one of the weld data points has a scatter value that is greater than a 1σ of 17°F and 28°F, respectively. Therefore, neither the plate nor the weld meets the criterion for credibility.

Criterion 4: The irradiation temperature of the Charpy specimens in the capsule should match the vessel wall temperature at the cladding/base metal interface within +/- 25°F.

The capsule specimens are located in the reactor between the thermal shield and the vessel wall and are positioned opposite the center of the core. The test capsules are in baskets attached to the thermal shield. The location of the specimens with respect to the reactor vessel beltline provides assurance that the reactor vessel wall and the specimens experience equivalent operating conditions such that the temperatures will not differ by more than 25°F. Hence, this criterion is met.

Criterion 5: The surveillance data for the correlation monitor material in the capsule should fall within the scatter band of the database for that material.

The Diablo Canyon Unit 1 surveillance program does contain correlation monitor material. NUREG/CR-6413, ORNL/TM-13133 contains a plot of residual vs. Fast fluence for the correlation monitor material (Figure 9 in the report). The data used for this plot is contained in Table 14. However, the data within this report only contains the two capsules and not Capsule V. In addition, it used the old fluence values. Thus, Table D-3 contains an updated calculation of Residual vs. Fast fluence.

235940

TABLE D-3
Calculation of Residual vs. Fast Fluence

Capsule	Fluence ($\times 10^{19}$ n/cm ²)	Fluence Factor (FF)	Measured Shift	RG 1.99 Shift (CF*FF) ^(a)	Residual (Meas.- RG Shift)
S	0.284	0.656	65.62	73.01	-7.39
Y	1.05	1.014	115.79	112.9	2.89
V	1.37	1.087	116.61	121.0	-4.39

Notes:

(a) Per NUREG/CR-6413, ORNL/TM-13133, the Cu and Ni values for the Correlation Monitor Material are 0.15 Cu and 0.65 Ni. This equates to a Chemistry Factor of 111.3°F from Reg. Guide 1.99 Rev. 2.

Table D-3 shows a 2σ uncertainty of less than 50°F, which is the allowable scatter in NUREG/CR-6413, ORNL/TM-13133. Hence, this criterion is met.

CONCLUSION:

Based on the preceding responses to all five criteria of Regulatory Guide 1.99, Revision 2, Section B and 10 CFR 50.61, the Diablo Canyon Unit 1 surveillance data is not credible. This is based on not satisfying the third criterion for credibility. It is recommended that PG&E review all current reactor vessel Integrity Evaluations (PTS and PT Curves) to assess the impact, if any, of non-credible data for the plate B4106-3 and weld heat #27204.

APPENDIX E

**VALIDATION OF THE RADIATION TRANSPORT
MODELS BASED ON NEUTRON DOSIMETRY
MEASUREMENTS**

E.1 Neutron Dosimetry

Comparisons of measured dosimetry results to both the calculated and least squares adjusted values for all surveillance capsules withdrawn from service to date at Diablo Canyon Unit 1 are described herein. The sensor sets from these capsules have been analyzed in accordance with the current dosimetry evaluation methodology described in Regulatory Guide 1.190, "Calculational and Dosimetry Methods for Determining Pressure Vessel Neutron Fluence."^[E-1] One of the main purposes for presenting this material is to demonstrate that the overall measurements agree with the calculated and least squares adjusted values to within $\pm 20\%$ as specified by Regulatory Guide 1.190, thus serving to validate the calculated neutron exposures previously reported in Section 6.2 of this report. This information may also be useful in the future, in particular, as least squares adjustment techniques become accepted in the regulatory environment.

E.1.1 Sensor Reaction Rate Determinations

In this section, the results of the evaluations of the three neutron sensor sets withdrawn to date as a part of the Diablo Canyon Unit 1 Reactor Vessel Materials Surveillance Program are presented. The capsule designation, location within the reactor, and time of withdrawal of each of these dosimetry sets were as follows:

<u>Capsule ID</u>	<u>Azimuthal Location</u>	<u>Withdrawal Time</u>	<u>Irradiation Time [EFPY]</u>
S	40°	End of Cycle 1	1.25
Y	40°	End of Cycle 5	5.87
V	4° → 40°	End of Cycle 11	14.27

* Capsule V was irradiated at a 4° location during Cycles 1 through 5 followed by irradiation at a 40° location during Cycles 6 through 11 when it was subsequently removed from service.

The azimuthal locations included in the above tabulation represent the first octant equivalent azimuthal angle of the geometric center of the respective surveillance capsules.

The passive neutron sensors included in the evaluations of Surveillance Capsules S, Y, and V are summarized as follows:

<u>Sensor Material</u>	<u>Reaction</u>	<u>Capsule S</u>	<u>Capsule Y</u>	<u>Capsule V</u>
	<u>Of Interest</u>			
Copper	$^{63}\text{Cu}(\text{n},\alpha)^{60}\text{Co}$	X	X	X
Iron	$^{54}\text{Fe}(\text{n},\text{p})^{54}\text{Mn}$	X	X	X
Nickel	$^{58}\text{Ni}(\text{n},\text{p})^{58}\text{Co}$	X	X	X
Uranium-238	$^{238}\text{U}(\text{n},\text{f})^{137}\text{Cs}$	X	X	X
Neptunium-237	$^{237}\text{Np}(\text{n},\text{f})^{137}\text{Cs}$	X	X	X
Cobalt-Aluminum*	$^{59}\text{Co}(\text{n},\gamma)^{60}\text{Co}$	X	X	X

* The cobalt-aluminum measurements for this plant include both bare wire and cadmium-covered sensors.

The copper, iron, nickel, and cobalt-aluminum monitors, in wire form, were placed in holes drilled in spacers at several radial locations within the test specimen array. As a result, gradient corrections were applied to these measured reaction rates in order to index all of the sensor measurements to the radial center of the respective surveillance capsules. Since the cadmium-shielded uranium and neptunium fission monitors were accommodated within the dosimeter block centered at the radial, azimuthal, and axial center of the material test specimen array, gradient corrections were not required for the fission monitor reaction rates. Pertinent physical and nuclear characteristics of the passive neutron sensors are listed in Table E-1.

The use of passive monitors such as those listed above does not yield a direct measure of the energy dependent neutron flux at the point of interest. Rather, the activation or fission process is a measure of the integrated effect that the time and energy dependent neutron flux has on the target material over the course of the irradiation period. An accurate assessment of the average neutron flux level incident on the various monitors may be derived from the activation measurements only if the irradiation parameters are well known. In particular, the following variables are of interest:

- The measured specific activity of each monitor,
- the physical characteristics of each monitor,
- the operating history of the reactor,
- the energy response of each monitor, and
- the neutron energy spectrum at the monitor location.

The radiometric counting of the neutron sensors from Capsules S and Y was carried out at the Westinghouse Analytical Services Laboratory at the Waltz Mill Site.^[E-2] The radiometric counting of the sensors from Capsule V was completed at the Pace Analytical Laboratory, also located at the Waltz Mill Site. In all cases, the radiometric counting followed established ASTM procedures. Following sample preparation and weighing, the specific activity of each sensor was determined by means of a high-resolution gamma spectrometer. For the copper, iron, nickel, and cobalt-aluminum sensors, these analyses were performed by direct counting of each of the individual samples. In the case of the uranium and neptunium fission sensors, the analyses were carried out by direct counting preceded by dissolution and chemical separation of cesium from the sensor material.

The irradiation history of the reactor over the irradiation periods experienced by Capsules S, Y, and V was based on the reported monthly power generation of Diablo Canyon Unit 1 from initial reactor startup through the end of the dosimetry evaluation period. For the sensor sets utilized in the surveillance capsules, the half-lives of the product isotopes are long enough that a monthly histogram describing reactor operation has proven to be an adequate representation for use in radioactive decay corrections for the reactions of interest in the exposure evaluations. The irradiation history applicable to Capsules S, Y, and V is given in Table E-2.

Having the measured specific activities, the physical characteristics of the sensors, and the operating history of the reactor, reaction rates referenced to full-power operation were determined from the following equation:

$$R = \frac{A}{N_0 F Y \sum \frac{P_j}{P_{ref}} C_j [1 - e^{-\lambda t_j}] [e^{-\lambda t_d}]}$$

where:

- R = Reaction rate averaged over the irradiation period and referenced to operation at a core power level of P_{ref} (rps/nucleus).
- A = Measured specific activity (dps/gm).
- N_0 = Number of target element atoms per gram of sensor.
- F = Weight fraction of the target isotope in the sensor material.
- Y = Number of product atoms produced per reaction.
- P_j = Average core power level during irradiation period j (MW).
- P_{ref} = Maximum or reference power level of the reactor (MW).
- C_j = Calculated ratio of $\phi(E > 1.0 \text{ MeV})$ during irradiation period j to the time weighted average $\phi(E > 1.0 \text{ MeV})$ over the entire irradiation period.
- λ = Decay constant of the product isotope (1/sec).
- t_j = Length of irradiation period j (sec).
- t_d = Decay time following irradiation period j (sec).

and the summation is carried out over the total number of monthly intervals comprising the irradiation period.

In the equation describing the reaction rate calculation, the ratio $[P_j]/[P_{ref}]$ accounts for month-by-month variation of reactor core power level within any given fuel cycle as well as over multiple fuel cycles. The ratio C_j , which was calculated for each fuel cycle using the transport methodology discussed in Section 6.2, accounts for the change in sensor reaction rates caused by variations in flux level induced by changes in core spatial power distributions from fuel cycle to fuel cycle. For a single-cycle irradiation, C_j is normally taken to be 1.0. However, for multiple-cycle irradiations, particularly those employing low leakage fuel management, the additional C_j term should be employed. The impact of changing flux levels for constant power operation can be quite significant for sensor sets that have been irradiated for many cycles in a reactor that has transitioned from non-low leakage to low leakage fuel management or for sensor sets contained in surveillance capsules that have been moved from one capsule location to another. The fuel cycle specific neutron flux values along with the computed values for C_j are listed in Table E-3. These flux values represent the cycle dependent results at the radial and azimuthal center of the respective capsules at the axial elevation of the active fuel midplane.

Prior to using the measured reaction rates in the least-squares evaluations of the dosimetry sensor sets, additional corrections were made to the ^{238}U measurements to account for the presence of ^{235}U impurities in the sensors as well as to adjust for the build-in of plutonium isotopes over the course of the irradiation. Corrections were also made to the ^{238}U and ^{237}Np sensor reaction rates to account for gamma ray induced fission reactions that occurred over the course of the capsule irradiations. The correction factors applied to the Diablo Canyon Unit 1 fission sensor reaction rates are summarized as follows:

Correction	Capsule S	Capsule Y	Capsule V
^{235}U Impurity/Pu Build-in	0.873	0.844	0.831
$^{238}\text{U}(\gamma, f)$	0.958	0.958	0.958
Net ^{238}U Correction	0.836	0.809	0.796
$^{237}\text{Np}(\gamma, f)$	0.985	0.985	0.985

These factors were applied in a multiplicative fashion to the decay corrected uranium and neptunium fission sensor reaction rates.

Results of the sensor reaction rate determinations for Capsules S, Y, and V are given in Table E-4. In Table E-4, the measured specific activities, decay corrected saturated specific activities, and computed reaction rates for each sensor indexed to the radial center of the capsule are listed. The fission sensor reaction rates are listed both with and without the applied corrections for ^{238}U impurities, plutonium build-in, and gamma ray induced fission effects.

E.1.2 Least Squares Evaluation of Sensor Sets

Least squares adjustment methods provide the capability of combining the measurement data with the corresponding neutron transport calculations resulting in a Best Estimate neutron energy spectrum with associated uncertainties. Best Estimates for key exposure parameters such as $\phi(E > 1.0 \text{ MeV})$ or dpa/s along with their uncertainties are then easily obtained from the adjusted spectrum. In general, the least squares methods, as applied to surveillance capsule dosimetry evaluations, act to reconcile the measured sensor reaction rate data, dosimetry reaction cross-sections, and the calculated neutron energy spectrum within their respective uncertainties. For example,

$$R_i \pm \delta_{R_i} = \sum_g (\sigma_{ig} \pm \delta_{\sigma_{ig}})(\phi_g \pm \delta_{\phi_g})$$

relates a set of measured reaction rates, R_i , to a single neutron spectrum, ϕ_g , through the multigroup dosimeter reaction cross-section, σ_{ig} , each with an uncertainty δ . The primary objective of the least squares evaluation is to produce unbiased estimates of the neutron exposure parameters at the location of the measurement.

For the least squares evaluation of the Diablo Canyon Unit 1 surveillance capsule dosimetry, the FERRET code^[E-6] was employed to combine the results of the plant specific neutron transport calculations and sensor set reaction rate measurements to determine best-estimate values of exposure parameters ($\phi(E > 1.0 \text{ MeV})$ and dpa) along with associated uncertainties for the three in-vessel capsules tested to date (a total of five capsules have been removed to date; two of the five are in storage).

The application of the least squares methodology requires the following input:

- 1 - The calculated neutron energy spectrum and associated uncertainties at the measurement location.
- 2 - The measured reaction rates and associated uncertainty for each sensor contained in the multiple foil set.
- 3 - The energy dependent dosimetry reaction cross-sections and associated uncertainties for each sensor contained in the multiple foil sensor set.

For the Diablo Canyon Unit 1 application, the calculated neutron spectrum was obtained from the results of plant specific neutron transport calculations described in Section 6.2 of this report. The sensor reaction rates were derived from the measured specific activities using the procedures described in Section E.1.1. The dosimetry reaction cross-sections and uncertainties were obtained from the SNLRML dosimetry cross-section library^[E-7]. The SNLRML library is an evaluated dosimetry reaction cross-section compilation recommended for use in LWR evaluations by ASTM Standard E1018, "Application of ASTM Evaluated Cross-Section Data File, Matrix E 706 (IIB)".

The uncertainties associated with the measured reaction rates, dosimetry cross-sections, and calculated neutron spectrum were input to the least squares procedure in the form of variances and covariances. The assignment of the input uncertainties followed the guidance provided in ASTM Standard E 944, "Application of Neutron Spectrum Adjustment Methods in Reactor Surveillance."

The following provides a summary of the uncertainties associated with the least squares evaluation of the Diablo Canyon Unit 1 surveillance capsule sensor sets.

Reaction Rate Uncertainties

The overall uncertainty associated with the measured reaction rates includes components due to the basic measurement process, irradiation history corrections, and corrections for competing reactions. A high level of accuracy in the reaction rate determinations is assured by utilizing laboratory procedures that conform to the ASTM National Consensus Standards for reaction rate determinations for each sensor type.

After combining all of these uncertainty components, the sensor reaction rates derived from the counting and data evaluation procedures were assigned the following net uncertainties for input to the least squares evaluation:

Reaction	Uncertainty
$^{63}\text{Cu}(n,\alpha)^{60}\text{Co}$	5%
$^{54}\text{Fe}(n,p)^{54}\text{Mn}$	5%
$^{58}\text{Ni}(n,p)^{58}\text{Co}$	5%
$^{238}\text{U}(n,f)^{137}\text{Cs}$	10%
$^{237}\text{Np}(n,f)^{137}\text{Cs}$	10%
$^{59}\text{Co}(n,\gamma)^{60}\text{Co}$	5%

These uncertainties are given at the 1σ level.

Dosimetry Cross-Section Uncertainties

The reaction rate cross-sections used in the least squares evaluations were taken from the SNLRML library. This data library provides reaction cross-sections and associated uncertainties, including covariances, for 66 dosimetry sensors in common use. Both cross-sections and uncertainties are provided in a fine multigroup structure for use in least squares adjustment applications. These cross-sections were compiled from the most recent cross-section evaluations and they have been tested with respect to their accuracy and consistency for least squares evaluations. Further, the library has been empirically tested for use in fission spectra determination as well as in the fluence and energy characterization of 14 MeV neutron sources.

For sensors included in the Diablo Canyon Unit 1 surveillance program, the following uncertainties in the fission spectrum averaged cross-sections are provided in the SNLRML documentation package.

Reaction	Uncertainty
$^{63}\text{Cu}(n,\alpha)^{60}\text{Co}$	4.08-4.16%
$^{54}\text{Fe}(n,p)^{54}\text{Mn}$	3.05-3.11%
$^{58}\text{Ni}(n,p)^{58}\text{Co}$	4.49-4.56%
$^{238}\text{U}(n,f)^{137}\text{Cs}$	0.54-0.64%
$^{237}\text{Np}(n,f)^{137}\text{Cs}$	10.32-10.97%
$^{59}\text{Co}(n,\gamma)^{60}\text{Co}$	0.79-3.59%

These tabulated ranges provide an indication of the dosimetry cross-section uncertainties associated with the sensor sets used in LWR irradiations.

Calculated Neutron Spectrum

The neutron spectra input to the least squares adjustment procedure were obtained directly from the results of plant specific transport calculations for each surveillance capsule irradiation period and location. The spectrum for each capsule was input in an absolute sense (rather than as simply a relative spectral shape). Therefore, within the constraints of the assigned uncertainties, the calculated data were treated equally with the measurements.

While the uncertainties associated with the reaction rates were obtained from the measurement procedures and counting benchmarks and the dosimetry cross-section uncertainties were supplied directly with the SNLRML library, the uncertainty matrix for the calculated spectrum was constructed from the following relationship:

$$M_{gg'} = R_n^2 + R_g * R_{g'} * P_{gg'}$$

where R_n specifies an overall fractional normalization uncertainty and the fractional uncertainties R_g and $R_{g'}$ specify additional random groupwise uncertainties that are correlated with a correlation matrix given by:

$$P_{gg'} = [1 - \theta] \delta_{gg'} + \theta e^{-H}$$

where

$$H = \frac{(g - g')^2}{2\gamma^2}$$

The first term in the correlation matrix equation specifies purely random uncertainties, while the second term describes the short-range correlations over a group range γ (θ specifies the strength of the latter term). The value of δ is 1.0 when $g = g'$, and is 0.0 otherwise.

The set of parameters defining the input covariance matrix for the Diablo Canyon Unit 1 calculated spectra was as follows:

Flux Normalization Uncertainty (R_n)	15%
--	-----

Flux Group Uncertainties (R_g , $R_{g'}$)	
---	--

($E > 0.0055$ MeV)	15%
(0.68 eV $< E < 0.0055$ MeV)	29%
($E < 0.68$ eV)	52%

Short Range Correlation (θ)	
--------------------------------------	--

($E > 0.0055$ MeV)	0.9
(0.68 eV $< E < 0.0055$ MeV)	0.5
($E < 0.68$ eV)	0.5

Flux Group Correlation Range (γ)	
---	--

($E > 0.0055$ MeV)	6
(0.68 eV $< E < 0.0055$ MeV)	3
($E < 0.68$ eV)	2

E.1.3 Comparisons of Measurements and Calculations

Results of the least squares evaluations of the dosimetry from the Diablo Canyon Unit 1 surveillance capsules withdrawn to date are provided in Tables E-5 and E-6. In Table E-5, measured, calculated, and best-estimate values for sensor reaction rates are given for each capsule. Also provided in this tabulation are ratios of the measured reaction rates to both the calculated and least squares adjusted reaction rates. These ratios of M/C and M/BE illustrate the consistency of the fit of the calculated neutron energy spectra to the measured reaction rates both before and after adjustment. In Table E-6, comparison of the calculated and best estimate values of neutron flux ($E > 1.0$ MeV) and iron atom displacement rate are tabulated along with the BE/C ratios observed for each of the capsules.

The data comparisons provided in Tables E-5 and E-6 show that the adjustments to the calculated spectra are relatively small and well within the assigned uncertainties for the calculated spectra, measured sensor reaction rates, and dosimetry reaction cross-sections. Further, these results indicate that the use of the least squares evaluation results in a reduction in the uncertainties associated with the exposure of the surveillance capsules. From Section 6.4 of this report, it may be noted that the uncertainty associated

with the unadjusted calculation of neutron fluence ($E > 1.0$ MeV) and iron atom displacements at the surveillance capsule locations is specified as 12% at the 1σ level. From Table E-6, it is noted that the corresponding uncertainties associated with the least squares adjusted exposure parameters have been reduced to 6% for neutron flux ($E > 1.0$ MeV) and 7% for iron atom displacement rate. Again, the uncertainties from the least squares evaluation are at the 1σ level.

Further comparisons of the measurement results with calculations are given in Tables E-7 and E-8. These comparisons are given on two levels. In Table E-7, calculations of individual threshold sensor reaction rates are compared directly with the corresponding measurements. These threshold reaction rate comparisons provide a good evaluation of the accuracy of the fast neutron portion of the calculated energy spectra. In Table E-8, calculations of fast neutron exposure rates in terms of $\phi(E > 1.0$ MeV) and dpa/s are compared with the best estimate results obtained from the least squares evaluation of the capsule dosimetry results. These two levels of comparison yield consistent and similar results with all measurement-to-calculation comparisons falling well within the 20% limits specified as the acceptance criteria in Regulatory Guide 1.190.

In the case of the direct comparison of measured and calculated sensor reaction rates, the M/C comparisons for fast neutron reactions range from 0.78-1.12 for the 15 samples included in the data set. The overall average M/C ratio for the entire set of Diablo Canyon Unit 1 data is 0.94 with an associated standard deviation of 8.3%. This value is used to determine the Best Estimate fluence ($E > 1.0$ MeV) and iron atom displacement values on a cycle wise basis. Table E-9 lists the Best Estimate values on a cycle by cycle basis for the fluence at the capsule center as shown.

In the comparisons of best estimate and calculated fast neutron exposure parameters, the corresponding BE/C comparisons for the capsule data sets range from 0.86–1.00 for neutron flux ($E > 1.0$ MeV) and from 0.88 to 1.02 for iron atom displacement rate. The overall average BE/C ratios for neutron flux ($E > 1.0$ MeV) and iron atom displacement rate are 0.91 with a standard deviation of 8.3% and 0.93 with a standard deviation of 8.3%, respectively.

Based on these comparisons, it is concluded that the calculated fast neutron exposures provided in Section 6.2 of this report are validated for use in the assessment of the condition of the materials comprising the beltline region of the Diablo Canyon Unit 1 reactor pressure vessel.

Table E-1

Nuclear Parameters Used In the Evaluation of Neutron Sensors

<u>Monitor Material</u>	<u>Reaction of Interest</u>	<u>Target Atom Fraction</u>	<u>90% Response Range (MeV)</u>	<u>Product Half-life</u>	<u>Fission Yield (%)</u>
Copper	$^{63}\text{Cu} (n,\alpha)$	0.6917	4.9 – 11.8	5.271 y	
Iron	$^{54}\text{Fe} (n,p)$	0.0585	2.1 – 8.3	312.3 d	
Nickel	$^{58}\text{Ni} (n,p)$	0.6808	1.5 – 8.1	70.82 d	
Uranium-238	$^{238}\text{U} (n,f)$	0.9996	1.2 – 6.7	30.07 y	6.02
Neptunium-237	$^{237}\text{Np} (n,f)$	1.0000	0.4 – 3.5	30.07 y	6.17
Cobalt-Aluminum	$^{59}\text{Co} (n,\gamma)$	0.0015	non-threshold	5.271 y	

Notes: The 90% response range is defined such that, in the neutron spectrum characteristic of the Diablo Canyon Unit 1 surveillance capsules, approximately 90% of the sensor response is due to neutrons in the energy range specified with approximately 5% of the total response due to neutrons with energies below the lower limit and 5% of the total response due to neutrons with energies above the upper limit.

236940

Table E-2

Monthly Thermal Generation During the First Eleven Fuel Cycles

Of The Diablo Canyon Unit 1 Reactor

(Reactor Power of 3338 MWt through October 6, 2000, and 3411 MWt thereafter)

<u>Year</u>	<u>Month</u>	<u>Thermal Generation (MWt-hr)</u>	<u>Year</u>	<u>Month</u>	<u>Thermal Generation (MWt-hr)</u>	<u>Year</u>	<u>Month</u>	<u>Thermal Generation (MWt-hr)</u>
1984	11	167071	1988	1	2035485	1991	3	0
1984	12	781228	1988	2	1710575	1991	4	1610788
1985	1	84750	1988	3	274544	1991	5	2161086
1985	2	497207	1988	4	0	1991	6	2392176
1985	3	1854601	1988	5	0	1991	7	2481053
1985	4	0	1988	6	0	1991	8	2482327
1985	5	1632108	1988	7	927368	1991	9	2350718
1985	6	2286901	1988	8	2358057	1991	10	2481357
1985	7	2435846	1988	9	2068428	1991	11	2197143
1985	8	2218873	1988	10	2427826	1991	12	2480444
1985	9	2374552	1988	11	2368095	1992	1	2480772
1985	10	2163216	1988	12	2404073	1992	2	2322063
1985	11	1523963	1989	1	2398489	1992	3	2138149
1985	12	1929994	1989	2	2207286	1992	4	2224782
1986	1	2424269	1989	3	2449786	1992	5	2410682
1986	2	2102251	1989	4	2162399	1992	6	2400268
1986	3	2406348	1989	5	2441421	1992	7	2418213
1986	4	2132185	1989	6	2363360	1992	8	2381626
1986	5	2490682	1989	7	2468579	1992	9	835392
1986	6	2163689	1989	8	2384230	1992	10	0
1986	7	1842336	1989	9	2400292	1992	11	1352555
1986	8	1366070	1989	10	439623	1992	12	2428355
1986	9	0	1989	11	0	1993	1	2483047
1986	10	0	1989	12	818953	1993	2	2065992
1986	11	0	1990	1	2433618	1993	3	2338926
1986	12	48788	1990	2	2037409	1993	4	2402015
1987	1	1140482	1990	3	2491017	1993	5	2481334
1987	2	2028965	1990	4	2377992	1993	6	2256675
1987	3	2277945	1990	5	2516299	1993	7	2482118
1987	4	2394500	1990	6	1585625	1993	8	2480942
1987	5	2118322	1990	7	2340515	1993	9	2400588
1987	6	2141394	1990	8	2473468	1993	10	2432353
1987	7	2381703	1990	9	2370556	1993	11	2401678
1987	8	2090122	1990	10	2443130	1993	12	1867363
1987	9	2375321	1990	11	2346761	1994	1	2437616
1987	10	2308588	1990	12	1793532	1994	2	2242952
1987	11	2347282	1991	1	2391971	1994	3	872868
1987	12	1817741	1991	2	27364	1994	4	0

Table E-2 cont'd

Monthly Thermal Generation During The First Eighteen Fuel Cycles

Of The Diablo Canyon Unit 1 Reactor

(Reactor Power of 3338 through October 6 2000 and 3411 MWt thereafter)

Year	Month	Thermal Generation (MWt-hr)	Year	Month	Thermal Generation (MWt-hr)	Year	Month	Thermal Generation (MWt-hr)
1994	5	546539	1997	7	2480639	2000	9	2391812
1994	6	2383038	1997	8	2466623	2000	10	400560
1994	7	2493803	1997	9	2394045	2000	11	695918
1994	8	2490277	1997	10	2361899	2000	12	2449052
1994	9	2407121	1997	11	2389197	2001	1	2385664
1994	10	2482344	1997	12	2468651	2001	2	2291938
1994	11	2398894	1998	1	2404594	2001	3	2537268
1994	12	2059217	1998	2	2188679	2001	4	2450959
1995	1	2425927	1998	3	2414420	2001	5	2537285
1995	2	2242278	1998	4	2336535	2001	6	2381547
1995	3	2449140	1998	5	2469944	2001	7	2533658
1995	4	2298107	1998	6	2360812	2001	8	2536196
1995	5	2485576	1998	7	2414420	2001	9	2455470
1995	6	2387434	1998	8	2414420	2001	10	2534575
1995	7	2479699	1998	9	2336535	2001	11	2177067
1995	8	2478524	1998	10	2414420	2001	12	2506152
1995	9	2070677	1998	11	2336535	2002	1	2537285
1995	10	0	1998	12	1572621	2002	2	2260854
1995	11	60824	1999	1	2474763	2002	3	2530637
1995	12	1650488	1999	2	500553	2002	4	2217016
1996	1	2482638	1999	3	1098455			
1996	2	2271956	1999	4	2396984			
1996	3	2045407	1999	5	2480081			
1996	4	2397718	1999	6	2396014			
1996	5	2480874	1999	7	2473999			
1996	6	2198496	1999	8	2474498			
1996	7	2329842	1999	9	2136320			
1996	8	1911123	1999	10	2214363			
1996	9	2398306	1999	11	2224383			
1996	10	2481168	1999	12	2464655			
1996	11	1686924	2000	1	2377796			
1996	12	2425633	2000	2	2298401			
1997	1	2470296	2000	3	2469797			
1997	2	2215833	2000	4	2352203			
1997	3	2479111	2000	5	1311575			
1997	4	1429228	2000	6	2400627			
1997	5	0	2000	7	2481168			
1997	6	2072263	2000	8	2479288			

236940

Table E-3

Calculated C_j Factors at the Surveillance Capsule Center

Core Midplane Elevation

Fuel Cycle	$\phi(E > 1.0 \text{ MeV}) [\text{n/cm}^2\text{-s}]$			C_j		
	Capsule S	Capsule Y	Capsule V*	S	Y	V*
1	7.23E+10	7.23E+10	2.24E+10	1.000	1.267	0.761
2		6.03E+10	1.94E+10		1.057	0.657
3		6.28E+10	1.60E+10		1.101	0.542
4		4.85E+10	1.63E+10		0.850	0.554
5		4.14E+10	1.54E+10		0.726	0.522
6			4.16E+10			1.411
7			4.11E+10			1.394
8			3.69E+10			1.252
9			3.87E+10			1.314
10			3.80E+10			1.289
11			3.84E+10			1.305
Average	7.23E+10	5.70E+10	2.95E+10	1.000	1.000	1.000

*Note: C_j factors based on the ratio of the cycle specific fast ($E > 1.0 \text{ MeV}$) neutron flux divided by the average flux over the total irradiation period were deemed unsuitable for Capsule V since reaction rates did not vary by constant values as a function of azimuthal position for this capsule. To a large extent, this was due to moving Capsule V from a 4° to 40° location following the fifth fuel cycle. As a result of this observation, the C_j terms that were utilized in the final Capsule V analysis were based on the individual reaction rates determined from the synthesized transport calculations. The final C_j terms for Capsule V, which are based on individual reaction rates, are reported on the next page of this table.

Table E-3 cont'd

Calculated C_j Factors at the Surveillance Capsule Center

Core Midplane Elevation

(Capsule V only)

Fuel Cycle	Capsule V Reaction Rates [rps/atom]						
	⁶³ Cu (n,α)	⁵⁴ Fe (n,p)	²³⁸ U (n,f)	²³⁷ Np (n,f)	⁵⁹ Co (n,γ)	⁵⁹ Co (n,γ)	⁵⁹ Co (n,γ) Cd
1	2.22E-17	1.99E-15	2.67E-15	8.37E-15	5.66E-14	7.12E-13	3.69E-13
2	1.96E-17	1.74E-15	2.33E-15	7.25E-15	4.88E-14	6.09E-13	3.16E-13
3	1.66E-17	1.45E-15	1.94E-15	5.99E-15	4.02E-14	5.01E-13	2.60E-13
4	1.71E-17	1.49E-15	1.99E-15	6.14E-15	4.10E-14	5.08E-13	2.63E-13
5	1.62E-17	1.40E-15	1.88E-15	5.79E-15	3.87E-14	4.79E-13	2.49E-13
6	2.78E-17	2.98E-15	4.10E-15	1.45E-14	1.12E-13	1.69E-12	8.94E-13
7	2.77E-17	2.96E-15	4.06E-15	1.44E-14	1.10E-13	1.66E-12	8.81E-13
8	2.50E-17	2.66E-15	3.65E-15	1.29E-14	9.89E-14	1.49E-12	7.90E-13
9	2.64E-17	2.80E-15	3.84E-15	1.36E-14	1.04E-13	1.56E-12	8.27E-13
10	2.60E-17	2.75E-15	3.77E-15	1.33E-14	1.02E-13	1.53E-12	8.10E-13
11	2.64E-17	2.79E-15	3.83E-15	1.35E-14	1.03E-13	1.55E-12	8.20E-13
Average	2.28E-17	2.27E-15	3.09E-15	1.05E-14	7.77E-14	1.12E-12	5.89E-13

Fuel Cycle	Capsule V C _j						
	⁶³ Cu (n,α)	⁵⁴ Fe (n,p)	²³⁸ U (n,f)	²³⁷ Np (n,f)	⁵⁹ Co (n,γ)	⁵⁹ Co (n,γ)	⁵⁹ Co (n,γ) Cd
1	0.97	0.88	0.86	0.80	0.73	0.64	0.63
2	0.86	0.76	0.75	0.69	0.63	0.55	0.54
3	0.73	0.64	0.63	0.57	0.52	0.45	0.44
4	0.75	0.65	0.64	0.58	0.53	0.45	0.45
5	0.71	0.62	0.61	0.55	0.50	0.43	0.42
6	1.22	1.31	1.32	1.38	1.44	1.51	1.52
7	1.21	1.30	1.31	1.37	1.42	1.49	1.50
8	1.09	1.17	1.18	1.23	1.27	1.34	1.34
9	1.16	1.23	1.24	1.29	1.34	1.40	1.40
10	1.14	1.21	1.22	1.26	1.31	1.37	1.37
11	1.16	1.23	1.24	1.28	1.33	1.39	1.39
Average	1.00	1.00	1.00	1.00	1.00	1.00	1.00

Table E-4

Measured Sensor Activities And Reaction Rates

Surveillance Capsule S

<u>Reaction</u>	<u>Location</u>	<u>Measured Activity (dps/g)</u>	<u>Saturated Activity (dps/g)</u>	<u>Radially Adjusted Saturated Activity (dps/g)</u>	<u>Radially Adjusted Reaction Rate (rps/atom)</u>
$^{63}\text{Cu} (n,\alpha) ^{60}\text{Co}$	Top	4.470E+04	3.146E+05	3.269E+05	4.987E-17
	Bottom	4.290E+04	3.019E+05	3.137E+05	4.786E-17
	Average				4.887E-17
$^{54}\text{Fe} (n,p) ^{54}\text{Mn}$	W-3 Charpy	1.130E+06	2.716E+06	2.830E+06	4.486E-15
	W-4 Charpy	1.130E+06	2.716E+06	2.830E+06	4.486E-15
	W-8 Charpy	1.150E+06	2.764E+06	2.880E+06	4.565E-15
	E-41 Charpy	1.330E+06	3.196E+06	2.739E+06	4.342E-15
	R-47 Charpy	1.350E+06	3.244E+06	2.780E+06	4.408E-15
	Average				4.457E-15
$^{58}\text{Ni} (n,p) ^{58}\text{Co}$	Middle Average	8.200E+06	4.785E+07	4.986E+07	7.137E-15 7.137E-15
$^{238}\text{U} (n,f) ^{137}\text{Cs} (\text{Cd})$	Middle	1.310E+05	4.634E+06	4.634E+06	3.043E-14
$^{238}\text{U} (n,f) ^{137}\text{Cs} (\text{Cd})$		Including ^{235}U , ^{239}Pu , and γ , fission corrections:			2.545E-14
$^{237}\text{Np} (n,f) ^{137}\text{Cs} (\text{Cd})$	Middle	9.970E+05	3.527E+07	3.527E+07	2.250E-13
$^{237}\text{Np} (n,f) ^{137}\text{Cs} (\text{Cd})$			Including γ , fission correction:		2.215E-13
$^{59}\text{Co} (n,\gamma) ^{60}\text{Co}$	Top	7.560E+06	5.321E+07	5.098E+07	3.326E-12
	Middle	7.350E+06	5.173E+07	4.956E+07	3.233E-12
	Bottom	7.870E+06	5.539E+07	5.307E+07	3.462E-12
	Average				3.340E-12
$^{59}\text{Co} (n,\gamma) ^{60}\text{Co} (\text{Cd})$	Top	4.030E+06	2.836E+07	2.454E+07	1.601E-12
	Middle	3.980E+06	2.801E+07	2.423E+07	1.581E-12
	Bottom	4.050E+06	2.851E+07	2.466E+07	1.609E-12
	Average				1.597E-12

Notes: 1) Measured specific activities are indexed to a counting date of February 2, 1987.

2) The average $^{238}\text{U} (n,f)$ reaction rate of 2.545E-14 includes a correction factor of 0.873 to account for plutonium build-in and an additional factor of 0.958 to account for photo-fission effects in the sensor.

3) The average $^{237}\text{Np} (n,f)$ reaction rate of 2.215E-13 includes a correction factor of 0.985 to account for photo-fission effects in the sensor.

Table E-4 cont'd

Measured Sensor Activities And Reaction Rates

Surveillance Capsule Y

<u>Reaction</u>	<u>Location</u>	<u>Measured Activity (dps/g)</u>	<u>Saturated Activity (dps/g)</u>	<u>Radially Adjusted Saturated Activity (dps/g)</u>	<u>Radially Adjusted Reaction Rate (rps/atom)</u>
$^{63}\text{Cu} (n,\alpha) ^{60}\text{Co}$	Top	1.23E+05	1.52E+05	1.45E+05	2.21E-17
	Bottom	1.28E+05	1.58E+05	1.51E+05	2.30E-17
	Average				2.26E-17
$^{54}\text{Fe} (n,p) ^{54}\text{Mn}$	W-09 Charpy	1.02E+06	1.15E+06	1.10E+06	1.74E-15
	W-16 Charpy	1.05E+06	1.19E+06	1.13E+06	1.80E-15
	E-49 Charpy	8.87E+05	1.00E+06	1.15E+06	1.83E-15
	E-56 Charpy	9.03E+05	1.02E+06	1.17E+06	1.86E-15
	Average				1.81E-15
$^{58}\text{Ni} (n,p) ^{58}\text{Co}$	Middle	9.58E+06	2.09E+07	1.99E+07	2.85E-15
	Average				2.85E-15
$^{238}\text{U} (n,f) ^{137}\text{Cs} (\text{Cd})$	Middle	4.68E+05	1.69E+06	1.69E+06	1.11E-14
$^{238}\text{U} (n,f) ^{137}\text{Cs} (\text{Cd})$		Including ^{235}U , ^{239}Pu , and γ , fission corrections:			8.84E-15
$^{237}\text{Np} (n,f) ^{137}\text{Cs} (\text{Cd})$	Middle	3.44E+06	1.24E+07	1.24E+07	7.94E-14
$^{237}\text{Np} (n,f) ^{137}\text{Cs} (\text{Cd})$			Including γ , fission correction:		7.82E-14
$^{59}\text{Co} (n,\gamma) ^{60}\text{Co}$	Top	1.38E+07	1.70E+07	1.62E+07	1.06E-12
	Middle	1.46E+07	1.80E+07	1.71E+07	1.12E-12
	Bottom	1.39E+07	1.71E+07	1.63E+07	1.06E-12
	Average				1.08E-12
$^{59}\text{Co} (n,\gamma) ^{60}\text{Co} (\text{Cd})$	Top	6.53E+06	8.05E+06	7.65E+06	4.99E-13
	Middle	7.42E+06	9.15E+06	8.69E+06	5.67E-13
	Bottom	6.37E+06	7.85E+06	7.46E+06	4.87E-13
	Average				5.18E-13

Notes: 1) Measured specific activities are indexed to a counting date of August 1, 2002.

2) The average $^{238}\text{U} (n,f)$ reaction rate of 8.84E-15 includes a correction factor of 0.831 to account for plutonium build-in and an additional factor of 0.958 to account for photo-fission effects in the sensor.

3) The average $^{237}\text{Np} (n,f)$ reaction rate of 7.82E-14 includes a correction factor of 0.985 to account for photo-fission effects in the sensor.

Table E-4 cont'd

Measured Sensor Activities And Reaction Rates

Surveillance Capsule V

Reaction	Location	Measured Activity (dps/g)	Saturated Activity (dps/g)	Radially Adjusted Saturated Activity (dps/g)	Radially Adjusted Reaction Rate (rps/atom)
$^{63}\text{Cu} (n,\alpha) ^{60}\text{Co}$	Top	3.80E+04	7.80E+04	8.12E+04	1.24E-17
	Bottom	3.81E+04	7.82E+04	8.14E+04	1.24E-17
	Average				1.24E-17
$^{54}\text{Fe} (n,p) ^{54}\text{Mn}$	R-48 Charpy	1.58E+06	2.55E+06	2.66E+06	4.22E-15
	R-42 Charpy	1.62E+06	2.62E+06	2.73E+06	4.33E-15
	H-2 Charpy	1.47E+06	2.37E+06	2.48E+06	3.93E-15
	S-58 Charpy	1.90E+06	3.07E+06	2.65E+06	4.19E-15
	S-52 Charpy	1.87E+06	3.02E+06	2.60E+06	4.13E-15
	W-2 Charpy	1.75E+06	2.83E+06	2.44E+06	3.86E-15
	Average				4.11E-15
$^{238}\text{U} (n,f) ^{137}\text{Cs} (\text{Cd})$	Middle	2.52E+05	1.64E+06	1.64E+06	1.08E-14
$^{238}\text{U} (n,f) ^{137}\text{Cs} (\text{Cd})$		Including ^{235}U , ^{239}Pu , and γ ,fission corrections:			8.64E-15
$^{237}\text{Np} (n,f) ^{137}\text{Cs} (\text{Cd})$	Middle	1.23E+05	7.99E+05	7.99E+05	5.10E-15
$^{237}\text{Np} (n,f) ^{137}\text{Cs} (\text{Cd})$		Including γ ,fission correction:			5.02E-15
$^{59}\text{Co} (n,\gamma) ^{60}\text{Co}$	Top	3.11E+06	6.38E+06	6.11E+06	5.98E-16
	Middle	2.82E+06	5.79E+06	5.54E+06	5.42E-16
	Bottom	3.01E+06	6.18E+06	5.91E+06	5.79E-16
	Average				5.73E-16
$^{59}\text{Co} (n,\gamma) ^{60}\text{Co} (\text{Cd})$	Top	1.53E+06	3.14E+06	2.77E+06	2.71E-16
	Middle	3.17E+04	6.51E+04	5.74E+04	5.62E-18
	Bottom	1.52E+06	3.12E+06	2.75E+06	2.69E-16
	Average				1.82E-16

Notes: 1) Measured specific activities are indexed to a counting date of March 30, 1985.

2) The average $^{238}\text{U} (n,f)$ reaction rate of 8.64E-15 includes a correction factor of 0.837 to account for plutonium build-in and an additional factor of 0.960 to account for photo-fission effects in the sensor.

3) The average $^{237}\text{Np} (n,f)$ reaction rate of 5.02E-15 includes a correction factor of 0.984 to account for photo-fission effects in the sensor.

Table E-5

Comparison of Measured, Calculated, and Best Estimate
Reaction Rates At The Surveillance Capsule Center

Capsule S

Reaction	Reaction Rate [rps/atom]			M/C	M/BE
	Measured	Calculated	Best Estimate		
$^{63}\text{Cu}(n,\alpha)^{60}\text{Co}$	4.89E-17	4.46E-17	4.69E-17	1.10	1.04
$^{54}\text{Fe}(n,p)^{54}\text{Mn}$	4.46E-15	5.01E-15	4.87E-15	0.89	0.92
$^{58}\text{Ni}(n,p)^{58}\text{Co}$	7.14E-15	6.91E-15	6.96E-15	1.03	1.03
$^{238}\text{U}(n,f)^{137}\text{Cs (Cd)}$	2.54E-14	2.50E-14	2.49E-14	1.02	1.02
$^{237}\text{Np}(n,f)^{137}\text{Cs (Cd)}$	2.21E-13	1.97E-13	2.10E-13	1.13	1.05
$^{59}\text{Co}(n,\gamma)^{60}\text{Co}$	3.34E-12	2.93E-12	3.32E-12	1.14	1.00
$^{59}\text{Co}(n,\gamma)^{60}\text{Co (Cd)}$	1.60E-12	1.53E-12	1.60E-12	1.04	1.00

Capsule Y

Reaction	Reaction Rate [rps/atom]			M/C	M/BE
	Measured	Calculated	Best Estimate		
$^{63}\text{Cu}(n,\alpha)^{60}\text{Co}$	3.67E-17	3.69E-17	3.58E-17	0.99	1.02
$^{54}\text{Fe}(n,p)^{54}\text{Mn}$	3.44E-15	4.02E-15	3.63E-15	0.86	0.94
$^{58}\text{Ni}(n,p)^{58}\text{Co}$	5.23E-15	5.54E-15	5.10E-15	0.94	1.02
$^{238}\text{U}(n,f)^{137}\text{Cs (Cd)}$	1.82E-14	1.98E-14	1.77E-14	0.92	1.03
$^{237}\text{Np}(n,f)^{137}\text{Cs (Cd)}$	1.24E-13	1.54E-13	1.30E-13	0.81	0.95
$^{59}\text{Co}(n,\gamma)^{60}\text{Co}$	2.35E-12	2.26E-12	2.35E-12	1.04	1.00
$^{59}\text{Co}(n,\gamma)^{60}\text{Co (Cd)}$	1.15E-12	1.18E-12	1.15E-12	0.97	1.00

Capsule V

Reaction	Reaction Rate [rps/atom]			M/C	M/BE
	Measured	Calculated	Best Estimate		
$^{63}\text{Cu}(n,\alpha)^{60}\text{Co}$	2.26E-17	2.32E-17	2.16E-17	0.97	1.04
$^{54}\text{Fe}(n,p)^{54}\text{Mn}$	1.81E-15	2.32E-15	1.97E-15	0.78	0.92
$^{58}\text{Ni}(n,p)^{58}\text{Co}$	2.85E-15	3.16E-15	2.77E-15	0.90	1.03
$^{238}\text{U}(n,f)^{137}\text{Cs (Cd)}$	8.84E-15	1.08E-14	9.24E-15	0.82	0.96
$^{237}\text{Np}(n,f)^{137}\text{Cs (Cd)}$	7.81E-14	8.06E-14	7.39E-14	0.97	1.05
$^{59}\text{Co}(n,\gamma)^{60}\text{Co}$	1.08E-12	1.13E-12	1.08E-12	0.95	1.00
$^{59}\text{Co}(n,\gamma)^{60}\text{Co (Cd)}$	5.18E-13	5.87E-13	5.20E-13	0.88	1.00

Table E-6

Comparison of Calculated and Best Estimate Exposure Rates

At The Surveillance Capsule Center

Capsule ID	$\phi(E > 1.0 \text{ MeV}) [\text{n/cm}^2\text{-s}]$			
	Calculated	Best Estimate	Uncertainty (1 σ)	BE/C
S	7.23E+10	7.26E+10	6%	1.00
Y	5.68E+10	5.05E+10	6%	0.89
V	3.04E+10	2.61E+10	6%	0.86

Notes: 1) Calculated results are based on the synthesized transport calculations taken at the core midplane following the completion of each respective capsules irradiation period.

Capsule ID	Iron Atom Displacement Rate [dpa/s]			
	Calculated	Best Estimate	Uncertainty (1 σ)	BE/C
S	1.22E-10	1.23E-10	7%	1.01
Y	9.56E-11	8.44E-11	7%	0.88
V	5.05E-11	4.39E-11	7%	0.87

Notes: 1) Calculated results are based on the synthesized transport calculations taken at the core midplane following the completion of each respective capsules irradiation period.

Table E-7a

Comparison of Measured/Calculated (M/C) Sensor Reaction Rate Ratios Including all Fast Neutron Threshold Reactions

Reaction	M/C Ratio		
	Capsule S	Capsule Y	Capsule V
$^{63}\text{Cu}(n,\alpha)^{60}\text{Co}$	1.10	0.99	0.97
$^{54}\text{Fe}(n,p)^{54}\text{Mn}$	0.89	0.86	0.78
$^{58}\text{Ni}(n,p)^{58}\text{Co}$	1.03	0.94	0.90
$^{238}\text{U}(n,p)^{137}\text{Cs (Cd)}$	1.02	0.92	0.82
$^{237}\text{Np}(n,f)^{137}\text{Cs (Cd)}$	1.12	0.81	0.97
Average	1.03	0.90	0.89
% Standard Deviation	8.7	8.2	9.8

Note: 1) The overall average M/C ratio for the set of 15 sensor measurements is 0.94 with an associated standard deviation of 8.3%.

Table E-7b

Comparison of Measured/Calculated Individual Sensor Reactions without Recourse to the Least Squares Adjustment Encompassing all In-Vessel and Ex-Vessel Dosimetry

Reaction	In-Vessel		Ex-Vessel		Combined	
	Average M/C	Unc. (1 σ)	Average M/C	Unc. (1 σ)	Average M/C	Unc. (1 σ)
$^{63}\text{Cu}(n,\alpha)^{60}\text{Co}$	1.02	7.0	0.87	8.0	0.95	10.6
$^{54}\text{Fe}(n,p)^{54}\text{Mn}$	0.84	5.7	0.84	11.1	0.84	0.0
$^{58}\text{Ni}(n,p)^{58}\text{Co}$	0.96	6.7	0.89	10.6	0.93	4.9
$^{238}\text{U}(n,p)^{137}\text{Cs (Cd)}$	0.92	10.0	0.96	11.4	0.94	2.8
$^{237}\text{Np}(n,f)^{137}\text{Cs (Cd)}$	0.97	16.0	0.98	13.1	0.91	0.7
Linear Average	0.94	6.7	0.91	6.0	0.91	4.3

Table E-8

Comparison of Best Estimate/Calculated (BE/C) Exposure Rate Ratios

Capsule ID	BE/C Ratio	
	$\phi(E > 1.0 \text{ MeV})$	dpa/s
S	1.00	1.02
Y	0.89	0.89
V	0.86	0.88
Average	0.92	0.93
% Standard Deviation	8.0	8.4

Table E-9

Best Estimate Fluence and Iron Atom Displacement Values on a Cycle-By-Cycle Basis

Cycle	Cumulative Operating Time {EFPY}	Best Estimate Values					
		$\phi(E > 1.0 \text{ MeV})$			Iron Displacements		
		{n/cm ² }			{dpa}		
		4°	40°	Capsule V*	4°	40°	Capsule V*
1	1.25	8.03E+17	2.59E+18	8.03E+17	1.34E-03	4.51E-03	1.34E-03
2	2.27	1.37E+18	4.36E+18	1.37E+18	2.28E-03	7.59E-03	2.28E-03
3	3.45	1.91E+18	6.48E+18	1.91E+18	3.18E-03	1.13E-02	3.18E-03
4	4.51	2.41E+18	7.96E+18	2.41E+18	4.01E-03	1.38E-02	4.01E-03
5	5.87	3.01E+18	9.58E+18	3.01E+18	5.01E-03	1.67E-02	5.01E-03
6	7.14	3.60E+18	1.11E+19	4.53E+18	5.99E-03	1.93E-02	7.64E-03
7	8.47	4.19E+18	1.27E+19	6.09E+18	6.98E-03	2.20E-02	1.04E-02
8	9.75	4.69E+18	1.40E+19	7.44E+18	7.81E-03	2.44E-02	1.27E-02
9	11.38	5.40E+18	1.58E+19	9.25E+18	8.98E-03	2.75E-02	1.58E-02
10	12.87	5.98E+18	1.75E+19	1.09E+19	9.96E-03	3.03E-02	1.87E-02
11	14.27	6.60E+18	1.91E+19	1.25E+19	1.10E-02	3.31E-02	2.14E-02
Projections	16.00	7.34E+18	2.10E+19		1.22E-02	3.64E-02	
Projections	24.00	1.08E+19	3.02E+19		1.80E-02	5.25E-02	
Projections	32.00	1.43E+19	3.94E+19		2.38E-02	6.85E-02	
Projections	40.00	1.78E+19	4.87E+19		2.97E-02	8.45E-02	
Projections	48.00	2.13E+19	5.79E+19		3.55E-02	1.00E-01	
Projections	54.00	2.39E+19	6.48E+19		3.98E-02	1.12E-01	

Notes: 1) * Capsule V was irradiated at a 4° capsule position for cycles 1-5 at which point it was moved to be irradiated in a 40° location until it was removed at the end of cycle 11.

Table E-10

Best Estimate Azimuthal Variation of Maximum Exposure Rates

And Integrated Exposures at the Reactor Vessel

Clad/Base Metal Interface

Cycle	Cycle Length [EFPS]	Cumulative Irradiation Time [EFPS]	Cumulative Irradiation Time [EFY]	Neutron Flux (E > 1.0 MeV) [n/cm ² -s]			
				0°	15°	30°	45°
1	3.94E+07	3.94E+07	1.25	6.14E+09	9.73E+09	1.23E+10	1.90E+10
2	3.23E+07	7.16E+07	2.27	5.40E+09	7.69E+09	1.06E+10	1.59E+10
3	3.72E+07	1.09E+08	3.45	4.39E+09	7.16E+09	1.08E+10	1.66E+10
4	3.34E+07	1.42E+08	4.51	4.49E+09	6.89E+09	8.68E+09	1.30E+10
5	4.31E+07	1.85E+08	5.87	4.25E+09	6.42E+09	8.01E+09	1.09E+10
6	4.01E+07	2.25E+08	7.14	4.44E+09	6.96E+09	8.07E+09	1.10E+10
7	4.18E+07	2.67 E+08	8.47	4.28E+09	6.88E+09	8.18E+09	1.08E+10
8	4.04E+07	3.08 E+08	9.75	3.81E+09	6.24E+09	7.50E+09	9.84E+09
9	5.13E+07	3.59 E+08	11.38	4.17E+09	6.36E+09	7.64E+09	1.02E+10
10	4.72E+07	4.06 E+08	12.87	3.71E+09	6.61E+09	7.95E+09	9.98E+09
11	4.58E+07	4.52 E+08	14.27	4.02E+09	7.46E+09	8.63E+09	1.00E+10
Projection	5.29E+07	5.05 E+08	16.00	4.18E+09	6.84E+09	8.16E+09	1.06E+10
Projection	2.53E+08	7.57 E+08	24.00	4.18E+09	6.84E+09	8.16E+09	1.06E+10
Projection	2.53E+08	1.01E+09	32.00	4.18E+09	6.84E+09	8.16E+09	1.06E+10
Projection	2.53E+08	1.26E+09	40.00	4.18E+09	6.84E+09	8.16E+09	1.06E+10
Projection	2.53E+08	1.51E+09	48.00	4.18E+09	6.84E+09	8.16E+09	1.06E+10
Projection	1.89E+08	1.70E+09	54.00	4.18E+09	6.84E+09	8.16E+09	1.06E+10

236340

Table E-10 cont'd

Best Estimate Azimuthal Variation of Maximum Exposure Rates

And Integrated Exposures at the Reactor Vessel

Clad/Base Metal Interface

Cycle	Cycle Length [EFPS]	Cumulative Irradiation Time [EFPS]	Cumulative Irradiation Time [EFPY]	Neutron Fluence (E > 1.0 MeV) [n/cm ²]			
				0°	15°	30°	45°
1	3.94E+07	3.94E+07	1.25	2.42E+17	3.83E+17	4.85E+17	7.46E+17
2	3.23E+07	7.16E+07	2.27	4.16E+17	6.31E+17	8.26E+17	1.26E+18
3	3.72E+07	1.09E+08	3.45	5.79E+17	8.97E+17	1.23E+18	1.88E+18
4	3.34E+07	1.42E+08	4.51	7.29E+17	1.13E+18	1.52E+18	2.31E+18
5	4.31E+07	1.85E+08	5.87	9.12E+17	1.40E+18	1.86E+18	2.78E+18
6	4.01E+07	2.25E+08	7.14	1.09E+18	1.68E+18	2.19E+18	3.22E+18
7	4.18E+07	2.67 E+08	8.47	1.27E+18	1.97E+18	2.53E+18	3.67E+18
8	4.04E+07	3.08 E+08	9.75	1.42E+18	2.22E+18	2.83E+18	4.07E+18
9	5.13E+07	3.59 E+08	11.38	1.64E+18	2.55E+18	3.22E+18	4.59E+18
10	4.72E+07	4.06 E+08	12.87	1.81E+18	2.86E+18	3.60E+18	5.06E+18
11	4.58E+07	4.52 E+08	14.27	1.99E+18	3.20E+18	3.99E+18	5.52E+18
Projection	5.29E+07	5.05 E+08	16.00	2.22E+18	3.56E+18	4.42E+18	6.08E+18
Projection	2.53E+08	7.57 E+08	24.00	3.27E+18	5.29E+18	6.48E+18	8.75E+18
Projection	2.53E+08	1.01E+09	32.00	4.33E+18	7.02E+18	8.54E+18	1.14E+19
Projection	2.53E+08	1.26E+09	40.00	5.38E+18	8.74E+18	1.06E+19	1.41E+19
Projection	2.53E+08	1.51E+09	48.00	6.43E+18	1.05E+19	1.27E+19	1.68E+19
Projection	1.89E+08	1.70E+09	54.00	7.22E+18	1.18E+19	1.42E+19	1.88E+19

Table E-10 cont'd

Best Estimate Azimuthal Variation of Fast Neutron Exposure Rates

And Iron Atom Displacement Rates At the Reactor Vessel

Clad/Base Metal Interface

Cycle	Cycle Length [EFPS]	Cumulative Irradiation Time [EFPS]	Cumulative Irradiation Time [EFPY]	Iron Atom Displacement Rate [dpa/s]			
				0°	15°	30°	45°
1	3.94E+07	3.94E+07	1.25	9.96E-12	1.56E-11	1.99E-11	3.06E-11
2	3.23E+07	7.16E+07	2.27	8.74E-12	1.23E-11	1.70E-11	2.57E-11
3	3.72E+07	1.09E+08	3.45	7.13E-12	1.15E-11	1.74E-11	2.68E-11
4	3.34E+07	1.42E+08	4.51	7.28E-12	1.10E-11	1.40E-11	2.10E-11
5	4.31E+07	1.85E+08	5.87	6.88E-12	1.03E-11	1.29E-11	1.76E-11
6	4.01E+07	2.25E+08	7.14	7.20E-12	1.11E-11	1.30E-11	1.77E-11
7	4.18E+07	2.67 E+08	8.47	6.94E-12	1.10E-11	1.32E-11	1.75E-11
8	4.04E+07	3.08 E+08	9.75	6.18E-12	9.99E-12	1.21E-11	1.59E-11
9	5.13E+07	3.59 E+08	11.38	6.76E-12	1.02E-11	1.23E-11	1.65E-11
10	4.72E+07	4.06 E+08	12.87	6.04E-12	1.06E-11	1.28E-11	1.61E-11
11	4.58E+07	4.52 E+08	14.27	6.55E-12	1.19E-11	1.39E-11	1.62E-11
Projection	5.29E+07	5.05 E+08	16.00	6.78E-12	1.09E-11	1.31E-11	1.71E-11
Projection	2.53E+08	7.57 E+08	24.00	6.78E-12	1.09E-11	1.31E-11	1.71E-11
Projection	2.53E+08	1.01E+09	32.00	6.78E-12	1.09E-11	1.31E-11	1.71E-11
Projection	2.53E+08	1.26E+09	40.00	6.78E-12	1.09E-11	1.31E-11	1.71E-11
Projection	2.53E+08	1.51E+09	48.00	6.78E-12	1.09E-11	1.31E-11	1.71E-11
Projection	1.89E+08	1.70E+09	54.00	6.78E-12	1.09E-11	1.31E-11	1.71E-11

230940

Table E-10 cont'd

Best Estimate Azimuthal Variation of Maximum Exposure Rates

And Integrated Exposures at the Reactor Vessel

Clad/Base Metal Interface

Cycle	Cycle Length [EFPS]	Cumulative Irradiation Time [EFPS]	Cumulative Irradiation Time [EFPY]	Iron Atom Displacements [dpa]			
				0°	15°	30°	45°
1	3.94E+07	3.94E+07	1.25	3.92E-04	6.13E-04	7.83E-04	1.21E-03
2	3.23E+07	7.16E+07	2.27	6.74E-04	1.01E-03	1.33E-03	2.04E-03
3	3.72E+07	1.09E+08	3.45	9.39E-04	1.44E-03	1.98E-03	3.03E-03
4	3.34E+07	1.42E+08	4.51	1.18E-03	1.81E-03	2.44E-03	3.73E-03
5	4.31E+07	1.85E+08	5.87	1.48E-03	2.25E-03	3.00E-03	4.49E-03
6	4.01E+07	2.25E+08	7.14	1.77E-03	2.70E-03	3.52E-03	5.20E-03
7	4.18E+07	2.67 E+08	8.47	2.06E-03	3.16E-03	4.07E-03	5.93E-03
8	4.04E+07	3.08 E+08	9.75	2.31E-03	3.56E-03	4.55E-03	6.57E-03
9	5.13E+07	3.59 E+08	11.38	2.65E-03	4.08E-03	5.19E-03	7.42E-03
10	4.72E+07	4.06 E+08	12.87	2.94E-03	4.58E-03	5.79E-03	8.18E-03
11	4.58E+07	4.52 E+08	14.27	3.24E-03	5.12E-03	6.43E-03	8.92E-03
Projection	5.29E+07	5.05 E+08	16.00	3.59E-03	5.70E-03	7.12E-03	9.82E-03
Projection	2.53E+08	7.57 E+08	24.00	5.31E-03	8.47E-03	1.04E-02	1.41E-02
Projection	2.53E+08	1.01E+09	32.00	7.02E-03	1.12E-02	1.38E-02	1.84E-02
Projection	2.53E+08	1.26E+09	40.00	8.73E-03	1.40E-02	1.71E-02	2.28E-02
Projection	2.53E+08	1.51E+09	48.00	1.04E-02	1.68E-02	2.04E-02	2.71E-02
Projection	1.89E+08	1.70E+09	54.00	1.17E-02	1.88E-02	2.29E-02	3.03E-02

To document the ex-vessel dosimetry program the following tables have been extracted from Reference E-8.

Capsule Identifications for Ex-Vessel Irradiations

Azimuth [degrees]	Capsule Identification - Cycle 1 Irradiation		
	Core Top	Core Midplane	Core Bottom
0.0	C	F	A
13.5		E	
33.8		D	
45.0		B	

Azimuth [degrees]	Capsule Identification - Cycle 2 Irradiation		
	Core Top	Core Midplane	Core Bottom
0.0	D	A	F
10.9		B	
35.1		C	
42.0 (48.0)		E	

Azimuth [degrees]	Capsule Identification - Cycles 3-4 Irradiation		
	Core Top	Core Midplane	Core Bottom
0.0	D	A	F
10.9		B	
35.1		C	
42.0 (48.0)		E	

Azimuth [degrees]	Capsule Identification - Cycles 5-6 Irradiation		
	Core Top	Core Midplane	Core Bottom
0.0	J	G	L
10.9		H	
35.1		I	
42.0 (48.0)		K	

Azimuth [degrees]	Capsule Identification - Cycles 7-10 Irradiation		
	Core Top	Core Midplane	Core Bottom
0.0		M	
10.9		N	
35.1		O	
42.0 (48.0)	P	Q	R

Contents of Multiple Foil Sensor Sets

Cycle 1 Irradiation

Capsule ID and Position	Bare or Cadmium Covered	Radiometric Monitor ID							SSTR
		Fe	Ni	Cu	Ti	Co	U Nat.	U Dep.	
A-1	Bare	A				9			DC-19
A-2	Cd Cov.	3	DU	3	CN/CU	3			
A-3	Cd Cov.						UN-05	U8-05	DC-23
B-1	Bare	B/7				7			DC-01
B-2	Cd Cov.	1	SI	1	CL/CK	1			
B-3	Cd Cov.						UN-06	U8-06	DC-09
C-1	Bare	C				8			DC-17
C-2	Cd Cov.	2	SH	2	CM	2			
C-3	Cd Cov.						UN-07	U8-07	DC-21
D-1	Bare	D				10			DC-02
D-2	Cd Cov.	4	DK	4	CP/CR	4			
D-3	Cd Cov.						UN-08	U8-08	DC-10
E-1	Bare	E				11			DC-03
E-2	Cd Cov.	5	DL	5	CT/CS	5			
E-3	Cd Cov.						UN-09	U8-09	DC-11
F-1	Bare	F				12			DC-04
F-2	Cd Cov.	6	DM	6	AU/CU	6			
F-3	Cd Cov.						UN-10	U8-10	DC-12

Cycle 2 Irradiation

Capsule ID and Position	Bare or Cadmium Covered	Radiometric Monitor ID					SSTR
		Fe	Cu	Nb	Co	U-238	
A-1	Bare	G	AK	S	AS	G	W2-7
A-2	Cd Cov.	H			A		W2-8
A-3	Cd Cov.						
B-1	Bare	N	AL	T	AR	H	W2-5
B-2	Cd Cov.	I			B		W2-6
B-3	Cd Cov.						
C-1	Bare	O	AM	N	AP	I	W2-3
C-2	Cd Cov.	J			C		W2-4
C-3	Cd Cov.						
D-1	Bare	P	AN	O	AN	J	W2-9
D-2	Cd Cov.	K			D		W2-10
D-3	Cd Cov.						
E-1	Bare	R	AO	P	AO	K	W2-1
E-2	Cd Cov.	L			E		W2-2
E-3	Cd Cov.						
F-1	Bare	S	AP	R	AM	M	W2-11
F-2	Cd Cov.	M			F		W2-12
F-3	Cd Cov.						

Cycles 3-4 Irradiation

Capsule ID and Position	Bare or Cadmium Covered	Radiometric Monitor ID							SSTR
		Fe	Ni	Cu	Ti	Co	U Dep.	Nb	
A-1	Bare	AA				G			W8-07
A-2	Cd Cov.	AB	K	AR	AA	H	O	G	
A-3	Cd Cov.								W8-08
B-1	Bare	AC				I			W8-05
B-2	Cd Cov.	AD	L	AS	AB	J	P	H	
B-3	Cd Cov.								W8-06
C-1	Bare	AE				K			W8-03
C-2	Cd Cov.	AF	M	AT	AC	L	R	I	
C-3	Cd Cov.								W8-04
D-1	Bare	AG				M			W8-09
D-2	Cd Cov.	AH	N	BG	AD	N	S	J	
D-3	Cd Cov.								W8-10
E-1	Bare	AI				O			W8-01
E-2	Cd Cov.	AJ	O	BH	AE	P	T	K	
E-3	Cd Cov.								W8-02
F-1	Bare	T				R			W8-11
F-2	Cd Cov.	U	P	BJ	AF	S	U	L	
F-3	Cd Cov.								W8-12

Cycles 5-6 Irradiation

Capsule ID and Position	Bare or Cadmium Covered	Radiometric Monitor ID							SSTR
		Fe	Ni	Cu	Ti	Co	U Dep.	Nb	
G-1	Bare	BA				AA			W23-7
G-2	Cd Cov.	CA	G	G	G	CA	G	G	
G-3	Cd Cov.								W23-8
H-1	Bare	BB				AB			W23-5
H-2	Cd Cov.	CB	H	H	H	CB	H	H	
H-3	Cd Cov.								W23-6
I-1	Bare	BC				AC			W23-3
I-2	Cd Cov.	CC	I	I	I	CC	I	I	
I-3	Cd Cov.								W23-4
J-1	Bare	BD				AD			W23-9
J-2	Cd Cov.	CD	J	J	J	CD	J	J	
J-3	Cd Cov.								W23-10
K-1	Bare	BE				AE			W23-1
K-2	Cd Cov.	CE	K	K	K	CE	K	K	
K-3	Cd Cov.								W23-2
L-1	Bare	BF				AF			W23-11
L-2	Cd Cov.	CF	L	L	L	CF	L	L	
L-3	Cd Cov.								W23-12

Cycles 7-10 Irradiation

Capsule ID and Position	Bare or Cadmium Covered	Radiometric Monitor ID							
		Fe	Ni	Cu	Ti	Co	Nb	U-238	Np-237
M-1	Bare	BA				BA			
M-2	Cd Cov.	AA	A	A	A	AA	A		
M-3	Cd Cov.							14	8
N-1	Bare	BB				BB			
N-2	Cd Cov.	AB	B	B	B	AB	B		
N-3	Cd Cov.							15	9
O-1	Bare	BC				BC			
O-2	Cd Cov.	AC	C	C	C	AC	C		
O-3	Cd Cov.							16	10
P-1	Bare	BD				BD			
P-2	Cd Cov.	AD	D	D	D	AD	D		
P-3	Cd Cov.							17	12
Q-1	Bare	BE				BE			
Q-2	Cd Cov.	AE	E	E	E	AE	E		
Q-3	Cd Cov.							18	13
R-1	Bare	BF				BF			
R-2	Cd Cov.	AF	F	F	F	AF	F		
R-3	Cd Cov.							19	14

The results of the dosimetry evaluations performed for the Diablo Canyon Unit 1 Ex-Vessel capsules withdrawn to date from locations opposite the core axial midplane are provided below. The data tabulations for each capsule evaluation include the following information:

- 1 - The Measured, Calculated, and Best Estimate reaction rates for each sensor.
- 2 - The Measurement to Calculation Ratio (M/C) and the Measurement to Best Estimate Ratio (M/BE) for each sensor.
- 3 - The Calculated and Best Estimate values of neutron flux ($E > 1.0$ MeV) and Iron atom displacement rate with associated uncertainties.
- 4 - The Best Estimate to Calculation Ratio (BE/C) for both neutron flux ($E > 1.0$ MeV) and Iron atom displacement rate.

The M/C and M/BE ratios for the individual sensors establish a comparison between measurement and calculation before and after the least squares evaluation. The reduction in these reaction rate ratios for the best estimate case is an indication of the improvement in the neutron spectrum and corresponding reduction in uncertainty brought about by the application of the least squares procedure. The comparisons of calculated and best estimate values of neutron flux ($E > 1.0$ MeV) and Iron atom displacement rate with associated uncertainties also provided an indication of the improved results obtained with the least squares procedure.

Capsule IDF

Azimuthal Location 0.0° Ex-Vessel

Axial Location Core Midplane

Irradiation Period Cycle 1

	Measured	Calculated	Best Est.	M/C	M/BE
Cu-63(n,a)Co-60	1.97E-19	2.24E-19	1.92E-19	0.88	1.03
Fe-54(n,p)Mn-54	1.37E-17	1.68E-17	1.41E-17	0.82	0.97
Ni-58(n,p)Co-58	1.98E-17	2.41E-17	2.03E-17	0.82	0.98
U-238(n,f)Cs-137 Cd	8.61E-17	9.52E-17	8.33E-17	0.90	1.03
Np-237(n,f)Cs-137 Cd	1.88E-15	1.68E-15	1.72E-15	1.12	1.09
Co-59(n,g)Co-60	4.22E-14	6.93E-14	4.27E-14	0.61	0.99
Co-59(n,g)Co-60 Cd	1.94E-14	2.59E-14	1.94E-14	0.75	1.00

	Calculated	% Unc.	Best Est.	% Unc.	BE/C
Flux(E > 1.0 MeV)	3.37E+08	14	3.03E+08	6	0.90
dpa/s	1.33E-12	14	1.26E-12	9	0.95

Capsule IDE

Azimuthal Location 13.5° Ex-Vessel

Axial Location Core Midplane

Irradiation Period Cycle 1

	Measured	Calculated	Best Est.	M/C	M/BE
Cu-63(n,a)Co-60	2.28E-19	2.97E-19	2.23E-19	0.77	1.02
Fe-54(n,p)Mn-54	1.65E-17	2.36E-17	1.71E-17	0.70	0.96
Ni-58(n,p)Co-58	2.41E-17	3.39E-17	2.47E-17	0.71	0.98
U-238(n,f)Cs-137 Cd	1.08E-16	1.37E-16	1.02E-16	0.79	1.06
Np-237(n,f)Cs-137 Cd	2.12E-15	2.43E-15	2.02E-15	0.87	1.05
Co-59(n,g)Co-60	4.98E-14	9.30E-14	5.10E-14	0.54	0.98
Co-59(n,g)Co-60 Cd	2.96E-14	3.95E-14	2.93E-14	0.75	1.01

	Calculated	% Unc.	Best Est.	% Unc.	BE/C
Flux(E > 1.0 MeV)	4.89E+08	14	3.74E+08	6	0.76
dpa/s	1.93E-12	14	1.57E-12	10	0.81

230940

Capsule IDD

Azimuthal Location 33.8° Ex-Vessel

Axial Location Core Midplane

Irradiation Period Cycle 1

	Measured	Calculated	Best Est.	M/C	M/BE
Cu-63(n,a)Co-60	3.11E-19	3.91E-19	3.10E-19	0.80	1.00
Fe-54(n,p)Mn-54	2.57E-17	3.30E-17	2.59E-17	0.78	0.99
Ni-58(n,p)Co-58	3.72E-17	4.81E-17	3.77E-17	0.77	0.99
U-238(n,f)Cs-137 Cd	1.67E-16	2.03E-16	1.61E-16	0.82	1.04
Np-237(n,f)Cs-137 Cd	3.06E-15	3.78E-15	3.07E-15	0.81	1.00
Co-59(n,g)Co-60	8.58E-14	1.35E-13	8.69E-14	0.64	0.99
Co-59(n,g)Co-60 Cd	4.56E-14	5.78E-14	4.54E-14	0.79	1.00

	Calculated	% Unc.	Best Est.	% Unc.	BE/C
Flux(E > 1.0 MeV)	7.44E+08	14	5.96E+08	6	0.80
dpa/s	3.00E-12	14	2.46E-12	9	0.82

Capsule IDB

Azimuthal Location 45.0° Ex-Vessel

Axial Location Core Midplane

Irradiation Period Cycle 1

	Measured	Calculated	Best Est.	M/C	M/BE
Cu-63(n,a)Co-60	3.73E-19	4.26E-19	3.68E-19	0.88	1.01
Fe-54(n,p)Mn-54	2.93E-17	3.63E-17	3.11E-17	0.81	0.94
Ni-58(n,p)Co-58	4.72E-17	5.30E-17	4.67E-17	0.89	1.01
U-238(n,f)Cs-137 Cd	2.32E-16	2.26E-16	2.03E-16	1.03	1.14
Np-237(n,f)Cs-137 Cd	3.73E-15	4.11E-15	3.76E-15	0.91	0.99
Co-59(n,g)Co-60	6.60E-14	1.32E-13	6.81E-14	0.50	0.97
Co-59(n,g)Co-60 Cd	4.06E-14	5.02E-14	4.00E-14	0.81	1.02

	Calculated	% Unc.	Best Est.	% Unc.	BE/C
Flux(E > 1.0 MeV)	8.34E+08	14	7.60E+08	6	0.91
dpa/s	3.15E-12	14	2.88E-12	9	0.91

Capsule IDA

Azimuthal Location 0.0° Ex-Vessel

Axial Location Core Midplane

Irradiation Period Cycle 2

	Measured	Calculated	Best Est.	M/C	M/BE
Cu-63(n,a)Co-60	1.88E-19	1.98E-19	1.86E-19	0.95	1.01
Fe-54(n,p)Mn-54	1.33E-17	1.46E-17	1.35E-17	0.91	0.99
Ni-58(n,p)Co-58					
U-238(n,f)Cs-137 Cd	7.87E-17	8.20E-17	7.62E-17	0.96	1.03
Np-237(n,f)Cs-137 Cd					
Co-59(n,g)Co-60	4.24E-14	5.81E-14	4.26E-14	0.73	1.00
Co-59(n,g)Co-60 Cd	1.72E-14	2.17E-14	1.73E-14	0.79	0.99

	Calculated	% Unc.	Best Est.	% Unc.	BE/C
Flux(E > 1.0 MeV)	2.89E+08	14	2.68E+08	8	0.93
dpa/s	1.12E-12	14	1.04E-12	11	0.93

Capsule IDB

Azimuthal Location 10.9° Ex-Vessel

Axial Location Core Midplane

Irradiation Period Cycle 2

	Measured	Calculated	Best Est.	M/C	M/BE
Cu-63(n,a)Co-60	2.00E-19	2.36E-19	1.99E-19	0.85	1.01
Fe-54(n,p)Mn-54	1.47E-17	1.82E-17	1.51E-17	0.81	0.97
Ni-58(n,p)Co-58					
U-238(n,f)Cs-137 Cd	9.41E-17	1.04E-16	8.84E-17	0.90	1.06
Np-237(n,f)Cs-137 Cd					
Co-59(n,g)Co-60	4.94E-14	7.28E-14	4.98E-14	0.68	0.99
Co-59(n,g)Co-60 Cd	2.36E-14	3.05E-14	2.36E-14	0.77	1.00

	Calculated	% Unc.	Best Est.	% Unc.	BE/C
Flux(E > 1.0 MeV)	3.68E+08	14	3.17E+08	8	0.86
dpa/s	1.46E-12	14	1.28E-12	12	0.88

235940

Capsule IDC

Azimuthal Location 35.1° Ex-Vessel

Axial Location Core Midplane

Irradiation Period Cycle 2

	Measured	Calculated	Best Est.	M/C	M/BE
Cu-63(n,a)Co-60	3.11E-19	3.54E-19	3.08E-19	0.88	1.01
Fe-54(n,p)Mn-54	2.45E-17	2.95E-17	2.53E-17	0.83	0.97
Ni-58(n,p)Co-58					
U-238(n,f)Cs-137 Cd	1.71E-16	1.80E-16	1.59E-16	0.95	1.08
Np-237(n,f)Cs-137 Cd	3.03E-15	3.31E-15	3.02E-15	0.92	1.00
Co-59(n,g)Co-60	8.55E-14	1.16E-13	8.62E-14	0.74	0.99
Co-59(n,g)Co-60 Cd	4.29E-14	4.96E-14	4.28E-14	0.86	1.00

	Calculated	% Unc.	Best Est.	% Unc.	BE/C
Flux(E > 1.0 MeV)	6.57E+08	14	5.88E+08	7	0.90
dpa/s	2.62E-12	14	2.39E-12	10	0.91

Capsule IDE

Azimuthal Location 42.0° Ex-Vessel

Axial Location Core Midplane

Irradiation Period Cycle 2

	Measured	Calculated	Best Est.	M/C	M/BE
Cu-63(n,a)Co-60	3.21E-19	3.68E-19	3.14E-19	0.87	1.02
Fe-54(n,p)Mn-54	2.44E-17	3.11E-17	2.56E-17	0.78	0.95
Ni-58(n,p)Co-58					
U-238(n,f)Cs-137 Cd	1.77E-16	1.93E-16	1.62E-16	0.92	1.09
Np-237(n,f)Cs-137 Cd	2.95E-15	3.56E-15	2.99E-15	0.83	0.99
Co-59(n,g)Co-60	7.65E-14	1.16E-13	7.71E-14	0.66	0.99
Co-59(n,g)Co-60 Cd	3.51E-14	4.66E-14	3.52E-14	0.75	1.00

	Calculated	% Unc.	Best Est.	% Unc.	BE/C
Flux(E > 1.0 MeV)	7.13E+08	14	5.99E+08	7	0.84
dpa/s	2.76E-12	14	2.37E-12	9	0.86

236940

Capsule IDA

Azimuthal Location 0.0° Ex-Vessel

Axial Location Core Midplane

Irradiation Period Cycles 3-4

	Measured	Calculated	Best Est.	M/C	M/BE
Cu-63(n,a)Co-60	1.55E-19	1.72E-19	1.55E-19	0.90	1.00
Fe-54(n,p)Mn-54	1.12E-17	1.25E-17	1.13E-17	0.90	0.99
Ni-58(n,p)Co-58	1.61E-17	1.79E-17	1.61E-17	0.90	1.00
U-238(n,f)Cs-137 Cd	6.46E-17	6.98E-17	6.34E-17	0.93	1.02
Np-237(n,f)Cs-137 Cd					
Co-59(n,g)Co-60	3.58E-14	5.05E-14	3.62E-14	0.71	0.99
Co-59(n,g)Co-60 Cd	1.70E-14	1.88E-14	1.69E-14	0.90	1.01

	Calculated	% Unc.	Best Est.	% Unc.	BE/C
Flux(E > 1.0 MeV)	2.45E+08	14	2.24E+08	7	0.91
dpa/s	9.60E-13	14	8.80E-13	11	0.92

Capsule IDB

Azimuthal Location 10.9° Ex-Vessel

Axial Location Core Midplane

Irradiation Period Cycles 3-4

	Measured	Calculated	Best Est.	M/C	M/BE
Cu-63(n,a)Co-60	1.82E-19	2.14E-19	1.81E-19	0.85	1.01
Fe-54(n,p)Mn-54	1.34E-17	1.63E-17	1.37E-17	0.82	0.98
Ni-58(n,p)Co-58					
U-238(n,f)Cs-137 Cd	8.26E-17	9.24E-17	8.07E-17	0.89	1.02
Np-237(n,f)Cs-137 Cd	1.61E-15	1.62E-15	1.54E-15	0.99	1.05
Co-59(n,g)Co-60	4.45E-14	6.43E-14	4.49E-14	0.69	0.99
Co-59(n,g)Co-60 Cd	2.16E-14	2.69E-14	2.16E-14	0.80	1.00

	Calculated	% Unc.	Best Est.	% Unc.	BE/C
Flux(E > 1.0 MeV)	3.27E+08	14	2.92E+08	7	0.89
dpa/s	1.30E-12	14	1.19E-12	10	0.92

236940

Capsule IDC

Azimuthal Location 35.1° Ex-Vessel

Axial Location Core Midplane

Irradiation Period Cycles 3-4

	Measured	Calculated	Best Est.	M/C	M/BE
Cu-63(n,a)Co-60	2.94E-19	3.34E-19	2.89E-19	0.88	1.02
Fe-54(n,p)Mn-54	2.23E-17	2.75E-17	2.31E-17	0.81	0.97
Ni-58(n,p)Co-58					
U-238(n,f)Cs-137 Cd	1.52E-16	1.66E-16	1.43E-16	0.92	1.06
Np-237(n,f)Cs-137 Cd					
Co-59(n,g)Co-60	7.50E-14	1.06E-13	7.56E-14	0.71	0.99
Co-59(n,g)Co-60 Cd	3.68E-14	4.50E-14	3.68E-14	0.82	1.00

	Calculated	% Unc.	Best Est.	% Unc.	BE/C
Flux(E > 1.0 MeV)	6.06E+08	14	5.24E+08	8	0.86
dpa/s	2.40E-12	14	2.13E-12	12	0.88

Capsule IDE

Azimuthal Location 42.0° Ex-Vessel

Axial Location Core Midplane

Irradiation Period Cycles 3-4

	Measured	Calculated	Best Est.	M/C	M/BE
Cu-63(n,a)Co-60	2.78E-19	3.50E-19	2.78E-19	0.79	1.00
Fe-54(n,p)Mn-54	2.29E-17	2.92E-17	2.34E-17	0.78	0.98
Ni-58(n,p)Co-58	3.46E-17	4.25E-17	3.46E-17	0.81	1.00
U-238(n,f)Cs-137 Cd	1.60E-16	1.80E-16	1.50E-16	0.89	1.07
Np-237(n,f)Cs-137 Cd					
Co-59(n,g)Co-60	6.52E-14	1.05E-13	6.60E-14	0.62	0.99
Co-59(n,g)Co-60 Cd	3.28E-14	4.23E-14	3.27E-14	0.78	1.00

	Calculated	% Unc.	Best Est.	% Unc.	BE/C
Flux(E > 1.0 MeV)	6.60E+08	14	5.58E+08	7	0.84
dpa/s	2.54E-12	14	2.19E-12	11	0.86

236940

Capsule IDG

Azimuthal Location 0.0° Ex-Vessel

Axial Location Core Midplane

Irradiation Period Cycles 5-6

	Measured	Calculated	Best Est.	M/C	M/BE
Cu-63(n,a)Co-60	1.58E-19	1.67E-19	1.56E-19	0.95	1.01
Fe-54(n,p)Mn-54	1.10E-17	1.22E-17	1.14E-17	0.90	0.96
Ni-58(n,p)Co-58	1.63E-17	1.73E-17	1.64E-17	0.94	0.99
U-238(n,f)Cs-137 Cd	7.41E-17	6.76E-17	6.62E-17	1.10	1.12
Np-237(n,f)Cs-137 Cd	1.24E-15	1.17E-15	1.21E-15	1.06	1.02
Co-59(n,g)Co-60	3.43E-14	4.71E-14	3.46E-14	0.73	0.99
Co-59(n,g)Co-60 Cd	1.48E-14	1.76E-14	1.48E-14	0.84	1.00

	Calculated	% Unc.	Best Est.	% Unc.	BE/C
Flux(E > 1.0 MeV)	2.37E+08	14	2.37E+08	6	1.00
dpa/s	9.19E-13	14	9.28E-13	9	1.01

Capsule IDH

Azimuthal Location 10.9° Ex-Vessel

Axial Location Core Midplane

Irradiation Period Cycles 5-6

	Measured	Calculated	Best Est.	M/C	M/BE
Cu-63(n,a)Co-60	1.80E-19	2.05E-19	1.78E-19	0.88	1.01
Fe-54(n,p)Mn-54	1.28E-17	1.56E-17	1.32E-17	0.82	0.97
Ni-58(n,p)Co-58	1.89E-17	2.23E-17	1.90E-17	0.85	0.99
U-238(n,f)Cs-137 Cd	8.20E-17	8.79E-17	7.61E-17	0.93	1.08
Np-237(n,f)Cs-137 Cd					
Co-59(n,g)Co-60	4.06E-14	5.87E-14	4.10E-14	0.69	0.99
Co-59(n,g)Co-60 Cd	2.05E-14	2.47E-14	2.05E-14	0.83	1.00

	Calculated	% Unc.	Best Est.	% Unc.	BE/C
Flux(E > 1.0 MeV)	3.11E+08	14	2.72E+08	7	0.87
dpa/s	1.22E-12	14	1.09E-12	11	0.89

235940

Capsule IDI

Azimuthal Location 35.1° Ex-Vessel

Axial Location Core Midplane

Irradiation Period Cycles 5-6

	Measured	Calculated	Best Est.	M/C	M/BE
Cu-63(n,a)Co-60	2.39E-19	2.66E-19	2.35E-19	0.90	1.02
Fe-54(n,p)Mn-54	1.79E-17	2.17E-17	1.87E-17	0.82	0.96
Ni-58(n,p)Co-58	2.78E-17	3.14E-17	2.76E-17	0.89	1.01
U-238(n,f)Cs-137 Cd	1.21E-16	1.30E-16	1.15E-16	0.93	1.05
Np-237(n,f)Cs-137 Cd	2.21E-15	2.38E-15	2.19E-15	0.93	1.01
Co-59(n,g)Co-60	6.45E-14	8.43E-14	6.49E-14	0.77	0.99
Co-59(n,g)Co-60 Cd	3.12E-14	3.58E-14	3.12E-14	0.87	1.00

	Calculated	% Unc.	Best Est.	% Unc.	BE/C
Flux(E > 1.0 MeV)	4.74E+08	14	4.23E+08	6	0.89
dpa/s	1.89E-12	14	1.73E-12	9	0.92

Capsule IDK

Azimuthal Location 42.0° Ex-Vessel

Axial Location Core Midplane

Irradiation Period Cycles 5-6

	Measured	Calculated	Best Est.	M/C	M/BE
Cu-63(n,a)Co-60	2.23E-19	2.67E-19	2.19E-19	0.84	1.02
Fe-54(n,p)Mn-54	1.65E-17	2.21E-17	1.75E-17	0.75	0.94
Ni-58(n,p)Co-58	2.63E-17	3.22E-17	2.60E-17	0.82	1.01
U-238(n,f)Cs-137 Cd	1.22E-16	1.36E-16	1.10E-16	0.90	1.11
Np-237(n,f)Cs-137 Cd	1.92E-15	2.48E-15	1.99E-15	0.77	0.96
Co-59(n,g)Co-60	5.44E-14	8.23E-14	5.49E-14	0.66	0.99
Co-59(n,g)Co-60 Cd	2.64E-14	3.29E-14	2.63E-14	0.80	1.00

	Calculated	% Unc.	Best Est.	% Unc.	BE/C
Flux(E > 1.0 MeV)	4.98E+08	14	4.05E+08	6	0.81
dpa/s	1.93E-12	14	1.60E-12	9	0.83

Capsule IDM

236940

Azimuthal Location 0.0° Ex-Vessel

Axial Location Core Midplane

Irradiation Period Cycles 7-10

	Measured	Calculated	Best Est.	M/C	M/BE
Cu-63(n,a)Co-60	1.46E-19	1.56E-19	1.44E-19	0.94	1.01
Fe-54(n,p)Mn-54	1.03E-17	1.13E-17	1.04E-17	0.91	0.99
Ni-58(n,p)Co-58	1.43E-17	1.62E-17	1.48E-17	0.88	0.97
U-238(n,f)Cs-137 Cd	6.29E-17	6.32E-17	5.98E-17	1.00	1.05
Np-237(n,f)Cs-137 Cd	1.24E-15	1.10E-15	1.16E-15	1.13	1.07
Co-59(n,g)Co-60	3.18E-14	4.53E-14	3.21E-14	0.70	0.99
Co-59(n,g)Co-60 Cd	1.38E-14	1.69E-14	1.38E-14	0.82	1.00

	Calculated	% Unc.	Best Est.	% Unc.	BE/C
Flux(E > 1.0 MeV)	2.22E+08	14	2.14E+08	6	0.97
dpa/s	8.67E-13	14	8.65E-13	9	1.00

Capsule IDN

Azimuthal Location 10.9° Ex-Vessel

Axial Location Core Midplane

Irradiation Period Cycles 7-10

	Measured	Calculated	Best Est.	M/C	M/BE
Cu-63(n,a)Co-60	1.70E-19	1.96E-19	1.67E-19	0.87	1.02
Fe-54(n,p)Mn-54	1.22E-17	1.49E-17	1.26E-17	0.82	0.97
Ni-58(n,p)Co-58	1.79E-17	2.13E-17	1.82E-17	0.84	0.98
U-238(n,f)Cs-137 Cd	7.87E-17	8.41E-17	7.50E-17	0.94	1.05
Np-237(n,f)Cs-137 Cd	1.64E-15	1.47E-15	1.52E-15	1.12	1.08
Co-59(n,g)Co-60	3.89E-14	5.69E-14	3.93E-14	0.68	0.99
Co-59(n,g)Co-60 Cd	1.96E-14	2.39E-14	1.96E-14	0.82	1.00

	Calculated	% Unc.	Best Est.	% Unc.	BE/C
Flux(E > 1.0 MeV)	2.98E+08	14	2.73E+08	6	0.92
dpa/s	1.17E-12	14	1.14E-12	9	0.97

Capsule IDO

Azimuthal Location 35.1° Ex-Vessel

Axial Location Core Midplane

Irradiation Period Cycles 7-10

	Measured	Calculated	Best Est.	M/C	M/BE
Cu-63(n,a)Co-60	2.25E-19	2.54E-19	2.22E-19	0.89	1.01
Fe-54(n,p)Mn-54	1.74E-17	2.07E-17	1.79E-17	0.84	0.97
Ni-58(n,p)Co-58	2.59E-17	3.00E-17	2.63E-17	0.86	0.98
U-238(n,f)Cs-137 Cd	1.18E-16	1.24E-16	1.13E-16	0.95	1.04
Np-237(n,f)Cs-137 Cd	2.53E-15	2.27E-15	2.35E-15	1.11	1.08
Co-59(n,g)Co-60	6.00E-14	8.11E-14	6.04E-14	0.74	0.99
Co-59(n,g)Co-60 Cd	2.85E-14	3.45E-14	2.85E-14	0.83	1.00

	Calculated	% Unc.	Best Est.	% Unc.	BE/C
Flux(E > 1.0 MeV)	4.52E+08	14	4.22E+08	6	0.93
dpa/s	1.80E-12	14	1.76E-12	9	0.98

Capsule IDQ

Azimuthal Location 42.0° Ex-Vessel

Axial Location Core Midplane

Irradiation Period Cycles 7-10

	Measured	Calculated	Best Est.	M/C	M/BE
Cu-63(n,a)Co-60	2.07E-19	2.52E-19	2.05E-19	0.82	1.01
Fe-54(n,p)Mn-54	1.65E-17	2.08E-17	1.71E-17	0.79	0.96
Ni-58(n,p)Co-58	2.53E-17	3.03E-17	2.54E-17	0.83	1.00
U-238(n,f)Cs-137 Cd	1.18E-16	1.28E-16	1.11E-16	0.92	1.06
Np-237(n,f)Cs-137 Cd	2.42E-15	2.34E-15	2.29E-15	1.03	1.06
Co-59(n,g)Co-60	5.14E-14	7.87E-14	5.19E-14	0.65	0.99
Co-59(n,g)Co-60 Cd	2.40E-14	3.15E-14	2.40E-14	0.76	1.00

	Calculated	% Unc.	Best Est.	% Unc.	BE/C
Flux(E > 1.0 MeV)	4.68E+08	14	4.19E+08	6	0.89
dpa/s	1.82E-12	14	1.70E-12	9	0.93

The results of the dosimetry evaluations performed for the Diablo Canyon Unit 1 Ex-Vessel capsules withdrawn to date from locations opposite the top and bottom of the active are provided following. The data tabulations for each capsule evaluation include the following information:

- 1 - The Measured, Calculated, and Best Estimate reaction rates for each sensor.
- 2 - The Measurement to Calculation Ratio (M/C) and the Measurement to Best Estimate Ratio (M/BE) for each sensor.
- 3 - The Calculated and Best Estimate values of neutron flux ($E > 1.0$ MeV) and Iron atom displacement rate with associated uncertainties.
- 4 - The Best Estimate to Calculation Ratio (BE/C) for both neutron flux ($E > 1.0$ MeV) and Iron atom displacement rate.

The M/C and M/BE ratios for the individual sensors establish a comparison between measurement and calculation before and after the least squares evaluation. The reduction in these reaction rate ratios for the best estimate case is an indication of the improvement in the neutron spectrum and corresponding reduction in uncertainty brought about by the application of the least squares procedure. The comparisons of calculated and best estimate values of neutron flux ($E > 1.0$ MeV) and Iron atom displacement rate with associated uncertainties also provided an indication of the improved results obtained with the least squares procedure.

Capsule IDC

Azimuthal Location 45.0° Ex-Vessel

Axial Location Core Top

Irradiation Period Cycle 1

	Measured	Calculated	Best Est.	M/C	M/BE
Cu-63(n,a)Co-60	1.04E-19	1.19E-19	1.07E-19	0.87	0.97
Fe-54(n,p)Mn-54	9.41E-18	1.03E-17	1.01E-17	0.91	0.93
Ni-58(n,p)Co-58	1.67E-17	1.50E-17	1.57E-17	1.11	1.06
U-238(n,f)Cs-137 Cd	8.49E-17	6.47E-17	6.99E-17	1.31	1.21
Np-237(n,f)Cs-137 Cd	1.10E-15	1.21E-15	1.21E-15	0.91	0.91
Co-59(n,g)Co-60	3.68E-14	4.09E-14	3.70E-14	0.90	0.99
Co-59(n,g)Co-60 Cd	1.77E-14	1.56E-14	1.76E-14	1.13	1.01

	Calculated	% Unc.	Best Est.	% Unc.	BE/C
Flux(E > 1.0 MeV)	2.40E+08	14	2.64E+08	6	1.10
dpa/s	9.36E-13	14	9.92E-13	9	1.06

Capsule IDA

Azimuthal Location 45.0° Ex-Vessel

Axial Location Core Bottom

Irradiation Period Cycle 1

	Measured	Calculated	Best Est.	M/C	M/BE
Cu-63(n,a)Co-60	1.38E-19	1.29E-19	1.41E-19	1.07	0.98
Fe-54(n,p)Mn-54	1.31E-17	1.11E-17	1.28E-17	1.18	1.02
Ni-58(n,p)Co-58					
U-238(n,f)Cs-137 Cd	8.02E-17	7.04E-17	8.13E-17	1.14	0.99
Np-237(n,f)Cs-137 Cd	1.53E-15	1.32E-15	1.52E-15	1.16	1.01
Co-59(n,g)Co-60	4.31E-14	4.41E-14	4.35E-14	0.98	0.99
Co-59(n,g)Co-60 Cd	2.27E-14	1.69E-14	2.24E-14	1.34	1.01

	Calculated	% Unc.	Best Est.	% Unc.	BE/C
Flux(E > 1.0 MeV)	2.62E+08	14	3.03E+08	7	1.16
dpa/s	1.02E-12	14	1.16E-12	9	1.13

236940

Capsule IDD

Azimuthal Location 42.0° Ex-Vessel

Axial Location Core Top

Irradiation Period Cycle 2

	Measured	Calculated	Best Est.	M/C	M/BE
Cu-63(n,a)Co-60	1.13E-19	1.35E-19	1.11E-19	0.84	1.02
Fe-54(n,p)Mn-54	8.36E-18	1.15E-17	9.14E-18	0.73	0.91
Ni-58(n,p)Co-58					
U-238(n,f)Cs-137 Cd	7.64E-17	7.13E-17	6.14E-17	1.07	1.24
Np-237(n,f)Cs-137 Cd	1.12E-15	1.32E-15	1.16E-15	0.85	0.97
Co-59(n,g)Co-60	3.58E-14	4.17E-14	3.60E-14	0.86	0.99
Co-59(n,g)Co-60 Cd	1.79E-14	1.70E-14	1.78E-14	1.05	1.01

	Calculated	% Unc.	Best Est.	% Unc.	BE/C
Flux(E > 1.0 MeV)	2.63E+08	14	2.31E+08	7	0.88
dpa/s	1.02E-12	14	9.37E-13	10	0.92

Capsule IDF

Azimuthal Location 42.0° Ex-Vessel

Axial Location Core Bottom

Irradiation Period Cycle 2

	Measured	Calculated	Best Est.	M/C	M/BE
Cu-63(n,a)Co-60	1.39E-19	1.36E-19	1.39E-19	1.02	1.00
Fe-54(n,p)Mn-54	1.18E-17	1.16E-17	1.19E-17	1.02	0.99
Ni-58(n,p)Co-58					
U-238(n,f)Cs-137 Cd	7.67E-17	7.28E-17	7.50E-17	1.05	1.02
Np-237(n,f)Cs-137 Cd					
Co-59(n,g)Co-60	4.14E-14	4.28E-14	4.16E-14	0.97	1.00
Co-59(n,g)Co-60 Cd	2.00E-14	1.75E-14	1.99E-14	1.14	1.01

	Calculated	% Unc.	Best Est.	% Unc.	BE/C
Flux(E > 1.0 MeV)	2.69E+08	14	2.78E+08	8	1.03
dpa/s	1.05E-12	14	1.09E-12	11	1.03

236940

Capsule IDD

Azimuthal Location 42.0° Ex-Vessel

Axial Location Core Top

Irradiation Period Cycles 3-4

	Measured	Calculated	Best Est.	M/C	M/BE
Cu-63(n,a)Co-60	9.72E-20	1.17E-19	9.62E-20	0.83	1.01
Fe-54(n,p)Mn-54	7.58E-18	9.79E-18	8.07E-18	0.77	0.94
Ni-58(n,p)Co-58					
U-238(n,f)Cs-137 Cd	6.10E-17	6.05E-17	5.43E-17	1.01	1.12
Np-237(n,f)Cs-137 Cd	1.20E-15	1.12E-15	1.15E-15	1.07	1.04
Co-59(n,g)Co-60	3.22E-14	3.59E-14	3.23E-14	0.90	1.00
Co-59(n,g)Co-60 Cd	1.56E-14	1.46E-14	1.55E-14	1.07	1.01

	Calculated	% Unc.	Best Est.	% Unc.	BE/C
Flux(E > 1.0 MeV)	2.23E+08	14	2.07E+08	7	0.93
dpa/s	8.69E-13	14	8.62E-13	10	0.99

Capsule IDF

Azimuthal Location 42.0° Ex-Vessel

Axial Location Core Bottom

Irradiation Period Cycles 3-4

	Measured	Calculated	Best Est.	M/C	M/BE
Cu-63(n,a)Co-60	9.98E-20	1.15E-19	1.01E-19	0.87	0.99
Fe-54(n,p)Mn-54	8.74E-18	9.71E-18	8.72E-18	0.90	1.00
Ni-58(n,p)Co-58					
U-238(n,f)Cs-137 Cd	5.65E-17	6.05E-17	5.51E-17	0.93	1.03
Np-237(n,f)Cs-137 Cd	9.83E-16	1.13E-15	1.01E-15	0.87	0.97
Co-59(n,g)Co-60	3.65E-14	3.63E-14	3.66E-14	1.01	1.00
Co-59(n,g)Co-60 Cd	1.74E-14	1.48E-14	1.72E-14	1.18	1.01

	Calculated	% Unc.	Best Est.	% Unc.	BE/C
Flux(E > 1.0 MeV)	2.23E+08	14	2.04E+08	7	0.91
dpa/s	8.77E-13	14	8.11E-13	9	0.92

Capsule IDJ

Azimuthal Location 42.0° Ex-Vessel

Axial Location Core Top

Irradiation Period Cycles 5-6

	Measured	Calculated	Best Est.	M/C	M/BE
Cu-63(n,a)Co-60	7.70E-20	9.04E-20	7.77E-20	0.85	0.99
Fe-54(n,p)Mn-54	6.26E-18	7.54E-18	6.80E-18	0.83	0.92
Ni-58(n,p)Co-58	1.10E-17	1.10E-17	1.05E-17	1.00	1.05
U-238(n,f)Cs-137 Cd	5.40E-17	4.65E-17	4.70E-17	1.16	1.15
Np-237(n,f)Cs-137 Cd	9.87E-16	8.60E-16	9.63E-16	1.15	1.02
Co-59(n,g)Co-60	2.60E-14	2.83E-14	2.61E-14	0.92	1.00
Co-59(n,g)Co-60 Cd	1.27E-14	1.15E-14	1.26E-14	1.10	1.01

	Calculated	% Unc.	Best Est.	% Unc.	BE/C
Flux(E > 1.0 MeV)	1.71E+08	14	1.80E+08	6	1.06
dpa/s	6.71E-13	14	7.30E-13	9	1.09

Capsule IDL

Azimuthal Location 42.0° Ex-Vessel

Axial Location Core Bottom

Irradiation Period Cycles 5-6

	Measured	Calculated	Best Est.	M/C	M/BE
Cu-63(n,a)Co-60	6.77E-20	8.66E-20	6.91E-20	0.78	0.98
Fe-54(n,p)Mn-54	5.68E-18	7.28E-18	5.95E-18	0.78	0.95
Ni-58(n,p)Co-58	9.62E-18	1.06E-17	9.09E-18	0.91	1.06
U-238(n,f)Cs-137 Cd	3.91E-17	4.53E-17	3.88E-17	0.86	1.01
Np-237(n,f)Cs-137 Cd	6.99E-16	8.49E-16	7.27E-16	0.82	0.96
Co-59(n,g)Co-60	2.72E-14	2.84E-14	2.72E-14	0.96	1.00
Co-59(n,g)Co-60 Cd	1.23E-14	1.15E-14	1.22E-14	1.07	1.01

	Calculated	% Unc.	Best Est.	% Unc.	BE/C
Flux(E > 1.0 MeV)	1.67E+08	14	1.45E+08	6	0.87
dpa/s	6.64E-13	14	5.89E-13	9	0.89

236940

Capsule IDP

Azimuthal Location 42.0° Ex-Vessel

Axial Location Core Top

Irradiation Period Cycles 7-10

	Measured	Calculated	Best Est.	M/C	M/BE
Cu-63(n,a)Co-60	7.25E-20	9.84E-20	7.53E-20	0.74	0.96
Fe-54(n,p)Mn-54	6.37E-18	8.14E-18	6.81E-18	0.78	0.94
Ni-58(n,p)Co-58	1.17E-17	1.18E-17	1.07E-17	0.99	1.09
U-238(n,f)Cs-137 Cd	4.57E-17	4.98E-17	4.69E-17	0.92	0.97
Np-237(n,f)Cs-137 Cd	1.05E-15	9.12E-16	9.93E-16	1.15	1.06
Co-59(n,g)Co-60	2.27E-14	2.92E-14	2.29E-14	0.78	0.99
Co-59(n,g)Co-60 Cd	1.15E-14	1.19E-14	1.14E-14	0.97	1.01

	Calculated	% Unc.	Best Est.	% Unc.	BE/C
Flux(E > 1.0 MeV)	1.83E+08	14	1.81E+08	6	0.99
dpa/s	7.08E-13	14	7.28E-13	9	1.03

Capsule IDR

Azimuthal Location 42.0° Ex-Vessel

Axial Location Core Bottom

Irradiation Period Cycles 7-10

	Measured	Calculated	Best Est.	M/C	M/BE
Cu-63(n,a)Co-60	7.59E-20	9.48E-20	7.99E-20	0.80	0.95
Fe-54(n,p)Mn-54	7.39E-18	7.90E-18	7.30E-18	0.94	1.01
Ni-58(n,p)Co-58	1.16E-17	1.15E-17	1.10E-17	1.01	1.05
U-238(n,f)Cs-137 Cd	4.05E-17	4.88E-17	4.69E-17	0.83	0.86
Np-237(n,f)Cs-137 Cd	9.42E-16	9.04E-16	9.20E-16	1.04	1.02
Co-59(n,g)Co-60	2.68E-14	2.92E-14	2.69E-14	0.92	1.00
Co-59(n,g)Co-60 Cd	1.30E-14	1.19E-14	1.29E-14	1.09	1.01

	Calculated	% Unc.	Best Est.	% Unc.	BE/C
Flux(E > 1.0 MeV)	1.80E+08	14	1.76E+08	6	0.98
dpa/s	7.04E-13	14	6.95E-13	9	0.99

Appendix E References

- E-1. Regulatory Guide RG-1.190, "Calculational and Dosimetry Methods for Determining Pressure Vessel Neutron Fluence," U. S. Nuclear Regulatory Commission, Office of Nuclear Regulatory Research, March 2001.
- E-2. RSAC-PGE-807, "Analysis of Neutron Dosimetry form Diablo Canyon Unit 1 Surveillance Capsule Y," Anderson, S. L. July 26, 1993.
- E-3. E. B. Norris, "Reactor Vessel Material Surveillance Program, Capsule S – Turkey Point Unit No. 3, Capsule S – Turkey Point Unit No. 4," Final Report SwRI Project No. 02-5131 and SwRI Project No. 02-5380, Southwest Research Institute, May 1979.
- E-4. P. K. Nair and E. B. Norris, "Reactor Vessel Material Surveillance Program for Turkey Point Unit No. 3: Analysis of Capsule V," Final Report SwRI Project No. 06-8575, Southwest Research Institute, August 1986.
- E-5. WCAP-14044, Revision 0, "Westinghouse Surveillance Capsule Neutron Fluence Reevaluation," April 1994.
- E-6. A. Schmittroth, *FERRET Data Analysis Core*, HEDL-TME 79-40, Hanford Engineering Development Laboratory, Richland, WA, September 1979.
- E-7. RSIC Data Library Collection DLC-178, "SNLRML Recommended Dosimetry Cross-Section Compendium", July 1994.
- E-8. WCAP-15780. "Fast Neutron Fluence and Neutron Dosimetry Evaluations for the Diablo Canyon Unit 1 Reactor Pressure Vessel." December 2001.

